



HAL
open science

Involvement of a ventral tegmental area-Amygdala pathway in anxiety and fear

Thomas Contesse

► **To cite this version:**

Thomas Contesse. Involvement of a ventral tegmental area-Amygdala pathway in anxiety and fear. Molecular biology. Université Côte d'Azur, 2022. English. NNT : 2022COAZ6015 . tel-04307313

HAL Id: tel-04307313

<https://theses.hal.science/tel-04307313v1>

Submitted on 26 Nov 2023

HAL is a multi-disciplinary open access archive for the deposit and dissemination of scientific research documents, whether they are published or not. The documents may come from teaching and research institutions in France or abroad, or from public or private research centers.

L'archive ouverte pluridisciplinaire **HAL**, est destinée au dépôt et à la diffusion de documents scientifiques de niveau recherche, publiés ou non, émanant des établissements d'enseignement et de recherche français ou étrangers, des laboratoires publics ou privés.

THÈSE DE DOCTORAT

Implication d'une voie neuronale allant
de l'aire tegmentale ventrale à
l'amygdale dans l'anxiété et la peur

Thomas CONTESSE

Institut de Pharmacologie Moléculaire et Cellulaire (IPMC)

**Présentée en vue de l'obtention
du grade de docteur en SVS**

d'Université Côte d'Azur

Dirigée par : Jacques BARIK,
Sebastian P Fernandez

Soutenu le : 23 septembre 2022

Devant le jury, composé de :

Dr Stéphane MARTIN, Président du jury, Université Côte d'Azur

Dr Frank MEYE, Rapporteur, University Medical Center Utrecht

Dr Marisela MORALES, Rapporteuse, National Institute on Drug Abuse

Dr Gisela VETERE, Examinatrice, Ecole Supérieure de Physique et de
Chimie Industrielles

Dr Jacques BARIK, Directeur de thèse, Université Côte d'Azur

Dr Sebastian P FERNANDEZ, Directeur de thèse, Université Côte d'Azur

Implication d'une voie neuronale allant de l'aire tegmentale ventrale à l'amygdale dans l'anxiété et la peur

Jury :

Président du jury

Dr. Stéphane MARTIN, Directeur de Recherche CNRS, Université Côte d'Azur

Rapporteurs

Dr. Frank MEYE, Professeur, University Medical Center Utrecht

Dr. Marisela MORALES, Directrice de Recherche, National Institute on Drug Abuse

Examineur

Dr. Gisela VETERE, Professeure, Ecole Supérieure de Physique et de Chimie Industrielles

Directeurs de thèse

Dr. Jacques BARIK, Maitre de Conférences, Université Côte d'Azur

Dr. Sebastian P FERNANDEZ, Chargé de Recherche CNRS, Université Côte d'Azur

Involvement of a ventral tegmental area-Amygdala pathway in anxiety and fear

Committee:

President of committee

Dr. Stéphane MARTIN, Group Leader, Côte d'Azur University

Reviewers

Dr. Frank MEYE, Assistant Professor, University Medical Center Utrecht

Dr. Marisela MORALES, Research Group Leader, National Institute on Drug Abuse

Examiner

Dr. Gisela VETERE, Professor, Ecole Supérieure de Physique et de Chimie Industrielles

Thesis supervisors

Dr. Jacques BARIK, Associate Professor, Côte d'Azur University

Dr. Sebastian P FERNANDEZ, Researcher, Côte d'Azur University

1. Abstract and keywords

Involvement of a ventral tegmental area-Amygdala pathway in anxiety and fear

Mental disorders are the leading cause of disability-adjusted life years worldwide. Traumatic experiences and social stress promote the onset of mental disorders including post-traumatic stress disorders (PTSD) and anxiety disorders. A lack of understanding in the etiology of these disorders have led current therapies to aim at treating symptoms rather than the underlying dysfunctions. Hence, a major clinical challenge is to unravel how individuals control their emotions and cope with stressful events. My PhD project addresses the fundamental mechanisms that underpin mental disorders where individuals cannot cope with stressful events leading to excessive fear and anxiety. While the ventral tegmental area (VTA) is a heterogeneous brain structure well-studied for its function in reward processing, this brain region also plays a role in signaling negative valence. Indeed, subpopulations of VTA neurons respond to aversive stimuli. This functional divergence could arise from the unique properties in distinct target-specific cell populations within the VTA. However, our understanding of the inputs and outputs of the VTA that could contribute to the onset of exacerbated anxiety and fear responses is currently very limited.

The central hypothesis of my PhD project is that VTA projection neurons are significant modulators of the main center of anxiety and fear: the amygdala. My project is designed to model and study these defensive behaviors in mice. Hence, my thesis addresses two distinct but overlapping aims:

(i) Dissecting VTA glutamatergic projections to the amygdala and their contribution to adaptive and pathological anxiety.

(ii) Assessing the inputs and outputs of VTA projection neurons regulating fear responses.

For my first aim, I studied the distribution pattern of VTA glutamatergic neurons and their axonal innervation of the amygdala through histological studies. My results are consistent with a growing body of evidence depicting the VTA as a structure comprised of well-compartmentalized cell populations with different functional roles. Secondly, relying upon electrophysiological tools and the use of the chronic social defeat (CSD) paradigm to induce anxiety disorders, I found alterations of both presynaptic and post-synaptic plasticity in VTA glutamatergic neurons projecting to the amygdala. This suggests a potentiation of the neuronal transmission for these efferences to the amygdala paralleled with the appearance of anxiety following CSD. Causality was shown using optogenetic tools to chronically activate these projecting neurons. Indeed, this modulation was sufficient to increase anxiety levels and induce similar change in synaptic plasticity as in CSD. Hence, this first aim strongly suggests a role of this neuronal projection in anxiety disorders.

My second aim was based upon the discovery that the laterodorsal tegmentum contribute to fear responses, namely freezing, through efferences to the VTA. I focused on unravelling the connectivity of the VTA with fear centers, and dissecting the contribution of individual cell-types to this newly discovered role. Using chemogenetic tools, I showed that activation of VTA-amygdala pathway is necessary for the manifestation of unconditioned freezing upon electric foot shock exposure. In contrast to my first aim, I showed in this second axis that VTA GABAergic projecting neurons to the amygdala, but not glutamatergic neither dopaminergic cells, are responsible for this fear response.

Overall, my thesis work brings new insights into the interconnectivity of two salience centers in the brain, namely the VTA and the amygdala. Moreover, my results suggest that stress challenges on this brain connections contribute to maladaptive anxiety. I propose that future circuit-based therapies could be targeted at the VTA-amygdala pathway to alleviates anxiety symptoms.

Keywords: VTA, Amygdala, LDTg, Stress, Anxiety, Fear

Implication d'une voie neuronale allant de l'aire tegmentale ventrale à l'amygdale dans l'anxiété et la peur

Les troubles mentaux sont la principale cause d'handicap au monde (OMS). Les expériences traumatiques et le stress social favorisent le développement des troubles mentaux tels que les troubles du stress post-traumatique et les troubles anxieux. Le manque de connaissance sur l'étiologie de ces troubles a conduit à ce que les thérapies ciblent les symptômes plutôt que les causes sous-jacentes de ces troubles. Ainsi, un enjeu clinique majeur est de comprendre comment les individus contrôlent leurs émotions et gèrent les situations stressantes.

Mon projet de thèse vise à étudier les mécanismes fondamentaux régulant les troubles mentaux où les individus sont submergés par le stress, tel que les désordres de l'anxiété et de la peur. L'ATV est une structure hétérogène connue pour son rôle dans la sensation de plaisir mais aussi pour son implication dans la valence négative où certaines de ses sous-populations neuronales sont activées par des stimuli aversifs. Cette diversité fonctionnelle pourrait être liée aux différentes sous-populations neuronales de l'ATV ainsi qu'à leurs différentes connections afférentes et efférentes. Néanmoins, l'interaction entre l'ATV et les structures régulant les comportements défensifs associés à l'anxiété et la peur reste mal compris.

L'hypothèse de ma thèse place l'ATV comme un important modulateur de l'activité de l'amygdale pouvant ainsi réguler l'anxiété et la peur. Mon projet est organisé sur l'utilisation d'un modèle de souris d'anxiété et de peur pour répondre à des objectifs distincts mais entrecroisés :

- Disséquer les projections glutamatergiques de l'ATV vers l'amygdale ainsi que leur contribution dans l'anxiété adaptative et pathologique
- Déterminer les afférences et efférences neuronales de l'ATV régulant la réponse de peur

J'ai complété mon premier objectif par des approches histologiques en cartographiant la distribution des neurones glutamatergiques de l'ATV et leurs innervations de l'amygdale. Ces résultats sont en accord avec une accumulation de preuves indiquant que l'ATV est une structure composée de populations neuronales compartimentalisées selon leurs fonctions.

A l'aide de techniques d'électrophysiologie et du modèle de défaite sociale chronique (DSC) afin d'induire des troubles anxieux de longue durée, nous avons trouvé des altérations de la plasticité pré- et post-synaptique suggérant une potentialisation de la transmission neuronale glutamatergique entre l'ATV et l'amygdale suite à un DSC. Par la suite, j'ai induit une activation chronique des projections glutamatergiques de l'ATV allant à l'amygdale via des techniques d'optogénétiques in vivo.

Cette modulation est suffisante pour augmenter l'anxiété et causer des changements de plasticité synaptique similaires à ceux retrouvés durant le DSC. Ainsi, cet axe de ma thèse suggère fortement un rôle de cette projections neuronale dans l'induction des troubles anxieux.

Mon second objectif est basé sur la découverte d'une régulation de la peur par des efférences du tegmentum latérodorsal allant à l'ATV. J'ai étudié ici la connectivité de l'ATV avec plusieurs centres de la peur où j'ai déterminé le type cellulaire et les connections responsables de cette régulation. Une modulation des projections de l'ATV allant à l'amygdale a été suffisantes pour altérer l'induction contextuelle de la peur. De plus, l'inhibition des projections GABAergiques de l'ATV vers l'amygdale ont réduit la réponse contextuelle de peur. Ainsi, le second axe de ma thèse a révélé le rôle des neurones GABAergiques de l'ATV projetant à l'amygdale dans l'induction de la peur.

En conclusion, mes travaux mettent en évidence la connectivité entre deux centres cérébraux de la saillance émotionnelle, l'ATV et l'amygdale. De plus, mon étude suggère que les effets du stress sur ces connections pourrait contribuer aux troubles anxieux. De future thérapies pourraient cibler le réseau neuronal ATV-Amygdale afin de soulager les symptômes des troubles anxieux.

Mots-clés : **ATV, Amygdale, LDTg, Stress, Anxiété, Peur**

II. Acknowledgements / Remerciements

I would like first and foremost to thank my two PhD supervisors Jacques BARIK and Sebastian P FERNANDEZ. I have the impression of having joined the lab not so long ago during my master, yet nearly five years have already passed. I cannot tell you how much your supervision was appreciated, you were always there for give me feedbacks and advice but also to check up on me to make sure everything was going well. I don't think it is common to have supervisors that keep a tab on you to make sure you get enough holidays for you to enjoy your life and your PhD. You've also both done a lot to ensure a good future in science for me by providing me with the opportunity to involve myself in other projects. All these reasons are why I have always been and will remain grateful to you. For everything you've done for me, I cannot thank you enough.

I would like to thanks next the team who I have worked with for quite a few years now. Loic BROUSSOT who has been a shadow supervisor of sort during my master internship and two years and a half of my PhD. You've always been there to help me and give me advice when I was crawling under work. You've also been a good friend during my PhD with whom I shared a lot of funny discussion at the labs and to make it a brighter place for me. Léa ROYON, your arrival to the lab for a master internship made my second year of PhD far better. You allowed my repetitive experiments to be far less boring during this second year by providing an interest in my work but also through your friendship. I was and am glad that you pursued with a PhD in our team. You are a good friend and co-worker that always supported me during this last very complicated year. For that, know that you will always have my support and from the bottom of my heart, thank you. Sebastien MORENO, even though you were the last to join us, you were not the least. You are always here to try help others and make our lab environment a funnier place. I'm happy for you to have been here for the last year of my PhD. I wish you the best for your future work and will always gladly assist you if I can provide you with some help. Maxime Villet, thank you for always offering help and for always being there to provide us with fun and a friendly presence. Jade DUNOT for being a friend and giving me supports in the worst period of my thesis.

I would like to also thanks the other members of the labs for always providing a listening hear in my project as well as giving me advice for many experiments. A special thanks to Helene MARIE for welcoming me into the team. For Ingrid BETHUS with whom I often discussed surgery procedure and who provided me with great advice allowing me to move forward in my project with less trials and errors. I also want to thanks Paula POUSINHA for always giving me good feedback on my projects and Carine GANDIN for her great gestion of our need in equipment in the lab.

I want to thank my IPMC group of PhD mates, the UTers and the patoublanc. To the UTers, namely Joris Leredde and Guillaume DAZIANO, I will never forget nor be grateful enough for the time I spent with you since my very beginning at the IPMC. I would never ever have had enjoyed so much my PhD without your friendship and the support we provided to one another during difficult times at the lab. I am happy to have witnessed your growth through the years from simple hesitating master student unsure about their future to a fully grown PhD and a technician of godly talents. To the patoublanc, thank you for your friendship and for all the enjoyable lunch breaks we took together. This element made my life at the lab something to look forward to. A special thank to Marie PRONOT, whose drive and cheerfulness helped me through my thesis.

I want to thank also the rest of the IPMC, who enables the IPMC to be a good place to work at.

Enfin, je tiens à remercier ma mère, mon père et mon frère qui m'ont supporté et ont facilité ma vie tout au long de ces quatre années de thèse. Sans votre soutien, garder le cap durant ma thèse aurait été bien plus compliqué. Je vous suis éternellement reconnaissant pour l'oreille attentive et tout le réconfort que vous m'avez apporté durant ces mes années de doctorat.

Table of contents

Introduction	14
I. Anxiety	15
A. Anxiety and stress definition	15
1) Anxiety definition.....	15
2) Stress definition	16
B. The four step mechanisms leading to defensive behaviors.....	18
1) The detection process.....	19
2) The identification step	21
3) The Evaluation process	24
4) Response initiation	25
C. The autonomic and behavioral response	28
1) The autonomic response	28
2) The behavioral response.....	31
D. Anxiety disorders	38
1) What are anxiety disorders?.....	38
2) The genetic and epigenetic of anxiety.....	40
3) Modelling anxiety disorders in mice.....	41
II. The amygdala	45
A. Anatomical organization	45
1) The basolateral group.....	46
2) The cortical-like group	48
3) The centromedial group	48
4) The intercalated cells of the amygdala.....	50
B. Functional role in physiological anxiety.....	50
C. Anxiety disorders and amygdala.....	55
1) The epigenetic scale.....	55
2) The synaptic scale	57
3) The structural scale.....	59
III. The ventral tegmental area.....	61
A. Anatomical organization	62
1) The regional sub-divisions	62
2) The heterogeneity of the VTA.....	65
B. Functional role of VTA neurons	72
1) VTA and valence processing	72
2) Defensive behaviors.....	79
.....	82
OBJECTIVES	82
.....	86
RESULTS	86

Axis 1: VTAgut→BLA pathway in anxiety	87
Axis 2: LDTg→VTA→BLA axis in fear response	116
.....	166
DISCUSSION AND PERSPECTIVES	166
.....	181
Annexes	181
Contributions non-related to the thesis project	182
First contribution	182
Second contribution	183
Third contribution	184
Thesis references table.....	185

Table of figures

- Fig. 1** – Schematic illustration concept of the stress response as defined by Hans Selye (p.18)
- Fig. 2** – Model of Calhoun and Tye of the four steps process leading to defensive behaviors (p.19)
- Fig. 3** – Schematic of the circuitry regulating defensive behaviors including a simplified representation of the different sensory detection pathways (p.20)
- Fig. 4** – Simplified schematic of the hormonal stress response: the SAM and HPA axis (p.28)
- Fig. 5** – Defensive behaviors implemented in rodents depending on the threat distance and escapability (p.32)
- Fig. 6** – Schematic representation of the amygdala subdivisions following the three main groups (p.46)
- Fig. 7** – Simplified schematic summary of afferences and efferences to the three main amygdaloid groups (p.49)
- Fig. 8** – Schematic of the intra-amygdala network regulating anxiety (p.51)
- Fig. 9** – Schematic summary of the functional role of the amygdala in processing anxiety (p.54)
- Fig. 10** – Schematic definition of the VTA and its sub-territories (p.65)
- Fig. 11** – Schematic representation of the distribution of dopamine neurons in the VTA of rodents (p.68)
- Fig. 12** – Schematic representation of glutamatergic neurons distribution in the VTA of rodents (p.69)
- Fig. 13** – Schematic representation of combinatorial neurons distribution in the VTA of rodents for glutamate-dopamine and glutamate-GABA neurons (p.72)
- Fig. 14** – Schematic summary of the afference and efference of the VTA mediating reward-related behaviors (p.76)
- Fig. 15** – Schematic summary of the afference and efference of the VTA mediating aversion-related behaviors (p.78)
- Fig. 16** – Acute optogenetic stimulation of VTA glutamate terminals in the CeA did not change anxiety levels in our study (p.95)
- Fig. 17** – VTA glutamate neurons exhibit enhance activity during aggression by conspecific (p.102)

List of abbreviations

A adrenaline	D1R type 1 dopamine receptor
AB accessory basal nucleus	DA dopamine
ACTH adrenocorticotrophic hormone	DAT dopamine transporter
AHA anterior hypothalamic area	DRD2 dopamine receptor 2
AMPA α -amino-3-hydroxy-5-methyl-4-isoxazolepropionic acid receptor	DREADD designer receptor exclusively activated by designer drug
AP anterior pituitary gland	DRN dorsal raphe nucleus
BA basal nucleus of the amygdala	DSM Diagnostic and Statistical Manual of Mental Disorders
BAOT bed nucleus of the accessory olfactory tract	DVC dorsal vagal complex
BDNF brain-derived neurotrophic factor	EC entorhinal cortex
BF basal forebrain	EPSC excitatory post-synaptic current
BLA basolateral amygdala	GABA/ GABA-A gamma-aminobutyric acid / GABA receptor type A
BMA basomedial amygdala	GAD generalized anxiety disorders
BNST bed nuclei of the stria terminalis	GAD65/67 glutamate decarboxylase 65/67
CALB calbindin	GC glucocorticoids
CamKII calmodulin-dependent protein kinase II	GR glucocorticoids receptor
CCK cholecystokinin	HPA hypothalamic-pituitary-adrenal
CeA central amygdala	vHPC ventral hippocampus
CeL centrolateral amygdala	HT2c serotonin receptor type 2 c
CeM centromedial amygdala	HTR2A serotonin receptor type 2 A
CFC contextual fear conditioning	HYP hypothalamus
CNS central nervous system	IC inferior colliculus
CoA anterior cortical nucleus	ICSS intracranial self-stimulation
CoP posterior cortical nucleus	IF interfascicular nucleus
CPA conditioned place aversion	IL infralimbic PFC
CRF corticotropin-releasing factor	TH-IR TH immunoreactive
CRF1R CRF receptor type 1	ITC intercalated cells
CRH corticotropin-releasing hormone	LA lateral amygdala
CRS chronic restraint stress	LC locus coeruleus
CS conditioned stimulus	

CSD chronic social defeat

LDTg laterodorsal tegmentum

LH lateral hypothalamus

LHb lateral habenula

LPOA lateral preoptic area

LS lateral septum

LTP long-term potentiation

MeA medial amygdala

MOS main olfactory system

MPN medial preoptic nucleus

MPOA medial preoptic area

MR mineralocorticoids receptor

MSN medium spiny neuron

MTDB mouse test defense battery

MTN midline thalamic nuclei

NA noradrenaline

NAc nucleus accumbens

NK1R neurokinin receptor type 1

NLOT nucleus of the lateral olfactory tract

NMDAR N-methyl-D-aspartate receptor

NTS nucleus of the solitary tract

PAG periaqueductal gray

PBN parabrachial nucleus

PBP parabrachial pigmented area

PFC prefrontal cortex

PFR parafasciculus retroflexus area

PKC δ protein kinase C delta type

PL prelimbic PFC

PAC periamygdaloid cortex

PMV/PMD ventral/dorsal preammillary nucleus

PN paranigral nucleus

PTSD post-traumatic stress disorders

PV parvalbumin

PVH paraventricular nucleus of the hypothalamus

RGN retinal ganglion cells

RLi rostral linear nucleus

RMTg rostromedial tegmental nucleus

SAM sympatho-adrenomedullary

SC superior colliculus

SN/SNC/SNL substantia nigra /SN compacta / SN lateral

SOM somatostatin

TH tyrosine hydroxylase

UCMS unpredictable chronic mild stress

US unconditioned stimulus

V1 primary visual cortex

VGAT vesicular GABA transporter

VGLUT1/2/3 vesicular glutamate transporter type 1/2/3

VIP vasoactive intestinal peptide

VMAT2 vesicular monoamine transporter 2

VMH ventromedial hypothalamic nucleus

VP ventral pallidum

VPR vasopressin receptor

VTA ventral tegmental area

VTT tail of the VTA

WAS water avoidance stress

THÈSE DE DOCTORAT

Introduction

Preface :

Before diving in the lengthy context of study surrounding my thesis, I will clarify that several of the axis of my thesis are closely related one to another. Therefore, during my first axis about anxiety, I will remain brief and superficial in terms of details provided surrounding the amygdala and the ventral tegmental area as they will be discussed further in depth in their own axis.

I. Anxiety

A. Anxiety and stress definition

1) Anxiety definition

Anxiety in its popular definition is acknowledged as an emotion characterized by feelings of tension, worried thoughts and physical somatic changes. It is an emotion felt by all animals that thoroughly impact decision making during our daily lives. While anxiety is often viewed simplistically as a negative consequence of stress, this behavior is intended to prevent harm by increasing our awareness toward future threats. Hence, the term anxiety is often misused in modern society to refer to anxiety disorders instead of a normal behavioral response. So, what is a “normal” or “physiological” anxious response? For example, it would be the type of response leading to cautiousness upon discovery of a new environment. A behavior that stays until a clear lack of danger has been established. It helps us increase our survival chance by limiting the risks of emotional or physical harm while still enabling discovery of resources important to our survival such as feeding points, safe places or even partners to fulfill basic social needs. Conversely, anxiety disorders can be simplified as deleterious anxious responses crippling our chances of discovery of the forementioned “resources”. As animals require daily access to these “resources” to thrive, anxiety and their related disorders have been key feature of defensive behaviors. Hence, anxiety and its causes have long been identified and partially characterized. Indeed, from a historical standpoint, anxiety is a term deriving from the Latin “angor” and was already defined during the Greco-Roman era as an illness that affected both body and mind. It was during this era that the basis of cognitive therapies was developed especially with appearance of the stoic movements whose core values of emotional control are still upheld to this day by psychologists. However, before the writing of the Diagnostic and Statistical Manual of Mental Disorders (DSMs), a clear meaning of anxiety was often variable depending on the era and culture.

Indeed, French and several other languages have long distinguished anxiety from anguish. While anxiety referred to a psychological feeling, anguish referred instead to the somatic response to anxiety impacting mainly muscle contractions. This distinction was abolished in the last century with the emergence of the DSMs where newer versions progressively led to a clear association between psychological features and somatic features. This association has been also linked with the progressive characterization of the different subtypes of anxiety, ranging from generalized anxiety disorders (GAD) to specific phobias. In spite of these many subtypes, one may ask, what is the core feature these disorders have in common? Albeit obvious, the feature is the presence of an exacerbated anxious response toward normally a low-threatening cue or even toward a non-threatening cue. Therefore, the careful balance between physiological and pathological anxiety are heavily dependent on the cue or “stressors” that one may have experienced and their outcome. Hence, to understand anxiety and its biological determinants, I will first explore the notion of stress before addressing the question of the brain circuitry governing anxiety.

2) Stress definition

So, what is stress? Like anxiety, stress in its broadest meaning is often associated with a negative connotation. Indeed, when we say stress, most people tend to picture anxiogenic situations such as, performing an interview for a life changing job, sitting down for a conversation about the future of a relationship or watching somebody get hurt. From such definition, one might assume that stress is only a harmful situation. However, defining stress is far more complex than one might surmise, as this term often loosely refers to both: “stressors” or the conditions that are going to dysregulate the homeostasis of an organism; but also refers to the “stress response” meaning the reaction of such organism to stressors in order to bring back a regulated homeostatic state. Hence, stress is tightly linked to the notion of homeostasis. This notion was brought by the physicians Claude Bernard and Walter Cannon, who respectively developed and coined the notion to define the delicate balance upon which animal life relies upon. Homeostasis is the state of internal, physical and chemical conditions maintained for optimal function of organisms. Because of its inherent definition, it is commonly thought that stressors are factors that are “bad” as they can only promote dysregulation of such balance. However, environments are prone to change and the ability of animals to adapt and to resist stressors is key to their survival. Animals therefore needs the ability to move from a stressors-induced unbalanced state also called allostatic state (McEwen & Stellar, 1993) to a balanced homeostatic state. The amount of efforts required to reach a homeostatic state (also called allostatic load) is defining where stress is beneficial or detrimental to the animal. Indeed, some stressors can be beneficial as long as the stress is mild and short enough not to impede the survival of an organism by draining too

much of its resources. Such cases will help the organism to build resilience against future stronger and longer stressors by promoting a controlled stress response. One example of resilience building can be cited from the story of the king Mithridates VI who ingested small quantities of poisons to help build an immunity from fear of being poisoned. While affecting only very specific metabolically tolerated stressors, his movement of building immunity through exposure to a mild stressor, also known as Mithridatism, is still used to this day for allergen or venom desensitization. This example, albeit not perfect, is one way to reflect the ability of organisms to adapt to stressors and to build resilience should the same stressors be again encountered with higher strength. This ability is key for survival as an organism can lack sufficient resources to return to a homeostatic state following stressors. It is during these times, when the stressor is too strong and exposure is too long that the deleterious effects of the stress response appear. The range of these effects can vary from development of psychiatric disorders such as generalized anxiety disorders (GAD) or major depressive events; to immunity depression. While the notion of homeostasis disruption by stressors has been acknowledged since Claude Bernard, the biological mechanisms of the stress response have not long been studied, starting with the pioneering work of Hans Selye (Selye, 1950).

In his work, Selye described the stress response in three sequential stages, namely, the alarm, the resistance and the exhaustion stages (Fig. 1). He described the alarm stage as the succession of the shock phase, when the body is affected by the stressor without a response yet, followed by the antishock phase, when the body identifies the stressors and start a strong response to it. During this phase occurs a joint induction of the hypothalamic-pituitary-adrenal axis (HPA) with activation of the sympathetic nervous system that leads to the increased released of both glucocorticoids and adrenalin. These hormones promote survival through the induction of a hypervigilant state by preparing the body for the “fight or flight” reaction. Following this stage, the resistance stage is set by the organism to better regulate the response to the stressor. While the goal of the alarm stage is to mobilize all resources to ensure survival with a quick response, the resistance stage goal is to better allocate resources in order to face a stressor that is not transient but maintained. This stage prevents a draining of resources that would otherwise occurs during the alarm stage. Hence, in this stage, activation of the parasympathetic system and HPA axis inhibitory feedback loops helps to lower the resources allocated for a long-term sustainability. Finally, the third and last stage to occurs is either, the exhaustion stage or the recovery stage. While the recovery stage obviously happens if the stressor is overcome, the exhaustion stage conversely happens if it is not. It is during this exhaustion stage that the deleterious effects of the stress response appears, when the stressor leads to psychological and somatic

maladaptation. This stage often occurs when both the period and strength of the stressor experienced are too important during the resistance stage.

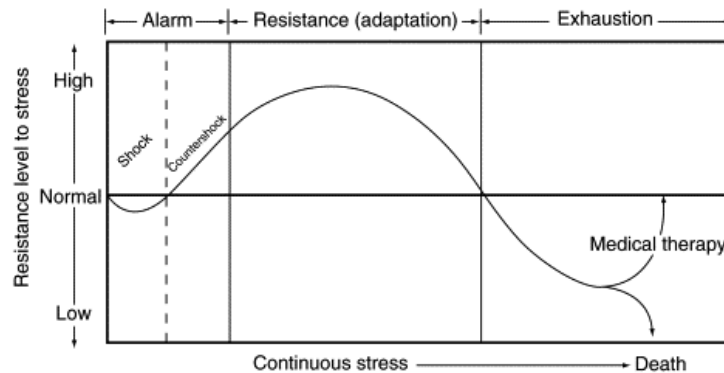


Fig. 1 – Schematic illustration concept of the stress response as defined by Hans Selye. Taken from (Brown & Waslien, 2003).

I have broadly defined here what are stressors and how they can impact the homeostasis of organisms. In the next paragraphs, I will further describe the sequence of events leading to the behavioral manifestation of defensive behaviors, from the detection and evaluation of psychological stressors that can trigger defensive behaviors, to the behavioral and somatic response in itself.

B. The four step mechanisms leading to defensive behaviors

As mentioned above, anxiety and fear are one of the possible consequences of a cascade of events. Following the model of (Calhoun & Tye, 2015), this cascade be divided in four steps from the detection of a stimulus to its identification as threatening to the evaluation of the context to the final response initiation when the somatic and behavioral effects of the anxious response are induced (Fig. 2). Hence, in this chapter, I will describe this four steps model of defensive behavior induction.

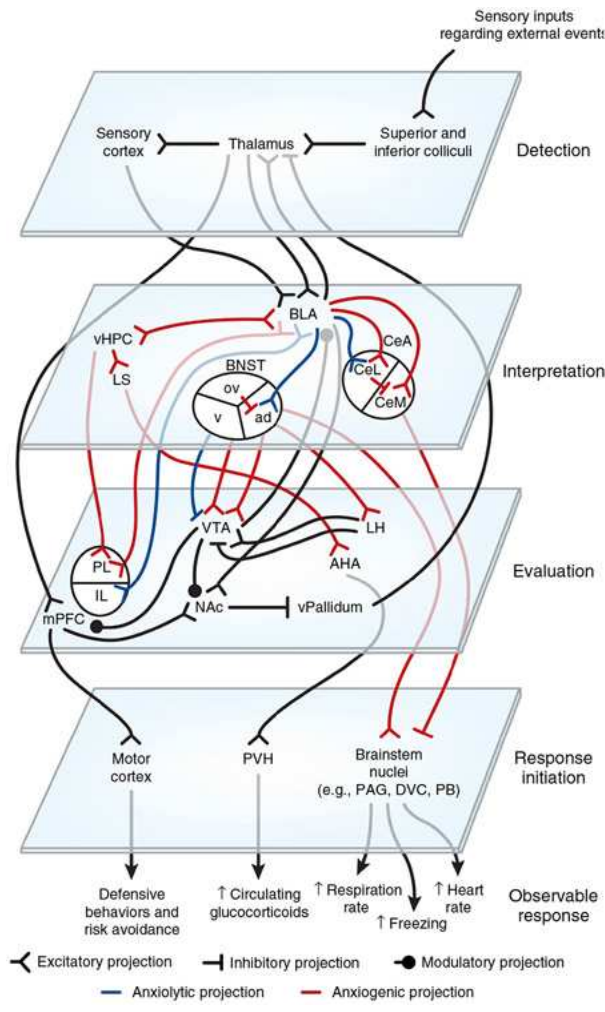


Fig. 2 – Model of Calhoun and Tye of the four steps process leading to defensive behaviors, taken from (Calhoun & Tye, 2015). Abbreviations: ad : anterodorsal BNST. AHA: anterior hypothalamic area. BNST: bed nuclei of the stria terminalis. BLA: basolateral amygdala. CeA: central amygdala. CeL: centrolateral amygdala. CeM : centromedial amygdala. DVC: dorsal vagal complex. IL: infralimbic division of the mPFC. LH: lateral hypothalamus. LS: lateral septum. mPFC : medial prefrontal cortex. NAc : nucleus accumbens. ov: oval nucleus of the BNST. PAG: periaqueductal grey. PB : parabrachial nucleus. PL: prelimbic division of the mPFC. PVH : paraventricular nucleus of the hypothalamus. v: ventral BNST. vHPC: ventral hippocampus. vPallidum: ventral pallidum. VTA: ventral tegmental area

1) The detection process

The first step is threat detection, where environmental cues are perceived. Therefore, this step heavily relies upon the sensory systems to gather visual, auditory, olfactory or even somatosensorial cue that could indicate the presence of a threat (Fig. 3). Hence, many structures are recruited in order to analyze the different types of inputs. For example, identification of visual inputs can be divided in mainly two different pathways involving distinct structures. These pathways diverge in the relays used to carry information from the retina to the amygdala and therefore in their role in threat detection. The first pathway recruited, named the “low-road” involves direct transmission from the retina to the pulvinar nucleus of the thalamus and then to the amygdala. This pathway allows for a coarse but fast transmission of the information to the amygdala for processing and rapid association of the cue. Therefore, this pathway has been shown to be involved in non-conscious threat perception and is crucial to enable a fast response to a threat (Krauzlis et al., 2013; L. Wang et al., 2022). The second

pathway, also called the “high-road”, allows for a higher level of integration and requires to transmit sensory inputs to the visual cortex for better representation of the information. This pathway also ends with information carried to the amygdala, but first the information transit from the retina to the lateral geniculate nucleus of the thalamus. The information is then brought to the visual cortices to increase the accuracy of the inputs provided to the amygdala. Hence, this pathway allows to further increase the level of analysis of the valence of the threat. (Diano et al., 2017; Koller et al., 2019; Pessoa & Adolphs, 2010).

Hence, while visual information is mainly integrated through the superior colliculus, auditory and somatosensorial inputs are integrated by the inferior colliculus and the downstream thalamus (Casseday et al., 2002; Lesicko et al., 2016; Yang et al., 2020).

While the goal of this first step is to gather the most precise information about the cue and its background, the second step require to assess if the cue is harmful, neutral or even positive. Hence, for this step, one of the most important structures for valence detection is required, namely, the amygdala.

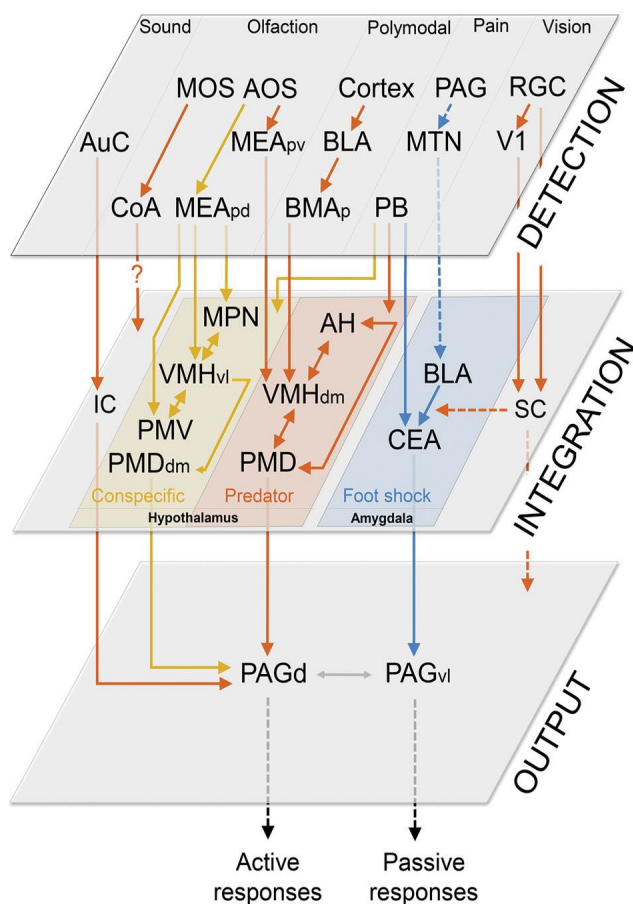


Fig. 3 – Schematic of the circuitry regulating defensive behaviors including a simplified representation of the different sensory detection pathways, taken from (Silva et al., 2016). Abbreviations: AuC: auditory cortex. BLA: basolateral amygdala. BMA: basomedial amygdala. CEA: central amygdala. CoA: cortical amygdala. IC: inferior colliculus. MEA: medial amygdala. MOS: main olfactory system. MPN: medial preoptic nucleus. MTN: midline thalamic nuclei. PAGd; dorsal periaqueductal gray (PAG). PBN: parabrachial nucleus. PMDdm: dorsomedial part of the dorsal premammillary nucleus. PMV: ventral premammillary nucleus. RGN : retinal ganglion cells. SC: superior colliculus. V1: primary visual cortex. vIPAG: ventrolateral part of the PAG. VMH : ventromedial hypothalamic nucleus.

2) The identification step

As previously mentioned, the detection process gathers sensory information to the amygdala in order to identify if the cue is threatening and the defensive strategy to adopt. It is therefore during this step that an emotional value is associated to the sensory inputs provided. For this association, several brain regions assign a valence to the cue. Amongst these structures, the amygdala stands out because of its integration of most sensory inputs (discussed more in depth in Axis 2). Indeed, excitatory inputs from thalamus and sensory cortices from both the low and high roads are integrated by the lateral (LA) and basolateral amygdala (BLA) (AGGLETON & MISHKIN, 1986; McDonald, 1998). These inputs and the ability for the BLA to promote either positive or negative salience through its downstream effectors, place the amygdala as a key structure in the interpretation step. The amygdala involvement in fear and anxiety-related behaviors have long placed this structure as an important mediator for negative valence encoding (for reference, see review of (Pignatelli & Beyeler, 2019)). However, the BLA also has a role in induction of positive valence which was first thought as specific of a projection to the nucleus accumbens (Namburi et al., 2015; Stuber et al., 2011); while more recent studies have shown the BLA to CeA connection also to contribute to positive valence encoding (J. Kim et al., 2017; Hao Li et al., 2022). Overall, those studies have highlighted a greater importance of the genetic profile of BLA cell population for its effects on valence (J. Kim et al., 2016, 2017; Hao Li et al., 2022; O'Neill et al., 2018). Yet, to our knowledge, as these discoveries are quite recent, few studies have been carried out to assess the genetic profile of other amygdala connections modulating assignment of valence. Hence, while the role of the connections from the BLA to CeA were amongst the first identified, other structures receiving projection from BLA are important for regulation of the interpretation process. These structures are the bed nuclei of the stria terminalis (BNST), the ventral hippocampus (vHPC) and the medial prefrontal cortex (mPFC). While all these regions are involved in the interpretation step, it is important to underline that they do not contribute in the same manner to valence assignment. Indeed, while some are important for fast anxious/fear response, others are important for slower but sustained anxious response. The fast anxious response requires BLA inputs to the CeA. Those inputs are known to target several subregions of the CeA with an overall effect resulting in excitation of the principal output nucleus of the amygdala, namely the centromedial amygdala (CeM). The resulting activation of the CeM is translated in the form of activation of numerous brainstem regions important for a quick induction of the somatic and behavioral response to a threat. Those regions and their role in response initiation will be further developed in the following paragraphs (B.3).

While the fast anxious or fear response initiation occurs before a comprehensive analysis of sensory stimuli, this response is necessary for survival for a danger that is too close to the animal.

However, this situation where “the fight or flight response” is paramount for survival is not the only situation where an anxious response is warranted. Indeed, threats can also be sufficiently distant not to enact a fight or flight response but a more adequate strategy for avoidance of the threat. In such case, a prolonged anxious response may be necessary as assessment of the threat must be sustained to dynamically select the most appropriate defensive behavior to ensure safety. These sustained anxious responses still require relay of sensory information to the BLA. However, for a sustained response, different downstream effectors of the BLA are recruited to enable long-term association of negative valence to a cue. Those effectors are the the bed nuclei of the stria terminal (BNST) (Davis et al., 2010), the ventral hippocampus (vHPC) and the medial prefrontal cortex (mPFC) (Calhoun & Tye, 2015). Hence, in the following paragraphs I will quickly describe the place of the vHPC and BNST in the circuitry of defensive behaviors.

The vHPC can trigger defensive behaviors as well as the activation of the hypothalamo-pituitary-adrenal (HPA) axis through a cascade of events (Ada C. Felix-Ortiz et al., 2013). During this cascade, the vHPC will first activate the lateral septum (LS). In turn, the LS will inhibit the anterior hypothalamic area (AHA) and therefore disinhibit the paraventricular nucleus of the hypothalamus (PVH), but also of the periaqueductal gray (PAG) (Anthony et al., 2014). The resulting excitation of the PVH is the first step for the induction of the HPA axis (Smith & Vale, 2006), while the activation of the ventrolateral PAG (vIPAG) will strongly contribute to the induction of the appropriate defensive behavior (Bandler & Shipley, 1994; Farook et al., 2004). Interestingly, while BLA→vHPC projections contribute to the induction of a sustained anxious state, a greater level of modulation of valence assignment is enabled through reciprocal connections from the vHPC to BLA (Herry et al., 2008).

Another downstream effector of the BLA involved in sustained anxiety and the interpretation process is the BNST. Indeed, in their study (Davis et al., 2010), Davis hypothesized that “phasic fear” (called in this thesis fast anxious or fear response) and “sustained fear” (called here sustained anxious response) are mediated through distinct pathway downstream of the BLA. In order to prove his assessment, Davis relied on protocols to measure the startle response of rats upon exposure to a conditioned stimulus that was previously associated with the administration of electric footshocks. Those protocols were carried following the inactivation of the BNST or the CeA with either local infusion of the AMPA receptor antagonist NBQX or with excitotoxic lesions. While inactivation of the CeA and BLA prevented the short-term fear response (more accurately discussed in Axis 2); the different results obtained consistently revealed that inactivation of the BNST or the upstream BLA were sufficient to abrogate the long-term startle response reflecting a lack of anxious response. In conclusion, this study proved the involvement of the BNST in sustained anxious responses while focusing on the lateral part of this region. While it has been argued that BNST mediate anxiety, more

recent studies have also revealed a role of the BNST in promoting fast fear response such as freezing (Goode et al., 2019). However, to fully understand the role of the BNST in valence interpretation and defensive behaviors, a rapid introduction of the functional connectivity of the BNST and its main divisions is required. Overall, the description provided here of the BNST role in the interpretation process is heavily simplified. Indeed, the BNST is comprised of many subregions (Bota et al., 2012) each receiving different inputs and emitting different efferences. The BNST can be divided in up to 18 subregions. These divisions have been associated to an important role in regulating valence with net opposite effects depending on the subregion activated. For example, activation of the oval nucleus subregion (ovBNST) promotes an anxiogenic response while the anterodorsal nucleus division (adBNST) enact the opposite (S. Y. Kim et al., 2013). In this study, Kim S.Y demonstrated that activation of BLA excitatory projections to the adBNST were driving a similar anxiolytic effect compared to direct optogenetic activation of the adBNST. This effect was described as the simultaneous occurrence of:

- A decrease of risk-avoidance through connections to the lateral hypothalamus.
- An increase of respiratory rate through modulation of the parabrachial nucleus.
- Positive valence signaling through the adBNST efferences to the VTA.

Hence, Kim S.Y and col. identified the inputs and outputs driving the anxiolytic effect of the adBNST activity. Furthermore, they proposed that ovBNST anxiogenic effects could be driven through modulation of the CeA or through direct inhibition of the adBNST. However, the inputs driving the activation of the ovBNST response also remain putative (Gungor & Paré, 2016).

This example I provided here highlight the complexity in the BNST connectivity which enables this structure to strongly contribute to valence assignment. While not being the main topic of this thesis, the complexity and the greater role of the BNST in valence can be further explored in the comprehensive review of Lebow (Lebow & Chen, 2016).

Overall, the interpretation process goal is to quickly assign a valence to a cue and to start the induction of both short-term (i.e fear) and longer-term response (i.e anxiety). However, assessing the threat of a stimulus is a process that requires flexibility in order to be able to dynamically review and correct assumptions should they be proven untrue. This step, downstream of the amygdala, the BNST and vHPC is comprised of structures providing feedback for valence assignment and somatic response initiation is called the evaluation process.

3) The Evaluation process

The third step of the anxiety process or evaluation step closely follow interpretation. This step's goal is to provide another level of analysis of the threatening cue in order to either, keep on/promote further the intensity of the anxious response, or to tone down the response should the cue's threat be lower than first assessed. Therefore, this step is heavily reliant upon an integrative system that can guide toward the best course of action. This integrative system is the mPFC, a key regulator of emotional states. Indeed, under non-threatening condition, the mPFC is known to enact a tight feedforward inhibitory control of the amygdala to prevent unreasoned anxious response. This "cortical brake" is known to be dysregulated during post-traumatic stress disorders (PTSD) or even uncontrollable stress (Datta & Arnsten, 2019). It has been proposed that in these pathologies, the effects are mediated through disruption of the tonic inhibition of the amygdala by the mPFC. However, the mPFC does not only contribute to negative valence evaluation. Indeed, two elements make the mPFC an important support in the analysis of the valence of a cue. The first element is the dense innervation of the PFC by sensory and limbic inputs which place the mPFC in the perfect place for improved integration of environmental context. The second element is the functional sub-territorialization of the PFC which can be divided in infralimbic (IL) and prelimbic (PL) PFC capable of mediating profound often opposite response over their target. Indeed, while mPFC prelimbic region has been revealed to be important for evaluation of negative valence, positive valence have also proven to be promoted through mPFC infralimbic connections to the BLA (Anthony A. Grace & Rosenkranz, 2002; Rosenkranz & Grace, 2001). Those connections have also proven to be reciprocal allowing the BLA to provide feedback to the PFC in order to improve assessment of the threat. Hence, the mPFC is capable of enacting a highly resolute modulation of valence assignment through its efferences in the context of fear and anxiety (Likhtik & Paz, 2015). However, this ability of the mPFC to dynamically modulate the outcome of the interpretation step is not only BLA dependant. Indeed, the mPFC provide modulatory inputs to the striatum and more precisely to the nucleus accumbens (NAc). These projections promote reinforcing behavior and are therefore contributing to the ability of the mPFC to induce assignment of a positive valence to a cue (Britt et al., 2012).

While the PFC is an important platform for further analysis of the context of a cue, other structures are important to make the evaluation process a dynamic process.

Indeed, as previously mentioned, the interpretation step and evaluation step overall require flexibility as the ability to change the perception of a cue is key for survival. For instance, an unknown animal scream can be mistakenly viewed as indicator of the proximity of a predator. Such scream would therefore trigger a wasteful anxious response. The ability to turn a previously thought

threatening cue into a non-threatening one upon sufficient exposure to this cue, also called habituation process is therefore key for survival not to waste energy or prevent resources seeking because of a wrong interpretation process (Mackintosh, 1987). Furthermore, the flexibility of the interpretation step is even more important because of the drive for basic needs. Indeed, it is often necessary for animal to proceed to search and gather resources for basic survival. In such scenario, it is important for the brain to possess ability to tone down the anxious response while promoting reward-seeking behaviors in order to promote exploration of environment in spite of threatening cues. Hence, the evaluation step relies strongly upon the reward system with the mesocortico-limbic system including the ventral tegmental area, the NAc and the hypothalamus. Since the VTA is a key region studied in my thesis, its role in reward seeking and valence assignment will be not be described here, but in axis 3.

Overall, the evaluation process is critical for the dynamic process of threat reassessment and can result in two simplistic outcomes. Either the cue was determined as non-threatening enough to warrant initiation of defensive behaviors, or the threat was assessed as real. While the former leads to negative feedback loop preventing further induction of the stress response, the latter results in the activation of efferent structures mediating the behavioral and visceral outcomes seen in defensive behaviors.

4) Response initiation

The fourth and last step of the stress response to a threat is the response initiation. As previously mentioned, the proximity of a threat warrants two different types of response: fear or anxiety. While these responses share some somatic features, they trigger the activation of complex but divergent cascades. For instance, a rapid fear response will lack the effects linked to the induction of the HPA axis that would be seen in sustained anxiety. Furthermore, the cortical conscious processing of a threat needed for complex defensive strategies (e.g. avoidance) takes also too much time to occur during fear. Hence, these differences warrant further explanation on the features of the response initiation seen in fear and anxiety. For these reasons, I will separately describe here the processes for fear and for anxiety.

So, how does the fear response initiate?

As previously mentioned, fast interpretation of a cue is heavily dependent on the amygdala. This structure is critical for fear response as it is placed at the interface between the interpretation system and known mediators of the visceral and behavioral stress response, namely the brainstem nuclei. These nuclei are mainly, but not limited to, the PAG, the parabrachial nucleus (PBN) and the

dorsal vagal complex (DVC). Amongst these nuclei, the DVC activation by the CeA following a threatening cue, triggers an increase of heart-rate (J. E. LeDoux et al., 1988; Viviani et al., 2011). This connection from the amygdala allows a fast-paced response to prepare the body for a potential upcoming “life or death” situation requiring all available resources for an intense muscular activity to fight or flee the threat. While important, the increase of heart-rate is not sufficient to prepare as best as possible against a threat. Hence, the visceral response is also characterized by an increased respiratory-rate to allow further preparation for intense activity. However, this response is not dependent on direct projections from the CeA but of projections from the adBNST to the DVC (S. Y. Kim et al., 2013). Finally, a fast stress response such as fear requires also implementation of the adapted behavior when cortical processing of the context has not yet been established. This behavioral process has long been associated with the PAG and more precisely with its different subregions. Indeed, the PAG can be dissociated in two main subregions involved in the different type of fear response, the ventrolateral (vlPAG) and the dorsal (dPAG) part. The vlPAG has been shown to be involved in freezing, a passive defensive behavior where an animal immobilize itself as to try and limit its own perception by a potential threat (Tovote et al., 2016). More precisely, this behavior can be mediated through the direct and indirect modulation of spinal motor circuits (Koutsikou et al., 2014), through efferences to the lateral reticular nucleus, the inferior olive and by influencing ascending sensorimotor pathway (Cerminara et al., 2009; Koutsikou et al., 2015). While freezing is useful against a close predator not aware of the prey, more active responses are needed in case of an attack attempt by a predator. It is in such situations that the dPAG plays an important role by mediating the “fight or flight” response (Deng et al., 2016). This response is triggered upon the attack by a threat and either results in active escape behaviors (i.e., flight response) most commonly seen in rodents or in the attempted aggression of the threat to deter the predator from further attack. Overall, the brainstem nuclei are at the crossroad between structures involved in valence interpretation and somatic effector, making them a well-placed interface for fear response initiation when speed is required. However, the fear response initiation is far more complex and do not only rely on the brainstem nuclei. Indeed, the visceral response observed during fear is not only characterized by an increase of respiratory and heart-rate, but also by mydriasis, urination, inhibition of sexual arousal, decreased digestion, muscular blood vessel dilatation, increased metabolism, etc. On the short term, these elements are the results of the action of the sympatho-adrenomedullary (SAM) axis, a fast-paced neuroendocrine response that is part of the autonomic response (further explored in the next chapter). Overall, the fear response is initiated upon proximity of a threat, requires fast acting processes and results in a rather raw simplistic behavior such as freezing or flight.

But what happens when the distance with the threat is greater?

In such situation, a process called anxious response initiation helps build a more sustainable response and is also often characterized by more complex defensive behavior such as active avoidance. Here, in this paragraph, I will discuss quickly the anxiety response initiation as this process shares many aspects of the fear response. Like the fear response, anxiety initiation is also dependent on the amygdala but also on its direct connections to the BNST (Davis et al., 2010). More recent studies have highlighted that central amygdala lateral portion (CeL) mediated this sustained anxious response through CRF release to the BNST (Asok et al., 2018). This modulation of the BNST neurons translate onto PVH CRF neurons where they contribute to the induction of the HPA axis (Herman et al., 1994). Although the fear response is dependent on the SAM axis, the anxiety response requires a more sustainable, less resource-draining process which is dependent on the HPA axis and the downstream production and release of glucocorticoids. However, while the induction of the HPA axis by the amygdala and the BNST is quick, the production of the stress hormones is lengthy. Indeed, while the SAM axis release of monoamine (noradrenaline and adrenaline) is almost instantaneous, the HPA axis requires several minutes for release of glucocorticoids with up to 30 minutes for peak of production. Furthermore, the glucocorticoids act as transcription factor following binding on their receptor. Hence, the slow-paced release of stress hormone and their slow but long-term effect are important not for fear responses but for sustained anxious states where a stressor can be present for a large amount of time. Because of the key importance of the SAM and HPA axis, I will further discuss their importance in the next chapter about the autonomic response.

However, before describing the hormonal stress response, it is important to note that the difference between initiation anxiety or fear is not only linked to stress hormones. More precisely, an important divergence between the two is related to the recruitment of cortical processing to establish more complex defensive strategies in anxiety. Indeed, while the fear response needs quickness and rely on a fast but raw interpretation by the amygdala, the anxious response relies strongly on the limbic-motor interface that is the mPFC. As mentioned previously, this structure receives dense sensory inputs from the thalamus and is reciprocally connected to limbic structures important for valence assignment. Because of these inputs and the strong connections of the mPFC to the motor cortex and brainstem nuclei, this structure orchestrates more elaborated responses to stress (Mogenson et al., 1980) that will be explored further in a next chapter.

Overall, both fear and anxiety share similar mechanisms but diverge mainly in the type of behavioral and endocrine response. Hence, in the next chapter, I will discuss about the endocrine response with the related SAM and HPA axis but also about the behavioral response and the different strategies often found in rodent to survive stressors.

C. The autonomic and behavioral response

1) The autonomic response

As previously mentioned, both the fear and the anxious response are processes that are not only dependent on neuronal circuitry. Indeed, these responses are also dependent on endocrine systems, respectively the SAM and HPA axis, where a hormonal response induce a quick or slow-paced mobilization of resource (see Fig. 4 for simplified overview). However, the complexity and interconnections of these two systems have led to the understanding that these systems are not exclusively linked to short or long-term response but participate in both although not with the same amplitude. Hence, in order to better understand the stress response, I will quickly describe each of these systems and discuss their interconnectivity.

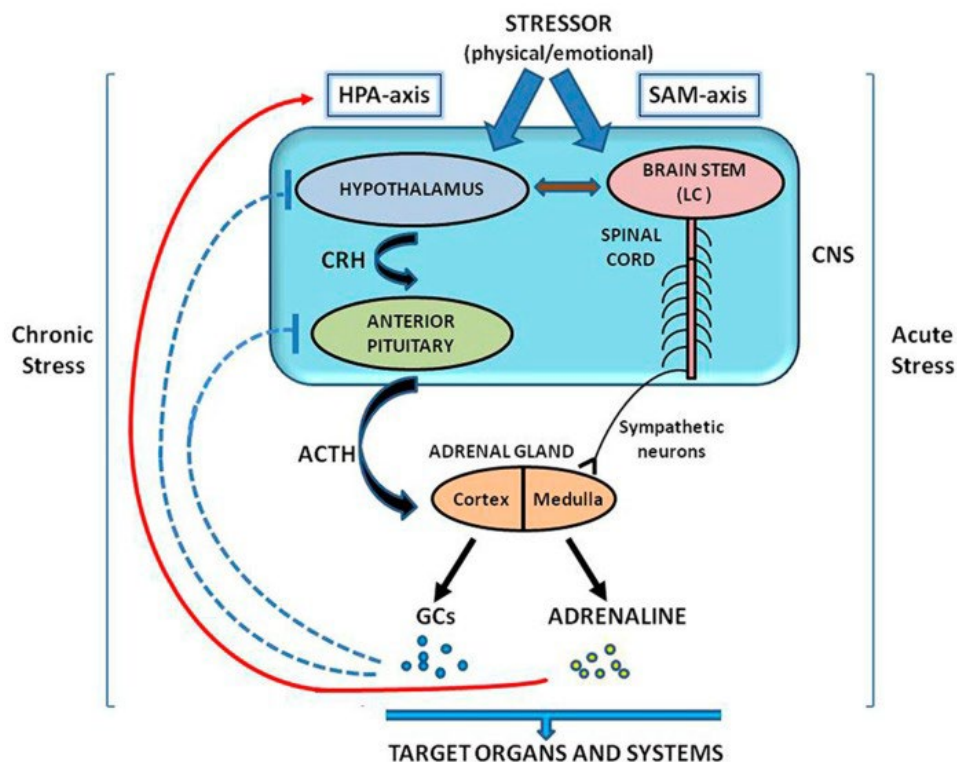


Fig. 4 – Simplified schematic of the hormonal stress response: the SAM and HPA axis, taken from (Baritaki et al., 2019). Of note, while only chronic stress is mentioned, sustained stress is also sufficient to induce the HPA-axis. Abbreviations: ACTH: adrenocorticotrophic hormone. CNS: central nervous system. CRH: corticotropin releasing hormone. GCs: glucocorticoids. HPA: hypothalamic-pituitary-adrenal. LC: locus coeruleus. SAM: sympatho-adrenal-medullary.

The SAM axis is principally known for mediating a fast intense response to stress through release of two types of catecholamines, namely adrenaline (A) and noradrenaline (NA). Indeed, upon highly threatening situation, this release triggers activation of the sympathetic nervous systems leading to a visceral response preparing the body for intense muscular activity (increase of respiratory and heart-rate, muscular blood vessel dilatation, increased metabolism, etc.). So how does this response occur?

Upon the interpretation of a threatening cue, the PVH, locus coeruleus (LC) and part of the medulla triggers the activation of preganglionic sympathetic neurons of the spinal cord. In turn, this activation induces both activation, of post-ganglionic noradrenergic neurons projecting directly to the organs mediating the visceral response (heart, muscle, gut, etc.) but also of the chromaffin cells of the medulla to produce circulating A and NA that will further modulate the visceral response mediated by efferent organs (Ulrich-Lai & Herman, 2009). However, the effect of the catecholamines is not restricted to visceral organs but also to the central nervous system (CNS). Because of the inability of the catecholamines to cross the blood brain barrier, the effect is mediated through projections of the spinal cord neurons to the LC and NTS that in turn target and modulate efferent limbic regions through release of NE (Tank & Wong, 2015). Overall, this effect of the A and NA on both the CNS and visceral organs is important as it enables different types of responses because of the diversity of receptors and their mediated effects (for a good review, see (McCorry, 2007)). Furthermore, the importance of the catecholamine system is underlined by its temporal resolution. Indeed, the post-ganglionic neurons release of NE on its effectors occurs with a resolution of milliseconds, while the secretion of catecholamines by the medulla requires more times but also enables longer action. This difference is explained by the degradation of catecholamines in the bloodstream through hepatic clearance while CNS NE is cleared at the synapse by reuptake transporters (McCorry, 2007) . Overall, this fast “neurotransmission” mediated by NE neurons and the release of circulating E allows for a fast transient response but may not be sufficient as a threat is not always short-lived. It is in such conditions, that a longer and more sustainable anxious response is required. This response is enabled by the HPA axis through the end release of glucocorticoids that I will further discuss here.

The first step of the HPA axis activation is the activation of the hypothalamus PVH corticotrophin release hormone (CRH) neurons. As previously mentioned, following different type of stressors, stress sensitive structures such as the LS, the BNST, the CeA and many others can modulate the activity of the PVH neurons in order to finely regulate the secretion of CRH. The CRH produced by the PVH is released in the portal blood vessel and carried to the corticotrope cells of the anterior pituitary gland (AP). Upon binding to their receptor in the AP, CRH triggers the synthetization and release of the previously called corticotropin, now named adrenocorticotropic hormone (ACTH). ACTH

is secreted through the hypophyseal portal system and is then brought to the zona fasciculata, a cortical layer of the adrenal gland, where it induces the synthesis and release of glucocorticoids (GC) into the bloodstream. Because of their ability to cross the blood brain barrier, the secreted GC are virtually capable of reaching all organs, and their effects are commonly divided in peripheral such as enhanced cardiovascular tone and increased energetic metabolism (Sapolsky et al., 2000) and the cerebral ones that I will further discuss here.

In order to understand the complexity of the neuronal modulation exerted by glucocorticoids, it is important to first address the question of the types of existing receptors, their localization in the brains and their mechanisms of action. The mineralocorticoids (MR) and glucocorticoids (GR) receptor are the two main GC receptor types while several orphan receptors lacking known ligands exists but won't be detailed here. Both MR and GR are nuclear receptors, however the MR expression is restricted to specific areas of the brain (Birmingham et al., 1979; Gomez-Sanchez, 2004), while the GR are ubiquitous. Furthermore, the MR have a high affinity for the GC, while the opposite for the GR is true. Hence, the localization and affinity of GR and MR underline their functional difference during the stress response. Indeed, the HPA axis is not only activated during stress, but produce basal levels of GC following an ultradian rhythm with highest GC levels during wake cycles. While these basal levels of GC lead to a constant level of binding of the MR because of their affinity, only an awakening or stress-related increase of the GC enables binding of the GR (Young et al., 2004). However, the binding of MR in physiological conditions do not indicate the absence of a MR role in modulating the stress response. Indeed, the brain expression of MR is mainly in limbic structures and is known to promotes resilience to stress (ter Heegde et al., 2015), restoration/maintenance of basal HPA axis activity and also to promote stress appraisal (Joëls & de Kloet, 2017). At the same time, GRs also play a role in the stress response by acting on several structures involved in valence processing such the BLA, the mPFC, the vHPC and the VTA (Joëls et al., 2012). Indeed, the GR are known to increase excitability of, the vHPC (Maggio & Segal, 2012), the BLA (Duarci & Paré, 2007) and the mPFC prelimbic region (Yuen et al., 2011). Furthermore, GR activation in the NAc is also necessary to trigger an increase of firing rates of VTA dopaminergic neurons in response to stress (Barik et al., 2013). Because of their properties of nuclear receptor of the family of the transcription factor, the MR and GR enables changes of gene expression and transcription. It is through these changes that long-term effects are mediated on the HPA axis on the actors of the stress response. However, both these receptors do not only mediate long-term effects but are also capable to enact fast action (from seconds to minutes) through non-genomic activation of GR (Timmermans et al., 2019) and MR (Groeneweg et al., 2012) located at the membrane. In spite of the aforementioned "fast" action of the GR and MR, activation of this receptors starts 15min following a stressor with the rise of the GC through activation of the HPA. Hence, because

of its length, the effects of the HPA axis activation are often perceived too late because of the transient nature of the stressors. As the HPA axis activation is linked to mobilization of resources for sustained alertness against a threat and is able to induce long-term changes, its activation can be nefarious if the threat is not present anymore. Hence, the HPA axis is tightly regulated with negative feedback loops provided by the GC on the PVH and the AP preventing the release of CRH and ACTH respectively (Gjerstad et al., 2018). This feedback is particularly important to allow flexibility in the ever-evolving interpretation of threats but also for the circadian and ultradian rhythm for the HPA axis. This flexibility however does not only rely upon this feedback but also on the cross-talk between the HPA and SAM axis. Indeed, the efficiency of the stress response is dependent on the coordinated activation of these two axes. This action is mediated through CRF modulation of the LC neurons and therefore of the SAM axis. CRF neurons inputs to the LC have been identified and include amongst others the CeA, the BNST and the PVH. Because of the excitatory effects of the CRH on the LC and of the place of the PVH in the regulation of the HPA axis, these elements underline the aforementioned crosstalk between the HPA and SAM axis (Valentino & Van Bockstaele, 2008).

Overall, the autonomic response is dependent on the parallel activation of two distinct neuroendocrine axis that act in a coordinated manner to provide the finest regulation of the visceral and behavioral response possible to stressors. While I have discussed here about the visceral effects, the effect of the endocrine response on behavior are wide because of the important expression of GR and MR in the brain. However, aside for the aforementioned examples of limbic structures, I will not delve deeper into other brain regions and mechanisms that the endocrine response may modulates. Instead, I will rather focus on the second joint element of the response initiation, namely, the defensive behaviors. Therefore, I will discuss in the next chapter the wide range of defensive behaviors enacted at the end of the stress response cascade.

2) The behavioral response

In the previous chapters, I discussed what is a stressor, how it is perceived and the physiological response triggered by it. However, the most important part of the response to a stressor is the behavioral strategies implemented. Indeed, the physiological response sole goal is to prepare the body for performing the physical activity needed during defensive behaviors. So, what are the defensive behavioral response that can be triggered against a threat? While I previously mentioned freezing, avoidance or even escape, the extent of defensive behaviors is greater than these mechanisms. Indeed, as the stressors can range from simple sound to complex social cues, a great number of defensive behaviors can be observed. Because of my interest in this thesis in the modulation of defensive

behaviors by the VTA and BLA, it is paramount to explain what are the different types of defensive behaviors and how can we measure them. Therefore, I will discuss in the next chapter, the wide range of defensive behaviors enacted at the end of the stress response cascade. Furthermore, as I used during my thesis a mouse animal model, the studies cited in the next paragraphs will be mainly based on the use of rodents.

a. The panel of defensive behaviors

I previously divided defensive behaviors in two categories: fear- and anxiety-related. This separation underlines how distance to the stressor is a critical parameter regulating the type of response warranted. Indeed, while fear is a present-based emotion based upon the threatening proximity of a stressor, anxiety is directed toward the future and rely upon anticipatory strategies linked to distant threat that could become dangerous. However, distance is not the only parameter regulating the choice a defensive behavior to implement. Indeed, escapable/inescapability toward a threat is another parameter upon which the choice of defensive behaviors is influenced (Carli & Farabollini, 2022) (Fig. 5).

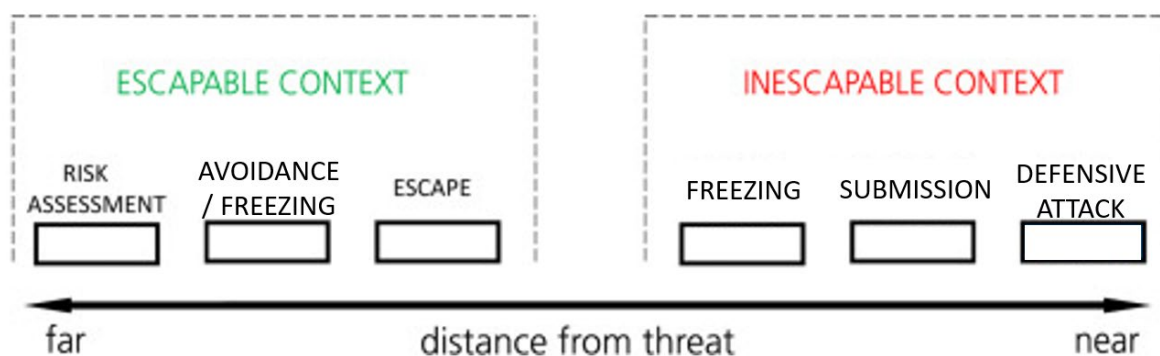


Fig. 5 – Defensive behaviors implemented in rodents depending on the threat distance and escapability, adapted from (Carli & Farabollini, 2022). Of note, submission is found in threat mediated by a conspecific while other mentioned defensive behavior can be found against both conspecific and predators.

In this section, I will explain the range of defensive behaviors in relationship to the distance of the threat, starting from the closest to the farthest. Hence, I will start with fear-related defensive behaviors. Such response, when adaptative, often occurs in the with the attack of a predator. In this situation, the escapability of the situation will lead to several different behaviors:

- Defensive fighting: If the threat is too close and escape is not possible, defensive fighting becomes the only appropriate answer do deter further attack and provide a needed respite to find an escape road. This behavior expression is different between species but retains some key features. It is comprised of two successive phases: threat then attack. While the threat

phase goal is based on appearing more menacing, the attack phase is to harm enough the predator to neutralize the predator, at least temporarily, by forcing him into a partial retreat. Hence, the first threat phase is often associated with a change of posture to appear bigger and more dangerous with an upright posture in mice (R. J. Blanchard et al., 1998). While this change most often occurs against conspecific attack, it remains an observable behavior against an inescapable predator. This upright posture is also often associated with sonic vocalization where animal emit a shriek to appear dangerous. It is also occurring with tail-rattling, where rodents slap their tails on the ground to emit booming noise in order to appear threatening. This behavior, albeit used in defensive postures is mostly found during aggressive behavior against conspecific (Godar et al., 2011; Kršiak et al., 1981). Together, these elements contribute to the first phase of the defensive fighting. Following the failure of this phase occurs the second step of attack. As mentioned before, the goal of this phase is to harm or neutralize the threat to provide a mean to escape. In rodent, this phase is characterized by more aggressive behavior divided in two types of observable attacks: lunge-and-bite vs jump attacks (R. J. Blanchard et al., 1998). Lunge-and-bite attacks are characterized by a rapid thrust or lunge of the animal followed by a bite directed at protruding part of the predator. During this attack, the rodent often uses his forepaws to push back from the predator once a bite has been delivered, hence helping its escape. While lunge-and-bite is a straightforward strategy, jump attacks relies on surprise as deterrent against a predator.

- Tonic immobility: this behavior occurs when a severe unescapable threat occurs, when an animal is cornered by a predator for instance. While sharing its immobility feature, it is important to note that this behavior is different from freezing. Indeed, this behavior's goal is often called as "playing dead" and is linked to hypotension and unresponsiveness while freezing is a more active behavior with different features (discussed further in the next paragraphs). Hence, tonic immobility relies on the hope that the predator will lose its interest in its prey. While this behavior can sometimes be useful, it is not a commonly found behavior and seems to be restricted to few rodent species.
- Submission: gregarious species are often motivated by the search of social interaction. However, such interactions are not always rewarding due to the existence of hierarchies between same-sex conspecific individuals. Hence, stressors can also be not a predator but a social one. In these situations, a classic response observed when the threat is not escapable is submission. This behavior widely differs following the species studied. In rodents, it can be characterized by three features: a flight response to signal defeat and avoid further hurt by

conspecific; a flaccid “freezing-like” response where the animal enables further interaction of the conspecific while not moving in order not to be perceived as challenging for domination; and finally, a subordinate posture, where the animal lay on the side with its flank exposed and its head reared to signal defeat and submission. Overall, these behaviors are important to prevent hurt by dominant conspecific and for groups interactions to prevent unrestricted fighting that could lead to injuries or death.

- Active escape: when a threat is close but escape roads are available, active escape provides a better alternative to a direct confrontation with a predator that is often stronger than its prey. This process, also known as flight response, is induced in order to distance the predator and found cover from further threat. Active escape is triggered upon the approach of a predator, when discovery by the predator is assumed. However, the pursuit by a predator is often a dynamic process with flight bouts intersped with moment of hiding or freezing.
- Freezing: While tight proximity to a threat leads to the aforementioned fight or flight response, further distance without potential to escape the threat induces freezing. Freezing is a universal response most commonly found in rodent where the animal presents sustained muscular tone to maintain apparent immobility. Hence, this behavior is induced when discovery is not yet ensured and helps the animal to remain undetected while plotting the best strategy for survival. For these reasons, this behavior is quickly induced and allows better threat assessment (D. C. Blanchard et al., 2011). This state is not only characterized by immobility however, but also by decreased heart-rate (i.e., Bradycardia). Freezing and bradycardia are respectively mediated by the activation of CeA projection to the PAG and to the dorsal vagal complex (Viviani et al., 2011). Furthermore, CeA projection to the PAG mediate immobility by downstream regulation of the medullar projections to the spinal cord motor neurons. Because of the dynamic aspect of defensive behaviors, freezing can be found in several situations. Indeed, freezing can be induced before, but also after flight following confrontation with a threat, when the threat is more distant. Hence, as freezing often occurs between flight response bouts, several studies have postulated that such behaviors are important in decision-making of the next active defensive behavior but the mechanisms remains to be explored (Klaassen et al., 2021).

- Avoidance: When a threat is distant and escapable, avoidance becomes the most common strategy. This behavior is akin to the flight response but does not occur with the same urgency. Hence, this behavior is simply characterized by moving away from the threatening stimulus while maintaining vigilant monitoring of the threat.

- Risk-assessment: when a stimulus is distant, risk-assessment allows for better appraisal of the valence of the cue. This behavior, while varying between species, is often characterized by the parallel induction or succession of several behaviors (D. C. Blanchard et al., 2003):
 - postural freezing: where an animal shifts its attention toward a cue by orienting itself toward the cue and stay immobile to increase discretion gather information about the stimulus.
 - Rearing: often found in rodents, where the animal stands up on its hind paws to gain better visibility of the cue.
 - Sniffing: where an animal uses its sense of smell to try and recognize the odor of a predator.
 - Stretching: when an animal is hiding and approach a stimulus while remaining close to its safety place. During this behavior, the animal stretches his body toward the stimulus to get slightly closer and gather more information.
 - Approach-avoidance: where an animal is dynamically moving toward and away from the stimulus several times to gather more and more information while often retreating to a safer place.

Overall, risk-assessment mainly occurs as a mechanism to promote vigilant exploration of foreign environments.

As evidenced here, both fear (from fighting to freezing) and anxiety (avoidance and risk-assessment) related response are comprised of several type of behavioral outputs. I will therefore quickly describe in the next paragraph the main behavioral test used to measure this response and their principles.

b. The test model for assessment of defensive behaviors

Defensive behaviors are associated with an autonomic response and a behavioral response. Here, I will focus on the test that can be used to measure defensive behaviors in the same model used during my thesis: mice. However, I will not go into the details of the test that can be carried to measure the autonomic response as the focus of my thesis was on the behavioral response. I will only state that

some physiological parameters such as heart and respiratory rates and biochemical markers such as circulating GC can be measured as they are changed during defensive behaviors.

Because of their fundamental difference, fear and anxiety measuring tests are based upon different principles. Indeed, many of the behavioral tests for mice to measure fear rely on the contextual association of a cue to a painful stimulus. However, while anxiety tests can also rely on the use of painful stimuli, the most commonly used test are ethologically relevant with the use of a non-painful aversive stimuli.

Here I will quickly describe available tests to measure the aforementioned defensive behaviors. The defensive fighting is a response difficult to assess as fight is a “last-resort” behavior exhibited only against an unescapable predator. Therefore, only the Mouse Test Defense Battery (MTDB) (D. C. Blanchard et al., 2003) is capable to enable recording of this defensive response by mice. In this test, mice are placed in a straight alley with an anesthetized rat following them. Upon reaching the end of the alley, the cornered test mouse may then exhibit such defensive behavior. Because of the material required, assessing defensive fight in mice remain complex and is rarely seen in the literature.

Submission is a response toward a dominant conspecific. As such, it can only be triggered with test relying on the interaction with other mice. Indeed, protocols like social defeat, where a mouse is attacked by a dominant conspecific can be used to measure submissive behaviors. However, such a protocol is highly stressful and can lead to injury of test mouse if not properly controlled. The tube test can also be used to measure submission. In this test, a mouse is placed against a conspecific in a tube, where moving forward only is possible. Hence, the submissive mouse will back away in this test. The simplicity of this test however is a great limit to the measure of submission as change of posture or flight response is not possible in this test.

Active escape is a key feature of the fear/anxious response. In order to record escape behavior, several techniques exist and can be divided in two main categories. The first category relies on conditioning with a learning phase where exposure to noxious stimuli (unconditioned stimulus, US) is paired with a specific context (conditioned stimulus, CS). In the second phase, re-exposure to the conditioned stimulus alone is sufficient to trigger flight behavior if an escape road is available. This test includes the active avoidance test where flight is measured after a noxious stimulus has been inflicted in one of the compartments following the US. The second category relies on better ethological paradigm that are more representative of the type of stressors that are encountered by animals. Hence, several tests exist where exposition to an acute non-painful stressor mimics a predator and elicit flight response. Amongst these tests figures the previously mentioned MTDB where a real, albeit

anaesthetized predator is used. Furthermore, the looming test also rely on visual inputs to elicits escape. In this test, the diving attack of an aerial predator is mimicked through the use of an image of a fast-expanding dark disk in the ceiling and the latency of the mice to flee to its nest is measured. Finally, tests relying upon auditory cue can be used to trigger and measure escape behavior. In this tests, flight response of mice can be measured following exposure to a 20 KHz sound alike to the ones emitted by predatory rats (Mongeau et al., 2003), or following a loud noise in the acoustic startle and flight test.

While escape eliciting test rely mainly on noxious or close threatening stimuli, freezing inducing test are based upon either unescapable noxious stimulus or unescapable distant threatening cues. Indeed, the main test used to measure such behavior is the previously mentioned contextual fear-conditioning (CFC) test, where electric footshock (US) are delivered with or without a cue in a specific inescapable context (CS). A strong freezing response is induced immediately after the footshocks or upon re-exposure to the CS alone after a day (necessary for fear memory formation). In a similar fashion, more ethological test exists for measure of freezing. These tests often rely on visual, auditory, or olfactory cues. Exposure to such visually threatening cues can be found in the looming test, where not only escape can be measured but also freezing. In this test, while escape is observed with a cue of a diving predator, freezing can be triggered by mimicking a circling flying predator through the movement of a small dark disk in the ceiling. Auditory-induced freezing can be measured in the looming sound test where mice are subjected to increasingly louder sound in order to mimic the auditory cue of an approaching predator (Z. Li et al., 2021). Finally, exposure to olfactory cues of predators such as fox urine in the form of trimethylthiazoline can be used to trigger freezing in mice (Takahashi et al., 2005). Overall, the diversity freezing-inducing test is a great tool to measure the different types of contexts that can lead to defensive behaviors.

While the mechanisms of freezing are important, threat can often be avoided when distant enough. Hence, several tests have been designed to measure avoidance. Similar to escape or freezing tests, avoidance can also be subdivided in the category of noxious learning test, and more innate ethological tests. The most common noxious learning-based test for avoidance is the passive avoidance test. In this test, mice are exposed to electrical foot shock (US) in a specific context (CS). Following learning, the latency of the mice to go back and explore the CS is measured and reflects the avoidance of a threatening stimulus. The more innate ethological tests often measure the latency and time spent by the mice to explore context associated with the aforementioned sensory cues. However, avoidance can also be measured in an ethological manner in the absence of threatening cues. Indeed, the most commonly used behavioral test to measure anxiety are based on the analysis of avoidance of a neutral albeit unknown environment and do not require specific cues. These tests are based on the exploration

of an environment that is unknown to the animals. Hence, these tests are often subdivided into anxiogenic zones where the animal would be more vulnerable to predator threats due to the lighting conditions and the absence of hiding spots; and more neutral zones where the animal can hide or where exposure to threat is less important. These tests are often found in the literature and consist mainly of the openfield, the zero maze or elevated-plus maze and the dark-light paradigms.

While these tests allow measure of avoidance, they are also used to measure risk-assessment behaviors in order to gain more insight on anxious behaviors. Indeed, the previously mentioned risk-assessment behaviors can be witnessed in such test, where for instance, approach-avoidance and stretching are often seen in the open anxiogenic zones of these tests.

Overall here, I have described what are stressors, how they are processed by the brain, the type of behavioral and peripheral response they trigger, and finally how can we measure this behavioral response in an animal model that shares many similarities to humans. All these processes and their understanding is key to unravel how anxiety is promoted. Therefore, these studies provide the necessary background to understand how dysregulation of brain circuitry can lead to anxiety-disorders. Hence, while I have discussed so far only of the mechanisms of normal, well-regulated defensive behaviors, I will now describe what is known about anxiety disorders, more precisely, how do they dysregulate the peripheral response and the brain control over defensive behaviors and the mouse models to study this disorder.

D. Anxiety disorders

Until now, I have discussed the circuitry of defensive behaviors and the observable response. However, I have focused on normal, non-pathological response while the hope of my thesis research was to identify a new neuronal projection that could play a role in the induction of anxiety disorders. The reason for my study and many others relies on the fact that anxiety disorders are wide and afflict a large part of the population with crippling consequences and a lack of efficiency in treatments. Hence, in this chapter, I will review what are anxiety disorders, how stressors can induce changes in the brain circuitry of anxiety and how it translates into behavioral and peripheral alterations. Finally, I will discuss the available techniques to model anxiety disorders in mice in laboratories.

1) What are anxiety disorders?

Anxiety disorders can be broadly defined as exacerbated anxiety against normally non-anxiogenic cue and/or sustained expectation apprehension. Following the reference diagnostic tool for psychiatric

disorders, the DSM-5 (American Psychiatric Association, 2013), anxiety disorders can be classified in different subtypes:

- separation anxiety disorder: the disorders occur mostly in children. It is characterized by excessive anxiety or distress linked to even temporary separation from an individual with strong emotional attachment (e.g. family or significant other)
- selective mutism: defined by a freezing response leading to an incapacity to speak in a precise context, often found during social situation requiring public speaking.
- specific phobia: intense fear or anticipatory anxiety directed at a cue that present little to no threat.
- social anxiety disorder (social phobia): persistent fear and anticipatory anxiety toward social interaction with unfamiliar person or in a situation where scrutiny by others appears possible.
- panic disorder: characterized by frequent and unexpected panic attack where the individual is overwhelmed by anxiety and fear and often exhibit strong anxiety about the next panic attack occurrence.
- Agoraphobia: fear and anticipatory anxiety of public spaces where panic attack can occur if an escape does not seem possible.
- generalized anxiety disorder: excessive and persistent feeling of anxiety toward everyday events
- substance/medication-induced anxiety disorder: excessive anxiety against mild stressor occurring following withdrawal effect of alcohol or other addictive substance abuse.
- anxiety disorder due to another medical condition: disorders directly caused by a medical condition such as hyperthyroidism.

Other stress-related conditions exist, such as post-traumatic stress disorders, but are no longer considered as a subclass of anxiety disorders but rather have been classified separately with trauma- and stressor-related disorders. Overall, anxiety disorders are the consequences of environmental and genetic factors. While environmental factors, ranging from psychological to physical stressors, have been previously discussed in the first chapter of this thesis, I will further explore in the following chapter how they contribute to the induction of anxiety disorders. As environmental factors effects are tightly linked to dysregulation of gene expression, I will first discuss of the genetic factors contributing to anxiety disorders. However, due to the complexity of the realization of large-scale genetic studies, the influence of genetic risk factors on the onset of anxiety disorders remains elusive. Hence, I will first discuss in the next paragraph what is known about these hereditary risk factors.

2) The genetic and epigenetic of anxiety

So far, several problems have hindered research and prevented the apparition of a clear consensus on the link between genetic and anxiety disorders. Indeed, while meta-analysis studies have suggested the existence of a strong heritability of anxiety disorders due to genetic factors (Hettema et al., 2001), no linkage studies have been carried for generalized anxiety disorder (GAD) but association studies have been yielded interesting results. Indeed, genome-wide association studies have revealed high correlation between GAD and several loci and single-nucleotide polymorphism. However, due to the variability in population studies, results obtained often differ between studies. Nevertheless, this is not the case with candidate-based gene studies, which rely on the analysis of gene that have already been involved in traits related to the stress response. Indeed, these studies have further hinter at the involvement of several systems in anxiety disorders:

- the serotonergic system where, for instance, the polymorphic region (*5-HTTLPR*) *S/S* that leads to a less active serotonin transporter (*SLC6A4*) has been associated with increased GAD chances (J. S. You et al., 2005). Furthermore, alleles resulting in a enhanced activity of the serotonin degrading enzyme, the monoamine oxidase A, have been associated with higher anxiety scores in adolescent (Voltas et al., 2015).
- The catecholaminergic system where a variant linked to lower activity form of the catechol-O-methyltransferase, an enzyme responsible for degrading catecholamines such as dopamine, has been associated with higher anxiety scores in women (Enoch et al., 2003).
- The neurotrophic systems where a polymorphism leading to a lower activity form of the brain-derived neurotrophic factor (BNDF) has associated with increased anxiety scores (Montag et al., 2010).

While the previous studies provide insights on anxiety-related genetic factors, variability in these studies highlight the need for further replication and direct study of their causal links to anxiety before a consensus can be reached (Gottschalk & Domschke, 2017). While my thesis is not including the genetic determinants of anxiety, it is important to underline the existence of such risk factors but also to understand that heredity might not be the only cause for the development of stress-related disorders. Indeed, for many years now, anxiety disorders have been tightly associated with environmental factors. More precisely, high intensity and/or repetition of stressors are the main risk factors for the induction of anxiety disorders. Indeed, even genetic risk factors are often not alone responsible for such disorders but instead induce greater vulnerability to the environmental factors responsible for the development of anxiety disorders. It is important to note that these two factors are reciprocally intertwined. On one side, genetic factors can promote vulnerability or resilience to

environmental factors. On the other side, environmental factors mediate their troublesome effects through long-term regulatory modulation of gene expression. Chronic stressors are known to regulate genetic expression through epigenetics mechanisms that modulate compaction of DNA and therefore alter its accessibility for transcription. These mechanisms are (Nieto et al., 2016) :

- DNA methylation: where a methyl group is added mainly on cytosine which trigger repression of genetic expression when occurs on CpGs islands located in promoter regions close to the transcription start (Jaenisch & Bird, 2003).
- Chromatin remodeling: where post-translational modifications targeting histones enable change of state of accessibility of the chromatin, from “open” where genes are accessible for transcription factor, to “close” where they are not. Many post-translational modifications are possible, such as and not limited to acetylation, methylation and phosphorylation. For more details, see (Kouzarides, 2007).
- Non-coding RNAs: where microRNAs (miRNAs) can bind to messenger RNAs to prevent their translation. While only recent and scarcely studied in the context of anxiety miRNAs are known to control many processes that could contribute to the induction of long-term adaptation in response to chronic stressors. Indeed, miRNA can modulate synaptic plasticity through regulation of dendritic spine development (Schratt et al., 2006), but also CRH signaling, synaptic vesicle fusion, excitatory post-synaptic transmission and other processes that could impact the induction of anxiety disorders (Murphy & Singewald, 2019; Narayanan & Schratt, 2020).

(for a more comprehensive review of epigenetic change in anxiety disorders, see (Persaud & Cates, 2022)).

So far, I have discussed what are anxiety disorders and the mechanisms through which they are induced, it is important to address the issue of the models that can be used to study these pathologies in laboratory.

3) Modelling anxiety disorders in mice

The main goal of studying the mechanisms underlying anxiety disorders is to gain enough insight in order to develop treatments to target the causes of the pathology rather than targeting the symptoms. Hence, as the biology of anxiety disorders is incredibly complex, the most accurate high-end tools such as optogenetics or live in-vivo calcium imaging are key to parse the circuitry anxiety and its molecular determinants. Their invasiveness has restricted the use of these tools to non-human

animals and highlight the need of animal models to study anxiety and its disorders. However, because of the evolutive differences between humans and other species, it is important to understand the relevance of the animal models studied. While many models exist, one if not the most common species used is the mouse. Several reasons guide this choice. First and foremost, is the development of molecular technologies enabling gene editing for which mice are well suited. It is these technologies that enables the use of the aforementioned high-end tools in animals. Secondly, an important similarity is found in neural structure organization and connectivity between humans and mammals including mice. These similarities increase the relevance of studies on neural circuitry underlying behaviors. It is however to be noted that mice do not have a cerebral cortex as developed as in humans and therefore do not provide a good model for the study of higher cognition and cannot emulate the full complexity of psychiatric disorders (Cryan & Holmes, 2005). The last reasons for the use of mice in the study of anxiety is practical. It is, the rapid and high reproduction rate and short length needed to reach adulthood. Overall, I provided here the reason for the use of mice as our referential animal model to study behaviors. However, to study anxiety disorders several models can be used to mimic in mice several of the human symptoms. Before describing these models, it is important to first detail the criterion used to assess their translational relevance. Models are mainly evaluated on the three following criterions:

- Predictive validity: this is the measure if a model's ability to mimic the human pathology unknown mechanisms. In order to have good predictive validity, pharmacological treatments used to treat human patients must have similar effects on animal model of the pathology as it indicates a great likelihood of sharing the elusive mechanisms of the pathology.
- Face validity: this is defined as the proximity between the animal model and the human phenotype of the pathology. This is one of the main limits of the mice models of psychological disorders as many symptoms can be emulated but unlike in humans, feelings and thoughts cannot be assessed.
- Construct validity: this is how well the etiology of the pathology is similar between humans and the animal model. For stress-related disorders, this validity refers to the ability for the same types of stressors to trigger the expected similar symptoms in Humans and the animal model.

Overall, several models exist to induce symptoms of anxiety disorders in animals. However, facing all three previous criterions can be difficult for these models. Here, I will not describe the genetic model as their contribution to study of anxiety substrate is important but an important limit exist. This limit is that genetic modification may have developmental effect detrimental to the understanding of circuitry and molecular mechanisms of anxiety. Therefore, I will focus here on models to study anxiety disorders relying on the use of chronic stressors. These stressors most commonly come under the form of chronic nociceptive stimuli and/or chronic psychological stimuli. However, painful stressors do not necessary reach the same levels of validity as would psychological stressors. The reason for this limit is linked to the low construct validity of model relying on painful stressors. Indeed, most of these models rely on the use of electric footshocks, the injections of pain-inducing substances or even exposure to cold. While these painful stimuli can sometimes be experienced in a non-artificial manner, the likelihood for them to occurs outside a laboratory setting on a chronic frequency is incredibly low. However, it is to be noted that chronic pain is often associated with anxiety disorders (Zhuo, 2016). While models of chronic noxious stress may use different type of stimuli compared to the chronic pain-afflicted patient, these models remain nonetheless relevant in the study of this association pain-anxiety. Psychological stressors are perhaps the most frequent stressors leading to anxiety disorders. The most used models for anxiety disorders are therefore relying on the use of chronic psychological stressors:

- The chronic social defeat stress (CSD) model: this model relies on exposure to an important social stressor in the form of repeated aggression by a foreign conspecific. In this protocol, mice are subjected to aggression by placing them inside the home cage of foreign mice selected for their heavily territorial and aggressive behaviour. In doing so, the mice become the intruder toward a stronger conspecific. This test has a great construct validity as recurrent social infighting, whether at work or at home, is a frequent phenomenon in our society. Furthermore, this model is also ethological because of the natural aspect of the stressor as this type of aggression is frequent in animals where social hierarchy and dominance are often contested by individual during the research of mates. Because of the repeated nature of the stressor, the CSD model is a good model to induce the development of anxiety disorders as well as depressive phenotype. Furthermore, generalized anxiety and often found comorbidities (such as weight changes, decreased libido or sleep cycle alterations) are replicated in this model, relating it to a strong face validity. However, this model is not perfect as the predictive validity of the CSD model for depression but not for anxiety disorders has been clearly

established. This element and the lack of possible discrimination between induction of anxiety disorders and depression makes the main limit of this model.

- The chronic restraint stress (CRS) model: this model is based on the forced sustained restraint of the animal to induce anxiety disorders. In this protocol, mice are usually placed in a semi-cylindrical tube with ventilation hole for a variable amount of time (from two to three hours daily) every day during one to three weeks. An alternate version of this protocol can also be used where the limbs are taped in order to immobilize the animal. Both these protocols produce a strong inescapable physical and mental stress on the animal leading to the development of both anxiety disorders and depressive-like phenotype. Unlike the CSD model, this model has poor ethological value and low construct validity as this type of stressors is not common in either human or mice. Furthermore, as to our knowledge, the CRS model has been mainly used to study depression, and therefore few studies have provided the necessary background to assess if this model presents face and predictive validity. However, in spite of this lack of studies, this model is subject to an effect of habituation where the animals are less impacted by the restraint upon re-exposure. Indeed, CRS has been associated with a decrease of HPA axis activity (Herman, 2013). Overall, these elements have led the CRS model's objectivity to be debated.
- The unpredictable chronic mild stress (UCMS) model: The objective of this model is to prevent the habituation effect that can occur in mildly stressful models of anxiety disorders. To achieve this goal, mice are subjected every day to a different stressor: restraint, disruption of light circadian rhythm, water or food depletion, threatening noise, placement in crowded cages, etc. This model presents a good construct validity because of the diversity of similar stressors encountered daily in human life. Similarly to CRS, the literature on UCMS predictive and face validity for anxiety disorders in mice is scarce. Furthermore, one of the main criticisms targeting the UCMS model is the low reproducibility of the results obtained with this model.

Overall, all the models for the study of anxiety disorders present advantages and limits. An important factor of note is the lack of discriminative validity between depression and anxiety disorders in most of the available models. In spite of this problem, the relative advantages of the CSD compared to other models have made it the best model for my thesis studies.

In conclusion, in this axis, I have introduced the definition of stress, which brain circuitry controls the stress-response and what type of mechanisms can be responsible for the maladaptive response found in anxiety disorders. Through this axis, I mentioned several times the decision not to delve deeper into the aforementioned mechanisms at a circuitry level because of the many structures involved. Hence, in the next axis of my thesis, I have decided to focus on two structures for their role in adaptive and pathological anxiety. These structures are comprised of a canonical key region in regulation of defensive behavior: the Amygdala; but also a structure heavily studied for its involvement in the reward system whose role in anxiety and defensive behaviors remains elusive: the ventral tegmental area.

II. The amygdala

As mentioned previously, the amygdala is a focal point for regulation of emotional behaviors. This structure has long been studied for its involvement in defensive behavior but also more recently proven to be involved in assignment of positive valence to events. As such, the amygdala lays at the crossroads of the limbic system and is particularly relevant when studying anxiety and its related disorders. Therefore, albeit amygdala was quickly aforementioned in the description of the anxiety process, a more detailed definition of the network present in the amygdala nuclei and their target is warranted. In the next chapter, I will describe the anatomical organization of the amygdala to provide a more integrated view of local microcircuitry tightly regulating amygdala control of emotions. This approach will give us the needed background to understand the function of the amygdala mediated through its efferences.

A. Anatomical organization

The amygdala is an almond-shaped telencephalic structure. The anatomical organization of the amygdala has been thoroughly parsed and has highlighted the incredible complexity of this structure. Indeed, the amygdala is not a single region but can be divided in up to 13 nuclei that can often be partitioned each into sub-nuclei with different histochemistry, cytoarchitectonics and connectivity properties. This complexity and the different functional relevance of the amygdala nuclei has led to several definition of its organization. Indeed, a first definition is based upon the evolutionary functionality of the amygdala with an olfactory derived division: the cortico-medial region; and neocortically evolved division with the basolateral region. More recent definition have highlighted the amygdala as a group of the basolateral complex, the cortical-like groups and centromedial groups (Sah et al., 2003). While other definitions exist, it is important to note the terminology of the amygdala

composition. More precisely, the basolateral amygdala can be the topic of confusion due to the extensive use of terms with different meaning about the regions encompassed. Indeed, many studies do not differentiate the basolateral nuclei comprised of the basal and accessory basal nuclei, from the lateral, basal and accessory basal nuclei of the basolateral region. In this thesis, I will use the definition of the amygdala as the clustering of three groups that I will further describe here (see also Fig. 6).

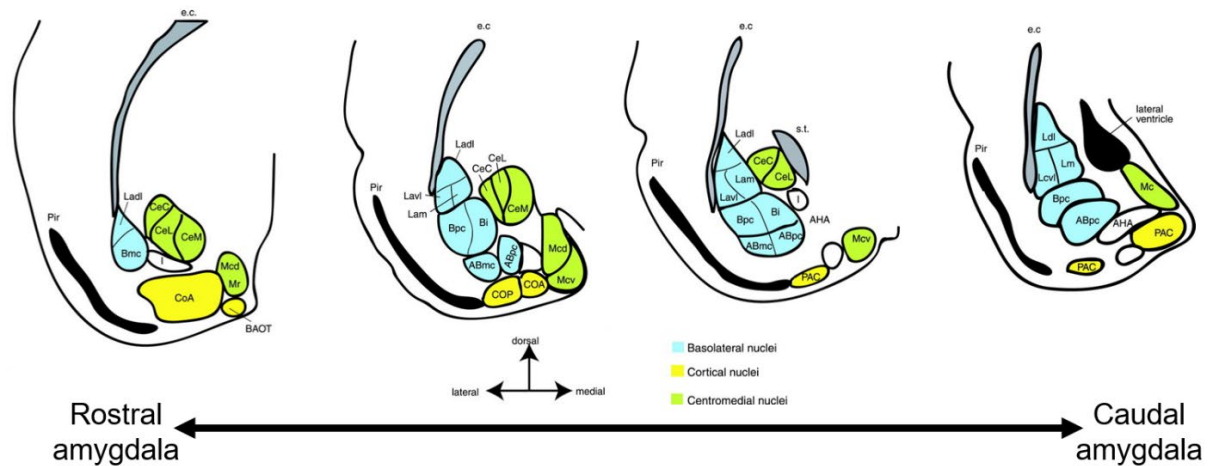


Fig. 6 – Schematic representation of the amygdala subdivisions following the three main groups, adapted from (Sah et al., 2003). Blue: basolateral group; Yellow: cortical-like group; green: centromedial group. Abbreviation: ABpc/ABmc : magnocellular/parvicellular division of the accessory basal nucleus. AHA: amygdalohippocampal area. BAOT: bed nucleus of the accessory olfactory tract. Bpc : parvicellular division of the basal nucleus. CeC: capsular division of the central amygdala. CeL: centrolateral amygdala. CeM: centromedial amygdala. CoA: anterior cortical nucleus. CoP: posterior cortical nucleus. e.c.: external capsule. I: intercalated nuclei. Ladi/Lam/Lavm: dorsolateral/medial/ventromedial subdivision of the lateral amygdala. Mc/Mcd/Mcv/Mr: dorsal/ventral/rostral subdivision of the medial amygdala. PAC: periamygdaloid cortex. Pir: piriform cortex. s.t.: stria terminalis.

1) The basolateral group

As previously mentioned, this group is comprised of the several nuclei that can be divided into other subnuclei. The importance of this group and their connectivity in my thesis warrants more details on their organization:

- lateral nucleus (LA): this nucleus is located in the dorsolateral part of the amygdala. The LA borders the dorsal striatum dorsally, the external capsule laterally, the central amygdala (CeA) medially and the BA ventrally. This nucleus can be subdivided based upon cytoarchitectonics

features into dorsolateral, ventrolateral and medial subdivisions. This nucleus possesses an important connectivity with its subdivisions but also with the other nuclei. Indeed, the ventrolateral LA projects to the medial subdivisions while the dorsal LA projects both to the medial and ventrolateral LA. The LA also send excitatory projection to the basomedial nucleus but also to other amygdala nuclei, albeit less profusely (Pitkänen et al., 1995). Because of the network of efference emitted by the LA and its profuse afference of sensory inputs, the LA is key to the interpretation of the valence of cues. Indeed, inputs from the thalamus, cortical and prefrontal cortex to the LA has led this region to be considered as a sensory gateway for the induction of defensive behaviors (Joseph E. LeDoux et al., 1990).

- the basal nucleus (BA): located ventral to the lateral nucleus, the BA is comprised of several subdivisions, namely the rostrally placed magnocellular subdivision and the more caudally located intermediate and parvocellular division. Similarly to the LA, the BA receives profuse sensory inputs from cortical and thalamic area. Furthermore, the BA has reciprocal connections with the LA, emits local excitatory efferences to the CeA and present interconnectivity with its subdivision. Indeed, the magnocellular divisions is reciprocally connected with the parvocellular division which in turn connects with the intermediate subdivision. The efferences of the BA are mainly the prefrontal cortex but also the hippocampus, the nucleus accumbens and the thalamus.
- accessory basal nucleus (AB): also called basomedial nucleus, it is located ventral to the BA and can be subdivided into magnocellular, intermediate and parvocellular subdivisions. This nucleus receives profuse afferents from the LA, while emitting strong connections to the centro-medial amygdala, leading this nucleus to be described as a bridge between the inputs subregion (i.e the LA) and the output structure of the amygdala (i.e the central amygdala). While the connection of the AB with the CeM infers a role of the AB in potentializing the anxious response, the efferences of the AB toward the adBNST and the vmPFC hints for a role of this subregion in promoting anxiolysis. Hence, this structure seems perfectly placed to further the interpretation step.

Overall, is it important to note the basolateral group is characterized as a cortical-derived structure because of its mainly glutamatergic populations. Indeed, the BLA is comprised of two neuronal types: the glutamatergic pyramidal cells (80-85% of the BLA) and of GABAergic interneurons (20% of the BLA) (Vereczki et al., 2021). This composition and the connectivity of the BLA allows it to enact fine regulatory control of the anxious response initiation.

2) The cortical-like group

While the BLA has long been associated as a cortical-like structure, it is not to be confused with the cortical-like group of amygdala nuclei. This group is placed at the surface of the brain and have a layered organization typical of cortical structures. The cortical-like group is comprised of the nucleus of the lateral olfactory tract (NLOT), the bed nucleus of the accessory olfactory tract (BAOT), the anterior cortical nucleus (CoA), the Posterior cortical nucleus (CoP) and the periamygdaloid cortex (PAC). These nuclei are located ventral to the BLA group and have particularly important role in modulating olfactory inputs. Indeed, the cortical-like nuclei receive important inputs from the different olfactory system structures. In turn, these nuclei have an important inter-connectivity and project to other amygdala nuclei.

3) The centromedial group

The centromedial group is the third group of the amygdala and is considered as an output subregion. It was separated from the cortical group based upon histochemical and developmental characteristics. This groups localized medially compared to the BLA is comprised of:

- the central amygdala (CeA): located medially to the BLA, this structure can be subdivided in four regions: the capsular, the lateral (CeL), the intermediate and the medial (CeM) subdivisions. While the CeA has received a lot of attention, the intermediate and capsular subdivisions have been poorly studied and the existence of the intermediate part in the mouse has been debated. Hence, the diversity of the nomenclature on this region often lead to confusion on these regions. Therefore, only the mainly studied subregions, namely the CeL and CeM will be described here. Similarly to other amygdala regions, the CeA is subject to an important local connectivity. Indeed, both the CeL and CeM are comprised of GABAergic projecting neurons and of inhibitory interneurons capable of enacting local inhibition of the main projection neurons. Furthermore, the CeL main projection neurons main outputs are the CeM projections neurons. Hence, the CeA local inhibitory circuitry enables the different subregions of this region to enact opposite effects on regulation of anxiety. This local circuitry is even more complex when the non-local inputs of the CeA are taken into consideration. Indeed, the CeA receive dense inputs from the basolateral region. These glutamatergic inputs from the lateral and basal nucleus are known to target both the CeL and CeM, hence enabling a even higher level of precision in the modulation of anxiety. The reach of the CeA in the regulation of anxiety and behaviors can be observed when the efferences of its projection neurons are viewed. Indeed, the CeA has extensive efference not only to the previously mentioned BNST or the PAG, but also through connections to the nucleus tractus solitarius, the ventral tegmental area, the hypothalamus, the basal forebrain and other

regions. Details of this complexity can be glanced in the following comprehensive reviews (Fadok et al., 2018; Gilpin et al., 2015).

- the medial amygdala (MeA): this region is located medially to the BLA and ventral to the CeA. This structure can also be subdivided in several territories: the rostral, the centro-ventral, the centro-dorsal and the caudal portion. Overall, the MeA receive major olfactory inputs from several structures that are important for odor detection of both conspecifics and potential predators (Tong et al., 2021). Many other inputs also targets the MeA, including afferences from nearby amygdaloid nuclei, such as the CeA and part of the BLA (Cádiz-Moretti et al., 2014). In turn, the MeA provide feedback to olfactory modulating structures such as the accessory olfactory bulb, the olfactory and vomeronasal amygdala. The hypothalamus, the hippocampus, also receive inputs from the MeA, (Pardo-Bellver et al., 2012).

Overall, these three groups of amygdaloid nuclei are highly interconnected and receive a profusion of afferences and efferences enabling an important role for the amygdala in the modulation of a wide range of behaviors including especially defensives behaviors (Fig. 7). However, all the amygdala nuclei cannot be classed in one of these groups.

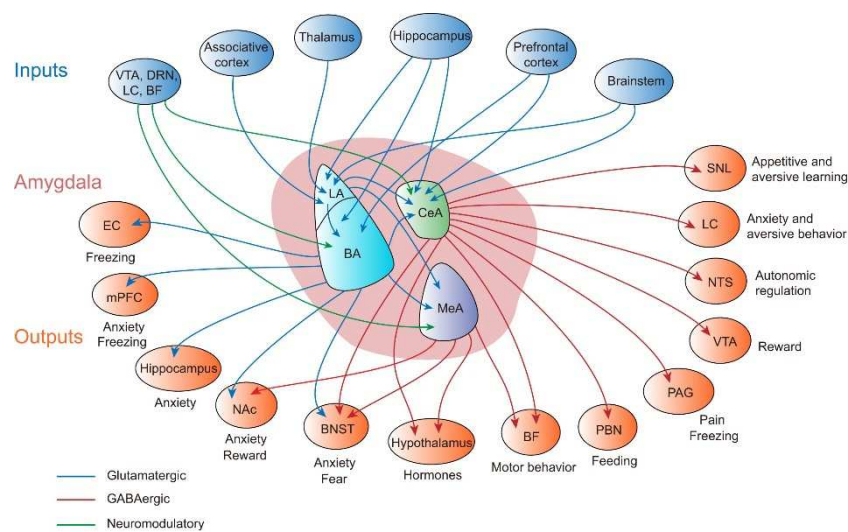


Fig. 7 – Simplified schematic summary of afferences and efferences to the three main amygdaloid groups, taken from (W. H. Zhang et al., 2021). The known major function of several output are also mentioned. Abbreviations; BA: basal amygdala. BF: basal forebrain. BNST: bed nucleus of the stria terminalis. CeA: central amygdala. DRN: dorsal raphe nucleus. EC: entorhinal cortex. LA: lateral amygdala. LC: locus coeruleus. MeA: medial amygdala. mPFC: medial prefrontal cortex. NAc: nucleus accumbens. NTS: nucleus of the solitary tract. PAG: periaqueductal gray. PBN: parabrachial nucleus. SNL: lateral substantia nigra. VTA: ventral tegmental area.

4) The intercalated cells of the amygdala

Indeed, although relatively poorly studied, the anterior amygdala area and the amygdalo-hippocampal area are also regions of the amygdala that do not belong to the previously cited groups. Another unclassified structure of importance in modulating the activity of the amygdala that requires a description is the is comprised in these nuclei and requires a description is the intercalated cells (ITCs) of the amygdala. The ITC are GABAergic neurons divided in three groups: the lateral ITCs (lITC), the ventromedial (vmITC) and dorsomedial ITCs (vdITC). These neurons are surrounding the BLA: laterally (lITC), medially and, ventrally (vmITC) or dorsally (vdITC). Overall, the three groups of ITCs inputs receive excitatory thalamic and auditory cortex inputs (Strobel et al., 2015). The ITCs groups differs mainly in their efferents as the lITCs target mainly the LA, while the dmITC principally inhibits the CeL and the vmITC. Their local connectivity with the amygdala subregions both afferent and efferent, makes them strong actors in the regulation of defensive behaviors. Indeed, several studies have showed the ITCs to be involved in gating fear and anxiety (Asede et al., 2015; Duvarci & Pare, 2014; G. Li et al., 2011; Palomares-Castillo et al., 2012).

B. Functional role in physiological anxiety

As previously described, the anatomy, the sub-territorialization and the connectivity of the amygdala are incredibly complex and enables the amygdala to regulate many behaviors. Because of this complexity, it is important to describe the mechanism through which the amygdala control anxiety. Hence, in the following chapters, I will provide a simplified view of the role amygdala in gating anxiety and the maladaptive adaptations afflicting this structure in anxiety disorders. In these chapters, because of their critical role in regulating anxiety, I will mainly focus on the role of the basolateral and the centromedial nuclei.

In the previous axis, I discussed the steps of the anxious process following the model proposed by (Calhoun & Tye, 2015). In this model, the amygdala is involved in the interpretation and evaluation process. Indeed, following detection of a cue, sensory inputs from all modalities (olfactory, somatosensory, gustatory and visceral, auditory, and visual) are carried mainly from cortical and thalamic regions towards the amygdala. These excitatory projections, although diverse, target mainly the BLA and more precisely the LA. In turn, first, the LA convey information mainly to the BA and the CeL leading to the activation of the CeM which trigger the activation of the region responsible for the observable anxiety effects (Fig. 8). This simplistic vision shows a multistep process for a sensory information to be integrated. I will now delve deeper in each step of this mechanism to provide a more comprehensive background for the involvement of the BLA in anxiety.

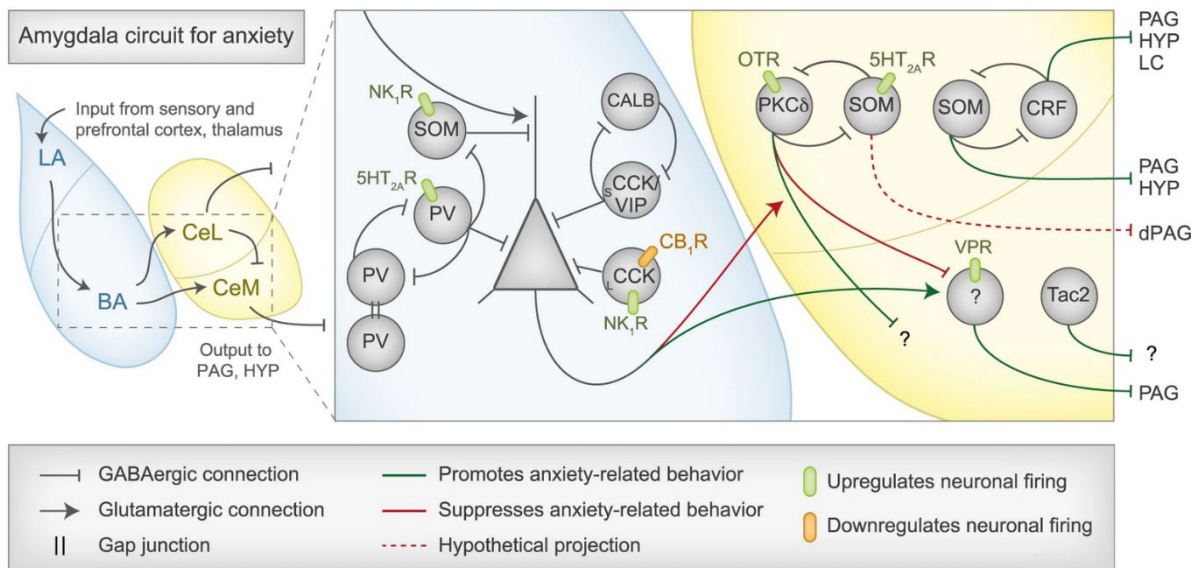


Fig. 8 – Schematic of the intra-amygdala network regulating anxiety, taken from (Babaev et al., 2018). Although simplified, these schematic highlights a part of the complexity of the intra-amygdala network that enable interpretation and processing of sensory stimuli to convey anxiety. Of note, this figure does not address the issue of the inhibitory network mediated by the intercalated cells. Abbreviations: BA : basal nucleus. CALB: calbindin. CeL: centrolateral amygdala. CeM: centromedial amygdala. CCK: cholecystokinin. CRF: corticotropin releasing factor. dPAG: dorsal periaqueductal grey. HT_R2A: serotonin receptor 2 A. HYP: hypothalamus. LC: locus coeruleus. NK_{1R}: neurokinin 1 receptor. OTR: oxytocin receptor. PAG: periaqueductal gray. PV: parvalbumin. SOM: somatostatin. Tac2: tachykinin 2. VIP: vasoactive intestinal peptide. VPR: vasopressin receptor.

The first step of sensory integration involves the LA and BA. Upon excitation of LA by sensory inputs, the LA neurons induce excitation of the BA principal glutamatergic neurons but also of the dmITC. Both these actions promote anxiety as excitation of BA principal neurons and dmITC both leads to activation of CeM. While BA principal neurons effects on CeM are direct, the results of dmITC activation are more complex. Indeed, dmITC are inhibiting two amygdala subregions: the CeL and the vmITCs. Both these regions are made of GABAergic neurons that keep the CeM under tight inhibition. Hence, this inhibition of the CeL and vmITC by the dmITC leads to disinhibition of the CeM and therefore an anxiogenic response. Overall, activation of the LA is an important step in promoting anxiety, however, under basal conditions, this structure, and more generally the amygdala, is under important inhibitory control to prevent unwarranted induction of anxious states. This strong inhibition of the amygdala is mainly mediated in a top-down manner by the prefrontal cortex inputs onto the BLA and through ITC mediated feedforward inhibition of amygdala nuclei. Indeed, the ventral mPFC (or infralimbic mPFC; IL) emit strong efferences toward the basomedial amygdala and the lateral ITC. While the anxiolytic effect of the connections to the basomedial amygdala are likely mediated through

basomedial amygdala feedforward inhibition to the CeL or to the vmITC (Adhikari et al., 2015), the IL connections to the lateral ITC promotes a feedforward inhibition of the LA. These inputs to the IITC are particularly important for maintenance of basal anxiety levels as they contribute to 70% of the cortical inhibition of the amygdala (Palomares-Castillo et al., 2012). Furthermore, several theories underline the importance of the IITC and have proposed the inactivation of IL→IITC inputs as a key mechanism for the induction of anxiety. These theories are based upon studies that first revealed that bath application of dopamine on brain slices led to Dopamine 1 receptor (D1R) mediated hyperpolarization of the ITC (Marowsky et al., 2005). Further studies have also identified the midbrain VTA and substantia nigra as the putative dopamine inputs responsible for this ITC-mediated disinhibition of the amygdala (Aksoy-Aksel et al., 2021). However, these studies have been carried out using ex-vivo electrophysiological experiments. Therefore, in-vivo studies linking directly these inputs to change in defensive behaviors remain to be established. Overall, these studies have highlighted the importance of the prefrontal cortex to prevent the induction of anxiety. However, this regulation is more complex as the different PFC inputs to the amygdala contribute in opposite ways to the induction of anxiety. Indeed, as previously mentioned, the IL projections to the amygdala are anxiolytic, but this is not the case of the dorsal mPFC (or prelimbic cortex). Indeed, the excitatory dmPFC inputs target the BA principal neurons and studies have hinted at a putative role for this projection in mediating threat-related behavior (Likhtik & Paz, 2015). Furthermore, because of its connectivity with the dmITC, the dmPFC inputs seems well placed to further enhance the induction of anxiety (Adhikari et al., 2015). It is also important to highlight that induction of anxiety in the amygdala is a dynamic process, especially in the BLA. Indeed, not only the BLA receives projections from the PFC but also emits reciprocal connections that controls anxiety. More precisely, optogenetic stimulation of BLA → mPFC promotes an anxiogenic effect while inhibition induces anxiolysis (A. C. Felix-Ortiz et al., 2016). Aside from reciprocal PFC connections, other projections from the BLA can be anxiogenic such as BLA → ventral hippocampus (Ada C. Felix-Ortiz et al., 2013) or can be anxiolytic such as BLA → adBNST. Therefore, the diversity of afferences and efferences of the BLA in conjunction with the local inhibitory circuitry enables a fine regulation of the anxiety levels. Until now, I have given details about the BLA and its connectivity to non-local regions involved in anxiety. However, the transmission of the information to the CeA is an important contributor to the induction of anxiety. Indeed, this contribution is due to the downstream connectivity of the CeA to several brainstem nuclei and more generally to stress-regulating regions. Similarly to the BLA, the CeA is a region tightly regulated by local GABAergic interneurons. This local inhibitory network with the afferences from the vmITC and dmITC enables a fine regulation of the activity of the CeA and of its effectors. In a simplified manner, this inhibitory network contributes to the gating of excitatory inputs from the BLA. Indeed, the BLA is comprised of excitatory projections capable to promote anxiety: from the LA to dmITC, from BA to the CeM and

from the BA to the PKC δ - cells of the CeL. While the projections from the BA to the CeM directly activate the output region of the amygdala, the activation of the projections from the LA to the dmITC lead to an inhibition of the projection neurons of the CeL which results in the direct disinhibition of the CeM. Finally, the inputs from the BA to the PKC δ - neurons of the CeL leads to a local inhibition of the CeL projections neurons (PKC δ +), therefore leading to the disinhibition of the CeM neurons. These discoveries on the integration of the BLA inputs by the CeA highlights once again the importance of local inhibitory network in gating anxious behaviors (see Fig. 9 for summary). While the CeA is not considered the main input integration region, the CeA also receives modulatory afferences from distant regions. More precisely, amongst its many distant inputs, the raphe nuclei, the parabrachial nuclei (Ito et al., 2021), the PVH, the vHPC, the mPFC, the BNST and cortical regions could contribute to the regulation of defensive behaviors through CeA modulation (Fadok et al., 2018). Of note, the projections from the PVH to the CeA are known to be involved in the previously mentioned “low-road”, where stimuli trigger a quick induction of fear through amygdala activation. Overall, these elements illustrate the complex regulation of the CeA by distant neuronal afferences. But what about the afferences of the amygdala and how do they mediate the somatic and behavioral effects of anxiety?

The next paragraph will be dedicated to the connectivity of the amygdala with the main effector structure mediating anxiety. The amygdala possesses an incredible number of outputs to diverse structures, hence listing each of these outputs and their respective role in anxiety would be tedious. Therefore, I will quickly describe the roles of the main known effectors in anxiety in two categories: somatic-response related and behavior-related.

- Amygdala somatic effectors of anxiety: as previously mentioned anxiety is associated with several autonomic effects. Indeed, activation of a projection from the CeA to the DVC following a threatening cue, triggers an increase of heart-rate (J. E. LeDoux et al., 1988; Viviani et al., 2011). The nucleus of the solitary tract (NST), a structure involved in the regulation of the autonomic respiratory and sympathetic motor response (Zoccal et al., 2014), also receive modulatory projection from the CeA (Gasparini et al., 2020). Several studies have also suggested a role of the CeA in promoting the activation of the HPA axis through facilitation of the serotonergic and noradrenergic transmission to the PVH (see review (Weidenfeld & Ovadia, 2017)).
- Amygdala behavioral effectors: the amygdala promotes its behavioral effects through a wide range of projections. For instance, the CeA project to the locus coeruleus (LC), a structure involved in many processes such as fight or flight response and stress reactivity. Selective optogenetic stimulation of CeA CRH projection to the LC was found to elicit anxiety (McCall et

al., 2015). Interestingly this projection may be bidirectionally involved in anxiety as the LC is known to emit efference to anxiety-related structures such as the BLA (Buffalari & Grace, 2007) and the CeA (Bouret et al., 2003). Furthermore, projections from the CeA to the PAG are known to play important role in the stress response. Indeed, connections to the vPAG produces freezing by disinhibition of ventrolateral periaqueductal grey excitatory outputs to pre-motor targets in the magnocellular nucleus of the medulla dorsal (Tovote et al., 2016). Inputs from the CeA to the lateral hypothalamus also promote avoidance (Weera et al., 2021). Finally, the CeA is interconnected with the BNST which may also underline another role of the CeA efference in promoting anxiety (Lebow & Chen, 2016). Overall, these examples underline the importance of the amygdala and the CeA in promoting anxiety through modulation of diverse effector regions.

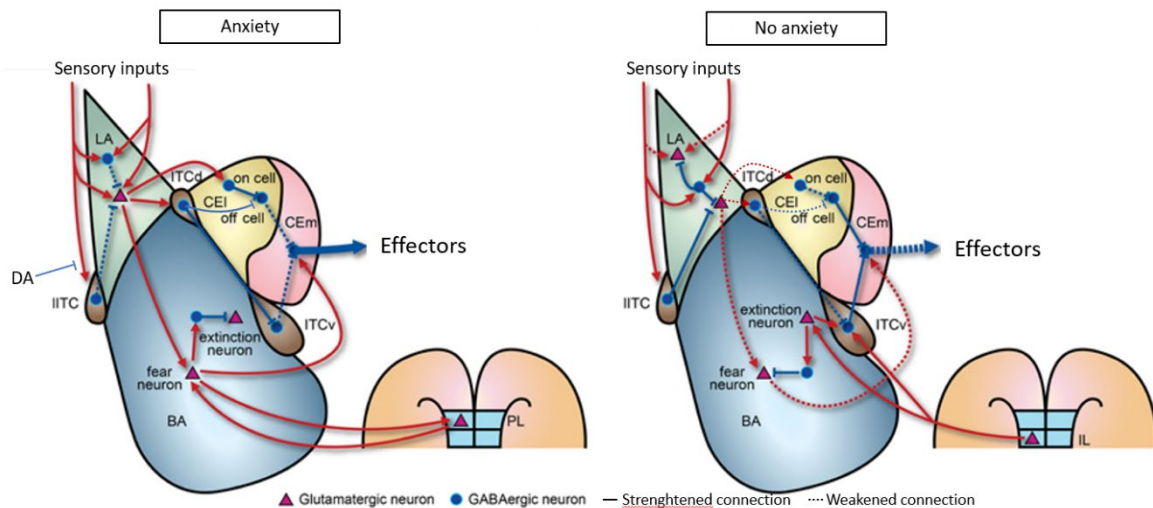


Fig. 9 – Schematic summary of the functional role of the amygdala in processing anxiety, adapted from (S. Y. Kim et al., 2013). This schematic highlights the importance of disinhibition of the ITCs in promoting anxiety by the amygdala. Abbreviations: BA: basal nucleus. CeL: centrolateral amygdala. CeM: centromedial amygdala. DA: dopamine. IL: infralimbic prefrontal cortex. ITC: intercalated cells. LA: lateral amygdala. PL : prelimbic prefrontal cortex.

Overall, I have here discussed at length about the involvement of the amygdala in anxiety and more generally in defensive behaviors. However, it is important to realize the amygdala also contribute to other non-defensive behaviors. These behaviors are mainly linked to emotional states such as reward learning and motivation, aggressive, sexual, and feeding (H. Cai et al., 2014) and appetitive behaviors (J. Kim et al., 2017). But also in cognitive function such as attention and explicit memories. While not the topic of my thesis, I will not delve deeper into these non-defensive roles of the amygdala.

C. Anxiety disorders and amygdala

As previously mentioned, anxiety disorders are proposed to result from the overactivation of the anxiety circuitry (Duval et al., 2015). While these maladaptations can virtually affect nearly every part of the circuitry, one key structure affected is the amygdala. Indeed, both animal and human studies have highlighted that anxiety disorders are generally associated with a hyperactivity of the amygdala (Shin & Liberzon, 2009). Neuroimaging studies in human have shown that post-traumatic stress disorders are associated with higher amygdalar activity and reactivity to stress while the infralimbic portion of the PFC, an important player in the prevention of amygdala hyperactivity has been shown to be less active (Pitman et al., 2012). Hyper-reactivity of the amygdala was also observed in human with GAD in an fMRI study (Nitschke et al., 2009). In patients with generalized anxiety disorders, similar change in the prefrontal connectivity to the amygdala were also found in a neuroimaging study (Etkin et al., 2009; Makovac et al., 2016). Furthermore, decrease of the serotonin reuptake transporter was also found in the amygdala of PTSD patients (Murrrough et al., 2011). As serotonin is thought to promote the excitation of the BLA in rodents following uncontrollable stress (Christianson et al., 2010), these change in PTSD patient also reflect the potential similarities in the mechanisms of anxiety-disorders in human and rodents. Overall, the previous example cited here provide a quick background on the dysregulation of the amygdala activity in anxiety disorders. For further information, we refer the viewer to the following review (Duval et al., 2015; Forster et al., 2012; X. Zhang et al., 2018). This dysregulation of the amygdala is tightly linked to maladaptations of the amygdala at several scales which I will introduce in the next paragraphs.

1) The epigenetic scale

As previously mentioned, several epigenetic changes can affect neurons of the anxiety circuitry. While epigenetic alterations were first believed to be induced in embryonic or in early-life stages, it has become increasingly evident these changes can take place across the entire lifespan. Here, I will not address the issue of epigenetic changes afflicting prenatal and early post-natal periods, for more information see the review (Gudsnuk & Champagne, 2012). I will rather focus on the epigenetic changes occurring during adulthood in the amygdala following stress.

So what are the epigenetic adaptations targeting the amygdala?

Several studies that have shown that stress induces epigenetic change inside that amygdala of rodents. However, the number of studies is scarce as the hippocampus, received most of the focus because of its center role in memory formation, a key process for adaptative behaviors. Nonetheless, studies on the amygdala have shown that chronic stress promotes DNA methylation on key target

genes. Indeed, in a study on rats using the repeated water avoidance stress (WAS) test, a psychological chronic stress model, GR and CRF gene expression was found altered (Tran et al., 2013). More precisely, WAS is associated with an increase methylation of GR promoter and therefore to a decrease of GR expression. Furthermore, WAS led to a decreased CRF methylation and the associated increase of CRF expression. While of great interest, this study was mainly carried at the transcriptional level and may not reflect directly translational level change. Nevertheless, this study suggested that chronic stress could induce a decrease of GR expression which in turn would lead to an increase of CRF expression directly in the CeA. As CeA CRF neurons have been involved in promoting anxiety through their efference to the dBNST (Pomrenze et al., 2019), the effects mediated by chronic stress on CeA CRF expression could be relevant in the study of anxiety disorders. Another study highlighted epigenetic change triggered by auditory fear conditioning in the lateral amygdala (Monsey et al., 2011). In this study, rats received foot shocks following an auditory cue and the levels of histone H3 acetylation and DNA methylation (DNMT3A) in the LA was measured. They found an increase in H3 acetylation and DNMT3A expression following auditory fear conditioning. Furthermore, they showed that acetylation of H3 and DNMT3A activity both enhance the long-term potentiation of thalamic and cortical inputs to the LA. While not directly studied in anxiety, these findings are particularly relevant as potentiation of these thalamic and cortical excitatory inputs may contribute to the activation of the LA and therefore to the induction of anxiety.

While the previous studies showed examples in the amygdala of DNA methylation and chromatin remodelling linked to stress, non-coding microRNAs (miRNA) may also strongly contribute to the regulation of anxiety levels. Indeed, a study of miRNA contribution to anxiety, Haramati et al., revealed that depletion of miRNA in the amygdala was sufficient to induce an anxious phenotype in mice (Haramati et al., 2011). Based upon this discovery, they identified an enhanced expression profile of miR-34c following acute restraint and chronic social defeat stress. As this miRNA regulates the responsiveness to CRF, these results highlight the potential importance of miRNA in regulating anxiety. Furthermore, this upregulation of miR-34c was found two-weeks after the last social defeat, hinting therefore a role of this miRNA in long-term anxiety disorders. Interestingly, another surprising study showed increased of CRF1R gene expression and DNA methylation at promoter site following chronic mild stress (Sotnikov et al., 2014). This study identifies another epigenetic mechanism of regulation of the HPA axis linked to stress that can be reverted through exposure to an enriched environment. Several other studies on rats have shown the upregulation by stress of miRNAs in the amygdala that may contribute to anxiety disorders (Balakathiresan et al., 2014; Meerson et al., 2010).

Overall, the previous studies prove the seemingly overlooked role of epigenetic modifications in the regulation of anxiety disorders. While I focused here on the amygdala, two facts are to be

reminded. First, epigenetic alterations contribute to anxiety disorders through many other limbic regions aside from the amygdala. Second, susceptibility and resilience to stress-induced anxiety disorders is thoroughly linked to genetics and early-development epigenetic modifications in the anxiety circuitry. Interestingly, while the field of epigenetic in human is new, several studies on blood sample have been performed. These studies have shown that patient suffering from different kinds of anxiety disorders had several methylation alterations on key genes known to be involved in anxiety disorders. While those studies did not focus on the amygdala, they still provide first evidence of similar epigenetic mechanisms between rodent model and human afflicted with anxiety disorders. These findings can be found in more details in the following reviews (Nieto et al., 2016; Schiele & Domschke, 2018).

2) The synaptic scale

While epigenetic modifications exact an important regulatory role on anxiety, what are the synaptic plasticity alterations found in the amygdala during anxiety disorders?

As previously mentioned, modulation of pre- and post-synaptic plasticity allows activity-dependant adaptations of neurotransmissions. Such adaptations have been described in animals after submission to chronic stress. Hence, in this paragraph I will detail the stress-induced synaptic maladaptation found throughout the amygdala:

- The basolateral amygdala: the LA is an important integrator of excitatory sensory inputs. As such, strong fear induction, found for instance in contextual fear conditioning test, leads to a potentiation of the thalamic auditory afferents to the LA. More precisely, fear conditioning led to a NMDAR-dependent long-term potentiation (LTP) of thalamic inputs to the LA (Pape & Pare, 2010). Furthermore, this long-term potentiation is also associated with an increased expression of post-synaptic AMPA GluR1 receptors (Rumpel et al., 2005; Yi et al., 2017) . NMDAR trafficking could also play a role in the stress -related plasticity at the LA as NR2B subunit are downregulated following fear-conditioning (Zinebi et al., 2003). While these effects are mediated through fear conditioning challenge, another study has shown the effect of chronic stress in the LA. Indeed, a study using the restraint model in rats has shown that chronic stress was associated with an hyperexcitability of the LA principal neurons (Rosenkranz et al., 2010). This hyperexcitability was associated with greater action potential firing and a decrease of the slow hyperpolarization potential likely mediated by a lower number or function of calcium-activated hyperpolarizing potassium channels. The increased action potential firing could also result from the repeated activation of CRF receptor during chronic stress (Rainnie et al., 2004). This activation led to the simultaneous increase of NMDAR-

mediated calcium influx with a dampened GABA_A-receptor mediated inhibition of the BLA (Liu et al., 2014). Furthermore, downstream to the NMDAR activation, this CRF receptor modulation led to an increase in activity of the CamKII signalling cascade. This cascade is particularly important in promoting synaptic plasticity as its recurrent stimulation enables it to become independent of NMDAR-mediated calcium influx while promoting LTP (Lisman et al., 2002). Hence, chronic stress induction of CRF can promote long-term adaptation in the BLA that favours increased excitatory transmission while impairing GABAergic inhibition of the BLA. Furthermore, chronic restraint stress in rodents was also associated with increased frequency of excitatory post-synaptic current (EPSC) in the BLA (Masneuf et al., 2014; M. Padival et al., 2013). Interestingly, other neurotransmitters may contribute to maladaptive anxiety-related hyperactivity of the BLA. Indeed, inescapable-stress induced anxiety was shown to be dependent on an increase of serotonergic tone from the raphe nucleus to the BLA (Christianson et al., 2010). Increased serotonin is thought to promote excitation of BLA principal neurons while reducing GABA-A inhibitory current by acting on BLA 5-HT_{2c} receptors. Furthermore, adrenoreceptor and noradrenergic BLA receptors have also been suggested as mediating the hyperactivity of the amygdala through modulation of GABAergic transmission of the BLA (Rajbhandari et al., 2015).

In summary, stress-induced increased anxiety is mainly linked to change of ion channels expression such as AMPAR and NMDAR and to CRF mediated effects that promotes hyperactivity of the BLA.

- The central amygdala: The CeA is the main output region of the amygdala because of its connectivity to somatic and behavioral effector of the stress response. As previously mentioned, anxiety is induced by an activation of the BLA → CeA pathway. Hence, if BLA is overactive, this also should translate in adaptation in the CeA. However, unlike the BLA, only few studies have shown a direct link between chronic stress induced maladaptive anxiety and CeA synaptic alterations. One study has shown chronic unpredictable stress increase the amplitude of evoked inhibitory post-synaptic currents and the number of GABAergic inputs received onto CeA CRF positive neurons (Partridge et al., 2016). Furthermore, this result was also associated with enhanced synaptic strength suggesting a heightened quantal efficacy or an increase of GABAergic axons. Since the CeA CRF neurons have been involved in promoting anxiety through their efference to the dBNST (Pomrenze et al., 2019), this stress-induced adaptation could contribute to maladaptive anxiety. As aforementioned, while to my knowledge few studies have shown direct link between anxiety disorders and CeA synaptic alterations, several research have focused on fear conditioning and acute stress. Indeed, in

their study, (Haohong Li et al., 2013) showed that fear conditioning elicited enhanced AMPAR- and NMDAR-mediated excitatory inputs from the LA to the CeL somatostatin (SOM+) neurons. As SOM+ neurons inhibit CeM projecting GABAergic neurons, this modulation of SOM+ activity is thought to disinhibit CeM activity leading to fear expression. While these effects have not been studied on longer time period, similar mechanisms could arise in anxiety disorders driven by chronic stress. Furthermore, a study using acute restraint stress has highlighted a decrease in CRF1R expression in the CeA associated with an increase of basal activity in this region (Ciccocioppo et al., 2014). As CRF1R is thought to facilitate release of GABA by CeA neurons, this downregulation of CRF1R could lead to different outcome depending on the effect on the CeL or CeM affected (Fadok et al., 2017). Overall so far, relatively few maladaptations have been found in the CeA in response to chronic stress. Yet, several mechanisms for chronic stress-related maladaptations in the CeA have been identified through the use of fear conditioning combined with local injection of different agonist/antagonists. However, I decided not to describe these mechanisms as they remain putative for now.

3) The structural scale

So far, I have detailed how epigenetic and synaptic molecular alterations are stress induced and contribute to anxiety disorder through potentiation of the amygdala. However, alterations also found at the structural level where shift of dendritic arborization and spines density can enable enhanced neuronal transmission in the amygdala. Here, I will therefore discuss the structural changes induced in anxiety disorders.

-At the dendritic level, the structural plasticity alterations are either change in the ramification of the dendrites or in the number and/or type of dendritic spines. Indeed, restraint stress has been associated with increase of dendritic spines in the BLA (Hill et al., 2012; Mitra et al., 2005). Interestingly, the restraint stress was associated with different effect depending on its repeated or acute nature. More precisely, chronic restraint was associated with increase of dendritic spines in both primary and secondary dendritic branches, while acute restraint was associated with an increase only on primary branches. The effect of this acute stress was described as a progressive increase of dendritic spines and was strikingly associated with a gradual development of anxious behaviors. Further study from (M. A. Padival et al., 2013) revealed the distribution in the LA and BA of the previously observed increase of dendritic spines in response to stress. They found that both LA and BA had larger number of spines. However, this rise was more important in BA neurons at intermediate and distal distances from the soma unlike for the LA where the shift in spine was greater at proximity of the soma. Furthermore, the BA was also the subject of a dendritic growth not found in the LA after chronic restraint. Overall, these

differences between the LA and BA in this stress-induced structural may results in different amplitude and kinetics of EPSCs arriving at the soma and therefore may contribute to different synaptic integration. However, the global contribution of this structural adaptation seems to be an increase in excitatory drive integration (M. Padival et al., 2013). This results are coherent with a more recent study where chronic restraint promoted dendritic hypertrophy in the BLA with larger spine head size and greater number of mature mushroom spines (J. Y. Zhang et al., 2019). As previously mentioned, chronic-stress induced anxiety is associated to both increased excitatory tone and dampened local inhibitory tone in the amygdala. Hence, the effect of chronic restraint on local inhibitory interneuron was assessed by (Gilabert-Juan et al., 2011). They study show that chronic stress is sufficient to decrease dendritic arborization in the interneurons LA and BLA while also decreasing gene expression of GABAergic signalling and synaptic plasticity markers. These results suggest that chronic stress also promotes maladaptive anxiety through decreased local inhibitory drive in the BLA complex. As structural plasticity is altered in both excitatory principal neurons and in inhibitory local interneurons in the BLA, what about the CeA?

To my knowledge, few studies have been carried on the chronic stress-induced structural alteration in the CeA. Two studies have provided opposite answers to this question. The first study assessed a lack of effect of chronic restraint stress on the dendritic organization of the CeA (Vyas et al., 2003). However, in a second study, dendritic arborization was not altered but a decrease of dendritic spines density in the CeA (Moreno-Martínez et al., 2022). This second study seems more in accordance with the role of the CeA in mediating anxiety. Furthermore, this decrease of density was also associated with a shift in shapes of the spines. More precisely, more immature thin spines and less mature mushroom and stubby spines were found in the CeA. These findings are particularly interesting as they would favour a lowered neuronal transmission to the CeA. However, the study of the whole CeA without distinction between CeL and CeM seems a bias for interpretation of these results. Indeed, putatively, a decreased neuronal transmission in the CeL would be coherent in increasing anxiety through a disinhibition of the CeM. However, this theory remains to be tested.

Lastly, an important aspect of the structural plasticity mediated by chronic stress is the nature of the stress. Indeed, I have until now described structural plasticity mediated by chronic restraint stress, however other models of chronic stress are often used as previously described. Amongst these models, the social defeat stress was used for my thesis because of its ethological relevance. So how does the CSD model impact structural plasticity in the amygdala? Relatively few studies on CSD have been carried. These studies revealed a dendritic hypertrophy on BLA principal neurons comparable to chronic restraint and similar increase of firing but no increase in synaptic density (Colyn et al., 2019;

Patel et al., 2018). Hence, while mediating different structural plasticity compared to chronic restraint, the few studies on the CSD model suggest that it also promotes hyperactivation of the amygdala.

In conclusion, the amygdala and more precisely here, the BLA complex and CeA are the targets of important structural remodelling in response to chronic stress that enables facilitation of amygdala activity and therefore of anxiety.

To summarize, chronic stress is responsible for alterations from the epigenetic to the structural scale. These adaptations targeting the amygdala are considered as maladaptive as they promote a vicious cycle. In this cycle, the amygdala dysregulation induces pathological anxious states which in turn fuel a machinery enabling further amygdala dysregulation. Overall, the hyperactivity of the amygdala and of its basolateral portion has been attributed to decreased local inhibitory tone and therefore increased excitatory facilitation in the BLA. While the sensory thalamic inputs to the BLA contribute to this excitatory transmission, other putative glutamatergic inputs could be involved in the amygdala hyperactivity. It is in this context that I studied the inputs of a midbrain structure inputs to the BLA. Hence, in the next axis, I will describe this structure organization and its functional relevance in the study of anxiety through putative excitatory regulation of the amygdala.

III. The ventral tegmental area

The ventral tegmental area (VTA) has been long-studied for the role of in reward-motivated behaviors, especially with its participation in the mesocorticolimbic system. Because of its role in reward, the VTA was the focus of many studies on addiction and depression, two pathologies linked to a dysregulation of the reward system. However, through the year, the view on the VTA evolved with the discovery of the prediction-reward system and therefore the involvement of VTA in processing negative valence (for review see (Bromberg-Martin et al., 2010)). These first evidences of VTA involvement in aversion led to the study of the VTA for its role in behaviors related to negative valence signalling that are defensive behaviors. Amongst the structures involved in defensives behaviors receiving modulatory inputs from the VTA, the amygdala stands out because of its important role in modulating anxiety and fear. While the influence of the VTA over the amygdala in defensive behaviors has long remained elusive, recent studies have begun to uncover the role of these connections. These experiments have illustrated the important role of dopaminergic and GABAergic transmission from the VTA to the amygdala in promoting defensive behaviors (Morel et al., 2022; Nguyen et al., 2021; Tang et al., 2020; Zhou et al., 2019). However, the contribution of VTA glutamatergic projection to the amygdala to defensive behaviors remains putative and require clarification. As one of the main goals of my PhD was to answer this question, therefore I will introduce in this chapter the VTA. I will describe

its heterogeneous organization and its known role in valence, salience and more generally in defensive behaviors to provide the background needed to understand the putative position of VTA glutamate neurons in the anxiety circuitry.

A. Anatomical organization

The ventral tegmental area is a midbrain structure located medial to the substantia nigra and between the lateral hypothalamus and the Raphe on an antero-posterior axis. The first anatomical definition of this structure came from studies on the opossum performed by Tsai in 1925 (C. Tsai, 1925). In his study, Tsai determined that the cell-free space overlying the sulcus, along with smaller cell size and close relationship to the tracti mammillo- and olfacto-tegmentalis, warranted a separation of this structure from the neighboring substantia nigra. Despite this definition, the anatomical border of the VTA has been hard to establish because of the presence of similar cell types compared to neighbouring structures without remarkable anatomical delimitation. The lack of clear consensus about the span of the VTA can be problematic as sub-regions exhibit obvious functional differences. Yet, the sub-regions belonging to the VTA varies depending on the cytoarchitectural, neurochemical and functional features. Hence an important variability in the boundary of the VTA is often seen depending on the experimenters and are too often not clearly stated. Hence, in the following paragraphs, I will not delve into the debate of the VTA span. Rather, I address the reader to see the review (Morales & Margolis, 2017; Trutti et al., 2019). Hence, in this paragraph I will give my definition of the VTA (see Fig. 10), adapted from the suggestion in the aforementioned review (Trutti et al., 2019). This definition is based upon the gathering of subregions most commonly cited in the literature as part of the VTA.

1) The regional sub-divisions

Two main definitions of the VTA have so far been mentioned. A first, older mention described the VTA as comprised of 4 subregions (Phillipson, 1979), namely: the parabrachial pigmented area (PBP), the paranigral nucleus (PN), the tail of the VTA (VTT) and the parafasciculus retroflexus area (PFR). This mention does not include the midline nuclei as part of the VTA, including the interfascicular nucleus (IF), the rostral and caudal lineate nucleus because of different cytoarchitectonic features. The second definition, used as reference here, include these midline nuclei and do not consider the VTT and PFR as part of the VTA. This definition is mainly based on the first description of the VTA DA neurons (also called A10 groups). Their location includes these midline nuclei where they are found profusely. Furthermore, this description also allows to define the VTA as a whole continuous area

rather than a clustering of non-contiguous nuclei. Therefore, in the next paragraph, I will quickly describe the nuclei comprised by the VTA following our model of the VTA:

a. The parabrachial pigmented area

This subregion was first defined by Phillipson in 1979 (Phillipson, 1979). Phillipson described the PBP as a mantle of small, oval or stellate shaped cells with haphazardous organization and no preferential orientation compared to its neighboring nuclei. The PBP is considered the largest VTA subnuclei. Indeed, the PBP was accounting for roughly half of the volume and half the number of cells of the VTA for different species, including the rat (50% and 40% respectively) and in humans (55% and 42% respectively) (Halliday & Törk, 1986). Compared to other neighboring structure, the PBP is located medial to the substantia nigra compacta and the medial terminus of the accessory optic tract. The PBP is also ventral to the magnocellular part of the red nucleus and to the deep mesencephalic nucleus. Compared to the other VTA subnuclei discussed later, the PBP is lateral to the IF, the rostral linear nucleus (RLi) and the CLi and dorsal to the paranigral nucleus. Because of its similarity compared to neighboring structures including the SN and the other VTA subnuclei, the PBP boundaries have been hard to describe. Indeed, first studies of Phillipson in 1979 showed the PBP as composed of two categories of neurons found in either the SNC or the VTA. These neurons were either “VTA-like” with a small to medium size and a stellate or fusiform shape. Moreover, these neurons often bear two to four primary dendrites that divided into varicose secondary dendrites with few dendritic spines. The second category was predominantly “SNC-like” neurons with larger sized cells of a fusiform shape with two to five thick dendrites and few dendritic varicosities but with an increased proportion of stubby and thin dendritic spines. Because of this architecture, the PBP was first believed to be a transition area between the VTA and the SN rather than a structure of its own. Aside from the SN, the PBP can also be identified from the other VTA subnuclei because of their cytoarchitectural features. Indeed, the PBP is comprised of neurons loosely organized without preferential orientation and send fiber dorsally toward the medial lemniscus, unlike neighbouring VTA regions. While primary pioneering studies of Phillipson in 1979 and 1987 allowed a morphological description of the PBP subnuclei, the basis for its separation from the remaining the VTA subnuclei came also from difference in connectivity from this region. Indeed, differences in afferences and efferences in the VTA subnuclei can be found underlining the diverse behavior modulated by the VTA (further described in Chapter X).

b. The paranigral nucleus

Phillipson described the catecholaminergic cells of the paranigral nucleus (PN) as small to medium sized and with stellate or fusiform shapes (Phillipson, 1979). The neurons of the PN possess an anteroposterior and horizontal orientation and are slightly tilted upward the interpeduncular nucleus. The PN was accounting for roughly a fourth of the volume and number of cells of the VTA for the rat (23% and 26% respectively) and in humans (18% and 37% respectively) (Halliday & Törk, 1986). When compared to neighboring structures, the PN is more ventral but shares a similar localization with the PBP. This structure was well described in humans (Nobin & Bjorklund, 1973) and its separation from other VTA nuclei was demonstrated through tyrosine hydroxylase immunohistochemistry on human brain (Pearson et al., 1983). Together with the PBP, the PN forms the lateral VTA (Morales & Margolis, 2017).

c. The rostral linear nucleus

The lineate nucleus previously called the nucleus linearis, includes both its rostral and caudal (or central) parts and was first identified by Taber in 1961. The lineate nucleus was first purely defined by the location of its dopaminergic neurons and was separated from its lateral counterpart, being the PBP and the PN. The RLi is comprised of cells of different size and shapes (Phillipson, 1979). The RLi accounts for a very small proportion of the VTA volume and number of cells in rats (5% and 3% respectively) and humans (5% and 2% respectively). The RLi, is located medially to the PN and PBP and dorsally to the IF. Together with the CLi and the IF, the RLi are parts of the medial VTA (Morales & Margolis, 2017).

d. The caudal lineate nucleus

The CLi is comprised of fusiform cells dorsoventrally oriented. The CLi accounts for a small proportion of the VTA volume and number of cells in rats (13% and 8% respectively) and humans (20% and 12% respectively). Akin to the RLi, the CLi is located medially to the PN and PBP and dorsally to the IF.

e. The interfascicular nucleus

The interfascicular nucleus (IF) is comprised of small, round or oval cells (Phillipson, 1979). The CLi accounts for a small proportion of the VTA volume and but relatively high number of cells in rats (9% and 23% respectively) and humans (18% and 37% respectively). The IF is placed medially to the PBP and PN and ventrally to the RLi and CLi.

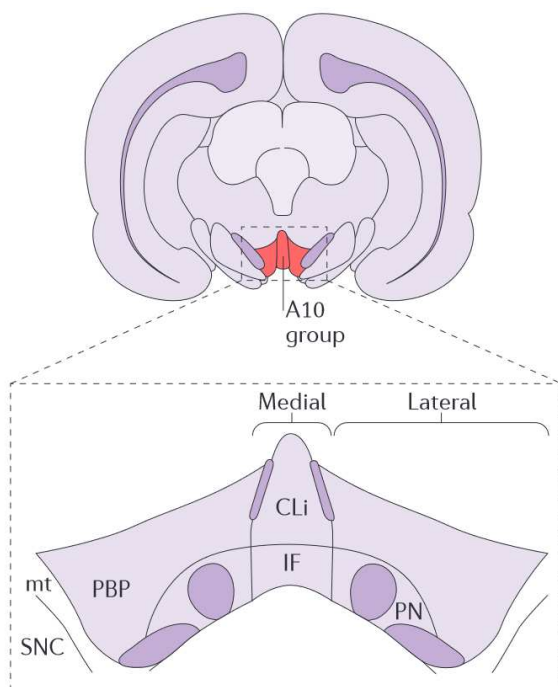


Fig. 10 – Schematic definition of the VTA and its sub-territories, taken from (Morales & Margolis, 2017). Top panel: the VTA, defined by the A10 group is coloured in red. Bottom panel: Divisions of the VTA into several nuclei and definition of lateral vs medial VTA. Of note, the rostral linear nucleus (RLi) belongs to this definition of the VTA but does not appear on this schematic as it is located more rostral. Abbreviations: CLi: caudal linear nucleus. IF: interfascicular nucleus. mt: medial terminal nucleus of the accessory optic tract. PBP: parabrachial pigmented nucleus. PN: paranigral nucleus. SNC: substantia nigra pars compacta.

2) The heterogeneity of the VTA

As mentioned above, the VTA can be anatomically subdivided in different subregions. However, some differences between these subdivisions can also be seen in their neurochemical properties. Indeed, while globally the VTA is comprised of 60% dopaminergic, 35% GABAergic and 5% glutamatergic neurons, these proportions vary depending on the subregions studied (Nair-Roberts et al., 2008; Yamaguchi et al., 2011). Furthermore, co-neurotransmitter release in VTA neurons is not rare (Morales & Margolis, 2017), hence providing another level of complexity. As recent studies have shown functional differences for these subregions, the understanding of the neurochemical properties of these subregions and their inputs has become increasingly relevant as to better understand the function of the VTA in a broad spectrum of behaviors. This heterogeneity is also seen in the network of inputs and outputs of the VTA. However, because of the great complexity of this network and their contribution to behaviors, I have decided to describe heterogeneity of the afferences and efferences of the VTA in a different upcoming chapter. Hence, in the next paragraph, I will describe the known neurochemical properties of the VTA and its subregions.

a. Dopamine neurons

The VTA has been studied extensively for its monoaminergic neurons, namely, the dopamine neurons. More precisely, a study of 1960 first identified several catecholamines expressing populations using the Falck–Hillarp formaldehyde fluorescence technique (Björklund & Dunnett, 2007). They were classified in 12 populations A1-A12 amongst which figures the VTA DA namely the A10 populations. Studies using immunohistochemistry for tyrosine hydroxylase (TH), a key enzyme in the production of the dopamine have revealed the dopamine neurons as the main VTA population comprising around 60% of its neurons (see fig. 11 for distribution of VTA-TH neurons). While small differences can be observed between species, the ratio of VTA dopaminergic neurons is generally well conserved. Dopaminergic neurons in the VTA of mice are more profusely found in lateral aspects of the VTA such as the PBP and the PN. In spite of these discoveries, the labeling of VTA neurons as dopaminergic has been recently reassessed. Indeed, studies in rats have shown that subsets of VTA TH expressing neurons can lack the expression of the vesicular monoamine transporter 2 (VMAT2) enzyme necessary for the vesicle's packaging of dopamine (X. Li et al., 2013). Similarly, the expression of dopamine cellular reuptake enzyme (DAT) has been found to be lacking for VTA TH positive neurons in both rats and mice (Lammel et al., 2008; Morales & Margolis, 2017). Finally, a large proportion of medial VTA neurons (RLi and IF) have been found in mice to be lacking TH protein expression while having TH mRNA (Yamaguchi et al., 2015). Although technical limitation could have led to identification of false negatives, these results suggest a lack or low number of DA neurons in the medial VTA. These recent discoveries put into perspectives previous studies that have often used TH labeling as indicator for dopamine neurons and may have overestimated the VTA dopaminergic transmissions capability. This problem however seems to be mainly restricted to the medial VTA.

While DA neurons seem compartmentalized to discrete subregions of the VTA, the heterogeneity of these neurons is also present in their electrophysiological properties. Indeed, differences in electrophysiological properties are present between the first characterized lateral VTA DA neurons and their medial VTA counterpart. However, before addressing this issue, it is important to describe what is known of the electrophysiological properties of the DA neurons.

The DA neurons were first describe as capable of four modalities of activity during in vivo recordings (Grace' And & Bunney3, 1984; A. A. Grace & Bunney, 1984) :

- hyperpolarized non-firing: inactive state linked to the inhibition or lack of activation of the neurons
- depolarization inactivation: inactive state resulting from a previous excitation preventing further depolarization.

- single-spike firing (also called tonic firing) : active state where the DA neurons emits trains of spike at irregular intervals
- burst firing (also called phasic firing): active state characterized by burst of spikes with consecutives spikes during a short period of time with a progressive decrease in amplitude but increase of duration.

The transition from tonic to phasic firing is a key element to increase neurotransmission. Hence, this mechanisms is thought to play an important role many behaviors both reward-related (Bass et al., 2013; Anthony A. Grace et al., 2007; H. C. Tsai et al., 2009) and aversion-related during restraint (Anstrom & Woodward, 2005) or even CSD (Cao et al., 2010) . However, in spite of the characterization of this model of firing, the electrophysiological identification of cells as “dopaminergic” has been a particular challenge. Indeed, a pioneering study of Margolis (Margolis et al., 2006), showed that electrophysiological parameters that were previously accepter as marker of dopaminergic neurons were not predictor of DA neurons as they were found in non-TH neurons. Furthermore, a later study has also highlighted the limitations of identifying DA neurons while proposing new profile for DA characterization through electrophysiology (Ungless & Grace, 2012). This new profile is however based upon the heterogeneity of the DA neurons in the VTA. Indeed, several studies indicated that medial and lateral VTA DA neurons did not share the same electrophysiological profiles. Identification in lateral VTA of DA neurons is reliable through classical properties associated to DA (long action potentials duration, slow tonic firing rate, burst firing, large hyperpolarization-activated cation current and response to dopamine agonists). However, this is not the case for the medial VTA DA which exhibit small to no hyperpolarization-activated cation current (Lammel et al., 2008; T. A. Zhang et al., 2010) and also have lesser response to dopamine agonist as evidenced in the medially located VTA mesocortical DA neurons (Chiodo et al., 1984). Hence, the DA neurons are heterogenous is the VTA with distinction in term of neurochemical and electrophysiological properties. However, this heterogeneity can also be found in their functionality which will be approached in the next chapter on the VTA modulatory properties.

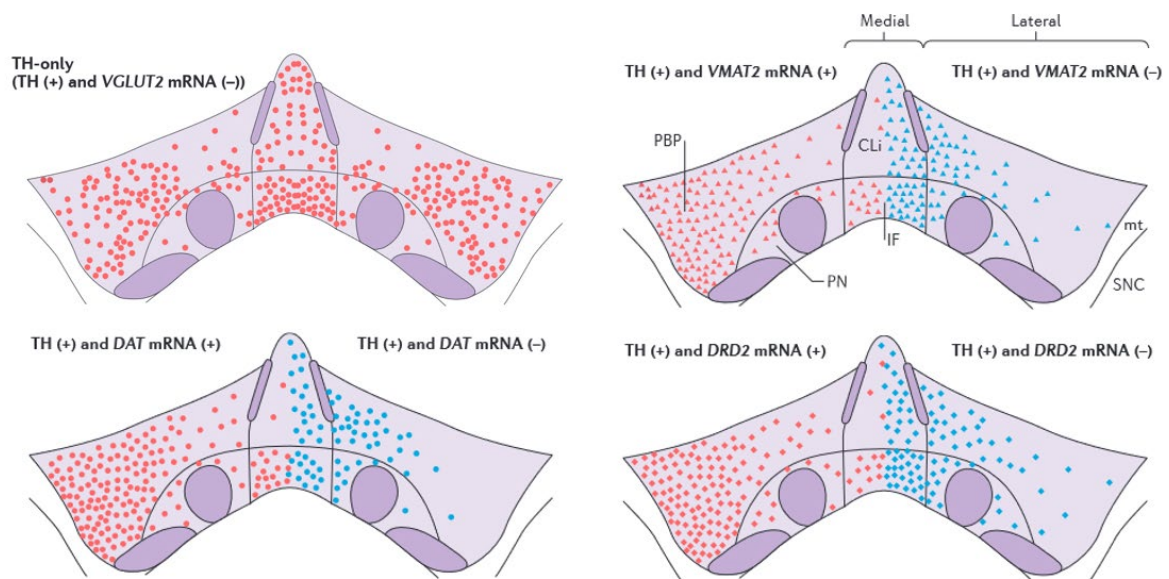


Fig. 11 – Schematic representation of the distribution of dopamine neurons in the VTA of rodents, taken from (Morales & Margolis, 2017). Importantly, TH neurons on this figure were identified with immunolabeling, hence limiting the chance of false positives. Notice that medial VTA neurons are TH positive but often lack VMAT2, DAT and dopamine receptor 2 (DRD2) mRNA, therefore leading to the conclusion that they are not capable of using DA as a neurotransmitter. Abbreviations: CLi: Caudal linear nucleus. IF: interfascicular nucleus. mt: medial terminal nucleus of the accessory optic tract. PBP: parabrachial pigmented nucleus. PN: paranigral nucleus. SNC: substantia nigra pars compacta.

b. GABAergic neurons

While DA neurons comprise the major portion of the VTA, the GABAergic neurons are nonetheless highly present with a third of the VTA neurons (Nair-Roberts et al., 2008). The GABA neurons can be identified by two means in the VTA: the expression of the glutamate decarboxylase enzymes 1 and 2 (also called GAD67 and 65 respectively) or the expression of the vesicular transporter VGAT. Unlike dopamine and glutamate neurons, GABA neurons are found through all the VTA with a higher density in the lateral part of the rostral VTA (Olson & Nestler, 2007). While the VTA GABA functional importance was thought at first to be limited to local inhibition of DA neurons, many studies have revealed a wider range in their role. Indeed, the presence of GABA neurons with mesocorticolimbic, mesoprefrontal and mesoaccumbal projections has led to a high interest in their study (more information in next chapter). The heterogeneity of the VTA GABA neurons is not only in their projections targets but also in genetic markers as well as electrophysiological parameters. Indeed, while the VTA GABA do not express traditional markers used for the different interneurons of the forebrain, several subsets of GABA neurons have been identified. These subsets are characterized by the expression of different transcription factors as putative markers (Lahti et al., 2016). In terms of

electrophysiological properties, two subsets of GABA neurons have been identified in the VTA (Korotkova et al., 2004). One subgroups has high firing rate (~ 8Hz) compared to the other (~ 0.7Hz) with no other change in electrophysiological properties. Overall, electrophysiological studies of VTA GABA neurons have revealed a different profiles compared to DA neurons (shorter action potentials duration, faster tonic firing rates, lack of burst firing, hyperpolarization-activated cation current less frequent and response to NMDAR antagonists) (Bouarab et al., 2019).

c. Glutamatergic neurons

The most recently discovered and also the least expressed in the VTA, the glutamate neurons are heterogeneously distributed in the VTA (Nair-Roberts et al., 2008; Yamaguchi et al., 2007). While identified as expressing VGLUT2, they are mainly found in the medial and anterior portion of the VTA where they outnumber TH-expression neurons (Fig. 12). In spite of their recent discovery (Kawano et al., 2006; Yamaguchi et al., 2007), several studies have shown that VTA glutamatergic neurons are involved in many rewarding and aversive processes (see next chapter on VTA projections for more details). Furthermore, they electrophysiological properties have already been assessed (Hnasko et al., 2012). Indeed, while several studies have strongly suggested that medial VTA glutamatergic neurons do not co-release DA (Yamaguchi et al., 2007, 2011), these neurons seems to closely share electrophysiological properties with medial VTA DA neurons (short action potentials duration, faster tonic firing rates than lateral VTA DA, hyperpolarization-activated cation current less frequent and variable response to DA agonists). Overall, these finding highlight a similarity in electrophysiological properties between medial VTA DA, glutamate and even with GABA neurons (aside from their response to NMDAR antagonists). Hence, the glutamatergic neurons contribute to the heterogeneity of the VTA.

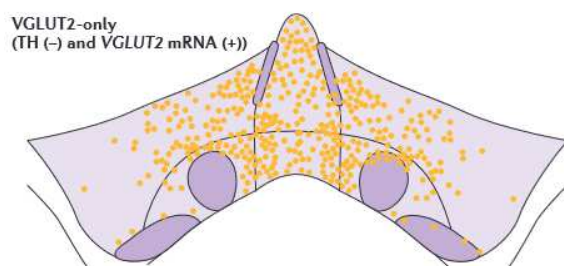


Fig. 12 – Schematic representation of glutamatergic neurons distribution in the VTA of rodents, taken from (Morales & Margolis, 2017). Yellow dots indicate VGLUT2 positive neurons. In striking contrast with TH positive neurons, VGLUT2 neurons are mainly located in the medial VTA.

d. Co-transmission neurons

So far, I have described the heterogeneity of the three cell-types comprising the VTA, however these cell-types are not mutually exclusive. Indeed, while a great portion of VTA neurons are specific of one neurotransmitter, several subsets of neurons can release two neurotransmitters

simultaneously. This ability of subsets of neurons to co-release neurotransmitters greatly increase the complexity of the VTA and the span of its actions. Hence, it is necessary to discuss the three main subsets of neurons capable of co-release (see Fig. 13 for distribution in the VTA):

- Dopamine-glutamate neurons : because of the previously mentioned issues with the identification of VTA DA neurons, the prevalence of this co-releasing population is variable between species and between VTA subregions (Yamaguchi et al., 2015). Indeed, rats VTA is comprised of TH-immunoreactive (TH-IR) neurons profusely found throughout all the VTA including the medial VTA (RLi and IF). However, this is not the case of mice medial VTA where little to no TH-IR is found. Hence, because of the prevalent medial location of VTA glutamate neurons, the number of dopamine/glutamate co-releasing neurons has been described as quite low especially in the medial VTA. Indeed, only 1% of VTA VGLUT2 neurons in the RLi were found to be also TH-IR (Yamaguchi et al., 2015). Furthermore, only 7% in the IF, 10% in the lateral PBP and PN and 20% in the CLi were found to be VGLUT2 neurons that were TH-IR in mice. While this study of Yamaguchi showed little medial VTA dopamine/glutamate co-release in mice, the lack of VMAT2 and DAT expression in this same area in rats underline a similar absence of co-release in the rats. However, these results are to be put in perspective as other studies relying on different technical methods have suggested a different proportion for DA/Glut co-releasing neurons. Indeed, in their study, Taylor et al., reported a higher proportion of VTA DA/glut co-releasing projection neurons (Taylor et al., 2014). Indeed, they found VGLUT2 neurons to be TH-IR up to 7% for the RLi, 18% for the IF, 32% for the PBP, 54% in the PN and 56% in the CLi. Furthermore, another study that did not distinguish the different VTA subregions also reported slightly high co-release levels with VGLUT2 neurons TH-IR up to 18% (Faget et al., 2016). Overall, the previous studies underlined a albeit low and differential corelease of DA for VGLUT2 neurons depending on the subregions of the VTA studied. Interestingly, a similar heterogeneity was also found in humans and primates where DA/glut neurons, conversely, were found more profusely in the lateral VTA. Because of their low prevalence, little is known to my knowledge about the electrophysiological properties of dopamine/glutamate co-releasing neurons. However, studies in VTA→NAc projections have illustrated the segregation of DA and glut release to different axonal domains (S. Zhang et al., 2015). Hence, such pattern suggests a fast excitatory neurotransmission by glutamate release, combined with a slower modulatory signalling by DA.
- Dopamine -GABA neurons: only a small subset of VTA neurons have been directly identified as co-releasing DA/GABA in rats and mouse. Indeed, several reports focused on identified a small population of TH-IR co-expressing GAD65 mRNA (González-Hernández et al., 2001; Olson &

Nestler, 2007). Importantly, as previously mentioned, the use of TH as marker of dopamine neurons is subject to caution. This is especially true following a study targeting the VTA → lateral habenula (LHb) neuron where stimulation of TH-CRE VTA neurons was associated with the synaptic release of GABA but not DA at the LHb (Stamatakis et al., 2013). However, while TH expression does not necessarily mean DA release, several studies have highlighted mechanisms of actual DA/GABA co-release. These studies proved the presence of co-release despite the lack of GABA synthesis enzymes or GABA vesicular transporters. Indeed, subsets of VTA TH-IR neurons have been found to release GABA onto striatal medium spiny neurons (MSN) while lacking usual marker of GABA neurons. This GABA release was found to be linked not to the neuronal synthesis of GABA but to an uptake of GABA from extracellular compartment. Following this uptake, the GABA is then packed for vesicular release by VMAT2 together with DA (Tritsch et al., 2014, 2016). Furthermore, alternative GABA synthesis pathway have been found to be expressed in DA neurons through the action of the aldehyde dehydrogenase 1a1 enzyme (J. I. Kim et al., 2015). Together, these different mechanisms account for the release of GABA by dopamine neurons.

- Glutamate-GABA neurons : co-release of Glut/GABA was first identified in the VTA in a major portion of the populations projecting to the LHb (Root, Mejias-Aponte, Zhang, et al., 2014). Interestingly, in the same study, Glut/GABA co-release was further characterized. Indeed, glutamate was found to be restricted to asymmetric synapses (usually classified as excitatory) and GABA to symmetric synapses (usually classified as inhibitory). This co-releasing neurons are found throughout all the VTA but are more concentrated in the medial anterior VTA (Root, Zhang, et al., 2018) where glutamate neurons are found more profusely. With the discovery of this intriguing population a recent study has characterized the electrophysiological properties of these neurons. This work showed that Glut/GABA neurons and Glut neurons had overall shared features. This included slightly hyperpolarized resting membrane potential, greater rheobase, lower spontaneous firing frequency and therefore a decreased excitability (Miranda-Barrientos et al., 2021). In spite of this characterization, the VTA Glut/GABA population remains elusive in its functional properties as solely inputs to the LHb and to the ventral pallidum (Yoo et al., 2016) have been so far identified.

The VTA is also comprised of a subsets of neurons expressing markers for all three neurotransmitters (Root, Mejias-Aponte, Zhang, et al., 2014). However so far, no study has successfully proven simultaneous co-release of these neurotransmitters in these neurons. In conclusion, the VTA possess an incredible anatomical and neurochemical heterogeneity that contributes to its functional

diversity. This heterogeneity is particularly important as the VTA is comprised of a complex network of neuronal afferent and efferent projections that differs between the different subregions of the VTA and the different neurochemical subsets. Hence, while I decided rather not to mention the networks of inputs and outputs of the VTA in this chapter but rather in the next. This separation was for me warranted by the incredible complexity of afferent and efferent projections and they respective contribution to specific behaviors through the regulation of the VTA and its downstream effectors.

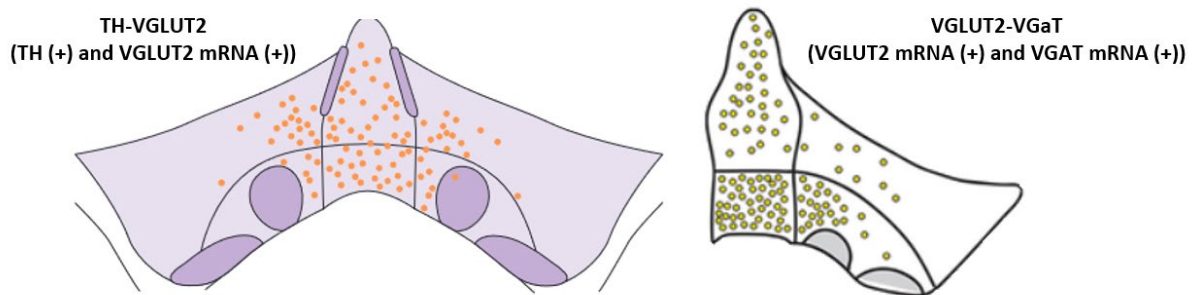


Fig. 13 – Schematic representation of combinatorial neurons distribution in the VTA of rodents for glutamate-dopamine and glutamate-GABA neurons, taken from (Morales & Margolis, 2017) and (Root, Zhang, et al., 2018). Of note, TH-VGLUT2 are located in the medial VTA, where TH-neurons have been shown to be unreliable in the dopaminergic nature (see previous chapter and Fig. 11). Combinatorial glutamate-GABA (VGLUT2-VGAT) neurons are also found more profusely in medial aspect of the VTA and are mainly found in the IF and medial PN.

B. Functional role of VTA neurons

The VTA has long been known as one if not the most prominent cerebral structure involved in reward. However, the view on the VTA has changed through the last decades with studies highlighting that aversion is also strongly regulated by this region. Hence, a more comprehensive view of the VTA has emerged, underlining its paramount role in valence processing and defensive behaviors. In this chapter, I will describe the known afferences and efferences of the VTA and how they mediate a wide range of behaviors. Because of my thesis is focused on defensive behaviors, I will mainly focus on this topic and will only quickly summarize the VTA role on other processes and behaviors.

1) VTA and valence processing

Amongst the diverse process regulated by the VTA, reward processing has been the focus of a lot of attention. Indeed, the VTA DA neurons have been thoroughly studied for their role in promoting reinforcement and reward through two main pathways: mesolimbic and mesocortical (colloquially known as the mesocorticolimbic pathway). The mesocorticolimbic pathway is comprised of VTA DA

projections toward the striatum including dorsal part (caudate putamen) and ventral parts (NAc) but also toward the prefrontal cortex. This pathway has been established as particularly important for reward-directed behaviors. Indeed, several studies have shown that drugs of abuse play on the reward system by acting on the mesolimbic pathway and promoting release of DA in the NAc (Di Chiara & Imperato, 1988). Furthermore, depletion of DA in the NAc decreases the rewarding effects of drugs of abuse (Gerrits & Van Ree, 1996). The mesolimbic pathway however is not only involved in drug-mediated reward but in a wide range of environmentally rewarding stimuli such as feeding (Martel & Fantino, 1996) and social interaction (O'Connell & Hofmann, 2011; Trezza et al., 2011; Van Kerkhof et al., 2014). However, this view of the VTA DA as promoting reinforcement is too simplistic. Indeed, several studies have shifted the view of the DA as encoding not simply positive valence but to encode the prediction error of rewards. This prediction is characterized by the switch from tonic to phasic activity of a subset of DA neurons when a reward that is unexpected or better expected is obtained (Schultz, 1998). Conversely, a smaller or unobtained reward is associated with a decrease of tonic activity and halting of phasic activity of these DA neurons (Bromberg-Martin et al., 2010). Overall, the involvement of the DA system for prediction error of reward is key for generating and sustaining motivation toward a stimulus and is thought to be an important player in the development of addictions (for good review on this system, see (Schultz, 2016)). While the DA mesocorticolimbic system is important for reward-processing as mentioned above, several studies have identified inputs and outputs of the VTA that signal reward (see Fig. 14 for summary):

- Local connections : the presence of local efferences onto DA neurons by GABA (see review (Bouarab et al., 2019)) and glutamate (H. L. Wang et al., 2015) is an important mechanism that can regulate VTA DA activity and therefore reward. Hence, it is important to note the nature and source of inputs to the VTA as well as the cell-type.
- The dorsal raphe nucleus (DRN) : Indeed, long-distance efferences from the DRN are targeting the VTA. Activation of vGluT3 DRN projections to the VTA has been shown to elicit release of DA to the NAc, hence promoting reward (J. Qi et al., 2014). Interestingly however, the serotonergic neurons of the DRN involvement in reward is still questioned. This debate is linked to the net inhibitory effect of 5-HT on DA neurons while rewarding effects are seen following optogenetic stimulation of 5-HT efferences to the VTA but these projections have also been found to express vGluT3 (Courtiol et al., 2021).
- The lateral hypothalamus : several studies based on the use of electrical stimulation of the LH have illustrated a role of the LH in promoting DA release in the NAc (Margules & Olds, 1962; Z. B. You et al., 2001). However, this technique has several limitations in its effects on broad structure (rather than specific discrete circuits) and its spatial restriction. The use of more

precise techniques such as optogenetics have allowed to dissect the underlying circuits responsible for the LH promotion of reward. More precisely, activation of neurotensin-expressing LH neurons is associated with an increased release of glutamate to the VTA and potentiation of glutamatergic transmission to VTA DA neurons (Kempadoo et al., 2013). Furthermore, the role of the LH in promoting reward has been further confirmed by studies on its neuropeptidergic transmission modulation of VTA DA (Perez-Bonilla et al., 2020) but also by action on its non-DA neurons where it promotes motivation (Schiffino et al., 2019). This action of the LH on non-DA seems to promote reward through GABAergic inputs to VTA GABA neurons. As VTA GABA are known to inhibit local VTA DA (discussed later), the resulting rewarding effect of LH GABA inputs is associated to the disinhibition of the VTA DA projecting to the NAc (Barbano et al., 2016; Nieh et al., 2016).

- The BNST : stimulation of BNST GABAergic inputs to the VTA has been shown to promote reward (Jennings et al., 2013). While the target of GABA BNST neurons remains elusive, it seems to preferentially innervate the VTA non-DA neurons. Furthermore, a more recent study has shown the PN to be preferentially targeted by BNST GABA while expression several neuropeptides that could further contribute to the activation of VTA DA neurons (Soden et al., 2022). Hence, from a mechanistic view, these results suggest that the BNST GABA could target the VTA GABA, therefore, leading to a disinhibition of VTA DA neurons. However, this hypothesis remains to be tested.
- The ventral pallidum: similarly to the BNST and the LH, the VP provides Glut and GABA projection to the VTA. This GABA projections also promotes reward through real-time place preference and reinforcement (Faget et al., 2018).
- The LHb : while strongly known for its role in mediating aversion (described latter), the LHb can also promotes reward through VTA GABA afferences. Indeed, an optogenetic stimulation of VTA TH neurons have shown to mediate reward with a notable absence of DA release but instead of GABA in the LHb (Stamatakis et al., 2013).
- The medial preoptic area (MPOA): the MPOA also provide Glut and GABA inputs to the VTA. The activation neurotensin peptidergic GABA inputs as well as purely GABA inputs to the VTA have been shown to promote reward through real-time place preference (McHenry et al., 2017). These GABA inputs are thought to target the GABA population of the VTA, however this mechanism remains putative and therefore to be tested.
- The lateral preoptic area (LPOA): the LPOA provides GABA inputs to the VTA. Surprisingly, activation of these input triggers aversion with reinforcement (assessed by intracranial self-stimulation protocol; ICSS). Furthermore, this modulation targets the VTA GABA population, and seems to induce a mixed excitation and inhibition of VTA DA neurons (Gordon-Fennell et

al., 2020). This discrepancy requires further investigation in order to better appreciate the role of the LPOA in reward.

- The laterodorsal tegmentum (LDTg): this small brainstem nuclei comprised of Glut, GABA and cholinergic neurons. This structure is important in mediating the phasic activity of VTA DA as LDTg inactivation prevent such bursting events (Lodge & Grace, 2006). Optogenetic activation of LDTg projection to the VTA further confirmed this role of the LDTg in mediating reward by promoting place preference (Lammel et al., 2012). This effect is thought to be mediated by cholinergic and glutamatergic LDTg neurons projecting to the VTA as their activation has been associated with conditioned place preference and therefore reward (Steidl et al., 2017; Xiao et al., 2016). Furthermore, this net rewarding effect of the activation of LDTg is associated with an increased DA activity in NAc projecting VTA neurons (Coimbra et al., 2021). Overall, the previously mentioned research and others have placed the LDTg as a key modulator of the VTA activity during positive valence signalling.
- The mPFC: the use of ex vivo electrophysiology and in vivo optogenetic confirmed the existence of a mPFC → VTA DA → NAc lateral shell. This excitatory projection was proven to promote reward through ICSS (Beier et al., 2015).
- VTA Non-DA mediated reward: while most of the reward pathway are linked to an increased dopaminergic activity in the mesocorticolimbic system, several key studies have identified that VTA glutamatergic neurons can promote reward-seeking behaviors independently of VTA DA modulation. Indeed, stimulation of VTA glut neurons has been associated with reward in a first study of (H. L. Wang et al., 2015). Stimulation of VTA glut → NAc pathways was then found to be rewarding (Yoo et al., 2016) and was dissected by (Zell et al., 2020) which showed that glutamatergic inputs to the NAc promote reinforcement independently of DA release.

Overall, I tried here to provide a background on the afferent and efferent structure of the VTA that can contribute to positive valence signalling (see Fig. 14 for summary). However, because of the towering number of studies on VTA DA involvement in rewarding processes, it is likely that other structures are involved and not mentioned here.

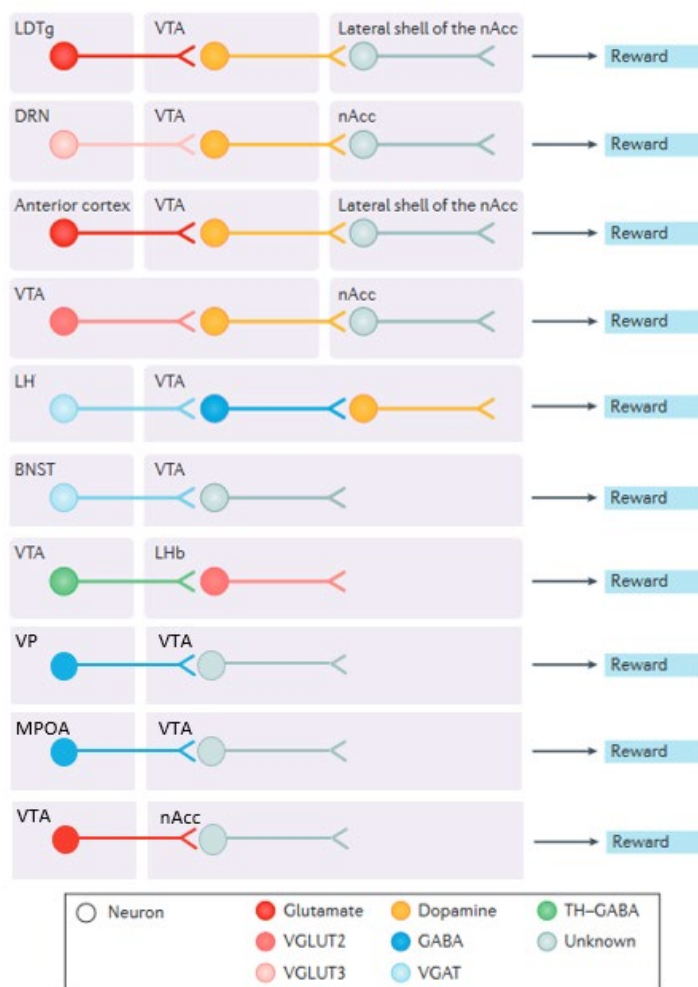


Fig. 14 – Schematic summary of the afference and efference of the VTA mediating reward-related behaviors, adapted from (Morales & Margolis, 2017). Abbreviations: BNST: bed nucleus of the stria terminalis. DRN: dorsal raphe nucleus. LDTg: laterodorsal tegmentum nucleus. LHb: lateral habenula. LH: lateral hypothalamus. MPOA: medial preoptic area. NAc: nucleus accumbens. TH: tyrosine hydroxylase. VGAT: vesicular GABA transporter. VGLUT: vesicular glutamate transporter. VTA: ventral tegmental area. VP: ventral pallidum.

As the VTA is key for the appraisal of a stimulus, it can also promote aversion. Hence, it is important to discuss the role of VTA signalling of aversion as VTA DA do not only signal reward (see Fig. 15 for summary). Indeed, a subset of VTA DA neurons targeting the mPFC and receiving glutamatergic excitatory projections from the LHb have been shown to signal aversion. More precisely, in their study, (Lammel et al., 2012) showed that activation of LHb→VTA neurons was associated with conditioned place aversion (CPA). Furthermore, they identified the LHb to preferentially connect to the mPFC projecting VTA DA neurons and prevented LHb induced CPA through the local injection of a dopamine antagonist in the mPFC. It is important to note that a subset of VTA DA neurons is activated in response to both rewarding or aversive events. Hence, these neurons have been shown not to directly modulate valence but rather emotional salience (Matsumoto & Hikosaka, 2009). Overall, DA

neurons are also important to modulate aversion, however, other neuronal populations of the VTA can contribute to signalling negative valence.

VTA GABA neurons can also promote aversion through non-local projections such as the ones to the DRN serotonergic neurons which been shown to promote real time place aversion (Y. Li et al., 2019). However, local VTA GABA neurons inhibition of VTA DA has been strongly associated with aversion. More precisely, stimulation of local VTA GABA was shown to elicit aversion through neurons inhibition of VTA DA neurons (Tan et al., 2012). In accordance with this VTA GABA local modulation of aversion, several others VTA pathways contribute to the induction of aversive response through putative VTA GABA-mediated feedforward inhibition of VTA DA. Indeed, while BNST, VP, LH and MPOA GABA afferences to the VTA promote reward, their glutamatergic counterparts promote aversion (Faget et al., 2018; Jennings et al., 2013; Nieh et al., 2016; G. W. Zhang et al., 2021). Of note, it has been proposed in a recent study that LH glutamate inputs to the VTA could mediate aversion through modulation of a specific VTA DA subpopulations targeting the ventral NAc medial shell (De Jong et al., 2019). Furthermore, a similar mechanism of VTA GABA mediated feedforward inhibition has been suggested to drive aversion for inputs from the LHb to the VTA (Omelchenko et al., 2009). Hence, a feedforward inhibition of the VTA DA would appears coherent for these glutamatergic afferences. Overall, these studies highlight the importance of VTA GABA transmission in mediating aversion. But what about the involvement in aversion of last VTA cell populations not yet mentioned, the glutamatergic neurons.

Several glutamatergic non-local projections from the VTA can mediate aversion. VTA glutamate neurons promote aversion through excitation of the LHb (and therefore potentially downstream rostromedial tegmental nucleus; RMTg). Indeed, stimulation of VTA VGLUT2 afferences to the LHb is associated with CPA (Root, Mejias-Aponte, Qi, et al., 2014). Interestingly, an indirect pathway with LHb glutamate projections to the RMTg (or tail of the VTA) can also contribute to aversion (Stamatakis & Stuber, 2012). Indeed, glutamatergic neurons of the LHb emit major efferences to the RMTg, which in turn provide GABAergic inputs to the VTA DA during aversive events (Jhou et al., 2009; Hao Li et al., 2019). Another study on the VTA inputs to the NAc has brought forth another way for the VTA glut neurons to mediate aversion. Indeed, in their study, (J. Qi et al., 2016) have found that optogenetic activation of glutamatergic mesoaccumbens pathway elicited aversion through feedforward inhibition of NAc medium spiny neurons.

Taken together, these studies suggests that VTA glut neurons may be shifted toward regulation of aversion rather than reward. Indeed, three VTA glut subsets have been identified following their activation pattern to aversive and rewarding stimulus (Root, Estrin, et al., 2018). One small subset

increases its activity in response to both aversive and reward stimulus, therefore signalling salience. However, the majority of the VTA VGLUT2 neurons belongs to two subsets where their activity is increased in response to an aversive stimulus, while either no change or decreased activity is observed in response to a rewarding stimulus. Furthermore, another study also highlighted the existence of VTA glut subsets that differently respond to aversive event (Montardy et al., 2019). These findings are of particular interest for my thesis project as activation during aversive events of VTA glut could be linked to a role of this neuronal population in promoting anxiety. However, more direct evidences have identified a role for the VTA and its glutamatergic population in mediating defensive behaviors and will be described in the next chapter.

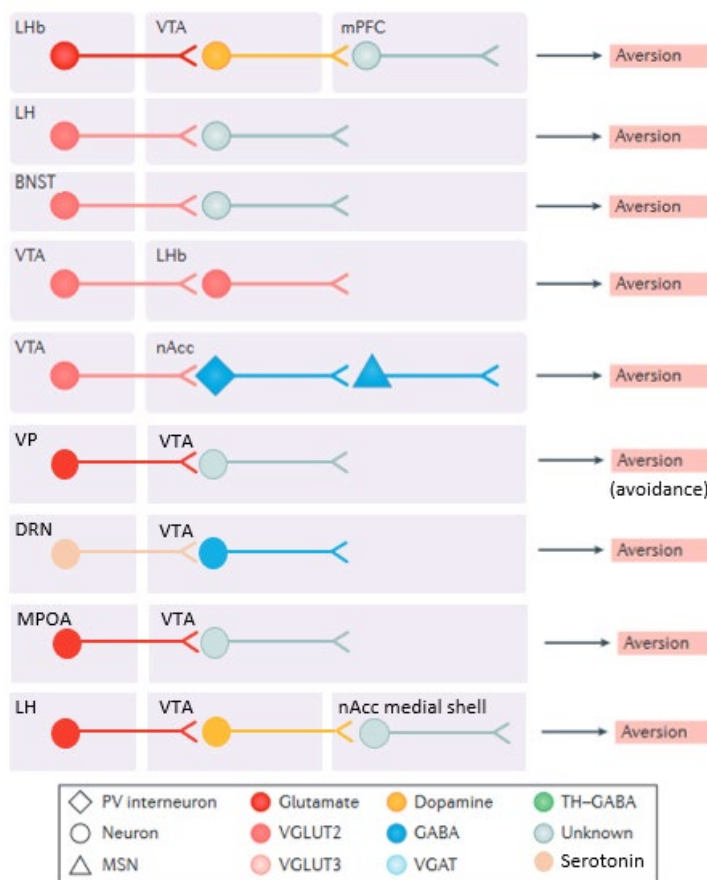


Fig. 15 – Schematic summary of the afference and efference of the VTA mediating aversion-related behaviors, adapted from (Morales & Margolis, 2017). Abbreviations: BNST: bed nucleus of the stria terminalis. DRN: dorsal raphe nucleus. LHb: lateral habenula. LH: lateral hypothalamus. MSN: medium spiny neuron. MPOA: medial preoptic area. mPFC: medial prefrontal cortex. NAc: nucleus accumbens. TH: tyrosine hydroxylase. VGAT: vesicular GABA transporter. VGLUT: vesicular glutamate transporter. VTA: ventral tegmental area. VP: ventral pallidum.

2) Defensive behaviors

The VTA role in mediating defensive responses have received little focus in comparison to the great number of studies on its role in valence assignment, addiction and depression. However, several studies have first suggested a role for the VTA DA neurons in defensive behaviors. Indeed, disruption of activation of VTA DA neurons in response to aversive event such as fear conditioning has been associated with the induction of generalized anxiety (Zweifel et al., 2011). Interestingly, this study and many others suggest that a decrease of VTA DA neurons activity is triggered in response to both aversion and anxiety/fear. However, a series of works on dopamine receptors expressed in the amygdala have highlighted incoherence with this simplistic view. Indeed, experiments of dopamine receptor blockade with local injection of dopamine 1 receptor antagonist in the amygdala were found to prevent fear (Lamont & Kokkinidis, 1998) and anxiety expression (De La Mora et al., 2005). Mechanistically, these effects on fear and anxiety are thought to be induced through the DA-mediated decrease of amygdaloid local inhibitory tone to the BLA and CeA (de la Mora et al., 2010). However, a putative increase of VTA DA activity would seem more coherent to promote the amygdala dopaminergic promotion of anxiety and fear. This example of confusing reports highlights a far more complex role of VTA DA in the modulation of defensive behaviors. As my thesis project is based upon the study of neuronal circuitry involved in anxiety, I have decided in this chapter to mainly describe here the known afference and efference of the VTA promoting defensive behaviors. While anxiety is not directly a behavior, I will refer to it in this chapter as a proxy for the expression avoidance and risk-assessment.

When studying the involvement of the VTA in mediating defensive behaviors, it is logical to assess the connectivity and modulatory effect of this region on known centers of anxiety and fear. For this reason, I will speak first of the connectivity of the VTA with one, if not, the main center in regulating defensive behaviors, the amygdala.

In spite of the identification of VTA DA inputs to the amygdala, the contribution of this neuronal population in promoting anxiety and fear as long remained putative. Indeed, for a long-time, only studies using pharmacological tools as mentioned above were carried out. These studies did not prove a causal link between fear and anxiety expression and direct modulation of VTA DA efferences to the amygdala. However, a recent study of (Morel et al., 2022) provided evidence of the direct involvement in anxiety of VTA DA neurons. In their study, Morel et al, showed that optogenetic silencing of VTA → BLA dopamine neurons is associated with an increased anxious phenotype while, conversely, activation is associated with a decrease in anxiety. Furthermore, they functionally distinguished VTA DA efference to the BLA from other efference to the NAc as modulation of VTA DA inputs to the BLA alone was associated with change in anxiety level while not affecting social interaction. Albeit surprising in the

light of the previous pharmacological studies showing that D1R blockade in the amygdala prevent anxiety expression, these results are consistent with another recent study about nicotine effect on VTA DA afference to the amygdala (Nguyen et al., 2021). In this study, optogenetic silencing of VTA DA projections to the amygdala (VTA DA → Amy) was found to elicit similar anxiogenic effect as nicotine. Conversely, optogenetic activation of VTA DA → Amy prevented the anxiogenic effect of nicotine. Overall, these two studies show indeed a causal link between VTA DA neurons activity and defensive behaviors. However, more work is required in order to better understand how an increase of VTA dopaminergic activity to the amygdala can simultaneously decrease anxiety levels while DA is thought to promote anxiety in the amygdala by removing the cortical brake on local inhibitory neurons (Aksoy-Aksel et al., 2021).

While the VTA DA have been identified to regulate defensive behaviors, other VTA inputs to the amygdala have also been shown to contribute. GABA neurons from the VTA have been shown to project to the CeM, where their activation promote flight-to-nest behavior (Zhou et al., 2019). More precisely, a structure important to convey information about visual threat, namely, the superior colliculus, provide excitatory inputs to VTA GABA which promote two parallel defensive behavior. On one hand, the previously mentioned flight-to-nest behavior is induced through GABA efference to the CeM and optogenetic activation of this superior colliculus (SC) glutamatergic projection to VTA GABA can elicit spontaneous flight-to-nest behavior. On the other hand, this same study suggests that SC-mediated feedforward inhibition onto VTA DA neurons do not alters flight-to-nest behavior but increase hiding behavior. Overall, this study has highlighted an important role of the VTA GABA neurons in promoting defensive behavior such as visual threat-evoked escape to safety and increase hiding time in a safe zone.

Last but not least, VTA glutamatergic neurons have also been recently involved in the modulation of defensive behaviors. Indeed, (Barbano et al., 2020) showed that genetic ablation of VTA VGLUT2 neurons was associated with a decrease in active escape behavior. Furthermore, they identified glutamatergic projection from the LH to be responsible for this effect by mainly targeting the VTA glut neurons. This study demonstrated a direct involvement in active escape of LH glut projection to VTA glut as optogenetic activation and inhibition of this projection was associated respectively with increase and decrease of active escape in response to a looming stimulus. Interestingly, this study had several surprising findings in comparison with the study on VTA GABA neurons involvement in flight-to-nest behavior (Zhou et al., 2019). Indeed, Barbano et al, also showed that VTA GABA ablation did not change flight behavior in response to looming stimulus or predator odor exposure. Furthermore, in a looming test with an available shelter, optogenetic inhibition of LH-VTA glut neurons did not change the time spent hiding in the shelter while activation of the same

projections decreased time spent in the shelter. Therefore, while VTA GABA neurons seems to promote hiding behavior, the VTA glut neurons rather promote escape behavior. Similarly to VTA GABA neurons, the involvement of VTA glut in defensive behavior has been recently linked to modulation of the amygdala. Indeed, a recent study has shown that VTA glut optogenetic activation of CeA terminals is associated to an increase of aversion as well as defensive behavior (Chen et al., 2022). Indeed, upon optogenetic stimulation of glutamatergic VTA→CeA neurons, an increase of avoidance, burrowing, escape and flight-to-shelter was recorded.

Taken together, the aforementioned studies have highlighted an important role for the VTA in mediating defensive behaviors through modulation of the amygdala. However, the VTA inputs to the amygdala are not restricted to the one listed above and further characterization of these inputs could provide better insights on the role of the VTA in mediating amygdala-regulated defensive behaviors. Furthermore, further studies are required because of the connectivity of the VTA with key region in the modulation of such behaviors. This requirement is even more relevant as afferent from these regions to the VTA have been shown to regulate defensive behaviors. Indeed, further research on, amongst others, the LH, LHb and BNST may highlight bidirectional pathway with the VTA in the regulation of defensive behaviors.

THÈSE DE DOCTORAT

OBJECTIVES

So far, I have described the circuitry and mechanisms of defensive behaviors related to fear and anxiety and how the amygdala and VTA have respective role in these behaviors. While amygdala hyperactivity is commonly found in anxiety disorders, the underlying mechanisms of silencing of local amygdalar inhibition network and of increased sensory excitatory transmission may not fully reflect how the amygdala promote defensive behaviors. Indeed, several studies have identified non-sensory modulatory projection that may contribute to the regulation of the amygdala. Because of its role in mediating aversion and its recently discovered role in mediating defensive behaviors, the VTA appears as a good candidate to contribute to this modulatory regulation of the amygdala.

The larger goal of my thesis was therefore to study how the VTA may promote defensive behaviors through its connectivity to the amygdala. To achieve this objective, my thesis was divided in the study of several VTA inputs and output that may regulate fear- and anxiety-related defensive behavior.

The first part of my thesis will parse the role of VTA glutamatergic neurons in promoting adaptative and maladaptive anxiety through modulation of the amygdala. I assessed here if VTA glutamatergic projection to the basolateral amygdala were capable to regulate amygdala activity and its downstream effect on anxiety. Hence, this part of my thesis can be subdivided in several axes:

- 1) Parsing the VTA glutamatergic connection to the amygdala
- 2) Assessing if stress affect the VTAglut→BLA neurons
- 3) Determining if VTAglut→BLA neurons contribute to the modulation of anxiety

The results I assembled for this first part of my thesis have crystallized in a first author-article that is currently in preparation and in a poster that I presented at the FENS Forum (July 9-13, 2022, Paris).

Synaptic potentiation of VTA glutamatergic efferents onto basoamygdala principal neurons underlies pathological anxiety

Contesse T, Royon L, Glanetas C, Fofu H, Georges F, Fernandez SP, Barik J
(in preparation)

The second part of my thesis will assess how a new non-canonical input to the VTA can promote a fear-related defensive behavior. We found here that the LDTg is capable regulating fear-induced freezing behavior. We therefore wondered what neurotransmitter release was associated with this defensive behavior and how the VTA integrate and transmit this input to the amygdala. Therefore, this part of my thesis was also subdivided in several objectives:

- 1) Mapping and characterizing which LDTg cell-types can promote freezing
- 2) Understanding how VTA integrates LDTg inputs to promote freezing
- 3) Assessing which structure downstream of the LDTg-VTA pathway mediates freezing

I participated in this part of my thesis by carrying all the in vivo optogenetic and several chemogenetic behavioral experiments. The results I gathered here allowed me to be credited as co-first author in an article soon to be published (accepted for publication) in *Molecular Psychiatry*.

A non-canonical GABAergic pathway to the VTA promotes unconditioned freezing

Broussot L*, Contesse T*, Costa-Campos R, Glangetas C, Royon L, Fofu H, Lorivel T, Georges F, Fernandez SP+, Barik J+

* These authors contributed equally to this work.; + co-last authors.

(accepted at *Molecular Psychiatry*)

My work in a team studying psychiatric disorders also led me to contribute during my thesis to several other projects. These secondary projects were not directly related to my thesis axes and therefore will not be discussed here (see annexes for the mentioned papers). These projects are the following:

- 1) I studied during my master internship the molecular pathways involved in the stress response in the striatum. My work during my thesis on this project as main experimenter led me to accumulate sufficient data to produce an article as first author published in 2021 that I presented in the form of a poster at the FENS 2020 online forum:

Dopamine and glutamate receptors control social stress-induced striatal ERK1/2 activation

Contesse T, Broussot L, Fofu H, Vanhoutte P, Fernandez S, Barik J
Neuropharmacology volume 190, Article number : 108534 (2021)

- 2) My contribution in generating histological and microscopy data for another project led me to be co-author on the following paper published in 2018:

Mesopontine cholinergic inputs to midbrain dopamine neurons drive stress-induced depressive-like behaviors

Fernandez S.P, Broussot L, Marti F, Contesse T, Mouska X, Soiza-Reilly M, Marie H, Faure P, Barik J

Nature Communications volume 9, Article number : 4449 (2018)

- 3) My contribution in performing stereotaxic viral injections for another project led me to be co-author in the following paper in preparation accessible in BioRxiv :

Dopamine and stress signalling interplay patterns of social organization in mice

Battivelli D, Vernochet C, Nguyen C, Zayed A, Meirsmann A.C, Messaoudene S, Fieggen A, Dreux G, Marti F, Contesse T, Barik J, Tassin J, Faure P, Parnaudeau S, Tronche F

In preparation, early access on BioRxiv, Article number: 856781

THÈSE DE DOCTORAT

RESULTS

Axis 1: Parsing VTA glutamatergic regulation of amygdala and its role in anxiety

Synaptic potentiation of VTA glutamatergic efferents onto basoamygdala principal neurons underlies pathological anxiety

Contesse T, Royon L, Glangetas C, Fofu H, Georges F, Fernandez SP, Barik J
(in preparation)

Summary

In the following study, we assess if VTA glutamatergic neurons can contribute to the induction of anxiety disorders through efferences to the BLA in mice. To parse the functional role of VTA projections to the BLA in the promotion of anxiety, we combined the use of optogenetic and chemogenetic tools with behavioral and electrophysiological recordings. We parsed the anatomical and functional connectivity of VTA glutamatergic efference to the BLA. We then tested if social stress can modulate the activity of these neurons. We modulated selectively this neuronal projection and measured the downstream consequence on anxious behaviors. Finally, we tested if modulation of the glutamatergic efference VTA→BLA can be used to induce or revert the apparition of anxiety disorders. Overall, we found that glutamatergic projection from the VTA regulate the activity of the BLA and their dysregulation promote anxious behaviors. Furthermore, while silencing this neuronal projection did not revert anxiety disorders, chronic activation led to a anxiety disorder-like phenotype in mice.

Contribution

This project has been the focal point of my PhD. The design of the project has been shared between me and my two supervisors and last authors: Sebastian P FERNANDEZ and Jacques BARIK. I have realised most of the stereotaxic viral injections and histochemical analysis, all the behavioral experiments and most of data analysis. Electrophysiological recordings were performed by Sebastian P FERNANDEZ. Single-cell PCR experiments were carried out by Sebastian P FERNANDEZ and Hugo FOFO. In vivo fiber photometry recordings were realised by Léa ROYON.

Synaptic potentiation of VTA glutamatergic efferents onto basoamygdala principal neurons underlies pathological anxiety

Short title: VTA glutamate pathway to Amygdala promote anxious disorders

Thomas Contesse^{1,2}, Léa Royon^{1,2}, Hugo Fofó^{1,2}, Christelle Glangetas³, François Georges³, Jacques Barik^{1,2*}, Sebastian P. Fernandez^{1,2*}

1 Université Côte d'Azur, Nice, France.

2 Institut de Pharmacologie Moléculaire & Cellulaire, CNRS UMR7275, Valbonne, France.

3 Université de Bordeaux, CNRS, IMN, UMR 5293, F-33000 Bordeaux, France

* These authors contributed equally to this work

Correspondence should be addressed to J.B. (barik@ipmc.cnrs.fr) and S.P.F. (fernandez@ipmc.cnrs.fr)

Keywords: Amygdala, Ventral tegmental area, Glutamate, Stress, Anxiety

ABSTRACT

Anxiety disorders are a major human blight afflicting high proportion of the population and being hard to diagnose. A lack of understanding of the functional neuronal network regulating anxiety is responsible for the lack of efficiency of treatment for these pathologies. The amygdala is a key structure that participates in the continuous detection and evaluation of environmental stimuli to generate appropriate motor, autonomic and hormonal responses to threats. Hyper-reactivity of the amygdala is a key trait in many anxiety clinical populations. In mice, stress exposure can increase the activity of amygdala neurons and innate anxiety and fear. Despite these evidences, the circuits mechanisms that leads to increase emotional output from the amygdala are not known.

Here, we study the contribution of a midbrain glutamatergic input to amygdala's hyperactivity associated with anxiety disorders. We showed that VTA Glu neurons preferentially innervate and synapse onto glutamatergic principal neurons in the basolateral amygdala. In vivo selective optogenetic activation of VTA Glu terminals in the basolateral amygdala was not sufficient to modulate basal anxiety levels in mice. However, fiber photometry measurement showed that VTA Glu neurons increase their activity during exploration of aversive areas of the zero-maze. Using the chronic social defeat paradigm, we demonstrate that heightened anxiety is associated with increased excitability of VTA Glu neurons projecting to the amygdala, and increased excitatory inputs to basolateral amygdala principal neurons. However, stress-induced anxiety was not reversed by chemogenetic silencing of this pathway. Instead, we provide evidence that exposure to chronic stress strengthens synaptic VTA \rightarrow BLA connectivity, and that artificial potentiation of these synapses by in vivo optogenetics was sufficient to increase innate anxiety. Taken together, our study uncovered a new pathway contributing to the induction of anxiety-disorders through dysregulation of amygdala activity.

INTRODUCTION

Anxiety is a normal and necessary response towards the uncertainty of a threat. This response helps drive animals towards caution and preparation should a threat be confirmed. In spite of their positive aspect on survival, when excessive, pathological, or triggered inappropriately, fear and anxiety form the basis of a variety of anxiety disorders. The span of anxiety disorders is far reaching from social anxiety to phobias and is linked with dysregulation of neuronal circuitry governing such behaviors (Duval et al., 2015).

Anxiety requires the continuous detection and evaluation of environmental stimuli to generate appropriate motor, autonomic and hormonal responses. Coordinated activity in the amygdala nuclei is pivotal in processing sensory inputs and identify them as aversive or potentially dangerous. It is hypothesized that increased emotional output from amygdala neuronal substrates is a putative mechanism underlying pathological anxiety. Indeed, a common feature observed in many anxiety-stricken clinical populations is heightened activity in the amygdala after exposure to negative stimuli (Bishop et al., 2004; Shin & Liberzon, 2009; Stein et al., 2007). However, the cellular mechanisms by which amygdalar neurons increase activity in anxious patients is still not clear.

The ventral tegmental area (VTA) is a cerebral structure known for its implication in both rewarding and aversive processes (Bouarab et al., 2019; Root et al., 2020). The VTA is a heterogeneous region comprised mainly of dopaminergic neurons but also of GABAergic and glutamatergic neurons (Morales & Margolis, 2017). VTA glutamatergic neurons have been shown to preferentially signal aversive events (Qi et al., 2016; Root et al., 2014, 2018), and to promote defensive behaviors such as active escape, avoidance, and hiding behaviors (Barbano et al., 2020; Chen et al., 2022).

However, in spite of these recent discoveries, the integration of VTA glutamatergic neurons into brain networks of anxiety regulation has not been explored. Previous work has demonstrated that exposure to chronic stress increases tonic activity in VTA DA neurons contributing to depressive-like but not to anxiety behaviours (Chaudhury et al., 2013). We therefore hypothesised that VTA glutamatergic neurons could be significant modulators of amygdala activity, contributing to pathological levels of anxiety. To test this, we combined the use of histological and optogenetic tools to first characterize the VTA glutamate connections to the amygdala. We then combined the use of pharmacogenetic/optogenetic tools, electrophysiological recording and behavioural analysis to assess the involvement of this

neuronal projection in modulation of both basal and pathological-like anxiety in mice. We highlight here the existence of a VTA glutamatergic projection capable of regulating anxiety through long-term modulation of basolateral amygdala (BLA) neurons.

MATERIALS AND METHODS:

Animals. All procedures were in accordance with the recommendations of the European Commission (2010/63/EU) for care and use of laboratory animals, and approved by the French National Ethical Committee. We used only vglut2-Cre mice. Experimental transgenic animals were heterozygous and backcrossed on a C57BL/6J background. Mice were housed 4-5 mice per cage on a 12h/12h light/dark cycle with lights on from 8:00 a.m. to 8:00 p.m. Mice had free access to food and water ad libitum. Enriched housing consisted of a chewing block of wood, a plastic igloo and cotton to facilitate nesting. All mice used in behavioural experiments were handled daily for one week before each test to limit any stress induced by intraperitoneal injections and connections to laser cables for *in vivo* optogenetic experiment. All tests were performed on adult mice that were at least 2 months old and littermates were used as controls. All the experiments were performed in accordance to the ARRIVE guidelines.

Reagents. Clozapine N-oxyde was purchased from Enzo Life (France), and Xylazine/Ketamine from Centravet (France). All drugs for *in vivo* administration were diluted in saline (0.9% NaCl).

Stereotaxic injections and optical fiber implantations. Stereotaxic injections were performed using a stereotaxic frame (Kopf Instruments) under general anaesthesia with xylazine and ketamine (10 mg/kg and 150 mg/kg, respectively). Anatomical coordinates and maps were adjusted from Paxinos. The injection rate was set at 100nl/min.

To identify innervation of Amygdala by VTA glutamatergic fiber, Vglut2-CRE mice (5-7 weeks old) were injected with AAV5-hSyn-DIO-mCherry (Addgene; titration $\geq 7 \times 10^{12}$ vg/mL) bilaterally (300nl/site) in the VTA (AP: -2.9mm, ML: ± 0.6 mm, DV: -4.7mm). Animal were given a 3 weeks' recovery period to allow sufficient viral expression.

To identify VTA neurons projecting to the amygdala, Vglut2-CRE mice were injected with a retrograde virus pAAV-FLEX-tdTomato (Addgene, Titration $\geq 7 \times 10^{12}$ vg/mL) bilaterally (200nl/site) in the BLA (AP: -0.9mm, ML: ± 3.22 mm, DV: -4.6mm). Animal were given a 3 weeks' recovery period to allow sufficient viral expression.

For specific *in vivo* fiber photometry recordings of VTA glutamate neurons, vGlut2-CRE mice were simultaneously injected with an AAV9 pGP-AAV-syn-jGCaMP8m-WPRE (Addgene, Titration $\geq 1 \times 10^{13}$ vg/mL) unilaterally (200nL) in the medial VTA (AP: -2.9mm, ML: ± 0.5 mm,

DV=-4.5mm) and implanted unilaterally with a fiber optic (400 μm core) 0.25mm above the VTA (AP: -2.9mm, ML: \pm 0.5mm, DV=-4.25mm).

To perform projection-specific modulation of VTA glutamatergic neurons, Vglut2-CRE mice were injected with an AAV5 pAAV-EF1a-double floxed-hChR2(H134R)-EYFP-WPRE-HGHpA (Addgene, Titration $\geq 1 \times 10^{13}$ vg/mL) bilaterally (300nl/site) in the VTA. Animals were given a 6 weeks' recovery period to allow sufficient viral expression.

For specific modulation of VTA glutamatergic terminals in the BLA, the previously mentioned mice were subjected to a second surgery 5 weeks after viral injection. During this surgery, mice were implanted with homemade optical fiber following the protocol of Sparta (2013). These optical fibers (200 μm core, 0.39 NA), were implanted bilaterally 0.5mm above the BLA (AP:-0.9mm, ML: \pm 3.22mm, DV:-4.1mm).

For projection- and neurotransmitter-specific manipulation, Vglut2-CRE mice were bilaterally injected with a retrograde AAV-retro/2-hSyn1-chI-dlox-EGFP_2A_FLPo(rev)-dlox-WPRE-SV40p(A) in the BLA and an AAV-8/2-hSyn1-dFRT-hM4D(Gi)- mCherry(rev)-dFRT-WPRE-hGHp(A) in the VTA (hereafter named $\text{Glut}^{\text{hM4}; \text{VTA} \rightarrow \text{BLA}}$).

***In vivo* fiber photometry recordings.**

GCaMP8m was excited at two wavelengths (490nm, calcium-dependent signal and 405 nm isosbestic control) by two light-emitting diodes reflected off dichroic mirrors and coupled into the photometry fiber. Both light streams were coupled to a high NA (0.48), large core (400 μm) optical fiber patch cord, which was mated to a matching brain implant in each mouse. GCaMP8m fluorescence and its isosbestic control channel were collected by the same fiber, passed through a GFP emission filter, and focused onto a photoreceiver (R810, RWD, China). Analysis of the resulting signals was then performed using custom-written Python scripts (Aquineuro, Bordeaux, FR). Changes in fluorescence (DF/F) were calculated by smoothing signals from the isosbestic control channel to correct for movement artifacts and photobleaching. Signals from the GCaMP channel were then normalized to changes in fluorescence across animals. The timing of relevant behavioral events was recorded by the same system and peri-events histograms were then constructed by averaging changes in fluorescence (DF/F) across repeated trials. Alternatively, averaged GCaMP signals were compared during exploration of open vs closed arms in the elevated O-maze.

***In vivo* optogenetic manipulation.**

After implantation, optical fibers were connected by a mating sleeve (ThorLabs, ADAL1-5) to patch-cords (Doric Lenses, MFP_200/240/900-0.22_1m_FC-ZF1.25(F)) to a fiber optic rotary joint (Doric Lenses FRJ_1x2i_FC-2FC_0.22) itself connected to a laser source (ThorLabs S1FC473MM). Mice were habituated to fiber optic connection for 20 min per day during the week preceding behavioural testing. On the day of experiment, mice performed behavioural tests after 10 min habituation following connection. The power of the blue (470 nm) laser was $10 \text{ mW}\cdot\text{mm}^{-2}$ as measured at the tip of the optic fiber. Light stimulation was delivered at 20Hz in pulses of 20 ms. Control group mice underwent the same procedure and received the same intensity of laser stimulation. Mice with misplaced viral injections or fiber optic implantations were excluded.

The Omaze test was divided in three equal periods of 1min30sec. Only the second period (from 1min30 to 3min) was matched with a light stimulation with aforementioned parameters.

The openfield test was divided in three equal periods of 5min. Only the second period (from 5min to 10min) was matched with a light stimulation with aforementioned parameters.

Mice undergoing chronic light stimulation received a light stimulation of 10min once per day during five consecutive days. 24h after the last stimulation, mice were subjected to the Omaze test as to only study long-term behavioral adaptations induced by the chronic light stimulation.

O-maze

The O-maze test was used to measure anxiety levels. Each mouse was placed in a circular maze consisting of two open arms and two closed arms alternating in quadrants (width of walking lane: 5 cm, total diameter: 55 cm, height of the walls: 12 cm, elevation above the floor: 60 cm) with an ambient light of 20 lux in the open arms. Mice movements were recorded during 5 minutes using a video camera placed above the maze. An experimenter blind to the experimental groups scored the time spent in the open arms.

Open-Field

The Open-field test was used to measure locomotor activity. Each mouse was placed in a 40x40 cm open field with an ambient light of 200 lux for 15 minutes and left to explore freely. Mice movements were recorded using a video camera placed above the apparatus. Distanced travel was automatically analysed using the software AnyMaze (Stoelting, France).

Ex-vivo patch-clamp recording

Mice were anesthetized (Ketamine 150 mg/kg / Xylazine 10 mg/kg) and transcardially perfused with aCSF for slice preparation. For VTA recordings, horizontal 250 μm slices were obtained in bubbled ice-cold 95% O₂/5% CO₂ aCSF containing (in mM): KCl 2.5, NaH₂PO₄ 1.25, MgSO₄ 10, CaCl₂ 0.5, glucose 11, sucrose 234, NaHCO₃ 26. Slices were then incubated in aCSF containing (in mM): NaCl 119, KCl 2.5, NaH₂PO₄ 1.25, MgSO₄ 1.3, CaCl₂ 2.5, NaHCO₃ 26, glucose 11, at 37°C for 1 h, and then kept at room temperature. For amygdala recordings, coronal 250 μm sections were obtained using the same solutions. Slices were transferred and kept at 30–32°C in a recording chamber superfused with 2.5 ml/min aCSF. Neurons were visualized by combined epifluorescent and infrared/differential interference contrast visualization using an upright microscope holding 5x and 60x objectives, with appropriate green and red fluorescent filters. Current-clamp and voltage-clamp experiments were obtained using a Multiclamp 700B (Molecular Devices, Sunnyvale, CA). Signals were collected and stored using a Digidata 1440A converter and pCLAMP 10.2 software (Molecular Devices, CA). In all cases, access resistance was monitored by a step of -10 mV (0.1 Hz) and experiments were discarded if the access resistance increased more than 20%. For current-clamp experiments internal solution contained (in mM): K-D-gluconate 135, NaCl 5, MgCl₂ 2, HEPES 10, EGTA 0.5, MgATP 2, NaGTP 0.4. Depolarizing (0-300 pA) or hyperpolarizing (0-450 pA) 800 ms current steps were used to assess excitability and membrane properties of VTA or amygdala neurons. For voltage-clamp experiments an internal solution containing (in mM) 130 CsCl, 4 NaCl, 2 MgCl₂, 1.1 EGTA, 5 HEPES, 2 Na₂ATP, 5 sodium creatine phosphate, 0.6 Na₃GTP and 0.1 spermine was used. Synaptic currents were evoked by light stimuli (5ms pulses, 470nm) at 0.1 Hz passed through the 60x objective. To assess AMPA-R/NMDA-R ratios, optical EPSCs were measured at V=+40mV in the absence and presence of the AMPA antagonist DNQX (10 μM), and picrotoxin (50 μM). AMPA I-V curves were constructed by isolating AMPA synaptic currents using the NMDA-R antagonist AP5 (50 μM), and picrotoxin (50 μM). In all cases, offline analyses were performed using Clampfit 10.2 (Axon Instruments, USA) and Prism (Graphpad, USA).

In a subset of neurons, single-cell PCR was carried out as previously described (Fernandez et al., 2016). In brief, after electrophysiological recording, the cytoplasmic content of the cell was harvested by applying gentle negative pressure to the pipette. Cell content was expelled into a tube where a reverse transcription reaction was performed in a final volume of 10 μl . cDNA sequences were thereafter amplified by conducting a multiplex nested PCR, designed to

simultaneously detect a series of molecular markers (see Table 1 for more information on the primers used).

Immunohistofluorescence

To achieve fixation of the brains, mice were anesthetized using a mix of ketamine (150 mg/kg) and xylazine (10 mg/kg) then underwent transcardial perfusion with cold phosphate buffer (PB 0.1 M Na₂HPO₄/NaH₂PO₄, pH 7.4) followed by paraformaldehyde (PFA 4%, diluted in PB 0.1M). Brains were left at 4°C in PFA 4% overnight, then cut into 60 µm free-floating slices. Sections were used to assess the correct location of stereotaxic viral injection for each animal and cannula implantation for *in vivo* optogenetic experiments.

For cFos labelling, brain sections containing the ventral tegmental area were incubated (30 min) in PBS-BT (PBS 0.5% BSA, 0.1% Triton X-100) with 10% normal goat serum (NGS). Sections were then incubated (4°C) in PBS-BT, 1% NGS, with primary anti-cFos (1:1000, Abcam anti-rabbit) for 36h. Sections were rinsed in PBS and incubated (2 h) in goat anti-rabbit Alexa488 secondary antibody (1:1000, Vector Laboratories, Burlingame, CA) in PBS-BT, 1% NGS. Sections were rinsed with PBS and incubated 5 min with DAPI before mounting with Moviol. Images for quantification of cFos-positive cells were acquired using a Axioplan2 epifluorescence microscope (Carl Zeiss).

For tyrosine hydroxylase (TH) labelling, brain sections containing the ventral tegmental area were incubated (30 min) in PBS-BT (PBS 0.5% BSA, 0.1% Triton X-100) with 10% normal goat serum (NGS). Sections were then incubated (4°C) in PBS-BT, 1% NGS, with primary anti-TH (1:1000, anti-mouse, MAB318 Milipore) for 24H. Sections were rinsed in PBS and incubated (2 h) in goat anti-mouse Alexa488 or Alexa647 secondary antibody (1:1000, Vector Laboratories, Burlingame, CA) in PBS-BT, 1% NGS. Sections were rinsed with PBS and incubated 5 min with DAPI before mounting with Moviol. Images for quantification of colabelling with cFos were acquired using a Axioplan2 epifluorescence microscope (Carl Zeiss).

Data analysis

Data were analysed using Prism (GraphPad, U.S.A.). Normality of the distribution was first tested using a Kolmogorov-Smirnov test. Depending of the number of groups and the results of the normality test, groups were then compared using a Student t-test, U of Mann-Whitney, or two-way analyses of variance (ANOVA) followed by post hoc Sidak's test. Data in the figures

are presented as mean \pm SEM. Statistical significance was conventionally established at * $p < 0.05$, ** $p < 0.01$, *** $p < 0.001$.

Table 1 – List of genes amplified by nested single-cell PCR, and the internal and external primer pairs used.

Acronym	Gene name GenBank accession number	External primer pair (Sequence 5' to 3')	Product size (bp)	Internal primer pair (Sequence 5' to 3')	Product size (bp)
GAD65	Glutamic acid decarboxylase 2 (Gad2) NM_008078	CCAAAAGTTACGGGCGG TCCTCCAGATTTGCGGTTG	375	CACCTGCGACCAAAAACCT GATTTGCGGTTGGTCTGCC	248
GAD67	Glutamic acid decarboxylase 1 (Gad1) NM-008077	TACGGGGTTCGCACAGGTC CCCAGGCAGCATCCACAT	598	CCCAGAAGTGAAGACAAAAGGC AATGCTCCGTAACAGTCGTGC	255
VGLUT1	Glutamate vesicular transporter, member 7 (Slc17a7) NM_182993	GGCTCCTTTTCTGGGGCTAC CCAGCCGACTCCGTTCTAAG	259	ATTCGCAGCCAACAGGGTCT TGGCAAGCAGGGTATGTGAC	153
VGLUT2	Glutamate vesicular transporter, member 6 (Slc17a6) NM_080853	ATGGAGTCGGTAAAAACAAGGATT TGGCTTTCCTTGATAACTTTGC	346	CGGGGAAAAGGGGATAAAG CGGTGGATAGTCTGTTGTTGA	286

RESULTS

A distinct glutamate-only projection from the VTA can modulate BLA PN activity

In order to determine if recently identified VTA glutamatergic projections to the amygdala could contribute to anxious behaviours, we first characterized these projections to better understand their place in the circuitry of anxiety. We used a viral approach to assess the territorial innervation of the amygdala by fibres of VTA glutamatergic neurons. Vglut2-CRE mice were injected with an anterograde CRE-dependant tracer virus (AAV5-hSyn-DIO-mCherry) and a quantification of labelled fibre density was performed in the lateral (LA; N=6), basolateral (BLA; N=6), centrolateral (CeL; N=5) and centromedial (CeM; N=4) parts of the amygdala (Figure.1.a). As seen from the chart and images, a higher fiber density was found in the basolateral (BLA) and centromedial amygdala (CeM) compared to other subregions (Figure.1.a). We then studied if this glutamatergic projection to the amygdala made functional. We injected a CRE-dependant virus expressing an excitatory opsin (AAV5-Dio-ChR2-YFP) in the VTA of Vglut2-CRE mice and measured if activation of the opsin was sufficient to trigger excitatory post-synaptic currents (oEPSC) in amygdala neurons (Figure.1.b Left panels). We found that channelrhodopsin activation induced oEPSC in most of BLA neurons (n=18/21) but fewer in the CeL (n=1/9) and the CeM (n=7/14). Additionally, the amplitude of the response was larger in BLA neurons (Figure.1.c). Synaptic currents were blocked by the AMPA antagonist DNQX, confirming glutamatergic nature of this VTA input. In a subset of neurons which presented oEPSCs, the cytoplasm was extracted and a single-PCR was performed to assess the glutamatergic (vGlut1 or vGlut2) or GABAergic (GAD65/67) nature of connected BLA neurons (Figure.1.b Right panels). We found that most of the neurons were glutamatergic vGlut1 expressing neurons while a small fraction was GAD65 expressing neurons (n=5; N=1). We then used a retrograde viral approach to determine if the VTA glutamate inputs to the amygdala were subject to territorialization or if they were evenly spread through the VTA (Figure.1.c). We therefore injected a CRE-dependant retrograde viral tracer (pAAV-FLEX-tdTomato) in the BLA of vGlut2-CRE mice and quantified the number of retrogradely labelled VTA glutamate neurons found inside the VTA. We found a high number of retrogradely labelled neurons inside the medial VTA and mostly in the rostral lineate nucleus compared to the low numbers found in the lateral VTA. We also assessed if those retrogradely labelled glutamate neurons are capable of co-transmission of dopamine (DA). Hence, we also performed a TH immunohistochemistry to label VTA DA neurons and determine the colocalization rate with the retrogradely labelled glutamate neurons (Figure.1.b bottom panels). Number of

neurons expressing both markers was extremely low, reaching 1.3% co-localization in the lateral VTA and 0.17% in the medial. Overall, these data indicate the presence of glutamate-only VTA neurons that can preferentially connect to BLA principal neurons.

VTA glutamate neurons are responsive to anxiogenic events but their modulation do not alter basal anxiety levels

We used in vivo fiber photometry recordings to assess if VTA glutamatergic neurons are responsive to anxiogenic cues. We injected a CRE-dependant virus expressing GCaMP8m (AAV9-Flex-GCaMP8m) in the VTA of vGlut2-CRE mice and implanted optical fiber on top of the VTA (Figure.2.a Left panel). We recorded the bulk calcium activity of VTA glutamatergic neurons during a zero-maze test where the animals are free to visit anxiogenic open arms or safe closed arms (N=4). We found that the exploration of the anxiogenic open arms increased calcium activity in VTA Glu neurons compared to exploration of closed arms (Figure.2.a). To unravel whether VTA Glu neurons can modulate anxiety levels, we conducted in vivo optogenetic activation of VTA glutamatergic terminals in the BLA during O-maze exploration. We injected a CRE-dependant virus expressing an excitatory opsin (AAV5-Dio-ChR2-YFP) in the VTA of Vglut2-CRE mice and implanted optical fiber on top of the BLA to activate BLA terminals (Figure.2.a right panel). We found that selective activation (N=20) did not alter basal anxiety levels as evidenced by the unchanged rate of exploration during the Omaze test in comparison to control mice (N=17).

Social stress is a common factor in anxiety disorders, which have been shown to increase anxiety in mice. Therefore, we question whether VTA Glu neurons are sensitive to social stress events. We injected a CRE-dependant retrograde viral tracer (pAAV-FLEX-tdTomato) in the BLA of vGlut2-CRE mice and performed an immunolabeling targeted against the immediate early gene cFOS (Figure.2.b). We quantified the number of retrogradely labelled VTA glutamatergic neurons found inside the VTA colocalising with cFOS labelling as a readout of neurons activated by social stress. We found that a single social defeat event increased the number of cFOS+ BLA-projecting VTA glutamatergic neurons compared to naïve mice (Figure.2.b; N=3). Finally, we wanted to assess the dynamic of VTA glutamate neurons activity during social defeat. We injected a CRE-dependant virus expressing GCaMP8m (AAV9-Flex-GCaMP8m) in the VTA of vGlut2-CRE mice and implanted optical fiber on top of the VTA. We then performed in vivo fiber photometry recording of the calcium activity of VTA glutamate neurons during social defeat session (Figure.2.c). We found that VTA glutamate neurons had increased activity upon aggression by a conspecific (N=4). Overall, these results

show that VTA glutamate efference to the BLA do not directly control basal level of anxiety but their responsiveness to a stronger stressor suggest a role in modulating pathological anxiety.

Chronic stress exposure increases VTA Glu output onto BLA neurons

We next assessed if chronic social defeat stress (CSD), a paradigm known to increase innate anxiety, could alter the activity of the VTA glutamate neurons connecting to the BLA. To achieve this goal we injected a CRE-dependent retrograde viral tracer (pAAV-FLEX-tdTomato) in the BLA of vGlut2-CRE mice and recorded the activity of labelled VTA glutamate neurons 24 hours after submitting the mice to a protocol of chronic social defeat (CSD) (Figure.3.a). Mice exposed to the CSD showed a significant decreased in the exploration of open arms in the O-maze compared to control (Figure.3.a)., Patch-clamp recordings, revealed that we that CSD decreased rheobase levels of retrogradely labelled VTA glutamate neurons between CSD (n=9) and naïve mice (n=10). Additionally, we found that BLA-projecting VTA Glu neurons from CSD mice (n=21; N=5) had significantly higher excitability compared to naïve mice (n=21; N=5). This increased VTA Glu input onto the BLA could contribute to heightened anxious behaviours. Hence, we tested if silencing this neuronal projection after CSD is sufficient to revert the stress-induced increase in anxiety. To achieve projection and neurotransmitter specificity in mice, we injected a retrograde CRE-dependent virus expressing flippase (AAV-DIO-Flp-eGFP) in the BLA and an anterograde Flippase-dependent virus expressing an inhibitory DREADD (AAV-hSyn-FRT-hM4-mCherry) in the VTA of VGLUT2-CRE mice. Mice were then subjected to the CSD protocol followed by a 5-day regimen of CNO injections (once/day, 1mg/kg, ip) or saline. Control mice received the same treatments, but were not subjected to CSD. Mice were then tested for anxiety levels using the O-maze. We found that both acute (data not shown) or 5-day chronic silencing of VTA glutamate efference to the BLA did not revert CSD-induced anxiety (N=10) compared to saline-injected control mice (N=9)(Figure.3.b). Overall, these results suggest that VTA glutamate efference to the BLA may contribute to the induction of anxiety disorders but not to sustain it.

Chronic social defeat stress induces post-synaptic adaptations in BLA neurons

Next, we wondered how BLA neurons receiving VTA glutamate afferences are impacted by chronic stress. We injected a CRE-dependent virus expression channelrhodopsin in the VTA of Vglut2-CRE mice (AAV5-Dio-ChR2-YFP). We then submitted mice to CSD and assessed synaptic input changes onto BLA principal neurons connected by VTA Glu terminals (Figure.4.a). We observed a significant increase in the frequency, but not amplitude, of spontaneous EPSCs in BLA neurons in mice that received CSD (Figures.4.b and 4.c), consistent with increased glutamatergic drive. To evaluate specific synaptic inputs from VTA Glu neurons, we used selective optogenetic stimulation (Figure.4.d). In BLA neurons from CSD mice, VTA Glu→BLA synapses were potentiated as revealed by an increased in AMPA-R/NMDA-R ratio (Figure.4.d). This effect was specific on this synaptic connection, as the same experiment carried out on glutamatergic inputs from the prefrontal cortex showed no changes in AMPA-R/NMDA-R ratio after CSD (Figure.4.e).

What mechanisms could underlie the increase ratio between AMPA and NMDA receptors? Membrane insertion of GluA1 AMPA subunits has been shown to mediate several forms of synaptic potentiation (Ge & Wang, 2021; McCormack et al., 2006; Rumpel et al., 2005). This insertion would favor GluA2-lacking AMPA receptors that feature inward rectification (Takahashi et al., 2003). Amplitudes of evoked AMPA EPSCs have been used to calculate a rectification index as a proxy for AMPA receptor trafficking (Takahashi et al., 2003). Using channelrhodopsin-assisted stimulation of VTA Glu inputs onto BLA neurons, we performed AMPA receptor I-V curves and calculated rectification index from current amplitudes at $V=-70\text{mV}$ and $V=+40\text{mV}$ (Figure.4.f). We observed that recordings from CSD mice showed significant smaller current amplitudes in positive voltages compared to controls (Figure.4.f Left panel). Consistent with this, rectification index was significantly higher in neurons from CSD mice compared to controls (Figure.4.f Right panel). Taken together, these data suggest that CSD results in synaptic potentiation of VTA Glu—BLA connectivity likely mediated by increased membrane trafficking of GluA1 AMPA subunits.

In vivo potentiation of VTA Glu→BLA synapses is sufficient to increase anxiety

Our previous results indicated that CSD drives selective adaptations in VTA Glu→BLA synaptic connectivity. We then asked whether mimicking these synaptic adaptations in vivo promotes pathological anxiety. We injected a CRE-dependant virus expressing channelrhodopsin (AAV5-DIO-ChR2-YFP) in the VTA of Vglut2-CRE mice and placed optical fiber on top of the BLA. Then, we subjected the mice to a chronic optogenetic stimulation protocol (pulses of 10mW, 20Hz, 20ms, once per day, during 10min) of the terminals in the BLA for five days and tested anxiety in a O-maze test 24 hours after the last stimulation (Figure.5.a). We observed that animals that received chronic stimulation spent significantly less time exploring the open arms of the O-maze, consistent with increased anxiety (Figure.5.a). Mice that received chronic stimulation, and their respective controls, were used for ex vivo patch-clamp recordings to assess synaptic connectivity between VTA Glu neurons and BLA neurons. We observed that in vivo chronic stimulation significantly increased AMPA-R/NMDA-R ratio and changed increased rectification in AMPA receptor I-V curves (Figures.5.c and 5.d). These changes were reminiscent of those previously observed after chronic stress, and suggest that synaptic potentiation of VTA Glu→BLA connections is a cellular mechanism of stress-induced pathological anxiety.

Discussion

Anxiety and its related disorders have long been studied and have revealed themselves to be hardwired in an incredibly complex neuronal circuitry. In this circuitry, the amygdala reign as a key structure that has received a lot of attention but its functions and mechanisms of action still remain elusive. We provide here a mechanism that could contribute to the amygdala hyper-reactivity found in anxiety disorders. We show that VTA glutamate neurons provides functional inputs to the BLA neurons that are sensitive to stress. Furthermore, only a chronic activation of these neurons increases anxiety levels and in a manner that share mechanistic similarities to chronic stress exposure, a paradigm known to induce heightened anxiety in mice (Golden et al., 2011). Our study provides new insights on amygdala pathological dysregulation of anxiety levels and could serve as a template for new studies to improve treatments of anxiety disorders.

Despite its well-known role in reward processing, more recent studies have shown that the VTA also plays a role in signalling aversion, and that subpopulations of neurons in this area are readily excited by aversive events such as a footshock, airpuff or even predator-like stimuli

(Cohen et al., 2012; Tan et al., 2012). This functional divergence could arise from the unique properties in distinct target-specific cell populations within the VTA. For example, VTA DA neurons projecting to the nucleus accumbens have long been implicated in reward signalling and motivation, however those projecting to the prefrontal cortex preferentially signals aversive events (Lammel et al., 2012, 2014). Further, two recent studies showed optogenetic manipulation of a VTA DA→amygdala pathway is sufficient to alter innate anxiety (Morel et al., 2022; Nguyen et al., 2021). Glutamatergic neurons in the VTA are selectively stimulated by aversive stimuli (Root et al., 2018) and optogenetic stimulation of these fibers in the nucleus accumbens or the lateral habenula has been shown to result in aversion (Lammel et al., 2012; Qi et al., 2016). In our study, we showed that this VTA population is activated by exploration of aversive areas of a maze and aversive social encounters, suggesting that they could be implicated in regulation of anxious responses. We provided evidence of functional connectivity between these neurons and the glutamatergic neurons of the basolateral amygdala, however in vivo optogenetic manipulation of this pathway did not alter exploration of an O-maze. A recent study showed that optogenetic stimulation of VTA Glu fibers within the central amygdala elicited a range of defensive behaviours including avoidance, burrowing, escape and flight-to-shelter (Chen et al., 2022). While it is possible that VTA Glu projections to the BLA do not modulate anxiety, it is important to note that this region is under a strong tonic feedforward inhibition by the prefrontal cortex in the absence of threatening stimuli. This inhibition is thought to be mediated by excitatory PFC inputs onto the intercalated cells of the amygdala (ITCs) and prevent the induction of anxiety under non-threatening situations (Palomares-Castillo et al., 2012). It is therefore possible that our acute optogenetic stimulation was not enough to overcome this strong inhibition. It could also explain the differential effect on anxiety of the optogenetic stimulation of VTA glutamate projections to the CeA (Chen et al., 2022). Indeed, a stimulation directly to the CeM would therefore bypass the upstream activation of the BLA normally required to activate the CeM under threatening stimuli (Tye et al., 2011). Overall, this evidence suggests that VTA Glu neurons are upstream modulators of amygdala activity with a potential role in anxiety modulation.

People suffering from social anxiety disorder show increased amygdala reactivity when exposed to social and non-social aversive cues (Kraus et al., 2018). This observation has been replicated in other related forms of anxiety including post-traumatic stress disorder (PTSD), specific phobias and generalized anxiety (Dilger et al., 2003; Nitschke et al., 2009; Rauch et al., 2006). Importantly, it has been shown that common anxiolytics can reduce hyper-reactivity

in patients, further validating the close correlation between amygdala function and symptoms levels (Forster et al., 2012). Based on these clinical observations, it has been hypothesized that increased emotional output from amygdala neuronal substrates is a putative mechanism underlying pathological anxiety. Despite this long-known association between amygdala reactivity and anxiety, little is known about the cellular and synaptic processes that contribute to this phenomenon. As with other neuropsychiatric conditions, anxiety disorders are highly heterogeneous with respect to genetic predisposing factors, behavioral manifestations of the symptoms and response to common treatments. However, stress has been suggested as a key element in the developmental root of these brain disorders. Indeed, intense emotional events or chronic exposure to stressful experiences can create a pathological shift in threat detection and value, leading to excessive anxiety (Hariri & Holmes, 2015; Roozendaal et al., 2009). Exposure to several stressors has been shown to increase innate anxiety and conditioned fear responses, and to increase the activity and responsiveness in basolateral amygdala neurons (Rosenkranz et al., 2010). We show here that exposure to chronic social defeat increases anxiety levels and excitatory drive into amygdala principal neurons. Further, chronic stress strengthened synaptic connectivity between VTA Glu and BLA neurons, and artificial potentiation of this synapse was sufficient to increase anxiety in mice. This data is in agreement with previous reports showing that stress exposure promotes neuronal remodeling of synaptic spines and dendritic branching in the basolateral amygdala, increasing synaptic input connectivity. Importantly, these morphological changes are well correlated with the levels of innate anxiety and enhancement of fear memory (Hariri & Holmes, 2015; Leuner & Shors, 2012; Vyas et al., 2003). Overall, these data suggest that hyperactivity of amygdala neurons could be mediated, or at least facilitated, by increased synaptic inputs from the VTA.

In conclusion, our study suggest that anxiety-disorders may be promoted by mechanism relying on the stress-induced activation of the VTA glutamate projections to the BLA PN.

REFERENCES

- Barbano, M. F., Wang, H. L., Zhang, S., Miranda-Barrientos, J., Estrin, D. J., Figueroa-González, A., Liu, B., Barker, D. J., & Morales, M. (2020). VTA Glutamatergic Neurons Mediate Innate Defensive Behaviors. *Neuron*, *107*(2), 368-382.e8. <https://doi.org/10.1016/J.NEURON.2020.04.024>
- Bishop, S. J., Duncan, J., & Lawrence, A. D. (2004). State anxiety modulation of the amygdala

- response to unattended threat-related stimuli. *The Journal of Neuroscience : The Official Journal of the Society for Neuroscience*, 24(46), 10364–10368. <https://doi.org/10.1523/JNEUROSCI.2550-04.2004>
- Bouarab, C., Thompson, B., & Polter, A. M. (2019). VTA GABA Neurons at the Interface of Stress and Reward. *Frontiers in Neural Circuits*, 13. <https://doi.org/10.3389/FNCIR.2019.00078>
- Chaudhury, D., Walsh, J. J., Friedman, A. K., Juarez, B., Ku, S. M., Koo, J. W., Ferguson, D., Tsai, H. C., Pomeranz, L., Christoffel, D. J., Nectow, A. R., Ekstrand, M., Domingos, A., Mazei-Robison, M. S., Mouzon, E., Lobo, M. K., Neve, R. L., Friedman, J. M., Russo, S. J., ... Han, M. H. (2013). Rapid regulation of depression-related behaviors by control of midbrain dopamine neurons. *Nature*, 493(7433), 532. <https://doi.org/10.1038/NATURE11713>
- Chen, S. Y., Yao, J., Hu, Y. D., Chen, H. Y., Liu, P. C., Wang, W. F., Zeng, Y. H., Zhuang, C. W., Zeng, S. X., Li, Y. P., Yang, L. Y., Huang, Z. X., Huang, K. Q., Lai, Z. T., Hu, Y. H., Cai, P., Chen, L., & Wu, S. (2022). Control of Behavioral Arousal and Defense by a Glutamatergic Midbrain-Amygdala Pathway in Mice. *Frontiers in Neuroscience*, 16, 415. <https://doi.org/10.3389/FNINS.2022.850193/BIBTEX>
- Cohen, J. Y., Haesler, S., Vong, L., Lowell, B. B., & Uchida, N. (2012). Neuron-type-specific signals for reward and punishment in the ventral tegmental area. *Nature*, 482(7383), 85–88. <https://doi.org/10.1038/NATURE10754>
- Dilger, S., Straube, T., Mentzel, H. J., Fitzek, C., Reichenbach, J. R., Hecht, H., Krieschel, S., Gutberlet, I., & Miltner, W. H. R. (2003). Brain activation to phobia-related pictures in spider phobic humans: an event-related functional magnetic resonance imaging study. *Neuroscience Letters*, 348(1), 29–32. [https://doi.org/10.1016/S0304-3940\(03\)00647-5](https://doi.org/10.1016/S0304-3940(03)00647-5)
- Duval, E. R., Javanbakht, A., & Liberzon, I. (2015). Neural circuits in anxiety and stress disorders: a focused review. *Therapeutics and Clinical Risk Management*, 11, 115. <https://doi.org/10.2147/TCRM.S48528>
- Fernandez, S. P., Cauli, B., Cabezaz, C., Muzerelle, A., Poncer, J. C., & Gaspar, P. (2016). Multiscale single-cell analysis reveals unique phenotypes of raphe 5-HT neurons projecting to the forebrain. *Brain Structure & Function*, 221(8), 4007–4025. <https://doi.org/10.1007/S00429-015-1142-4>

- Forster, G. L., Novick, A. M., Scholl, J. L., & Watt, M. J. (2012). The Role of the Amygdala in Anxiety Disorders. *The Amygdala - A Discrete Multitasking Manager*. <https://doi.org/10.5772/50323>
- Ge, Y., & Wang, Y. T. (2021). GluA1-homomeric AMPA receptor in synaptic plasticity and neurological diseases. *Neuropharmacology*, *197*, 108708. <https://doi.org/10.1016/J.NEUROPHARM.2021.108708>
- Golden, S. A., Covington, H. E., Berton, O., & Russo, S. J. (2011). A standardized protocol for repeated social defeat stress in mice. *Nature Protocols*, *6*(8), 1183. <https://doi.org/10.1038/NPROT.2011.361>
- Hariri, A. R., & Holmes, A. (2015). Finding translation in stress research. *Nature Neuroscience*, *18*(10), 1347–1352. <https://doi.org/10.1038/NN.4111>
- Kraus, J., Frick, A., Fischer, H., Howner, K., Fredrikson, M., & Furmark, T. (2018). Amygdala reactivity and connectivity during social and non-social aversive stimulation in social anxiety disorder. *Psychiatry Research: Neuroimaging*, *280*, 56–61. <https://doi.org/10.1016/J.PSYCHRESNS.2018.08.012>
- Lammel, S., Lim, B. K., & Malenka, R. C. (2014). Reward and aversion in a heterogeneous midbrain dopamine system. *Neuropharmacology*, *76*(0 0), 351–359. <https://doi.org/10.1016/J.NEUROPHARM.2013.03.019>
- Lammel, S., Lim, B. K., Ran, C., Huang, K. W., Betley, M. J., Tye, K. M., Deisseroth, K., & Malenka, R. C. (2012). Input-specific control of reward and aversion in the ventral tegmental area. *Nature*, *491*(7423), 212–217. <https://doi.org/10.1038/nature11527>
- Leuner, B., & Shors, T. J. (2012). Stress, anxiety, and dendritic spines: what are the connections? *Neuroscience*, *251*, 108–119. <https://doi.org/10.1016/J.NEUROSCIENCE.2012.04.021>
- McCormack, S. G., Stornetta, R. L., & Zhu, J. J. (2006). Synaptic AMPA receptor exchange maintains bidirectional plasticity. *Neuron*, *50*(1), 75–88. <https://doi.org/10.1016/J.NEURON.2006.02.027>
- Morales, M., & Margolis, E. B. (2017). Ventral tegmental area: Cellular heterogeneity, connectivity and behaviour. *Nature Reviews Neuroscience*, *18*(2), 73–85. <https://doi.org/10.1038/NRN.2016.165>

- Morel, C., Montgomery, S. E., Li, L., Durand-de Cuttoli, R., Teichman, E. M., Juarez, B., Tzavaras, N., Ku, S. M., Flanigan, M. E., Cai, M., Walsh, J. J., Russo, S. J., Nestler, E. J., Calipari, E. S., Friedman, A. K., & Han, M. H. (2022). Midbrain projection to the basolateral amygdala encodes anxiety-like but not depression-like behaviors. *Nature Communications* 2022 13:1, 13(1), 1–13. <https://doi.org/10.1038/s41467-022-29155-1>
- Nguyen, C., Mondoloni, S., Le Borgne, T., Centeno, I., Come, M., Jehl, J., Solié, C., Reynolds, L. M., Durand-de Cuttoli, R., Tolu, S., Valverde, S., Didienne, S., Hanneke, B., Fiancette, J. F., Pons, S., Maskos, U., Deroche-Gamonet, V., Dalkara, D., Hardelin, J. P., ... Faure, P. (2021). Nicotine inhibits the VTA-to-amygdala dopamine pathway to promote anxiety. *Neuron*, 109(16), 2604-2615.e9. <https://doi.org/10.1016/J.NEURON.2021.06.013>
- Nitschke, J. B., Sarinopoulos, I., Oathes, D. J., Johnstone, T., Whalen, P. J., Davidson, R. J., & Kalin, N. H. (2009). Anticipatory activation in the amygdala and anterior cingulate in generalized anxiety disorder and prediction of treatment response. *The American Journal of Psychiatry*, 166(3), 302–310. <https://doi.org/10.1176/APPI.AJP.2008.07101682>
- Palomares-Castillo, E., Hernández-Pérez, O. R., Pérez-Carrera, D., Crespo-Ramírez, M., Fuxe, K., & Pérez De La Mora, M. (2012). The intercalated paracapsular islands as a module for integration of signals regulating anxiety in the amygdala. *Brain Research*, 1476, 211–234. <https://doi.org/10.1016/J.BRAINRES.2012.03.047>
- Qi, J., Zhang, S., Wang, H. L., Barker, D. J., Miranda-Barrientos, J., & Morales, M. (2016). VTA glutamatergic inputs to nucleus accumbens drive aversion by acting on GABAergic interneurons. *Nature Neuroscience*, 19(5), 725–733. <https://doi.org/10.1038/NN.4281>
- Rauch, S. L., Shin, L. M., & Phelps, E. A. (2006). Neurocircuitry Models of Posttraumatic Stress Disorder and Extinction: Human Neuroimaging Research—Past, Present, and Future. *Biological Psychiatry*, 60(4), 376–382. <https://doi.org/10.1016/J.BIOPSYCH.2006.06.004>
- Root, D. H., Barker, D. J., Estrin, D. J., Miranda-Barrientos, J. A., Liu, B., Zhang, S., Wang, H. L., Vautier, F., Ramakrishnan, C., Kim, Y. S., Fenno, L., Deisseroth, K., & Morales, M. (2020). Distinct Signaling by Ventral Tegmental Area Glutamate, GABA, and Combinatorial Glutamate-GABA Neurons in Motivated Behavior. *Cell Reports*, 32(9), 108094. <https://doi.org/10.1016/J.CELREP.2020.108094>
- Root, D. H., Estrin, D. J., & Morales, M. (2018). Aversion or Salience Signaling by Ventral

Tegmental Area Glutamate Neurons. *IScience*, 2, 51.
<https://doi.org/10.1016/J.ISCI.2018.03.008>

Root, D. H., Mejias-Aponte, C. A., Qi, J., & Morales, M. (2014). Role of Glutamatergic Projections from Ventral Tegmental Area to Lateral Habenula in Aversive Conditioning. *The Journal of Neuroscience*, 34(42), 13906. <https://doi.org/10.1523/JNEUROSCI.2029-14.2014>

Roozendaal, B., McEwen, B. S., & Chattarji, S. (2009). Stress, memory and the amygdala. *Nature Reviews. Neuroscience*, 10(6), 423–433. <https://doi.org/10.1038/NRN2651>

Rosenkranz, J. A., Venheim, E. R., & Padival, M. (2010). Chronic Stress Causes Amygdala Hyperexcitability in Rodents. *Biological Psychiatry*, 67(12), 1128–1136. <https://doi.org/10.1016/j.biopsych.2010.02.008>

Rumpel, S., LeDoux, J., Zador, A., & Malinow, R. (2005). Postsynaptic receptor trafficking underlying a form of associative learning. *Science (New York, N.Y.)*, 308(5718), 83–88. <https://doi.org/10.1126/SCIENCE.1103944>

Shin, L. M., & Liberzon, I. (2009). The Neurocircuitry of Fear, Stress, and Anxiety Disorders. *Neuropsychopharmacology* 2010 35:1, 35(1), 169–191. <https://doi.org/10.1038/npp.2009.83>

Stein, M. B., Simmons, A. N., Feinstein, J. S., & Paulus, M. P. (2007). Increased amygdala and insula activation during emotion processing in anxiety-prone subjects. *The American Journal of Psychiatry*, 164(2), 318–327. <https://doi.org/10.1176/AJP.2007.164.2.318>

Tan, K. R., Yvon, C., Turiault, M., Mirzabekov, J. J., Doehner, J., Labouèbe, G., Deisseroth, K., Tye, K. M., & Lüscher, C. (2012). GABA Neurons of the VTA Drive Conditioned Place Aversion. *Neuron*, 73(6), 1173. <https://doi.org/10.1016/J.NEURON.2012.02.015>

Tye, K. M., Prakash, R., Kim, S. Y., Fenno, L. E., Grosenick, L., Zarabi, H., Thompson, K. R., Gradinaru, V., Ramakrishnan, C., & Deisseroth, K. (2011). Amygdala circuitry mediating reversible and bidirectional control of anxiety. *Nature* 2011 471:7338, 471(7338), 358–362. <https://doi.org/10.1038/nature09820>

Vyas, A., Bernal, S., & Chattarji, S. (2003). Effects of chronic stress on dendritic arborization in the central and extended amygdala. *Brain Research*, 965(1–2), 290–294. [https://doi.org/10.1016/S0006-8993\(02\)04162-8](https://doi.org/10.1016/S0006-8993(02)04162-8)

ACKNOWLEDGMENTS

This work was supported by the Centre National de la Recherche Scientifique (CNRS), the Université Côte d'Azur, the Fondation pour la Recherche sur le Cerveau and Rotary – Espoir en Tête to J.B., the Fédération pour la Recherche Médicale (FRMDEQ20180339159 to J.B.). T.C. is a recipient fourth-year PhD fellowship from the FRM (FDT202106012968). L.R. is a recipient of a PhD fellowship from the FRM.

AUTHOR CONTRIBUTIONS

T.C., L.R., and S.P.F. performed stereotaxic surgery. T.C. and L.R. performed behavioral experiments. T.C. and H.F. performed microscopy. L.R. performed in vivo fiber photometry recordings. S.P.F. and C.G. performed electrophysiology. F.G. and J.B. provided intellectual inputs. T.C., J.B. and S.P.F. designed the project and wrote the manuscript. All authors provided feedback on writing the manuscript. The authors declare no conflict of interest. All data needed to evaluate the conclusions in the paper are present in the paper and/or the Supplementary Materials.

FIGURES AND FIGURES LEGENDS

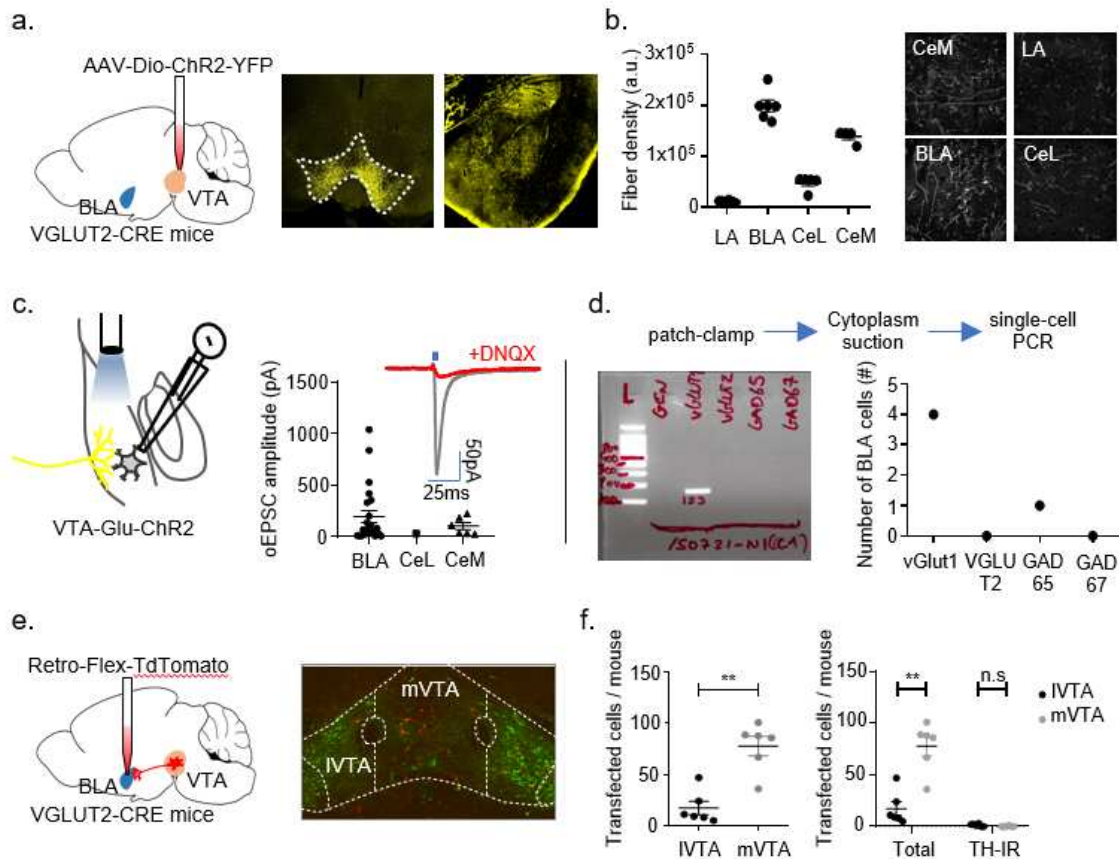


Figure 1. Medial VTA glutamate-only neurons preferentially make functional efferences to the BLA PNs. (a) Left panel: vGlut2-CRE mice were injected with AAV-Dio-ChR2-YFP in the VTA. Three weeks later, mice were sacrificed and the quantity of YFP labelled fibers was assessed in the amygdala subregions. Right panel: Representative microscopy images of the injection site and of the amygdala innervation. (b) Quantification of the fiber density innervating the amygdala subregions and representative microscopy images. (c) Left panel: vGlut2-CRE mice were injected with AAV-DIO-ChR2-YFP in the VTA. Six weeks later, the oEPSCs found in the BLA were recorded. Right panel: Amplitude of the evoked oEPSCs recorded in each subregion of the amygdala and representative trace of an EPSC and its response to an AMPA receptor antagonist: DNQX. (d) A single cell-PCR was performed on the extracted cytoplasm of BLA neurons exhibiting oEPSCs. (e) Left panel: vGlut2-CRE mice were injected with retrograde AAV-Flex-TdTomato in the BLA. Three weeks later, mice were sacrificed and the number of transfected cells found inside VTA medial (mVTA) and lateral (lVTA) part was counted. Right panel: Representative microscopy images of retrogradely transfected neurons (red) in the VTA with TH-immunolabeling (green). (f) Left panel:

Retrogradely labelled cells were counted in major divisions of the VTA. Right panel: Quantification of the number of retrogradely VTA glutamate neurons co-labelled for TH (TH-IR) inside the major divisions of the VTA.

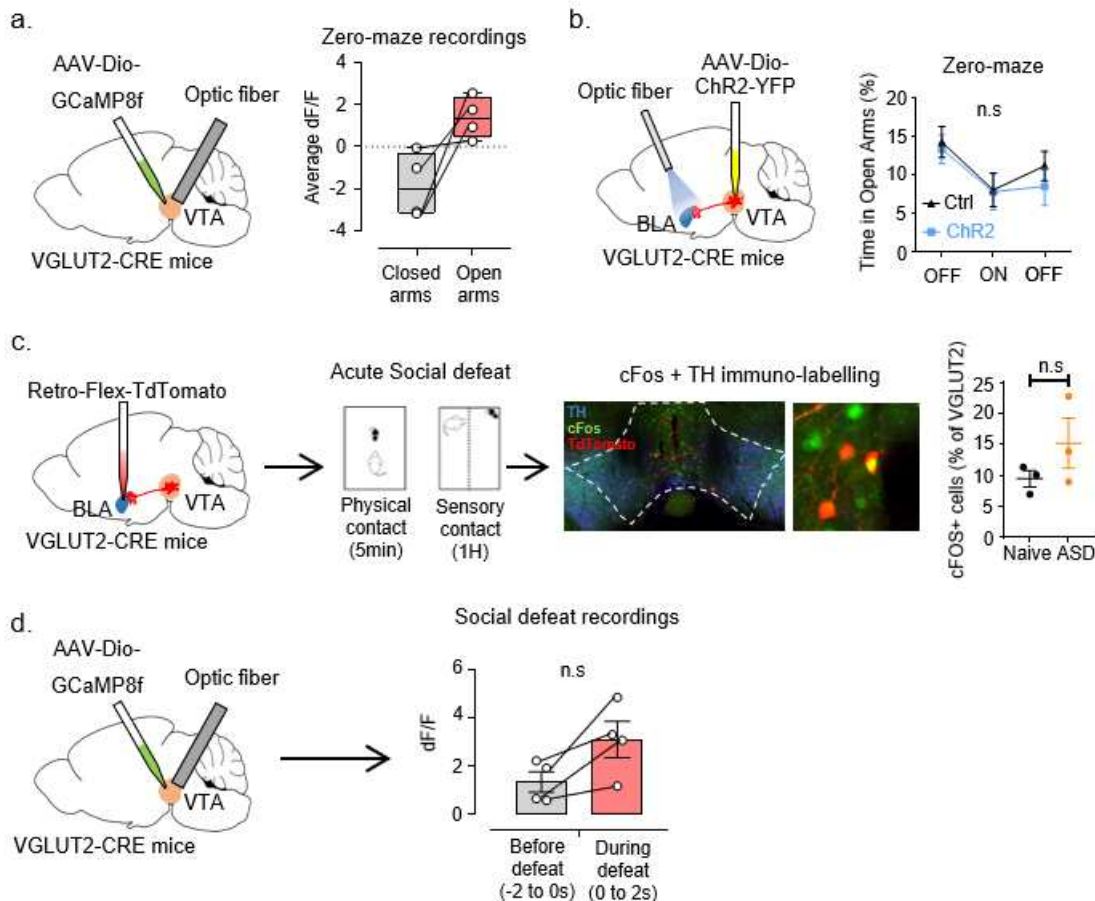


Figure 2. VTA glutamatergic inputs to the BLA are responsive to stress but do not modulate basal anxiety levels. (a) Left panel: vGlut2-CRE mice were injected with AAV-Dio-GCaMP8f in the VTA and implanted with an optical fiber placed over the VTA. Three weeks later, mice were put in the zero-maze test while the activity of VTA glutamate neurons was recorded. Right panel: Quantification of the activity of VTA glutamate neurons upon exploration by the mice of the closed or open arms of the zero-maze. (b) vGlut2-CRE mice were injected with AAV-Dio-ChR2-YFP in the VTA and were implanted five weeks later with an optical fiber placed over the BLA. Two weeks later, mice anxiety levels were measured in a zero-maze test divided in three phases of 1min30 each. The ON phase is paired with an optogenetic stimulation of the VTA glutamate efference to the BLA (pulses of 10mW, 20Hz, 20ms). (c) vGlut2-CRE mice were injected with a retrograde AAV-Flex-TdTomato in the BLA. Three weeks later, mice were subjected to an acute social defeat session (5min) before being

sacrificed one hour after. An immunostaining against cFOS (green) and TH (blue) was performed. The number of vGlut2 retrogradely-labelled neurons (red) co-labelled for cFOS was quantified. **(d)** vGlut2-CRE mice were injected with AAV-Dio-GCaMP8f in the VTA and implanted with an optical fiber placed over the VTA. Three weeks later, mice were subjected to an acute social defeat session (5min). The activity of VTA glutamate neurons was recorded before and during aggression by a dominant conspecific.

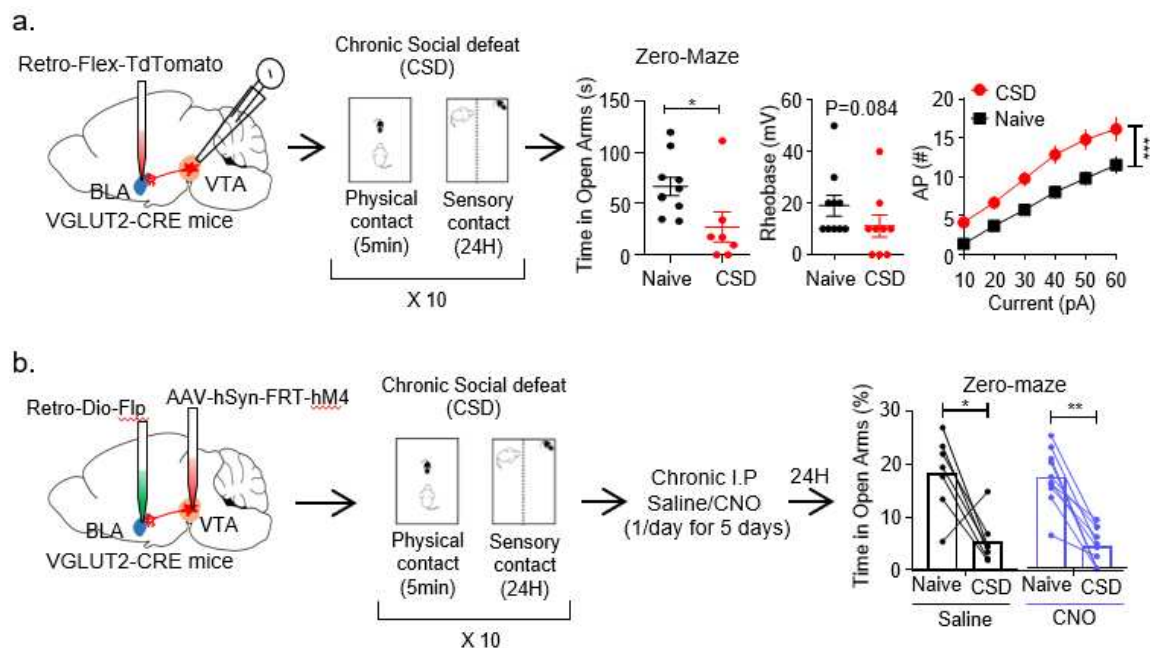


Figure 3. Chronic chemogenetic silencing of VTA glutamate efference to the BLA do not revert chronic stress-induced anxiety. **(a)** vGlut2-CRE mice were injected with a retrograde AAV-Flex-TdTomato in the BLA. Three weeks later, mice were subjected to a chronic social defeat protocol (5min/ day during 10 days). 24 hours after the last social defeat session, mice anxious phenotype was confirmed in the zero-maze and ex vivo electrophysiological recordings of BLA projecting VTA glutamate neurons was performed. **(b)** vGlut2-CRE mice were injected with a retrograde AAV-Dio-Flippase in the BLA and with an AAV-FRT-hM4-mCherry in the VTA. Three weeks later, mice anxiety levels were tested in the zero-maze before subjecting to a chronic social defeat protocol (5min/ day during 10 days). 24 hours after the last social defeat session, mice were chronically injected either with saline or CNO once per day, during 5 days. 24 hours after the last injection, mice were subjected to a zero-maze to assess anxiety levels after CSD.

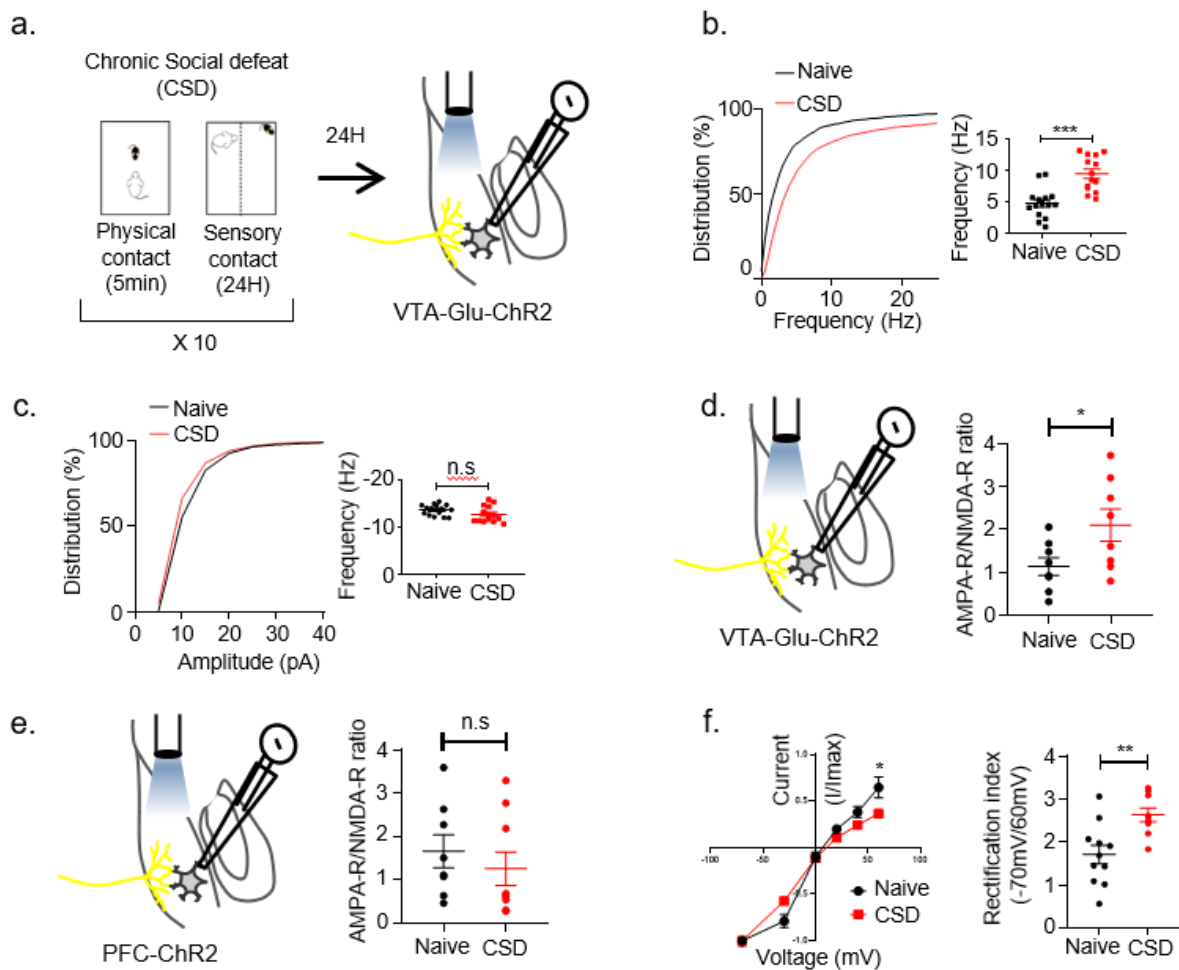


Figure 4. Chronic social defeat stress induces synaptic plasticity alterations of the BLA neurons receiving glutamatergic projections from the VTA but not the PFC. (a) Schematic representation of the protocol used from b. to e. vGlut2-CRE mice were injected with AAV-Dio-ChR2-YFP in the VTA. Five weeks later, mice were subjected to a chronic social defeat protocol (5min/ day during 10 days). 24 hours after the last social defeat session, post-synaptic adaptations of BLA neurons receiving functional inputs from the VTA glutamate neurons were measure through ex vivo electrophysiological recordings. (b) Cumulative distribution of spontaneous EPSCs frequency in VTA glutamate connected BLA neurons of mice subjected to the protocol described in a. (c) Cumulative distribution of EPSCs amplitude of VTA glutamate connected BLA neurons of mice subjected to the protocol described in a. (d) vGlut2-CRE mice were injected with AAV-Dio-ChR2-YFP in the VTA. Five weeks later, mice were subjected to a chronic social defeat protocol (5min/ day during 10 days). 24 hours after the last social defeat session, post-synaptic AMPA/NMDA-R ratio of BLA neurons receiving functional inputs from the glutamate neurons from the VTA were measured through ex vivo electrophysiological

recordings. (e) Mice were injected with AAV-ChR2-YFP in the PFC. Mice were subjected to the same protocol as described in b. and post-synaptic AMPA/NMDA-R ratio of BLA neurons receiving functional inputs from the glutamate neurons from the VTA were measured through ex vivo electrophysiological recordings. (f) I-V curve and rectification Index of AMPA currents recorded in VTA glutamatergic connected BLA neurons of mice subjected to the protocol described in a.

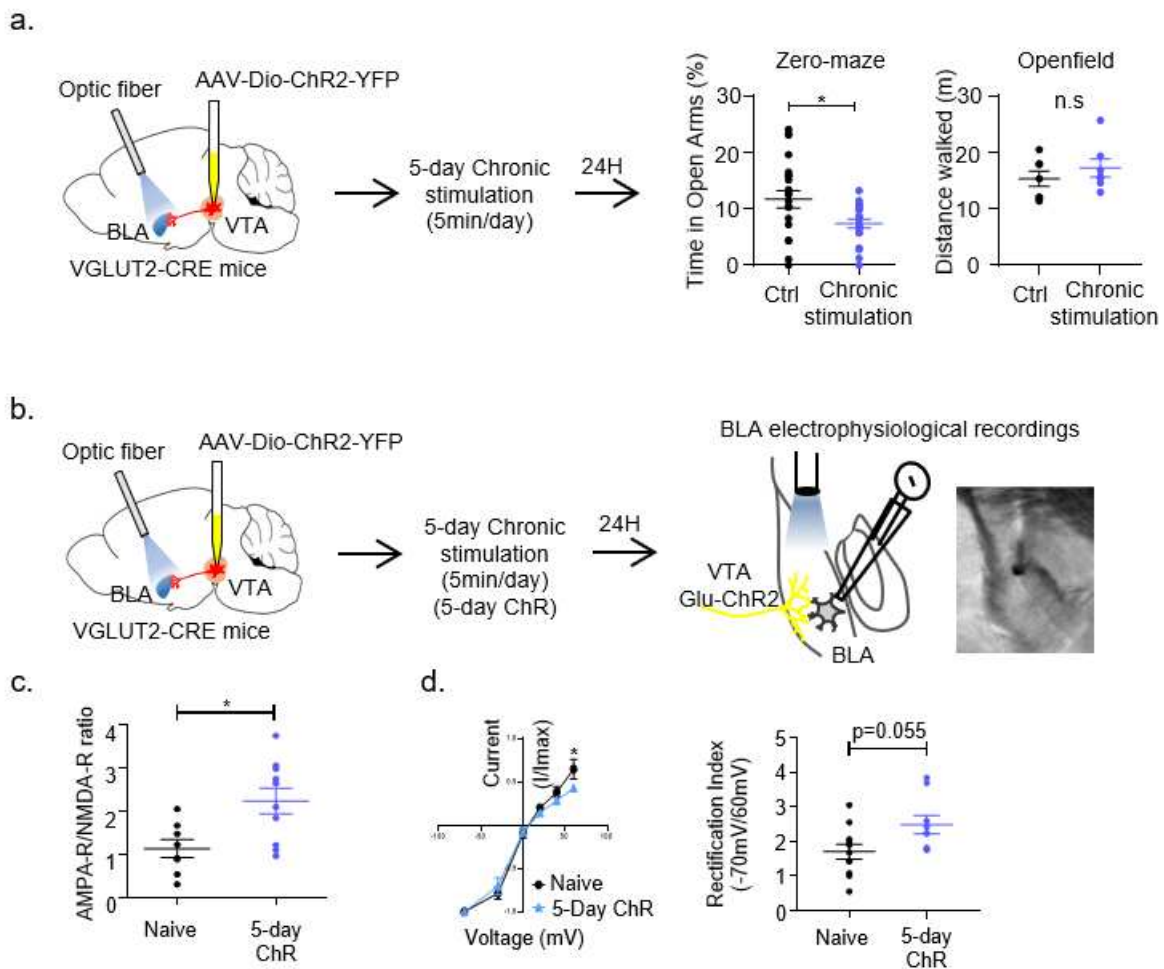


Figure 5. Chronic stimulation of VTA glutamate efference to the BLA triggers anxiety and post-synaptic adaptations similar to mice exposed to CSD. (a) vGlut2-CRE mice were injected with AAV-Dio-ChR2-YFP in the VTA and were implanted five weeks later with an optical fiber placed over the BLA. Two weeks later, mice were subjected to a chronic stimulation of VTA glutamate efference to the BLA once per day, during five days (10 min stimulation, pulses of 10mW, 20Hz, 20ms). 24 hours after the last stimulation, mice anxiety levels were measured in the zero-maze and locomotor activity in the openfield. (b) vGlut2-CRE mice were subjected to the same protocol as in a., however 24 hours after the last social defeat session, post-synaptic adaptations were measured through ex vivo electrophysiological

recordings for BLA neurons receiving functional inputs from VTA glutamate neurons. **(c)** Measure of the AMPA/NMDA-R ratio of BLA neurons receiving VTA glutamate afference for mice subjected to the protocol described in b. **(d)** I-V curve and rectification Index of voltage-clamp recording of VTA glutamate connected BLA neurons of mice subjected to the protocol described in b.

Axis 2: Circuit dissection of VTA contribution to fear responses

A non-canonical GABAergic pathway to the VTA promotes unconditioned freezing

Brousot L*, Contesse T*, Costa-Campos R, Glangetas C, Royon L, Fofo H, Lorivel T, Georges F, Fernandez SP, Barik J

* These authors contributed equally to this work.

(Accepted for publication at Molecular Psychiatry)

Summary

In the following study, we determine if the VTA plays a non-canonical role in stress-induced fear response in mice. We measure freezing, a tonic immobility characteristic of fear response in mice when a threat is distant or unidentified. We combined here the use of optogenetic and chemogenetic tools with behavioral and electrophysiological recordings. We sequentially parsed the influence of different LDTg inputs to the VTA in mediating freezing response. We also assessed what efferent structure downstream to the VTA could regulate the observed stress-induced freezing response. Overall, we found that GABA inputs to BLA projecting VTA GABAergic neurons modulate the freezing response.

Contribution

While secondary to my thesis project, this study has taken important part of the end of my PhD. The design of the project has been shared between the first co-author Loïc BROUSSOT and my two supervisors and last authors: Sebastian P FERNANDEZ and Jacques BARIK. I have participated in the stereotaxic viral injections and histochemical analysis. Furthermore, I have performed all the in vivo optogenetic and many of the chemogenetic in vivo experiments. Furthermore, I have participated in the design and realization of many behavioral experiments required during the revision of this article in the journal Molecular Psychiatry. Electrophysiological recordings were performed by Sebastian P FERNANDEZ and Renan CAMPOS. Microscopy images were obtained by Hugo FOFO, Loïc BROUSSOT and me. Most of the behavioral experiment were carried out by Loïc BROUSSOT and me. Data analysis was performed by Loïc BROUSSOT.

A non-canonical GABAergic pathway to the VTA promotes unconditioned freezing

Loïc Brousot^{1,2*}, Thomas Contesse^{1,2*}, Renan Costa-Campos^{1,2}, Christelle Glangetas³, Léa Royon^{1,2}, Hugo Fofó^{1,2}, Thomas Lorivel², François Georges³, Sebastian P. Fernandez^{1,2,4} and Jacques Barik^{1,2,4}.

1 Université Côte d'Azur, Nice, France.

2 Institut de Pharmacologie Moléculaire & Cellulaire, CNRS UMR7275, Valbonne, France.

3 Université de Bordeaux, CNRS, IMN, UMR 5293, F-33000 Bordeaux, France.

4 Co-last and co-corresponding authors.

* These authors contributed equally to this work.

Correspondence should be addressed to J.B. (barik@ipmc.cnrs.fr) and S.P.F. (fernandez@ipmc.cnrs.fr)

Keywords: laterodorsal tegmentum, ventral tegmental area, GABA, stress, freezing

Abstract

Freezing is a conserved defensive behavior that constitutes a major stress-coping mechanism. Decades of research have demonstrated a role of the amygdala, periaqueductal gray and hypothalamus as core actuators of the control of fear responses, including freezing. However, the role that other modulatory sites provide to this hardwired scaffold is not known. Here, we show that freezing elicited by exposure to electrical foot shocks activates laterodorsal tegmentum (LDTg) GABAergic neurons projecting to the VTA, without altering the excitability of cholinergic and glutamatergic LDTg neurons. Selective chemogenetic silencing of this inhibitory projection, but not other LDTg neuronal subtypes, dampens freezing responses but does not prevent the formation of conditioned fear memories. Conversely, optogenetic-activation of LDTg GABA terminals within the VTA drives freezing responses and elicits bradycardia, a common hallmark of freezing. Notably, this aversive information is subsequently conveyed from the VTA to the amygdala via a discrete GABAergic pathway. Hence, we unveiled a circuit mechanism linking LDTg-VTA-amygdala regions, which holds potential translational relevance for pathological freezing states such as post-traumatic stress disorders, panic attacks and social phobias.

INTRODUCTION

Stress is a key motor of adaptation. The stress response is mostly beneficial as it promotes survival. Whenever a living organism is presented with an environmental stressful stimulus such as a threat, it activates dedicated cerebral circuitries to select the most adaptive response among a diverse repertoire of defensive behaviours¹. These innate and learned responses have been shaped by natural selection and conserved in both invertebrates and vertebrates. Defensive behaviours vary according to the nature of the stimulus as well as internal factors such as behavioural inhibition and anxiety traits^{2,3}. In terms of behavioural outputs, defensive behaviours range from passive strategies such as freezing to active fight-or-flight responses, and the switch between these passive/active modes is essential for behavioural flexibility^{1,4,5}.

Freezing is a universal fear response characterized by a total lack of movement, aside breathing, due to a tense body posture when a threat is encountered. Freezing is cardinal in stress-coping processes as it corresponds to a state of hypervigilance, enabling decision-making and consequently building the most pertinent behavioural strategy. Although freezing has relevance for the etiology of threat-related disorder such as post-traumatic stress disorders (PTSD), panic attacks and social phobias⁶⁻⁹, the underpinning neuronal circuits and cellular substrates are far from being understood. A large body of evidence indicates that cerebral structures such as the periaqueductal gray (PAG), the hypothalamus, or the amygdaloid complex play a major role in the detection, integration and response to unconditioned and conditioned threats in both rodents and humans^{2,10,11}. Indeed, decades of work using different approaches ranging from lesions, pharmacological interventions and electrical stimulations to more recent opto- and pharmaco-genetic tools positioned the amygdala as a core unit in this hierarchical network of fear defensive system¹¹. The lateral amygdala computes information from sensory and associative inputs from cortices and thalamic nuclei that is conveyed to the central amygdalar output nucleus^{2,11}. This latter influences the activity of PAG

and hypothalamic pathways to subsequently influence the activity of the medulla and pons resulting in changes in viscera function, muscle contraction and pain sensitivity¹². Yet, in light of the impact of stress on the brain, stress-coping is likely to recruit key modulatory brain networks, which could shape freezing responses. Uncovering these pathways is an important step to fully understand the etiology of fear responses such as freezing, and to build a comprehensive functional map of these underlying interconnected subcortical and cortical regions. In humans, this distributed defensive network can suffer unduly activation and persistent deregulations sustained by epigenetic and synaptic changes, which clinically manifest as states of intense distress, peri-traumatic reactions and PTSD¹³.

The laterodorsal tegmental nucleus (LDTg) is interconnected with limbic regions and responds to somatosensory, visual and auditory stimuli¹⁴. Although primarily studied for its role in reward-oriented behaviours¹⁵⁻¹⁷ and paradoxical sleep^{18,19}, recent work indicates that the LDTg can convey stress-related information^{20,21}. The LDTg constitutes a strong modulator of the motivational balance regulating appetitive and negatively-valenced behaviours. As part of the reticular formation, the LDTg contributes also to behavioral arousal thus facilitating sensory integration^{22,23}, which is a key component affecting fear responses. Hence, we hypothesized that the LDTg could contribute to defensive behaviour such as freezing responses. To test this, we combined electrophysiological *in vivo* and *ex vivo* recordings and behavioural analyses to assess electric shocks-induced freezing. To causally link the LDTg to freezing responses, we employed pharmacogenetic and optogenetic approaches in virally-tagged brain circuits. We uncover a non-canonical pathway implicating LDTg GABAergic projection to the ventral tegmental area (VTA), which subsequently impact amygdalar neurons to regulate unconditioned freezing responses.

MATERIAL AND METHODS

Animals

All procedures were in accordance with the recommendations of the European Commission (2010/63/EU) for care and use of laboratory animals and approved by the French National Ethical Committee (#9185-2017020911476246 and #16459-2018061116303066). We used male C57BL/6J mice (Janvier Labs, France), vGAT-CRE mice (The Jackson Laboratory, stock number: 028862), vGluT2-CRE mice²⁴, and ChAT-CRE mice (The Jackson Laboratory, stock number: 006410). Transgenic mice were heterozygous and backcrossed on a C57BL/6J background. Mice were housed 4-5 mice per cage on a 12h/12h light/dark cycle with lights on from 8:00 a.m to 8:00 p.m. Mice had free access to food and water ad libitum. Enriched housing consisted of a chewing block of wood, a plastic igloo and cotton to facilitate nesting. All mice used in behavioural experiments were handled daily for one week before each test to limit any stress induced by intraperitoneal injections and connections to laser cables for *in vivo* optogenetic experiment. All tests were performed on adult mice that were at least 2 months old and littermates were used as controls. All the experiments were performed in accordance to the ARRIVE guidelines.

Reagents and drug administration

Clozapine-N-Oxide (CNO) was purchased from Enzo Life (France), Ketamine and Xylazine from Centravet (France), and picrotoxin from Sigma-Aldrich (France). All drugs for *in vivo* administration were diluted in saline solution 0.9% NaCl. Mice received either saline (10 mL/kg) or CNO (1 mg/kg) as previously described in²⁰.

Viral tools

Viruses were purchased from the following facilities: Addgene (plasmid #50475 AAV8-hSyn-hM4D(Gi)-mCherry, plasmid #44362 AAV8-hSyn-DIO-hM4D(Gi)-mCherry, plasmid #44361 AAV8-hSyn-DIO-hM3D(Gq)-mCherry, plasmid #20298 AAV5-EF1a-double floxed-hChR2(H134R)-EYFP-WPRE-HGHpA, plasmid #20297 AAV5-EF1a-double floxed-hChR2(H134R)-mCherry-WPRE-HGHpA) and Plateforme de vectorologie de Montpellier (Canine Adenovirus type 2, CAV-2-Cre). For modulation in a projection- and cell-type specific manner we used viruses from Zurich vector core facility (identifier: v190-8 AAV-8/2-hSyn1-dFRT-hM4D(Gi)-mCherry(rev)-dFRT-WPRE-hGHp(A), identifier:v171-retrograde ssAAV-retro/2-hSyn1-chi-dlox-EGFP_2A_FLPo(rev)-dlox-WPRE-SV40p(A)), Titers for AAVs and CAV-2-Cre were $\geq 10^{12}$ ppl/mL and $\geq 10^{13}$ ppl/mL respectively.

Stereotaxic injections

Stereotaxic injections were performed using a stereotaxic frame (Kopf Instruments). General anaesthesia was achieved using a mix of ketamine (150 mg/kg) and xylazine (10 mg/kg). All viruses were injected bilaterally at a rate of 100 nL/min for a final volume of 200 nL per site (except for VTA for which we injected 300 nL). Mice were 5-6 weeks-old at the time of surgery and were given at least a 3-week recovery period for pharmacogenetic experiments and 6 weeks for optogenetic tests to allow sufficient viral expression. Stereotaxic coordinates (antero-posterior: AP; Mediolateral: ML; dorsoventral: DV) were based on the Paxinos atlas of the adult mouse brain²⁵, and adapted as we performed surgeries on young mice. They are given here in millimetres (mm) from bregma for AP and ML coordinates, DV is taken from skull at the site of injection. Coordinates were as followed: LDTg: AP -4.70, ML ± 0.50 , DV -3.60; VTA: AP -2.80, ML ± 0.60 , DV -4.70; CeA: AP -0.75, ML ± 3.00 , DV -5.05; vIPAG: AP -4.00, ML ± 0.60 , DV -2.50; BLA: AP -1.30, ML ± 3.20 , DV -4.60; LS: AP +1.0, ML ± 0.2 , DV -3.35.

To silence LDTg neurons, an AAV8-hSyn-hM4D(Gi)mCherry was injected bilaterally in the LDTg of C57Bl6J mice.

To specifically silence LDTg cholinergic, glutamatergic and GABAergic neurons, an AAV8-hSyn-DIO-hM4D(Gi)mCherry was injected bilaterally in the LDTg of ChATCre, vGluT2Cre and vGATCre mice respectively.

For projection-specific silencing, wild-type mice were bilaterally injected with CAV-2-Cre in the periaqueductal gray (PAG), central amygdala (CeA) or VTA and with a hSyn-DIO-hM4D(Gi)-mCherry in the LDTg (hereafter named LDTg^{hM4→PAG}, LDTg^{hM4→CeA}, LDTg^{hM4→VTA} mice). For selective manipulation of VTA^{g→BLA} projections we injected bilaterally a CAV-2-Cre in the BLA and a hSyn-DIO-hM4D(Gi)-mCherry in the VTA.

To selectively activate LDTg to VTA projections we injected a CAV-2-Cre in the VTA and a hSyn-DIO-hM3D(Gq)-mCherry in the LDTg of wild-type mice (hereafter named LDTg^{hM3→VTA}).

For projection- and neurotransmitter-specific manipulation, vGATCre mice were bilaterally injected with a retrograde AAV-retro/2-hSyn1-chi-dlox-EGFP_2A_FLPo(rev)-dlox-WPRE-SV40p(A) in the VTA and an AAV-8/2-hSyn1-dFRT-hM4D(Gi)-mCherry(rev)-dFRT-WPRE-hGHp(A) in the LDTg (hereafter named GAT^{hM4; LDTg→VTA}).

***In vivo* optogenetic manipulation.**

Optical fibres (200 µm core, 0.39 NA, made following the protocol of²⁶ were implanted bilaterally into the VTA with a 15° angle (AP: -2.8 mm; ML: - 1.5 mm; DV: - 4.2 mm), 4-5 weeks after viral injection. Fibre optics were connected by a mating sleeve (ThorLabs, ADAL1-5) to patch-cords (Doric Lenses, MFP_200/240/900-0.22_1m_FC-ZF1.25(F)) to a fibre optic rotary joint (Doric Lenses FRJ_1x2i_FC-2FC_0.22) itself connected to a laser source (ThorLabs S1FC473MM). Mice were habituated to fibre optic connection for 30 min per day during the week preceding behavioural testing. On the day of experiment, mice performed behavioural tests after 10²¹min habituation following connection. The power of the blue (470 nm) laser was 10 mW.mm⁻² as measured at the tip of the optic fibre. Light

stimulation was delivered at 50Hz in pulses of 20 ms for periods of 1 min. Control group mice underwent the same procedure and received the same intensity of laser stimulation. Mice with misplaced viral injections or fibre optic implantations were excluded. The stimulation parameters were based on both the *ex-vivo* electrophysiological recordings performed in our laboratory and also published literature²¹.

For the conditioned place aversion test, we used two distinct chambers (with different visual and tactile cues) connected by a neutral compartment. On day 1, control and vGAT-Cre ChR2 mice freely explored the apparatus during 20 min. From day 2 to 4, mice were randomly assigned to a paired chamber (pairing was counterbalanced) and received light stimulation (50Hz frequency, 20 ms duration, delivered at 5min duration with 5min intervals). Two conditioning sessions of 20 min were conducted each day, so that mice received light stimulation in the paired chamber and no light stimulation in the unpaired chamber (am and pm sessions counterbalanced). On day 5, mice freely explored the apparatus in absence of stimulation. Results are expressed as different between the time spent (s) in paired chamber between day 5 (test) and day 1 (pre-test).

Behavioural testing

In all behavioural tests, unless otherwise stated, mice were housed in a habituation room adjacent to the experimental room at least one hour before the beginning of the test. Unless otherwise stated, saline or CNO were injected 30 min before behavioural testing. After each test, mice were temporarily housed in a new cage to avoid social interaction with untested mice until they were all tested and finally returned to their home cages.

Freezing paradigm

To measure electric shock-induced freezing, each mouse was placed individually in a soundproof test chamber containing a floor made of a grid with 27 stainless-steel rods (diameter 4 mm) spaced 1 cm apart and connected to a generator to allow shock delivery (Shocker LE 100-26 Panlab Harvard Apparatus Bioseb). Mice were left to freely explore the apparatus for 3 minutes and then received three consecutive electrical foot shocks (intensity: 0.7 mA, duration: 2 s) with a 58 s interval between each shock. Mice remained in the test chamber 1 min after the last foot shock. Activity levels of mice were recorded through a high-precision sensor plate placed beneath the floor grid (Load cell coupler LE 111 Panlab Harvard Apparatus Bioseb) to assess the variations of weight induced by the movements of the mice. Each test was also recorded using a video camera (Samsung SDP-860) placed above the apparatus. Freezing was defined as total lack of movement aside from breathing for a cumulative duration of at least two seconds. An experimenter blind to the experimental conditions manually scored the freezing behaviour of each mouse using the video recordings.

The subthreshold version of the freezing paradigm used with the activatory hM3 DREADD system was run over two days. On the first day, mice were placed in the test chamber as described above and left to explore freely for 5 minutes. On the second day, mice received a saline or CNO injection and immediately introduced in the test chamber. Mice were left 1 minute to explore freely and then received two electrical foot shocks (intensity: 0.7 mA, duration: 2 s; 58s interval). Mice were then left undisturbed for 15 minutes and freezing behaviour was assessed using the same method as described above during the last five minutes of the test.

All mice employed in the freezing and its subthreshold version were not re-used in other behavioral tests.

For *in vivo* optogenetic manipulations, mice were put in the same test box and left free to explore the apparatus for 5 min (habituation, OFF). Then, they received intracerebral illumination for 1 min (ON), and then 1 min without illumination (OFF). No electrical shocks were delivered. To test for aversive

memory formation, mice were re-exposed 24h after to the same context 24h. The video camera was placed on the side of the test chamber for further behavioural analyses.

O-maze

The O-maze test was used to measure anxiety levels. Each mouse was placed in a circular maze consisting of two open arms and two closed arms alternating in quadrants (width of walking lane: 5 cm, total diameter: 55 cm, height of the walls: 12 cm, elevation above the floor: 60 cm) with an ambient light of 200 lux in the open arms. Mice movements were recorded during 5 minutes using a video camera placed above the maze. An experimenter blind to the experimental groups scored the time spent in the open arms.

Open-Field

The Open-field test was used to measure locomotor activity. Each mouse was placed in a 40x40 cm open field with an ambient light of 200 lux for 5 minutes and left to explore freely. Mice movements were recorded using a video camera placed above the apparatus. Distanced travel was automatically analysed using the software AnyMaze (Stoelting, France).

Hargreaves Test

The Hargreaves test was used to measure pain sensitivity. Each mouse was placed in a small transparent plastic compartment in a room lit by red light for 30 minutes of habituation. Then, a radiating infrared source (intensity: $190 \pm 1 \text{ mW.cm}^2$) was placed under the rear paw of the mice and the latency to withdraw the paw was measured. Each day, two measures were taken for each rear paw with at least 1 min between each measure and the mean latency was calculated. The test was repeated

during three days with one day of interval between each trial. Only the results of the last two trials were analysed by a blind experimenter. Of note, the mice which underwent the Hargreaves test were first tested in the O-maze and then Open-field with 4 days interval between each test to avoid potential effect of pre-CNO exposure.

***Ex vivo* patch-clamp recording**

Mice were anaesthetised (ketamine 150 mg/kg, xylazine 10 mg/kg) and transcardiacally perfused with aCSF for slice preparation. For LDTg recordings, 250µm coronal slices were obtained in bubbled ice-cold (95% O₂ / 5% CO₂) aCSF containing (in mM): KCl 2.5, NaH₂PO₄ 1.25, MgSO₄ 10, CaCl₂ 2.5, glucose 11, sucrose 234, and NaHCO₃ 26. Slices were then incubating in aCSF containing (in mM): NaCl 119, KCl 2.5, NaHPO₄ 1.25, MgSO₄ 1.3, CaCl₂ 2.5, NaHCO₃ 26, and glucose 11 at 37°C for 15 min, and then kept at room temperature. Slices were transferred and kept at 32-34°C in a recording chamber superfused with 2.5 mL/min aCSF. Visualised whole-cell voltage-clamp or current-clamp recording techniques were used to measure synaptic responses or excitability respectively, using an upright microscope (Olympus France). Current-clamp experiments were obtained using a Multiclamp 700B (Molecular Devices, Sunnyvale, CA). Signals were collected and stored using a Digidata 1440 A converter and pCLAMP 10.2 software (Molecular Devices, CA). In all cases, access resistance was monitored by a step of -10 mV (0.1 Hz) and experiments were discarded if the resistance increased more than 20%. Internal solution contained (in mM): K-D-gluconate 135, NaCl 5, MgCl₂, HEPES 10, EGTA 0.5, MgATP 2, and NaGTP 0.4. Depolarizing (0-300 pA) or hyperpolarizing (0-450 pA) 800 ms current steps were used to assess excitability and membrane properties of LDTg and VTA neurons. For VTA recordings, 250 µm horizontal slices were obtained as before, and incubated in aCSF for 1h at 37°C before recording started.

To probe for functional synaptic connections within the VTA, we injected vGATCre mice with an AAV-DIO-ChR2-YFP in the LDTg and an AAV-hSyn-DIO-mCherry in the VTA. This allows us to identify VTA

GABAergic neurons expressing mCherry while opto-genetically activating GABAergic LDTg terminals. In another batch of mice, we performed the same injections in the LDTg and putative VTA DA neurons were identified based on classical criteria and as previously done^{20,27}. To unambiguously identify VTA glutamatergic neurons, we injected vGluT2Cre mice with AAV-hSyn-DIO-mCherry in the VTA and a non cre-dependent AAV-hSyn-ChR2-YFP in the LDTg. We pharmacologically isolated the GABAergic component of the optogenetic stimulation using glutamatergic receptor antagonists (AP5 50 μ M and DNQX 10 μ M) and cholinergic receptor antagonists (mecamylamine 10 μ M and atropine 1 μ M). Last, to record VTA^{→BLA} neurons, we injected vGATCre mice with an AAV-DIO-ChR2-YFP in the LDTg and a retroAAV-hSyn-tdTomato in the BLA. VTA horizontal sections were prepared as previously done²⁰. Whole-cell voltage-clamp recordings of fluorescent-tagged neurons in VTA were performed using the same internal solution as before with $V_m = -40$ mV in the presence of DNQX to block AMPA currents. Photocurrents were induced by optical illumination (0.1 Hz) with 5ms blue light pulses delivered by a LED through the objective light path. Twenty sweeps were averaged offline, and peak amplitude was measured to assess light-evoked current size. GABA-A receptors mediated currents were blocked using picrotoxin (Sigma, France) bath applied to a final concentration of 50 μ M.

In all cases, offline analysis was performed using Clampfit 10.2 (Axon Instruments, U.S.A.) and Prism (Graphpad, U.S.A.).

Immunohistofluorescence

To achieve fixation of the brains, mice were anesthetized using a mix of ketamine (150 mg/kg) and xylazine (10 mg/kg) then underwent transcardial perfusion with cold phosphate buffer (PB 0.1 M Na₂HPO₄/NaH₂PO₄, pH 7.4) followed by paraformaldehyde (PFA 4%, diluted in PB 0.1M). Brains were left at 4°C in PFA 4% overnight, then cut into 40 μ m free-floating slices. Sections were used to assess the correct location of stereotaxic viral injection for each animal and cannula implantation for *in vivo* optogenetic experiments.

For cFos labelling, brain sections containing the nucleus accumbens, amygdala or lateral septum were incubated (30 min) in PBS-BT (PBS 0.5% BSA, 0.1% Triton X-100) with 10% normal goat serum (NGS). Sections were then incubated (4°C) in PBS-BT, 1% NGS, with primary anti-cFos (1:1000, Abcam anti-rabbit 1:1000, Cat Ab190289) for 36h. Sections were rinsed in PBS and incubated (2 h) in goat anti-rabbit Alexa488 secondary antibody (1:1000, Vector Laboratories, Burlingame, CA; Cat goat anti-rabbit Alexa488 secondary antibody (1:1000, Vector Laboratories, Burlingame, CA; Cat. DI-1488-1.5) in PBS-BT, 1% NGS. Sections were rinsed with PBS and incubated 5 min with DAPI before mounting with Mowiol. Images for quantification of cFos-positive cells were acquired using a TCS SP5 confocal microscope (Leica Microsystems). An experimenter blind to treatment counted manually using ImageJ. Counting was done on two adjacent brain sections and the two hemispheres for each region analyzed. A mean value was averaged for each mouse and plotted for each experimental condition (i.e. Control or Chr2) as cFos+ cells/mm².

***In vivo* single-unit neuron recordings**

We performed as previously published ^{28,29}. Briefly, stereotaxic surgeries for electrophysiology experiments were performed under 1.0-1.5% isoflurane (in 50% air/50% O₂; 1L/min) anesthesia. A glass micropipette filled with 2 % pontamine sky blue solution in 0.5 % sodium acetate was lowered into the VTA (-3.16 mm/bregma, 0.5 mm/midline, 3.5-4.5 mm/brain surface) ²⁵. Extracellular potentials were recorded with an Axoclamp-2B amplifier and filter (300 Hz/0.5 Hz) ³⁰. Spikes were collected online (CED 1401, SPIKE 2; Cambridge Electronic Design; UK). VTA dopamine neurons were identified according to well-established electrophysiological features ^{31,32}, which included the following (i) an action potential with ≥ 1.1 ms (measured from the start of action potential to the negative trough), (ii) spontaneous firing rate (≤ 10 Hz) (iii) single and burst spontaneous firing patterns composed by 2 to 10 spikes *in vivo*. The onset of a burst was defined with an interspike interval lower than 80 msec and the end of the burst with an interspike interval higher than 160 ms ³³. Putative VTA GABA neurons were

identified according to well-established electrophysiological criteria (i) an action potential < 1 ms ; (ii) VTA boundary was defined 100 μ m dorsal to the first VTA DA neuron^{33–36}. Several parameters for VTA dopamine neuron firing and bursting were analyzed over a 100-second period: the cumulative probability distribution of the firing rate and the bar graphs with the mean \pm SEM, the bursting rate, the percentage of spikes in burst (% SIB). Firing frequency of GABA neurons was analyzed over a 100-second period. Results are expressed as mean \pm SEM.

Heart rate recordings

Heart rate was recorded using the MouseOx Pulse non-invasive oximeter (Starr Life Sciences). Briefly, mice were shaved around the neck area 24h before recordings. On the recording day, individual mice were anesthetized and maintained under 1.0-1.5% isoflurane (in 50% air/50% O₂; 1L/min). The neck collar and system were set up according to manufacturer instructions, and optic fibres were connected to the head to stimulate LDTg GABA terminals in the VTA. After obtaining a baseline of 10 min, 3 photo-stimulation protocols were delivered at 50Hz for 1 min, separated by 2min. Heart-rate was acquired at 5 Hz sampling rate, and analyzed using Excel. Heart rate deviations from baseline were calculated by building a z-score of the whole trace using the mean and SD. Data are expressed as mean \pm SEM.

Data analysis

Data were analysed using Prism (GraphPad, U.S.A.). Normality of the distribution was first tested using a Kolmogorov-Smirnov test. Depending of the number of groups and the results of the normality test, groups were then compared using a Student t-test, U of Mann-Whitney, or two-way analyses of variance (ANOVA) followed by post hoc Sidak's test. Data in the figures are presented as mean \pm SEM. Statistical significance was conventionally established at *p<0.05, **p<0.01, ***p<0.001.

RESULTS

LDTg inputs to the VTA bidirectionally control freezing

To assess the involvement of the LDTg in processing freezing, we used a chemogenetic approach to remotely silence LDTg neurons prior administration of electrical foot shocks. Wild-type C57BL/6J mice were injected into the LDTg with inhibitory DREADD (AAV-hSyn-hM4D-mCherry), hereafter referred to as LDTg^{hM4} mice (Fig. 1a, left panel). As depicted in the activity chart, foot shock delivery produced a decrease in locomotor activity and an increased time spent in freezing postures (Fig. 1a, middle panel). Quantification of freezing in saline-treated mice showed a gradual increase in this behaviour after each foot shock. In contrast, silencing of LDTg neurons engendered a pronounced and significant downward shift of the freezing response curve (Fig. 1a, right panel). This reduction of freezing was not caused by changes in locomotor activity, anxiety levels or pain sensitivity since saline- and CNO-treated LDTg^{hM4} mice showed similar responses in the open-field, elevated O-maze and Hargreaves test (Fig. 1b, c, d respectively). Importantly, reduced freezing did not impair aversive memory formation since re-exposure to the same context 24h after (Day 2) produced comparable conditioned-freezing responses in both groups (Fig. S1). These results demonstrate that activity in LDTg neurons is necessary for fear freezing manifestation but not memory formation of an aversive event.

To unravel the circuitry that links LDTg and freezing, we carried projection-specific chemogenetic manipulations of LDTg projections to the ventrolateral periaqueductal gray (vlPAG) and the central amygdala (CeA), two regions classically linked to the control of freezing responses^{11,37}. We therefore injected a retrograde CAV-2-Cre in either the vlPAG or the CeA and a Cre-dependent inhibitory DREADD (AAV-hSyn-DIO-hM4D-mCherry) in the LDTg to independently manipulate LDTg^{→vlPAG} or LDTg^{→CeA} projections. We validated this approach by immuno-histofluorescence as we observed mCherry-positive neurons in the LDTg and red fibres within the CeA and vlPAG (Fig. S2a and b respectively). Silencing LDTg^{→vlPAG} or LDTg^{→CeA} projections did not alter the freezing response that was similar in mice

receiving either saline or CNO (Fig. S2a and b respectively). Next, given the rising interest of the VTA in aversion processing^{38,39}, and the dense projections arising from the LDTg⁴⁰⁻⁴³, we hypothesized that this pathway could be involved in freezing behaviours. Indeed, silencing LDTg^{→VTA} projections triggered a significant downward shift of the freezing response (Fig. 1e), resembling results obtained with full LDTg silencing (Fig. 1a). Given this result, we hypothesized that activating this pathway may exacerbate fear responses to a mild aversive challenge. Thus, we used excitatory DREADD (AAV-hSyn-DIO-hM3D-mCherry) in order to stimulate LDTg^{→VTA} projections while exposing mice to only two foot-shocks. CNO-injected mice exhibited a strong freezing response indicating that a mild stress challenge primed LDTg^{→VTA} projections (Fig. 1f). These results point to the specificity of discrete LDTg circuits to the aversive processing of electric shocks.

LDTg GABAergic neurons are required for freezing

To assess which LDTg cell types are involved in the regulation of the freezing response, we individually silenced each neuronal population. We therefore injected a Cre-dependent AAV-hSyn-DIO-hM4-mCherry in vGlut2-Cre, ChAT-Cre or vGAT-Cre transgenic mouse lines, enabling the selective manipulation of glutamate, cholinergic or GABAergic neurons respectively. The fear response induced by electric shocks in CNO-treated LDTg^{Glut-hM4} and LDTg^{ChAT-hM4} mice was comparable to that of saline-treated controls (Fig. 2a and b, respectively). In striking contrast, freezing was markedly reduced in CNO-injected LDTg^{GABA-hM4} mice (Fig. 2c right panel), pinpointing to a key role of LDTg GABAergic transmission in electric shock-elicited freezing responses.

Electric shocks sensitize GABAergic projections to the VTA that are required for freezing

The previous results showed that independent silencing of either GABAergic LDTg neurons or LDTg^{→VTA} projections is sufficient to dampen the elicited freezing response. To test whether LDTg GABA neurons projecting to the VTA may be key in this process, we next manipulated the LDTg in a neurotransmitter- and projection-specific manner using a double intersectional strategy. We first injected in the VTA of

vGAT-Cre mice a retrograde AAV-DIO-flp that allows the expression of the flippase (flp) in a Cre-dependent manner (i.e. in GABAergic LDTg^{→VTA} neurons). Next, a flippase-dependent inhibitory DREADD (AAV-hSyn-FRT-hM4-mCherry) was injected in the LDTg. While saline-treated LDTg^{GABA→VTA-hM4} mice exhibited a normal freezing response, CNO-treated mice demonstrated a significant downward shift of the freezing curve (Fig. 3a). This provides strong evidence of the key regulatory role of this GABAergic projection over the fear response.

Can exposure to aversive foot shocks alter the cellular properties of LDTg^{→VTA} GABAergic neurons in order to promote fear responses? We performed *ex-vivo* whole-cell patch-clamp recordings in virally-tagged LDTg^{→VTA} GABAergic neurons. For this, vGAT-Cre mice were injected in the VTA with a retrograde AAV-FLEX-tdTomato (Fig. 3b). Mice were submitted to 3 consecutive electrical foot shocks as described for the behavioural testing, and recorded immediately after. Control mice were exposed to the chamber without receiving foot shocks. Exposure to foot shocks triggered an increased excitability of GABAergic LDTg^{→VTA} neurons evidenced by a higher discharge frequency to depolarizing current injections when compared to non-shocked mice (Fig. 3b, right panel). Importantly this adaptation was not accompanied by any significant effect on passive membrane properties of the cell such as membrane resistance, membrane capacitance or resting membrane potential (Fig. S3a, b, c). To test whether electric shocks could alter the activity of other LDTg cell types we applied the same procedure to ChAT-Cre and vGluT2-Cre mice and recorded cholinergic and glutamatergic LDTg^{→VTA} neurons. In contrast to what we observed for projecting LDTg GABA neurons, electrical shocks failed to modify the excitability profile of cholinergic and glutamatergic neurons projecting to the VTA (Supplementary Fig. 5a). However, projecting GABAergic LDTg neurons do not only target the VTA. Hence, we last tested whether electrical shocks could alter the function of GABAergic neurons independently of the targeted brain regions. For this, vGAT-Cre mice were injected in the vIPAG with a retrograde AAV-FLEX-tdTomato. Whereas we found an enhanced sensitivity of GABAergic LDTg^{→VTA} neurons, the excitability profile of GABAergic LDTg^{→vIPAG} neurons remained unaltered (Supplementary Fig. 5b). Thus, foot-shocks affect the activity of a discrete GABAergic LDTg pathway.

Optogenetic stimulation of LDTg GABA terminals within the VTA drives freezing

Our data gathered so far indicate that electric shocks trigger freezing by priming LDTg GABAergic LDTg^{→VTA} neurons. In order to test whether freezing could be induced without an aversive experience, we employed selective optogenetic stimulation in freely-behaving mice. We injected a Cre-dependent AAV-hsyn-DIO-hChR2-YFP in the LDTg of vGAT-Cre mice and bilaterally implanted optic fibres above the VTA. Light stimulation of ChR2 expressed on LDTg GABAergic terminals in the VTA was sufficient to induce significant freezing in absence of any aversive stimulus (Fig. 4a). Mice stopped freezing once the stimulation was turned off, indicative of a dynamic cellular process. Importantly, when mice were re-exposed to the same context 24h after in the absence of light stimulation, no conditioned freezing was observed (Supplementary Fig. S6a). Additionally, we evaluated whether pairing light stimulation in a defined context could trigger conditioned place aversion. Three daily pairings were done and mice were tested in absence of light stimulation. Of note, the distance travelled by ChR2 mice in the unpaired chamber was higher than in the paired chamber as expected, where light stimulation induced immobility (Supplementary Fig. 6b). Nevertheless, both control and ChR2 mice spent similar amount of time in the paired chamber during the pre-test and test sessions (Fig. 4b). This indicates that activation of LDTg GABAergic terminals in the VTA does not produce aversive memories.

To differentiate whether optogenetic stimulation elicited unconditioned freezing or purely a motor arrest, we performed telemetric measurements of heart rate. This was done in anaesthetised mice to avoid confounding changes in heart function and physical activity. Light stimulation in ChR2 mice resulted in a significant heart rate deceleration (i.e. bradycardia), which was not observed in control mice (Fig. 4c). Overall, this optogenetic experiment mimics two hallmarks of unconditioned freezing, namely immobility and bradycardia. Nevertheless, since this intervention does not trigger fear memories, and freezing being the sum of different physiological responses, including halted motor activity, we speculate that this artificial circuit recruitment may not fully recapitulate emotional responses to threatful stimuli.

Optogenetic stimulation of LDTg GABA terminals in the VTA activates the amygdala

Although some studies implicated the VTA in the formation of conditioned freezing responses^{44,45}, its role in unconditioned immediate freezing to threat as well as its output targets are unknown. To understand the circuits mediating LDTg GABA freezing response, we used optogenetic stimulation of LDTg GABA fibres over the VTA as before, and mice were sacrificed 90 min after light stimulation to conduct brain mapping of cFos expression (Fig. 5a). We have narrowed down our analyses to two brain structures known to play major roles in freezing, the amygdala¹¹ and the lateral septum⁴⁶. As a major target of the VTA and considering its role in motor responses, we also analyzed the reactivity of the nucleus accumbens (NAc). Activation of LDTg GABA terminals within the VTA elicited a striking activation in both the amygdala and lateral septum but not in the NAc (Fig. 5b, c and Supplementary Fig. 7a, b respectively).

In light of these results, we next tested whether modulating VTA^{→BLA} or VTA^{→LS} projections would affect freezing responses. Using an intersectional viral strategy, we expressed an inhibitory DREADD in VTA^{→BLA} (Fig. 5d) or in VTA^{→LS} (Fig. 5e) neurons and exposed mice to electric foot shocks. A significant decrease in freezing was only observed when silencing VTA^{→BLA} projections but not VTA^{→LS} pathway (Fig. 5d and e respectively). These results point to the specificity for discrete VTA targets in the freezing response.

Connectivity of GABA LDTg inputs to VTA cell types compared to VTA^{→BLA} neurons

Do LDTg GABAergic neurons directly modulate VTA^{→BLA} projecting neurons or do they encroach on VTA micro-circuits? To test this hypothesis, we probed for functional connectivity between this LDTg inhibitory input and the three VTA cell types (i.e. GABA, DA and Glu neurons) as well as VTA projecting neurons as described in Methods. Following photostimulation of LDTg terminals we found 24% of cells (7/29) connected with VTA^{→BLA} projecting neurons (Supplementary Fig. 8a). In striking contrast, 91% of VTA GABA cells (20/22) received GABA inputs from the LDTg (Supplementary Fig. 8b). These outward currents were blocked by picrotoxin, indicating that this response was through GABA-A receptors

(Supplementary Fig. 8f). Also, GABAergic LDTg neurons made functional contacts with putative 95% of VTA DA neurons (19/20). Instead, only 33 % of VTA Glu neurons (7/21) received GABA inputs from the LDTg (Supplementary Fig. 6d). Amongst the connected cells, the amplitude of optical inhibitory post synaptic currents (oIPSCs) was larger in VTA GABA and DA neurons when compared to VTA Glu cells or VTA^{→BLA} projecting neurons (Supplementary Fig. 6e). This first set of data indicates a more pronounced functional connectivity with the VTA micro-circuits over projecting ones, with a preference for DA and GABA VTA neurons.

GABA LDTg inputs affect VTA inhibitory signalling controlling freezing

Results from the connectivity analysis suggest that silencing GABAergic LDTg^{→VTA} neurons should preferentially modulate VTA GABAergic or DA neurons activity. To test this possibility, and to have a more comprehensive view of LDTg control over VTA function, we performed *in vivo* recordings in anaesthetised animals while silencing GABAergic LDTg^{→VTA} projections (Fig. 6a). In saline-treated mice, putative GABAergic VTA neurons exhibited a classical firing pattern of activity (Fig. 6b) similar to previous reports^{34–36}. In contrast, CNO-treated mice exhibited a strong leftward shift of the firing rate distribution of putative VTA GABA neurons, reflecting a marked decreased in activity (Fig. 6b). To determine whether silencing GABAergic LDTg^{→VTA} pathway had a broader impact onto VTA homeostasis, we additionally recorded *in vivo* the activity of VTA DA neurons. The firing rate distribution (Fig. 6c), the bursting activity and the four main modes of firing patterns of VTA DA neurons⁴⁷ did not differ between saline- and CNO-treated groups (Supplementary Fig. 9).

VTA GABA neurons can be long-range neurons or they could modulate VTA function via local connectivity^{34,35,48–50}. To try to solve this issue we sought to identify the nature of the neurotransmitter conveying freezing-related information to the amygdala. We therefore silenced in a projection- and neurotransmitter-specific manner DA, Glu and GABA VTA^{→BLA} neurons while submitting mice to electric

foot-shocks to elicit freezing. Only the silencing of GABAergic VTA^{→BLA}, but not DA or Glu, neurons decreased freezing (Fig. 6d, Supplementary Fig. 10a and b, respectively).

Overall, this set of data link an inhibitory input from the LDTg to VTA GABA function and provides evidence of a coordinated response of LDTg-VTA-amygdala macro-circuit during aversive processing (Supplementary Fig. 11).

DISCUSSION

While many brain regions have been identified to support freezing responses, the role that modulatory sites provide to this hardwired scaffold is not known. Our results provide a novel framework to understand how aversive experiences trigger rapid cellular changes ultimately leading to defensive behaviors. We show here that activity of LDTg GABAergic inputs to the VTA is necessary for the manifestation of freezing behaviors in response to imminent danger. Optogenetic stimulation of this projection is sufficient to promote freezing in absence of threat and recruitment of amygdala substrates. Our study demonstrates an uncovered role of this pathway in adaptive defensive behaviors to threat, which provides novel insights of stress coping circuits.

Macro- and micro-circuits of brain defensive network.

The brain defensive network includes several interconnected cortical and subcortical areas essential for threat detection and processing in order to timely drive defensive responses^{37,51,52}. Functional imaging studies in humans and extended molecular, cellular and circuit dissections in rodents positioned the amygdala, periaqueductal gray and prefrontal cortex as core actuators of the control of fear responses, which include freezing. While a large body of evidence provides solid ground for macro- and local-circuit governing conditioned freezing responses¹¹, a detailed comprehension of the cellular mechanisms and sequence of events eliciting unconditioned freezing behaviour is still lacking. This is highly relevant since the symptoms and pathogenesis of threat-related disorders rely on both learned and innate fear responses^{10,53}. In our study we demonstrate that electric foot shocks trigger an immediate increase in excitability of inhibitory LDTg projecting neurons to the VTA. The silencing of this specific projection has selective impact onto the function of VTA GABAergic neurons, without altering the firing of VTA DA cells. Furthermore, we dissected VTA outputs and observed that silencing of VTA GABAergic projections to the amygdala dampens unconditioned freezing responses to foot-shocks. In a recent study, selective optogenetic inhibition of VTA DA terminals in the amygdala impaired the acquisition of aversive memories but did not impact unconditioned freezing to foot-

shocks⁵⁴. This suggests that different VTA to amygdala neurotransmitter populations contribute to unconditioned and conditioned freezing.

Supporting a role of the VTA in defensive responses, two recent reports linked VTA GABA and glutamatergic neurons with innate defensive behaviour^{48,55}. Indeed, exposure to predator odor or to looming stimulus elicited a transient activation of VTA glutamate neurons associated with escape behaviours⁵⁵. Also, the onset of looming-evoked escape behaviours correlated with Ca²⁺ transients in VTA GABA neurons⁴⁸. In accordance with our study, the authors reported that direct optogenetic stimulation of this global neuronal population produced freezing followed by flight-to-nest behavior. This clearly reveals an emerging role for the VTA in escape defensive behaviours. Yet, although VTA neurons have been shown to react to foot shocks³⁴, their involvement in eliciting rapid fear responses remained uncovered. Here, we broadened the role of VTA in defensive responses by showing the triggering of freezing by solely modulating a GABA input from the pontine region. Studies addressing the role of the VTA in positive and negative valence have by far focussed onto the role of VTA DA neurons. Here, in the experiments we carried out, we could not implicate this neuronal population, but however, we identified a role for long-range VTA GABAergic neurons. This suggests that similarly to VTA DA neurons, GABAergic long-range neurons are likely to appear as, at least in part, segregated neuronal population computing distinct environmental stimuli and internal demands, in order to drive different facets of behavioral responses ranging from modulation of morphine rewarding properties, to associative learning and unconditioned freezing (present study)^{49,56,57}.

Overall, in these macro- and micro-circuits of brain defensive behaviors we revealed, one putative model would be that electric shocks activate GABAergic LDTg neurons to produce disinhibition of VTA^{→BLA} neurons via the modulation of local VTA neurons, putatively GABA⁵⁰.

The LDTg-VTA axis: positive and negative valence.

To navigate in complex and rapidly evolving environments, mammals must adapt their behaviors to gain access to vital resources while avoiding harmful situations. These behavioural responses are finely

tuned by both rapid and enduring cellular adaptations when facing rewarding and/or aversive challenges⁵⁸. Dysregulation of this homeostatic balance leads to inappropriate choices and increases the risk of developing psychiatric conditions⁵⁹. Historically, the LDTg-VTA axis has been heavily linked with reward processing and reinforcement^{60,61}. The LDTg is an important modulator of VTA dopamine firing activity and consequently forebrain dopamine release^{20,62,63}. Pharmacological and lesions studies have highlighted its key role in attributing reward value to stimuli, and mediating several cellular and behavioural adaptations to addictive substances such as cocaine and nicotine⁶⁴. Projection-specific manipulations revealed its contribution to appetitively motivated and rewarding behaviors^{16,43}, with distinct contribution of cholinergic and glutamatergic LDTg projections to these processes⁴². Indeed, selective optogenetic stimulation in the VTA of LDTg glutamatergic or cholinergic terminals is rewarding, reflected by the number of time spent and entries into a stimulus-paired chamber⁴². Recent evidence point to a partial involvement of GABAergic inputs to the VTA in the reinstatement of cocaine seeking behaviors⁶⁵. Despite these solid proofs of the LDTg-VTA axis involvement in positive stimuli processing, our present work calls into question this accepted view and demonstrates a causal implication of LDTg inhibitory inputs to the VTA in processing immediate aversive challenges. Our results are supported by evidence showing that optogenetic manipulation of local LDTg interneurons impact innate fear induced by olfactory cues²¹. This is likely to affect LDTg outputs and modulate downstream target activity, including the LDTg-VTA axis identified here. Also, our previous work demonstrated that overactivation of LDTg cholinergic inputs to VTA dopamine neurons following social aggression triggered the appearance of depressive-like symptoms²⁰. More recently, a neuron-derived trophic molecule, neuregulin-1, has been shown to be increased in the LDTg following chronic social defeat stress and to promote depressive-like behaviors by impinging on VTA DA neurons activity⁶⁶. Last, in utero exposure to the stress hormones glucocorticoids induces motivational deficits, which can be counteracted by modulating LDTg-VTA projections⁶⁷. Altogether, this suggests that salient environmental stimuli, either rewarding or aversive, would recruit independent populations of LDTg neurons, and that the early polarization of positive and negative networks was an oversimplification

⁶⁸. Thus, cholinergic/glutamatergic and GABAergic LDTg neurons might encode complementary motivational states, promoting approach or defence, respectively, via projections to the VTA. Approach and defence responses require the coordinated involvement of motor centres. In particular, the pedunculopontine nucleus (PPN), a closely related centre in the brainstem, sends ascending projections to most basal ganglia nuclei, notably the substantia nigra (SN), controlling motor responses²³. For example, optogenetic activation of PPN cholinergic terminals within the SN increases locomotion¹⁷. A recent bioRxiv report shows that GABAergic PPN neurons make synapses onto SN DA neurons, and that their activation impairs exploratory locomotion and halts movement initiation, but did not produce freezing responses⁶⁹. Overall, distinct GABAergic projections from the LDTg and PPN to the VTA and SN, respectively, are likely to convey complementary signals driving fear and motor responses. Future work is needed to understand a potential role of the PPN^{→SN} GABAergic pathway in response to aversive stimuli such as footshocks, and a putative crosstalk between these parallel brainstem projections.

Conclusions

Uncovering modulatory regions like the one described here is paramount to understand natural responses to threat stimuli. Importantly, the pathway identified here was restricted to the induction of unconditioned freezing and did not produce aversive memory formation. Furthermore, understanding synaptic and cellular adaptations on these circuits might help us understand the underlying mechanisms contributing to symptoms of pathological conditions. Future studies will need to identify the molecular actuators driving these circuits (mal)adaptations in order to target them with classic pharmacological drugs. Alternatively, future therapeutic approaches involving brain modulation techniques might be able to capitalize from the present findings.

REFERENCES

1. Blanchard, R. J., Flannelly, K. J. & Blanchard, D. C. Defensive behaviors of laboratory and wild *Rattus norvegicus*. *J. Comp. Psychol.* **100**, 101–107 (1986).
2. Mobbs, D., Headley, D. B., Ding, W. & Dayan, P. Space, Time, and Fear: Survival Computations along Defensive Circuits. *Trends Cogn. Sci.* **24**, 228–241 (2020).
3. Sapolsky, R. M. Stress and the brain: individual variability and the inverted-U. *Nat. Neurosci.* **18**, 1344–1346 (2015).
4. Blanchard, D. C. & Blanchard, R. J. Ethoexperimental approaches to the biology of emotion. *Annu. Rev. Psychol.* **39**, 43–68 (1988).
5. Shuhama, R., Del-Ben, C. M., Loureiro, S. R. & Graeff, F. G. Animal defense strategies and anxiety disorders. *An. Acad. Bras. Cienc.* **79**, 97–109 (2007).
6. Rizvi, S. L., Kaysen, D., Gutner, C. A., Griffin, M. G. & Resick, P. A. Beyond Fear: The Role of Peritraumatic Responses in Posttraumatic Stress and Depressive Symptoms Among Female Crime Victims. *J. Interpers. Violence* **23**, 853–868 (2008).
7. Buss, K. A., Davidson, R. J., Kalin, N. H. & Goldsmith, H. H. Context-Specific Freezing and Associated Physiological Reactivity as a Dysregulated Fear Response. *Dev. Psychol.* **40**, 583–594 (2004).
8. Schmidt, N. B., Richey, J. A., Zvolensky, M. J. & Maner, J. K. Exploring Human Freeze Responses to a Threat Stressor. *J. Behav. Ther. Exp. Psychiatry* **39**, 292–304 (2008).
9. Niermann, H. C. M. *et al.* Defensive freezing links Hypothalamic-Pituitary-Adrenal-axis activity and internalizing symptoms in humans. *Psychoneuroendocrinology* **82**, 83–90 (2017).
10. Silva, B. A., Gross, C. T. & Gräff, J. The neural circuits of innate fear: detection, integration, action, and memorization. *Learn. Mem.* **23**, 544–555 (2016).
11. Tovote, P., Fadok, J. P. & Lüthi, A. Neuronal circuits for fear and anxiety. *Nat. Rev. Neurosci.* **16**, 317–331 (2015).
12. Kozłowska, K., Walker, P., McLean, L. & Carrive, P. Fear and the Defense Cascade: Clinical Implications and Management. *Harv. Rev. Psychiatry* **23**, 263–287 (2015).
13. Baldwin, D. V. Primitive mechanisms of trauma response: An evolutionary perspective on trauma-related disorders. *Neurosci. Biobehav. Rev.* **37**, 1549–1566 (2013).
14. Wang, X. *et al.* Brain-wide Mapping of Mono-synaptic Afferents to Different Cell Types in the Laterodorsal Tegmentum. *Neurosci. Bull.* (2019) doi:10.1007/s12264-019-00397-2.
15. Coimbra, B. *et al.* Role of laterodorsal tegmentum projections to nucleus accumbens in reward-related behaviors. *Nat. Commun.* **10**, 4138 (2019).
16. Steidl, S. & Veverka, K. Optogenetic excitation of LDTg axons in the VTA reinforces operant responding in rats. *Brain Res.* **1614**, 86–93 (2015).
17. Xiao, C. *et al.* Cholinergic Mesopontine Signals Govern Locomotion and Reward through Dissociable Midbrain Pathways. *Neuron* **90**, 333–347 (2016).

18. Dort, C. J. V. *et al.* Optogenetic activation of cholinergic neurons in the PPT or LDT induces REM sleep. *Proc. Natl. Acad. Sci.* **112**, 584–589 (2015).
19. Lu, J., Sherman, D., Devor, M. & Saper, C. B. A putative flip–flop switch for control of REM sleep. *Nature* **441**, 589–594 (2006).
20. Fernandez, S. P. *et al.* Mesopontine cholinergic inputs to midbrain dopamine neurons drive stress-induced depressive-like behaviors. *Nat. Commun.* **9**, 4449 (2018).
21. Yang, H. *et al.* Laterodorsal tegmentum interneuron subtypes oppositely regulate olfactory cue-induced innate fear. *Nat. Neurosci.* **19**, 283–289 (2016).
22. Fuller, P. M., Sherman, D., Pedersen, N. P., Saper, C. B. & Lu, J. Reassessment of the structural basis of the ascending arousal system. *J. Comp. Neurol.* **519**, 933–956 (2011).
23. Mena-Segovia, J. & Bolam, J. P. Rethinking the Pedunculopontine Nucleus: From Cellular Organization to Function. *Neuron* **94**, 7–18 (2017).
24. Borgius, L., Restrepo, C. E., Leao, R. N., Saleh, N. & Kiehn, O. A transgenic mouse line for molecular genetic analysis of excitatory glutamatergic neurons. *Mol. Cell. Neurosci.* **45**, 245–257 (2010).
25. George Paxinos & Keith B.J. Franklin. *Paxinos and Franklin's the Mouse Brain in Stereotaxic Coordinates, Compact: The Coronal Plates and Diagrams.* (2019).
26. Sparta, D. R. *et al.* Construction of implantable optical fibers for long-term optogenetic manipulation of neural circuits. *Nat. Protoc.* **7**, 12–23 (2011).
27. Morel, C. *et al.* Nicotinic receptors mediate stress-nicotine detrimental interplay via dopamine cells' activity. *Mol. Psychiatry* (2017) doi:10.1038/mp.2017.145.
28. Glangetas, C. *et al.* Ventral Subiculum Stimulation Promotes Persistent Hyperactivity of Dopamine Neurons and Facilitates Behavioral Effects of Cocaine. *Cell Rep.* **13**, 2287–2296 (2015).
29. Bariselli, S. *et al.* SHANK3 controls maturation of social reward circuits in the VTA. *Nat. Neurosci.* **19**, 926–934 (2016).
30. Georges, F. & Aston-Jones, G. Activation of Ventral Tegmental Area Cells by the Bed Nucleus of the Stria Terminalis: A Novel Excitatory Amino Acid Input to Midbrain Dopamine Neurons. *J. Neurosci.* **22**, 5173–5187 (2002).
31. Ungless, M. A., Magill, P. J. & Bolam, J. P. Uniform Inhibition of Dopamine Neurons in the Ventral Tegmental Area by Aversive Stimuli. *Science* **303**, 2040–2042 (2004).
32. Grace, A. A. & Bunney, B. S. Intracellular and extracellular electrophysiology of nigral dopaminergic neurons--1. Identification and characterization. *Neuroscience* **10**, 301–315 (1983).
33. Ungless, M. A. & Grace, A. A. Are you or aren't you? Challenges associated with physiologically identifying dopamine neurons. *Trends Neurosci.* **35**, 422–430 (2012).
34. Tan, K. R. *et al.* GABA Neurons of the VTA Drive Conditioned Place Aversion. *Neuron* **73**, 1173–1183 (2012).
35. Bocklisch, C. *et al.* Cocaine Disinhibits Dopamine Neurons by Potentiation of GABA Transmission in the Ventral Tegmental Area. *Science* **341**, 1521–1525 (2013).

36. Steffensen, S. C., Svingos, A. L., Pickel, V. M. & Henriksen, S. J. Electrophysiological Characterization of GABAergic Neurons in the Ventral Tegmental Area. *J. Neurosci.* **18**, 8003–8015 (1998).
37. Rozeske, R. R. & Herry, C. Neuronal coding mechanisms mediating fear behavior. *Curr. Opin. Neurobiol.* **52**, 60–64 (2018).
38. Brischoux, F., Chakraborty, S., Brierley, D. I. & Ungless, M. A. Phasic excitation of dopamine neurons in ventral VTA by noxious stimuli. *Proc. Natl. Acad. Sci.* **106**, 4894–4899 (2009).
39. Bromberg-Martin, E. S., Matsumoto, M. & Hikosaka, O. Dopamine in Motivational Control: Rewarding, Aversive, and Alerting. *Neuron* **68**, 815–834 (2010).
40. Omelchenko, N. & Sesack, S. R. Laterodorsal tegmental projections to identified cell populations in the rat ventral tegmental area. *J. Comp. Neurol.* **483**, 217–235 (2005).
41. Dautan, D. *et al.* Segregated cholinergic transmission modulates dopamine neurons integrated in distinct functional circuits. *Nat. Neurosci.* **19**, 1025–1033 (2016).
42. Steidl, S., Wang, H., Ordonez, M., Zhang, S. & Morales, M. Optogenetic excitation in the ventral tegmental area of glutamatergic or cholinergic inputs from the laterodorsal tegmental area drives reward. *Eur. J. Neurosci.* **45**, 559–571 (2017).
43. Lammel, S. *et al.* Input-specific control of reward and aversion in the ventral tegmental area. *Nature* **491**, 212–217 (2012).
44. Pignatelli, M. *et al.* Synaptic Plasticity onto Dopamine Neurons Shapes Fear Learning. *Neuron* **93**, 425–440 (2017).
45. Tang, W., Kochubey, O., Kintscher, M. & Schneggenburger, R. A VTA to Basal Amygdala Dopamine Projection Contributes to Signal Salient Somatosensory Events during Fear Learning. *J. Neurosci.* **40**, 3969–3980 (2020).
46. Mongeau, R., Miller, G. A., Chiang, E. & Anderson, D. J. Neural Correlates of Competing Fear Behaviors Evoked by an Innately Aversive Stimulus. *J. Neurosci.* **23**, 3855–3868 (2003).
47. Mameli-Engvall, M. *et al.* Hierarchical Control of Dopamine Neuron-Firing Patterns by Nicotinic Receptors. *Neuron* **50**, 911–921 (2006).
48. Zhou, Z. *et al.* A VTA GABAergic Neural Circuit Mediates Visually Evoked Innate Defensive Responses. *Neuron* S0896627319304805 (2019) doi:10.1016/j.neuron.2019.05.027.
49. Brown, M. T. C. *et al.* Ventral tegmental area GABA projections pause accumbal cholinergic interneurons to enhance associative learning. *Nature* **492**, 452–456 (2012).
50. Omelchenko, N. & Sesack, S. R. Ultrastructural Analysis of Local Collaterals of Rat Ventral Tegmental Area Neurons: GABA Phenotype and Synapses onto Dopamine and GABA Cells. *Synap. N. Y. N* **63**, 895–906 (2009).
51. Fadok, J. P., Markovic, M., Tovote, P. & Lüthi, A. New perspectives on central amygdala function. *Curr. Opin. Neurobiol.* **49**, 141–147 (2018).
52. Roelofs, K. Freeze for action: neurobiological mechanisms in animal and human freezing. *Philos. Trans. R. Soc. B Biol. Sci.* **372**, (2017).
53. Ressler, K. J. Translating Across Circuits and Genetics Toward Progress in Fear- and Anxiety-

Related Disorders. *Am. J. Psychiatry* **177**, 214–222 (2020).

54. Tang, W., Kochubey, O., Kintscher, M. & Scheggia, R. A VTA to Basal Amygdala Dopamine Projection Contributes to Signal Salient Somatosensory Events during Fear Learning. *J. Neurosci. Off. J. Soc. Neurosci.* **40**, 3969–3980 (2020).
55. Barbano, M. F. *et al.* VTA Glutamatergic Neurons Mediate Innate Defensive Behaviors. *Neuron* (2020) doi:10.1016/j.neuron.2020.04.024.
56. Li, Y. *et al.* Rostral and Caudal Ventral Tegmental Area GABAergic Inputs to Different Dorsal Raphe Neurons Participate in Opioid Dependence. *Neuron* **101**, 748–761.e5 (2019).
57. Bouarab, C., Thompson, B. & Polter, A. M. VTA GABA Neurons at the Interface of Stress and Reward. *Front. Neural Circuits* **13**, (2019).
58. Hu, H. Reward and Aversion. *Annu. Rev. Neurosci.* **39**, 297–324 (2016).
59. Lammel, S., Lim, B. K. & Malenka, R. C. Reward and aversion in a heterogeneous midbrain dopamine system. *Neuropharmacology* **76, Part B**, 351–359 (2014).
60. Kohlmeier, K. A. Off the Beaten Path: Drug Addiction and the Pontine Laterodorsal Tegmentum. *ISRN Neurosci.* **2013**, (2013).
61. Maskos, U. The cholinergic mesopontine tegmentum is a relatively neglected nicotinic master modulator of the dopaminergic system: relevance to drugs of abuse and pathology. *Br. J. Pharmacol.* **153**, S438–S445 (2008).
62. Forster, G. L. & Blaha, C. D. Laterodorsal tegmental stimulation elicits dopamine efflux in the rat nucleus accumbens by activation of acetylcholine and glutamate receptors in the ventral tegmental area. *Eur. J. Neurosci.* **12**, 3596–3604 (2000).
63. Lodge, D. J. & Grace, A. A. The laterodorsal tegmentum is essential for burst firing of ventral tegmental area dopamine neurons. *Proc. Natl. Acad. Sci. U. S. A.* **103**, 5167 (2006).
64. Kohlmeier, K. A. & Polli, F. S. Plasticity in the Brainstem: Prenatal and Postnatal Experience Can Alter Laterodorsal Tegmental (LDT) Structure and Function. *Front. Synaptic Neurosci.* **12**, (2020).
65. Hernandez, N. S. *et al.* GLP-1 receptor signaling in the laterodorsal tegmental nucleus attenuates cocaine seeking by activating GABAergic circuits that project to the VTA. *Mol. Psychiatry* 1–15 (2020) doi:10.1038/s41380-020-00957-3.
66. Wang, H. *et al.* The laterodorsal tegmentum-ventral tegmental area circuit controls depression-like behaviors by activating ErbB4 in DA neurons. *Mol. Psychiatry* (2021) doi:10.1038/s41380-021-01137-7.
67. Coimbra, B. *et al.* Impairments in laterodorsal tegmentum to VTA projections underlie glucocorticoid-triggered reward deficits. *eLife* **6**,
68. Carlezon, W. A. & Thomas, M. J. Biological substrates of reward and aversion: A nucleus accumbens activity hypothesis. *Neuropharmacology* **56**, 122–132 (2009).
69. Gut, N. K., Yilmaz, D., Kondabolu, K., Huerta-Ocampo, I. & Mena-Segovia, J. Selective inhibition of goal-directed actions in the mesencephalic locomotor region. 2022.01.18.476772 (2022) doi:10.1101/2022.01.18.476772.

ACKNOWLEDGMENTS

We thank E.J. Kremer and the Plateforme de Vectorologie de Montpellier for providing CAV-2-Cre. We thank Dr Massimo Mantegazza for providing vGAT-Cre mice. We thank all the staff from the animal facilities for their technical support.

AUTHOR INFORMATION

L.B., T.C. and L.R. performed behavioral experiments. L.B., T.C. and H.F. performed microscopy. S.P.F. and R.C.C. performed *ex vivo* recordings. C.G. and F.G. carried out *in vivo* electrophysiological recordings. T.L. provided technical supports for behavioral analyses. L.B., S.P.F. and J.B. designed the project and wrote the manuscript. All authors provided feedback on writing the manuscript.

ETHICS DECLARATIONS

The authors declare no conflict of interest.

FUNDINGS

This work was supported by the Centre National de la Recherche Scientifique (CNRS), the Université Côte d'Azur, the Labex Signallife, the Fédération pour la Recherche sur le Cerveau and Rotary - Espoir en Tête, the Fondation pour la Recherche Médicale (FRM DEQ20180339159) to J.B. L.B. is a recipient of a PhD fellowship from the FRM as well as a fourth-year PhD fellowship from the FRM (FDT201904007874). T.C. is a recipient fourth-year PhD fellowship from the FRM (FDT202106012968). L.R. is a recipient of a PhD fellowship from the FRM.

FIGURE LEGENDS

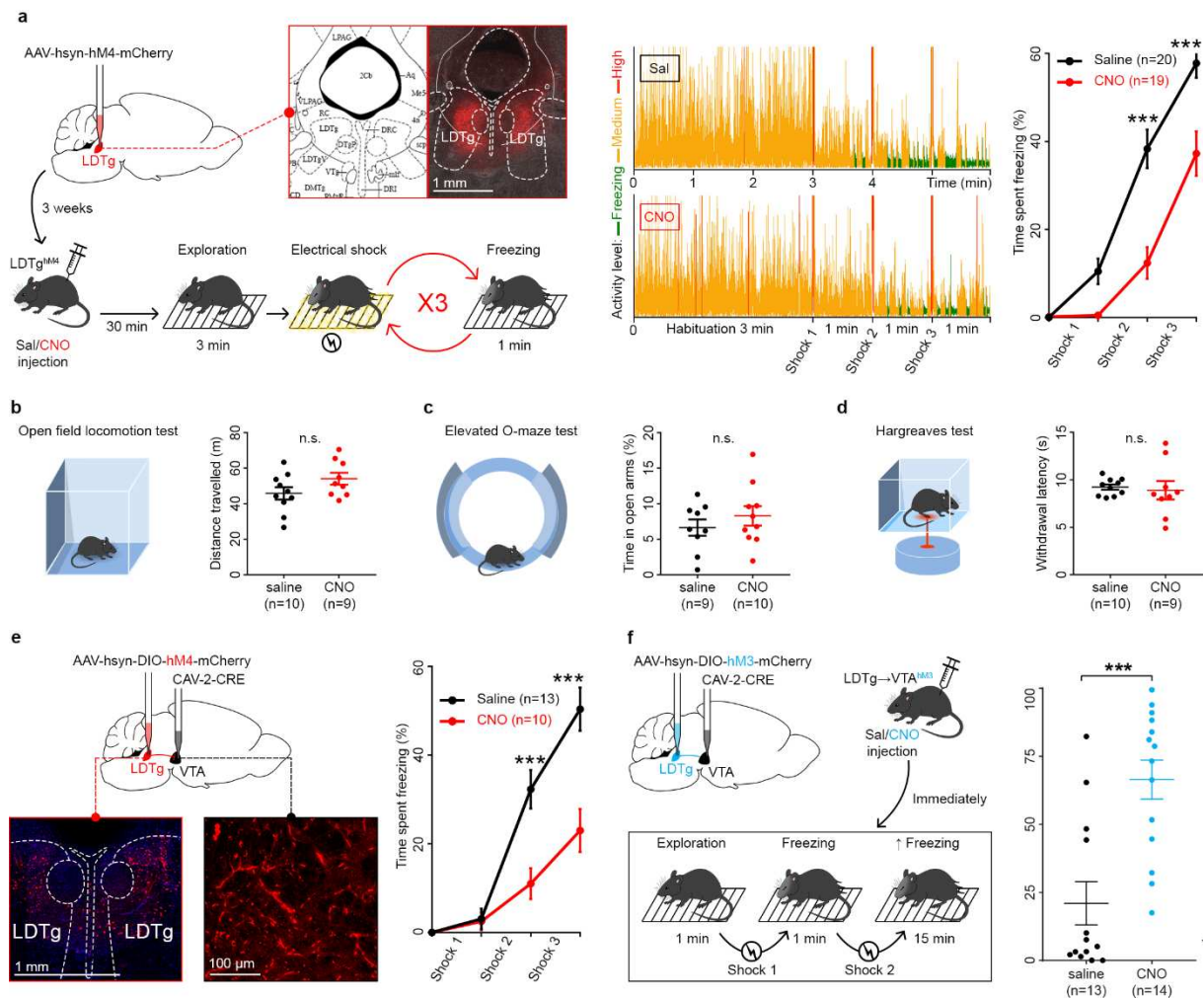


Fig. 1. LDTg inputs to the VTA bidirectionally control freezing. (a) Left panel: wild-type mice were injected with AAV-hsyn-hM4-mCherry in the LDTg. Microscopy image, opposed to coronal LDTg anatomy from reference²⁵, shows red fluorescence at correct injection site. Three weeks later, LDTg^{hM4} mice received saline or CNO injection 30 minutes prior to exposure to three electrical foot shocks. Middle panel: representative traces showing activity of mice during the test. Right panel: freezing responses to electrical foot shocks are decreased in mice treated with CNO compared to saline. Points represent mean \pm S.E.M. percentage of time spent freezing during the following time

intervals: 0-3 min, 3-4 min, 4-5 min, and 5-6 min. Interaction treatment x shocks $F(3, 111) = 10.12$; repeated measures two-way ANOVA followed by Sidak's comparison test, *** $P < 0.001$). (b) Locomotor activity in open-field was not affected by LDTg inhibition ($P = 0.1072$, t-test). (c) Anxiety levels were not affected in O-maze test ($P = 0.3741$, t-test). (d) Pain sensitivity was not affected in Hargreaves test ($P = 0.7339$, t-test). (e) Wild-type mice were injected with AAV-hsyn-DIO-hM4-mCherry in LDTg and CAV-2-CRE in VTA. Chemogenetic silencing of LDTg projections to VTA reduces freezing. Interaction treatment x shocks $F(3, 63) = 11.56$; repeated measures two-way ANOVA followed by Sidak's comparison test, *** $P < 0.001$). (f) Hyperactivation of LDTg projections to VTA increases freezing. Same injections as "e" except hM4 (Gi-coupled, inhibitory) was replaced with hM3 (Gq-coupled, excitatory). Mice received only two shocks and their freezing response was measured 10 min after the last shock delivery, for 5 min. Percentage of time mice spent freezing (*** $P < 0.001$, Mann-Whitney test).

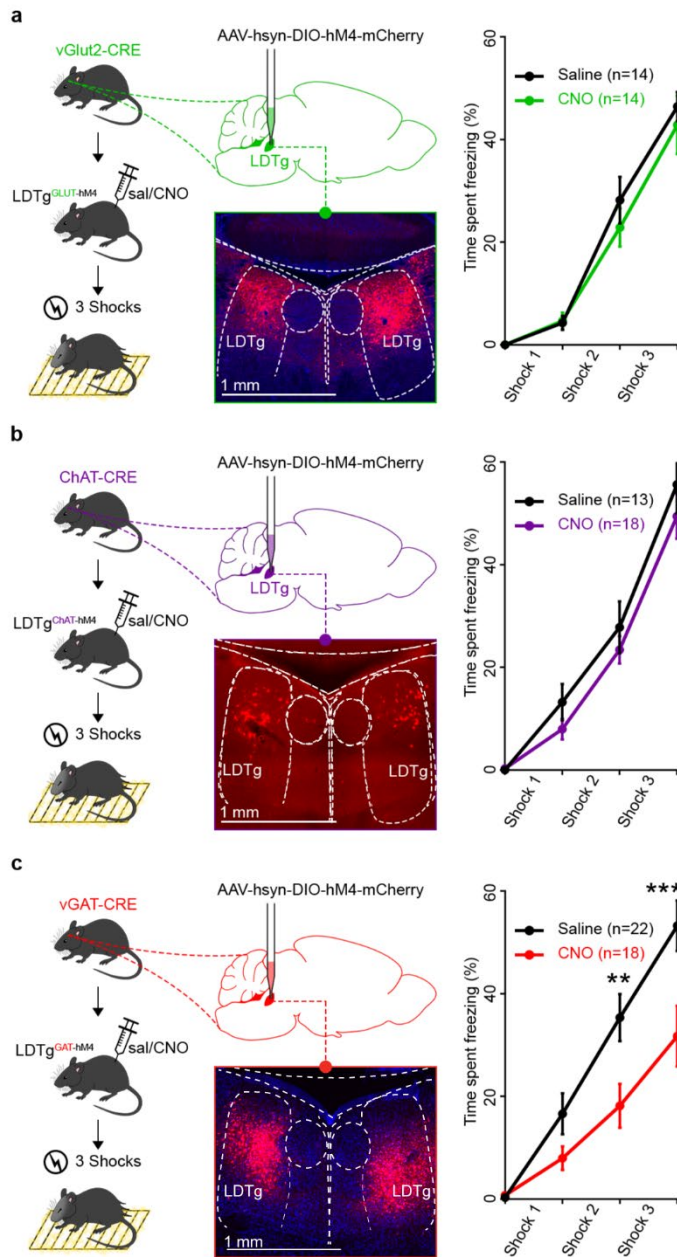


Fig. 2. LDTg GABAergic neurons but not cholinergic or glutamatergic cells control freezing. (a) Silencing glutamatergic LDTg neurons does not alter freezing. vGlut2-cre mice received injection of AAV-hsyn-DIO-hM4-mCherry in LDTg then underwent freezing paradigm; microscopy image shows mCherry expression at injection site. Percentage of time mice spent freezing on each interval, same as Fig. 1 (interaction treatment x shocks $F(3, 78) = 0.4895$; repeated measures two-way ANOVA followed by Sidak's comparison test, $P=0.6906$). **(b)** Silencing cholinergic LDTg neurons does not alter freezing. Same as above except mice were ChAT-cre (interaction treatment x shocks $F(3, 87) = 0.4895$; repeated measures two-way ANOVA followed by Sidak's comparison test, $P=0.6117$). **(c)**

Silencing GABAergic LDTg neurons reduces freezing. Same as above except mice were vGAT-cre (interaction treatment x shocks $F(3, 114) = 5.646$; repeated measures two-way ANOVA followed by Sidak's comparison test, ** $P < 0.01$, *** $P < 0.001$).

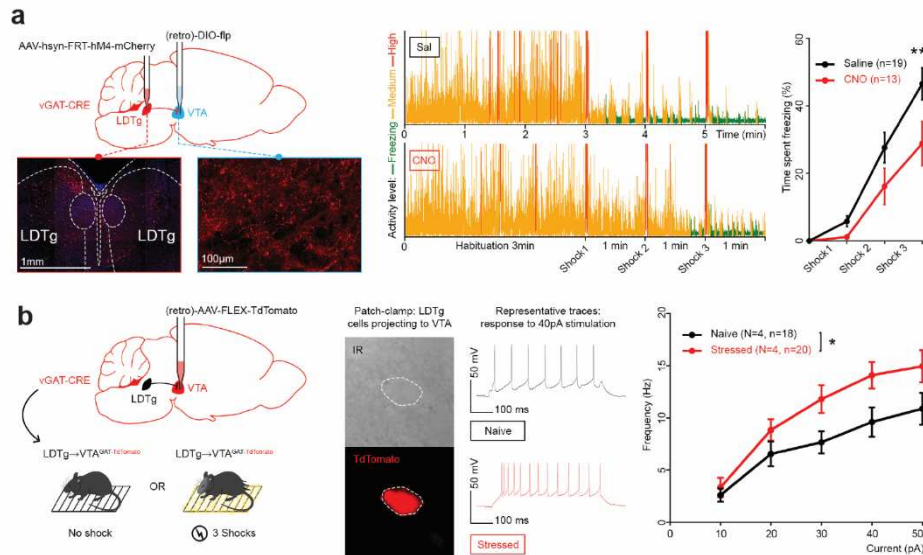


Fig. 3. LDTg GABAergic projections to VTA control freezing and are sensitized by acute stress.

(a) Silencing GABAergic LDTg projections to VTA reduces freezing. Left panel: vGAT-cre mice received injections of AAV-hsyn-FRT-hM4-mCherry in LDTg and retrograde DIO-flp in VTA then followed the same protocol as Fig. 1: microscopy images show mCherry-expressing cell bodies (injection site) and fibres in VTA. Middle panel: Representative traces showing activity of mice during the test. Right panel: Percentage of time mice spent freezing on each interval. Interaction treatment x shocks $F(3, 90) = 3.088$; repeated measures two-way ANOVA followed by Sidak's comparison test, ** $P < 0.01$).

(b) GABAergic LDTg projections to VTA are sensitized by acute stress. Left panel: vGAT-cre mice were injected with retrograde AAV-FLEX-tdTomato in VTA then received either 3 shocks (Stressed) or no shock (Naive). Middle left panel: Microscopy images of GABAergic cell projecting to VTA in LDTg with transmission light (top) or emitting red fluorescence (bottom). Middle right panel: Representative voltage traces responses to a 40pA current injection for each condition. Right panel: excitability profile of LDTg GABAergic neurons projecting to VTA in control or stressed mice. Plots depict action potential frequency after increasing current injection steps. Interaction treatment x current $F(4, 144)$

= 1.866); Treatment factor $F(1, 36) = 5.082$; repeated measures two-way ANOVA followed by Sidak's comparison test, * $P < 0.05$).

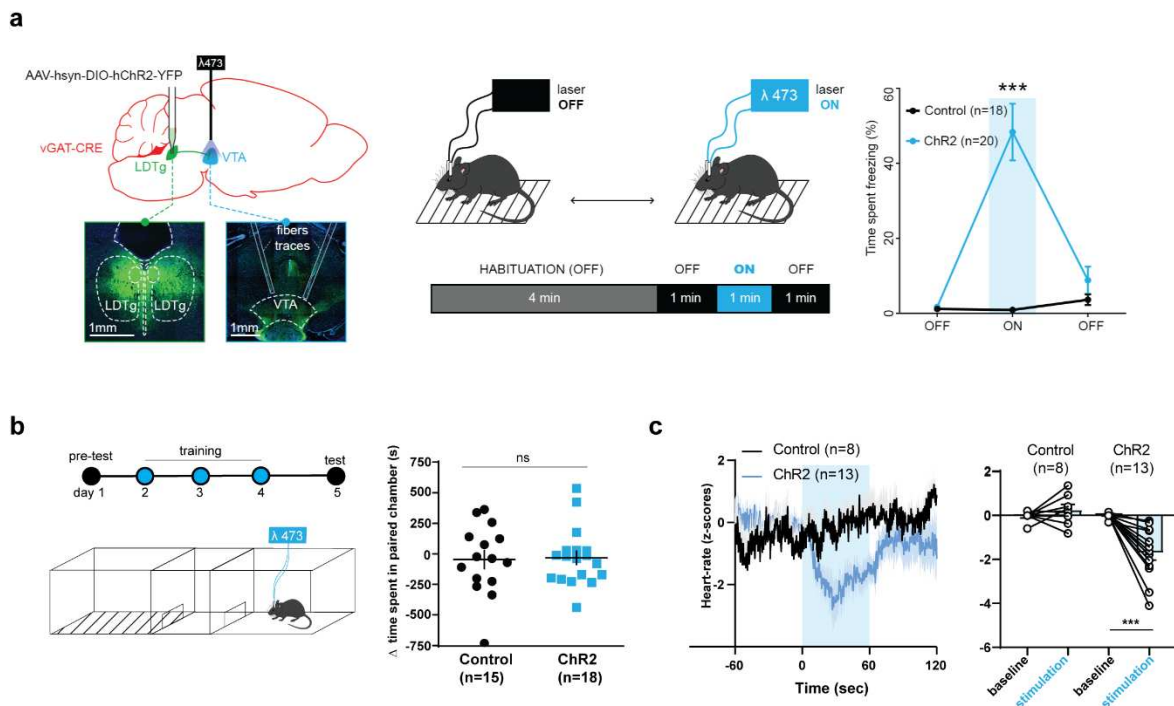


Fig. 4. Activation of LDTg GABAergic inputs to the VTA induce freezing in absence of aversive experience. (a) Optogenetic *in vivo* activation of GABAergic LDTg terminals within the VTA induces spontaneous freezing. Left panel: vGAT-cre mice were injected with either AAV-hsyn-DIO-hChR2-YFP (ChR2) or AAV-hsyn-DIO-YFP (control) in LDTg and implanted with optic fibres above the VTA; microscopy images show green fluorescence at injection site and YFP expression at injection site and YFP-expressing fibres with optic fibres traces at implantation site in the VTA. Middle panel: Experimental timeline. Right panel: Percentage of time mice spent freezing depicted as mean \pm S.E.M. on the following intervals (Interaction group \times light $F(2, 30) = 4.166$; repeated measures two-way ANOVA followed by Sidak's comparison test, * $P < 0.001$). (b) Control and ChR2 mice received light stimulation in the paired compartment and no light stimulation in the unpaired side. Following 3 pairings on each side mice were allowed to freely explore the conditioning apparatus. Optogenetic *in vivo* activation of GABAergic LDTg terminals failed to induce place aversion ($t_{31} = 0.1606$ $P = 0.8735$). (c) Using telemetry monitoring of heart rate in anesthetized mice, light stimulation in ChR2 mice**

elicited bradycardia that was not observed in control animals when laser was turned ON (t7=1.128
P=0.2966 control; t12=5.191 P<0.001 Chr2).

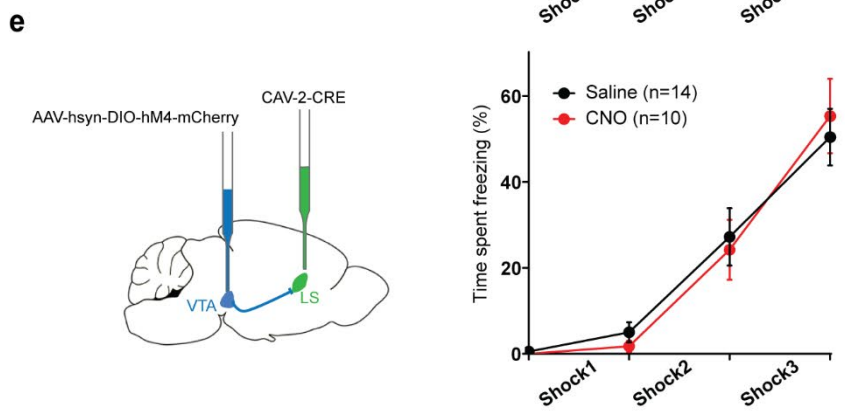
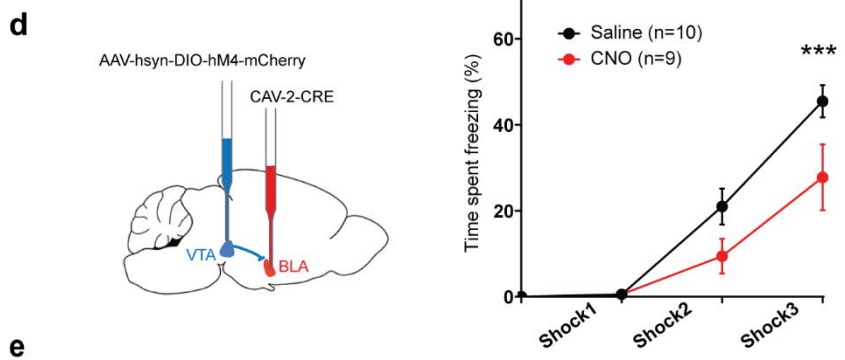
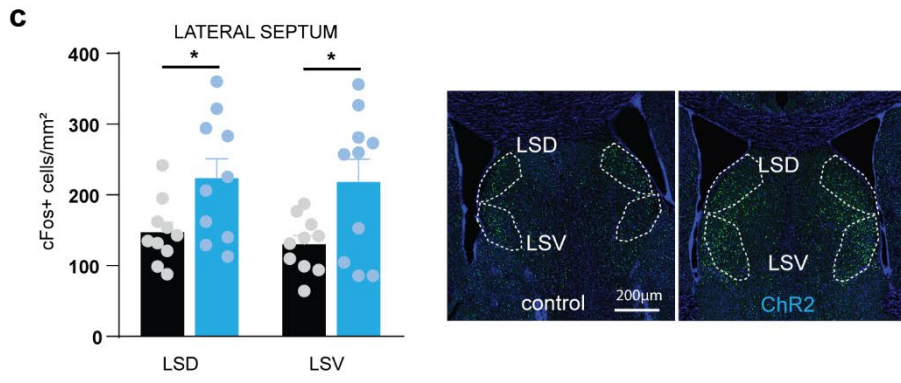
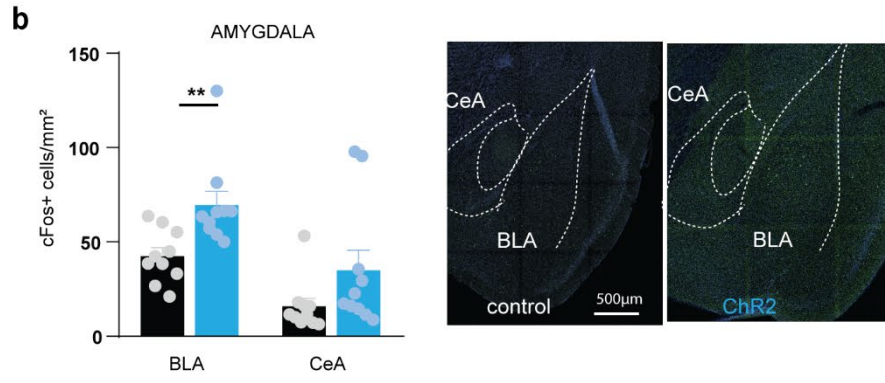
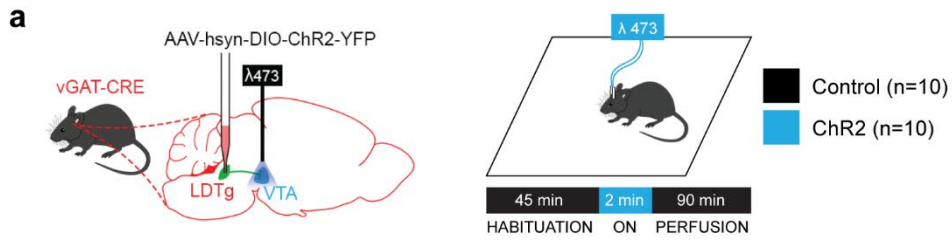


Fig. 5. Stimulation of GABAergic LDTg terminals within the VTA triggers amygdala activation required for freezing. (a) Control and vGAT-Cre ChR2 mice were sacrificed 90 min after light stimulation as depicted in the experimental timeline (left panel). cFos-positive neurons were counted in **(b)** the basolateral and central amygdala (BLA and CeA respectively), **(c)** the dorsal and ventral part of the lateral septum (LSD and LSV respectively). **(d)** In WT mice, chemogenetic silencing of VTA projections to the BLA (Interaction treatment x shocks $F(3, 51) = 3.604$; repeated measures two-way ANOVA followed by Sidak's comparison test, $** P < 0.01$), reduces freezing. **(e)** Chemogenetic silencing of VTA projections to the LS does not modify freezing behavior (Interaction treatment x shocks $F(3, 66) = 0.3606$; repeated measures two-way ANOVA followed by Sidak's comparison test, $P = 0.7817$) . * $P < 0.05$, $** P < 0.01$.

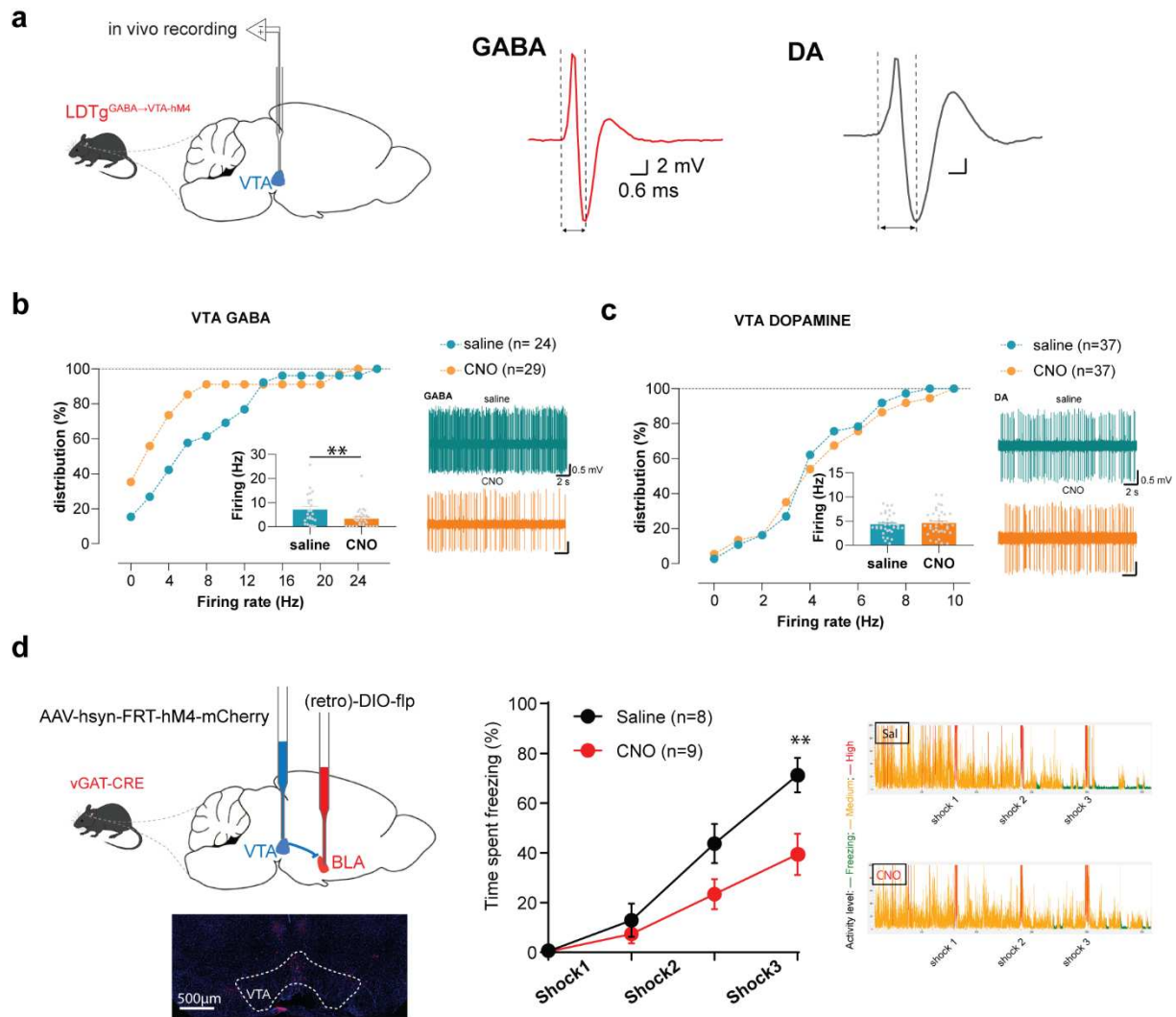
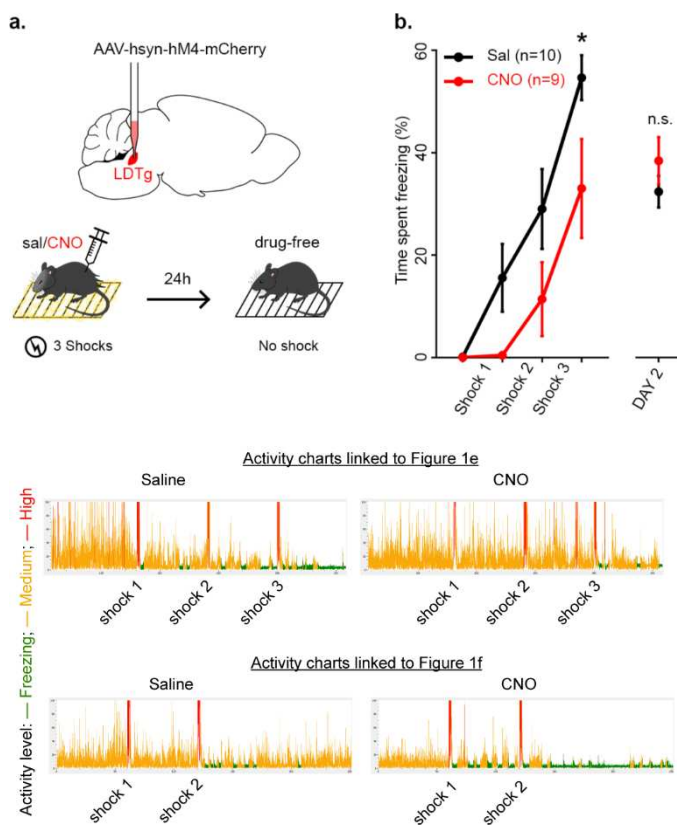


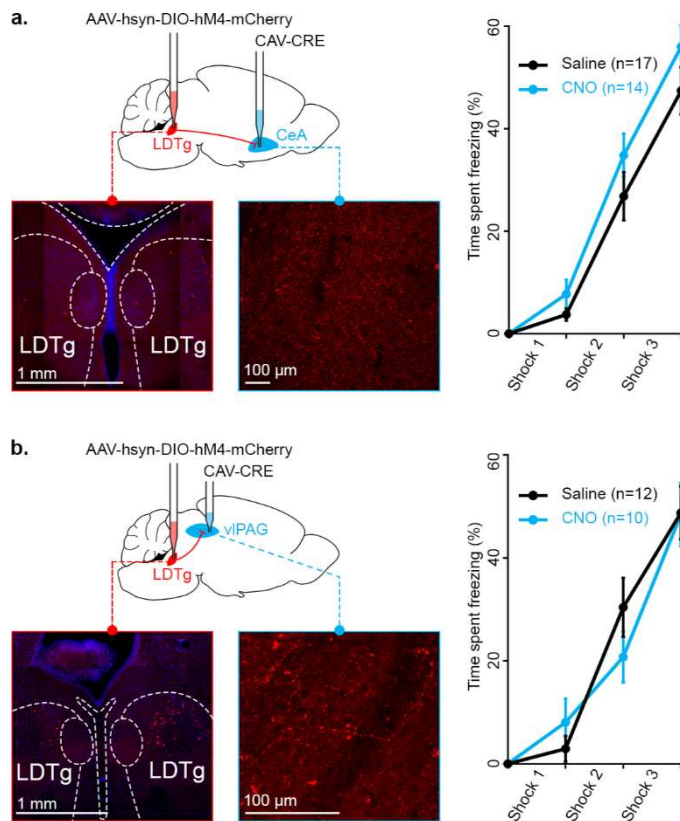
Fig. 6. The LDTg is an upstream regulator of the $VTA \rightarrow BLA$ pathway, which controls freezing. (a) *In vivo* recordings were performed in the VTA of anesthetized $LDTg^{GABA \rightarrow VTA-hM4}$ mice and the activity of putative VTA GABA or DA neurons was analysed upon systemic administration of saline or CNO. The cumulative probability distribution of the firing rate, as well as the firing frequency (inset) are presented for putative VTA GABA (b) and VTA DA neurons (c). Representative traces for each experimental condition are presented. Silencing of LDTg GABAergic inputs to VTA selectively decreases the activity of VTA GABA neurons without altering VTA DA firing. $P < 0.01$ Mann-Whitney test. (d) vGATCre mice received injection of AAV-hSyn-FRT-hM4-mCherry in the VTA and retro AAV-DIO-Flp in the BLA, and then underwent freezing paradigm. Microscopy image shows mCherry expression at VTA**

injection site. Selective silencing of GABAergic VTA^{→BLA} neurons diminished freezing responses (Interaction treatment x shocks $F(3, 45) = 4.947$; repeated measures two-way ANOVA followed by Sidak's comparison test, ** $P < 0.01$).

SUPPLEMENTARY FIGURES LEGENDS



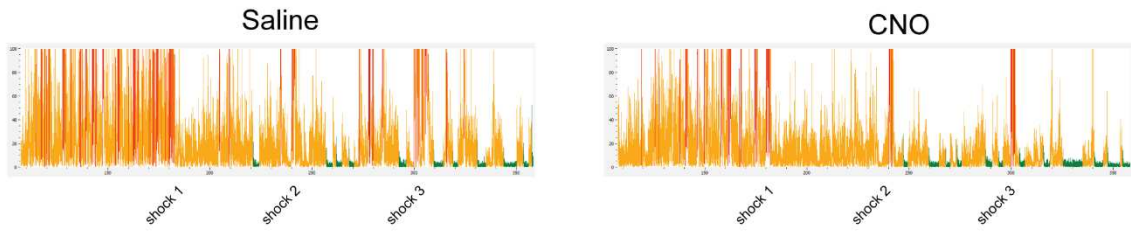
Supplementary Figure 1. Silencing of LDTg does not alter aversive memory formation. (a) Wild-type mice were injected with an AAV-hsyn-hM4-mCherry in the LDTg. Mice received either saline or CNO 30 min before receiving 3 consecutive electrical foot shocks. Mice were re-exposed in a drug-free state 24h to the same context without shocks. **(b)** Freezing responses did not differ between the 2 groups when re-exposed to the same context 24h after. DAY 1: Interaction treatment x shocks $F(3,51) = 0.1732$; Treatment factor $F(1, 17) = 6.423$; repeated measures two-way ANOVA followed by Sidak's comparison test, * $P < 0.05$. DAY 2: $P = 0.2839$, t-test.



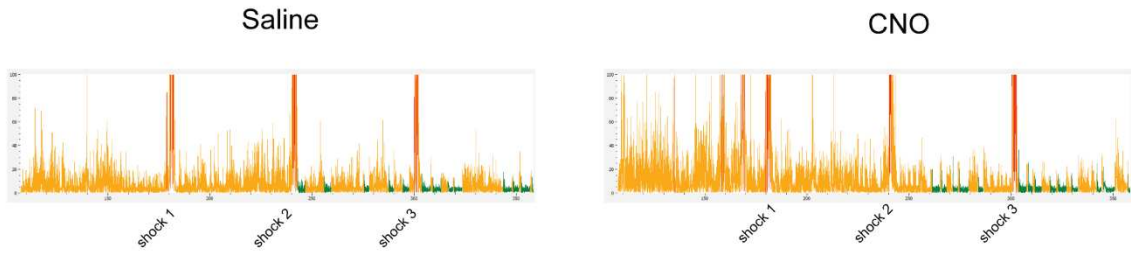
Supplementary Figure 2. Selective silencing of LDTg projections to the CeA or vlPAG does not alter freezing. Wild-type mice were injected with an AAV-hsyn-DIO-hM4-mCherry in the LDTg and a retrograde CAV-2-Cre in either (a) the central amygdala (CeA) or (b) ventrolateral periaqueductal gray (vlPAG). (a) Microscopy images show red fluorescence in LDTg and red fibres within the CeA. Silencing LDTg projections to CeA does not alter freezing. Interaction treatment x shocks $F(3, 87) = 0.997$; repeated measures two-way ANOVA followed by Sidak's comparison test, $P=0.3982$. (b) Microscopy images show mCherry expression in LDTg and mCherry-expressing fibres within the vlPAG. Silencing LDTg projections to vlPAG does not alter freezing. Interaction treatment x shocks $F(3, 63) = 1.592$; repeated measures two-way ANOVA followed by Sidak's comparison test, $P=0.2001$.

Activity level: — Freezing; — Medium; — High

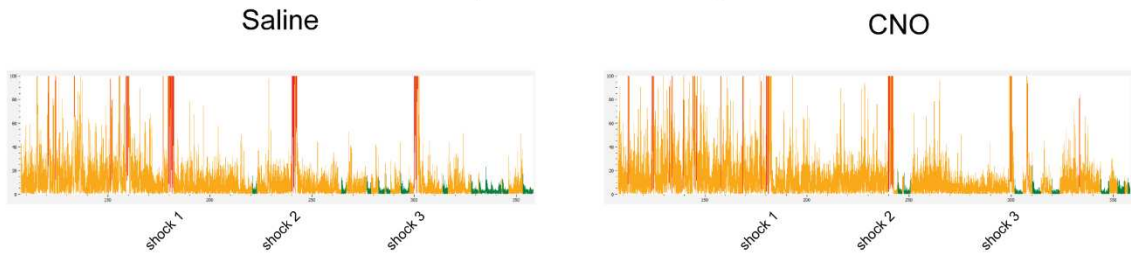
Activity charts linked to Figure 2a



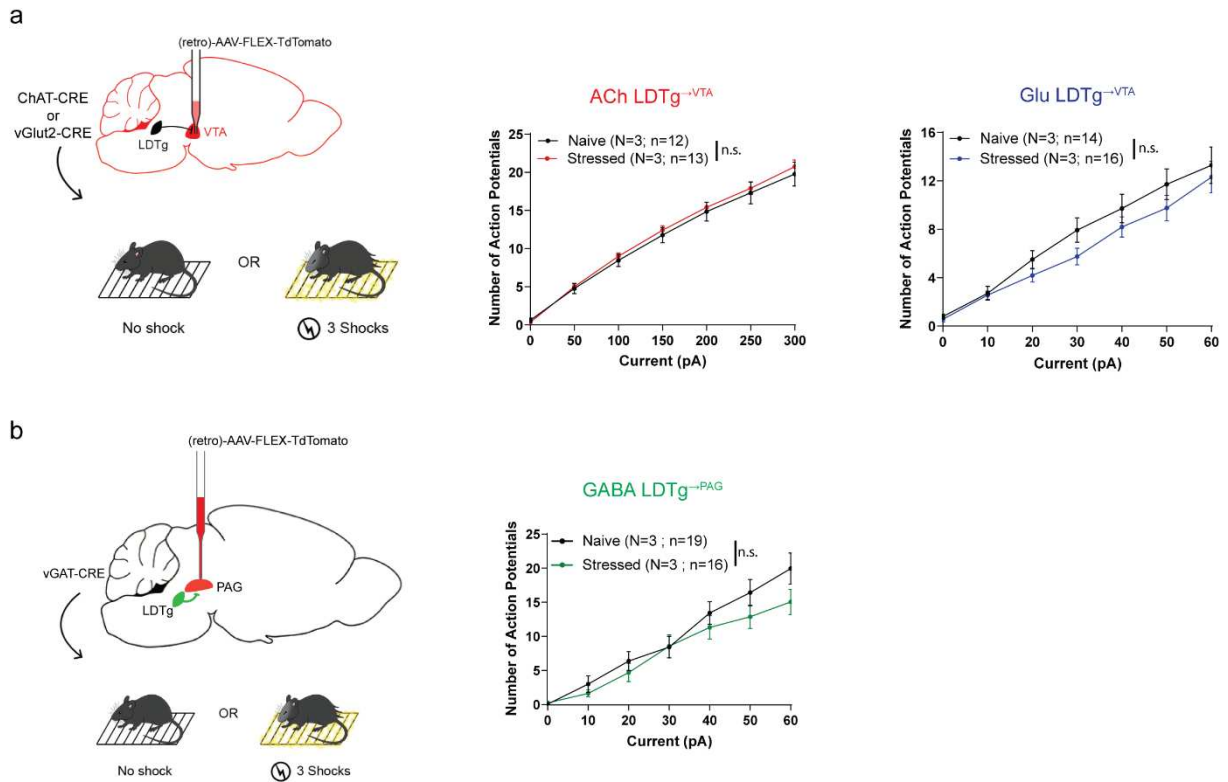
Activity charts linked to Figure 2b



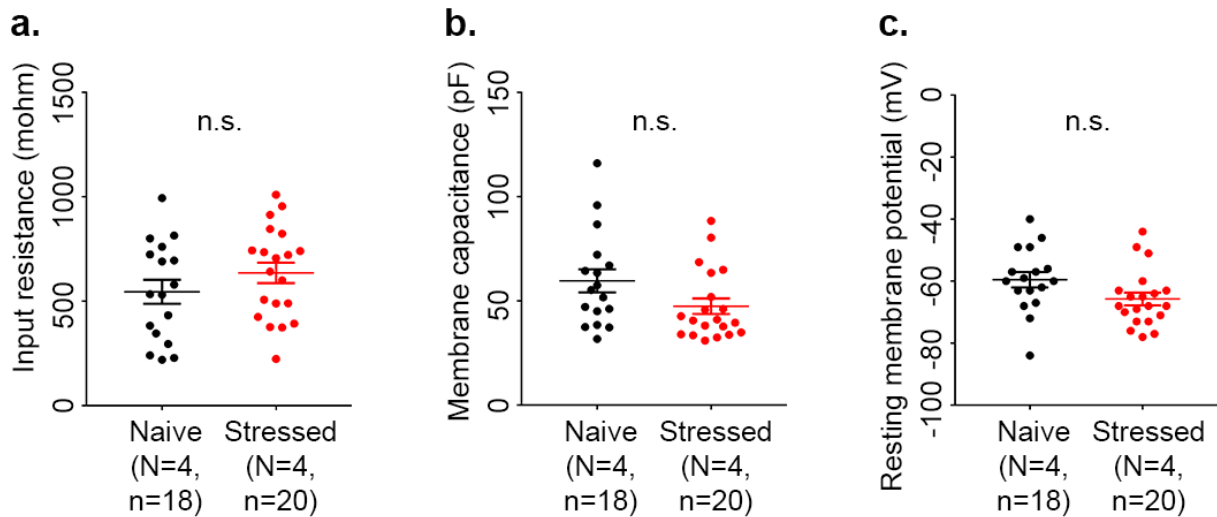
Activity charts linked to Figure 2c



Supplementary Figure 3. Examples of activity levels when silencing (or not) glutamatergic (2a), cholinergic (2b) or GABAergic (2c) LDTg neurons.

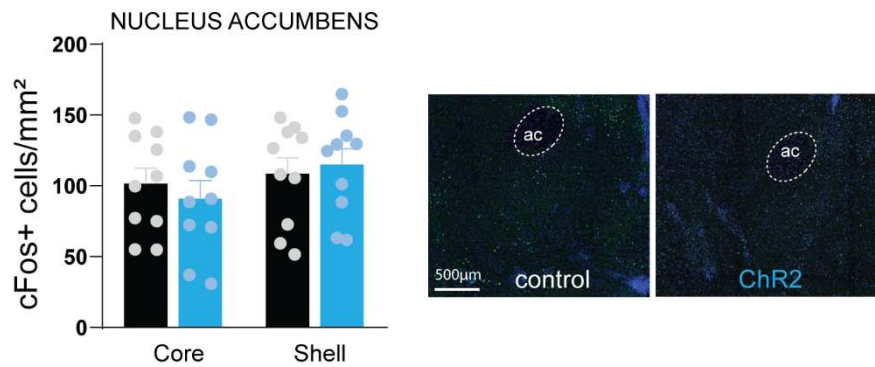
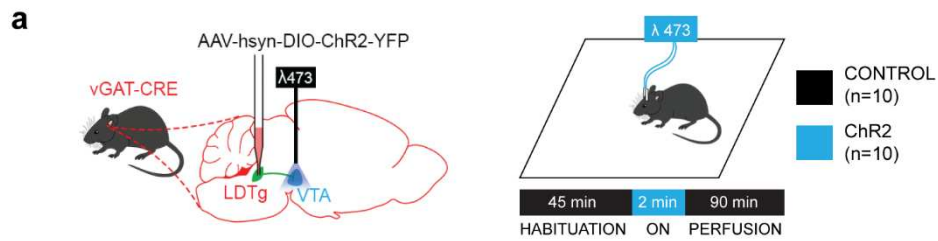


Supplementary Figure 4. Passive membrane properties of LDTg GABAergic neurons projecting to the VTA are unaffected by acute stress. (a, b, c) Measure of input resistance, membrane capacitance and resting membrane potential respectively in mice that received either three electrical foot shocks (stressed) or no shock (naïve) just before ex-vivo patch-clamp recording. All plots depict mean \pm S.E.M. (a) Input resistance ($P=0.2367$, t-test). (b) Membrane capacitance ($P=0.0694$, Mann-Whitney test). (c) Resting membrane potential ($P=0.0604$, t-test).



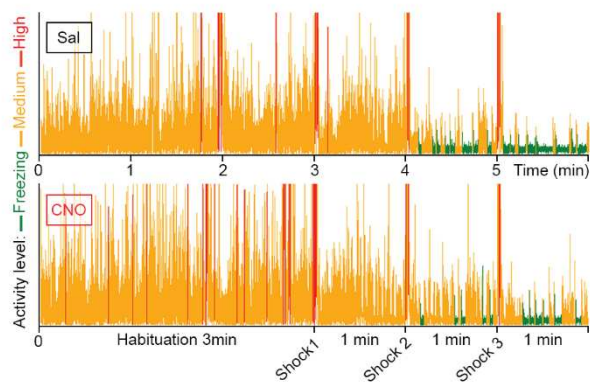
Supplementary Figure 5. Discrete cellular effects of foot-shocks.

(a) Left panel: ChaT-Cre and vGluT2-Cre mice were injected with retrograde AAV-FLEX-tdTomato in the VTA then received either 3 shocks (Stressed) or no shock (Naive). Neither cholinergic (Middle panel) nor glutamatergic (Right panel) projections to VTA are affected by stress as shown by the similar profiles of excitability between the 2 conditions. (b) Left panel: vGAT-Cre mice were injected with retrograde AAV-FLEX-tdTomato in the VTA and treated as in 'a'. Right panel: the excitability profile of LDTg GABAergic neurons projecting to the vIPAG do not differ between control or stressed mice. Statistical comparisons were made using repeated measures two-way ANOVA followed by Sidak's comparison test, revealing no significant differences.



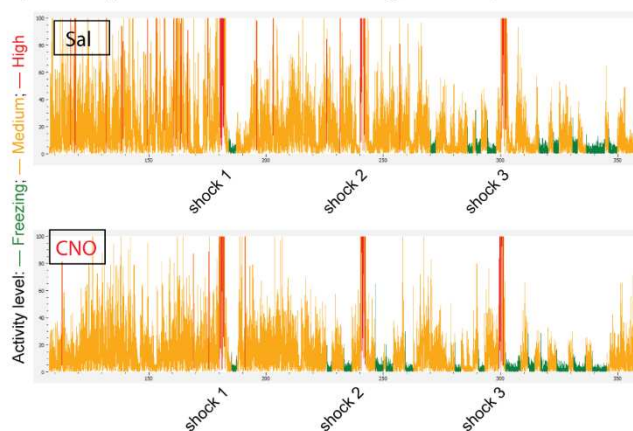
b

Activity charts linked to Figure 5d



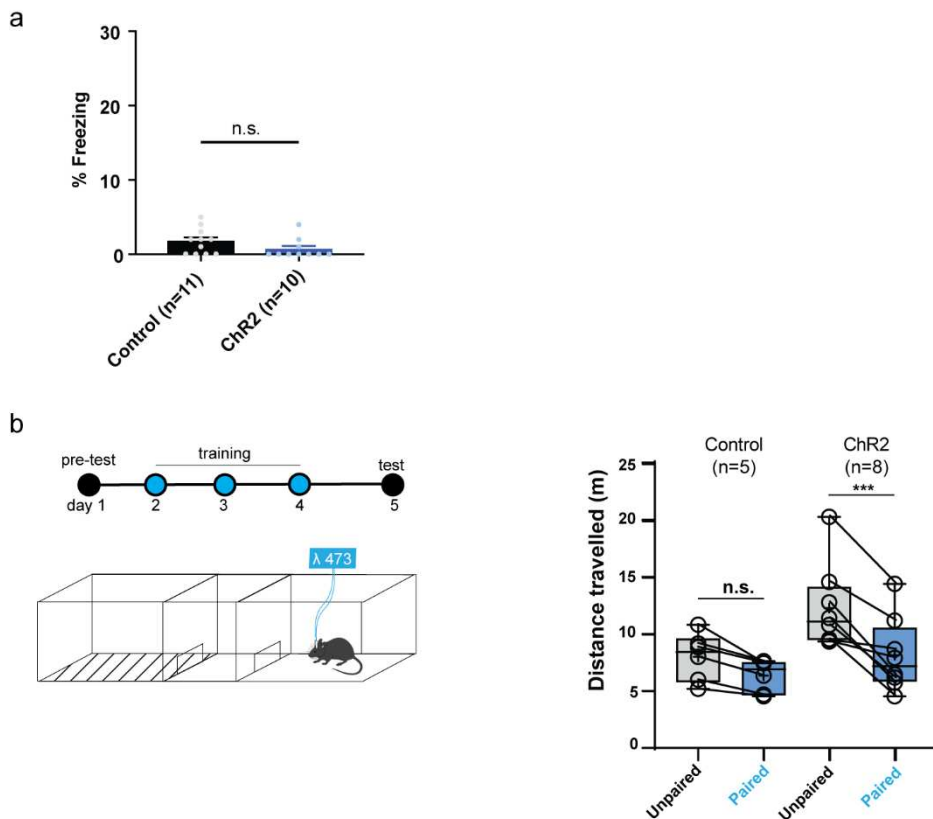
c

Activity charts linked to Figure 5e

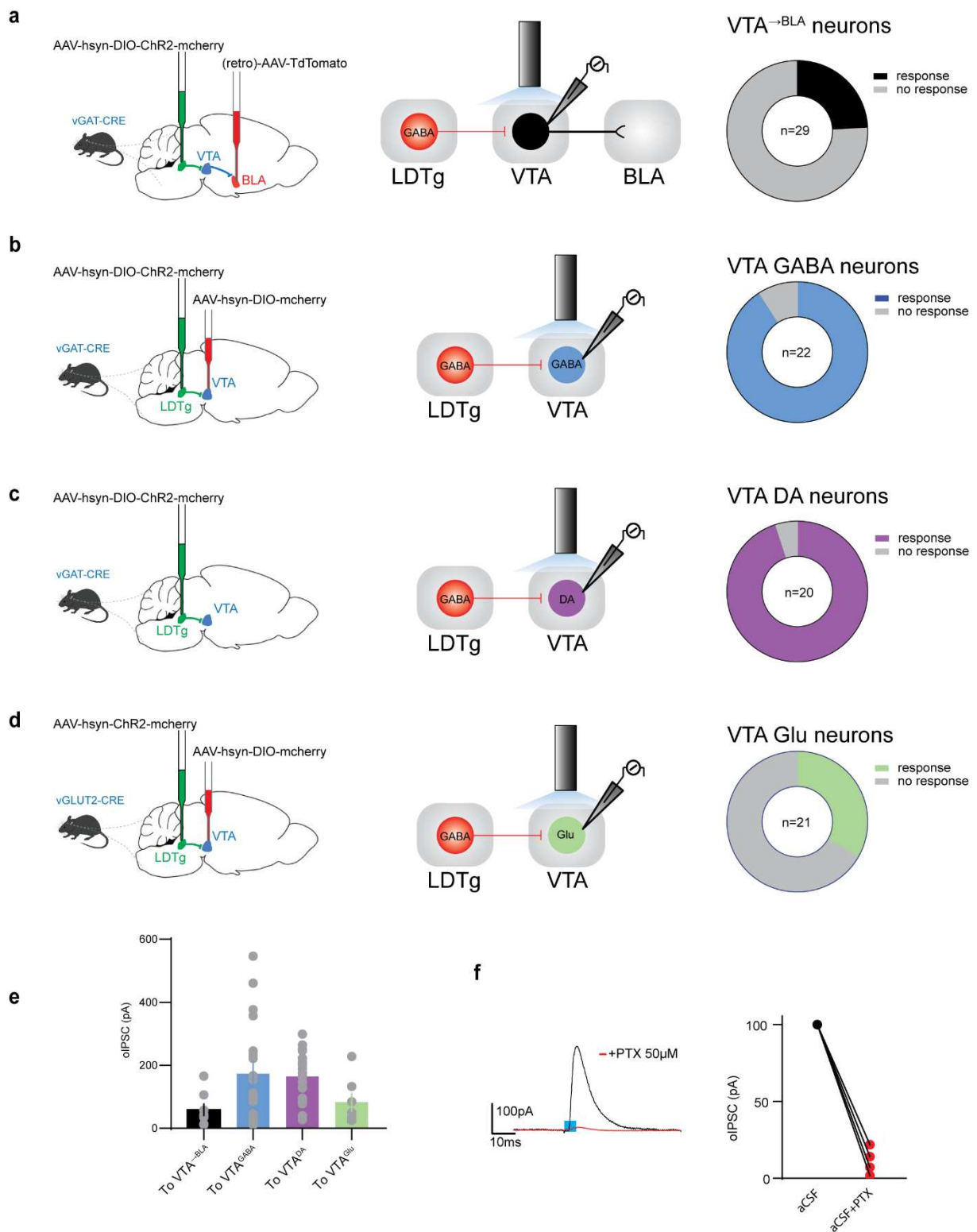


Supplementary Figure 6. Effects of photoactivation of LDTg GABAergic terminals does on aversive memory and distance travelled. (a) Control and ChR2 mice photo-stimulated in Fig. 2a were re-

exposed to the same context 24h after. Data indicate an absence of conditioned freezing. (b) The mean of the distance travelled over the 3 days of conditioning has been measured in the paired and unpaired chambers for control and Chr2 mice. Repeated measures two-way ANOVA followed by Sidak's comparison test, $P=0.0672$ for control and $P<0.001$ for Chr2 groups.

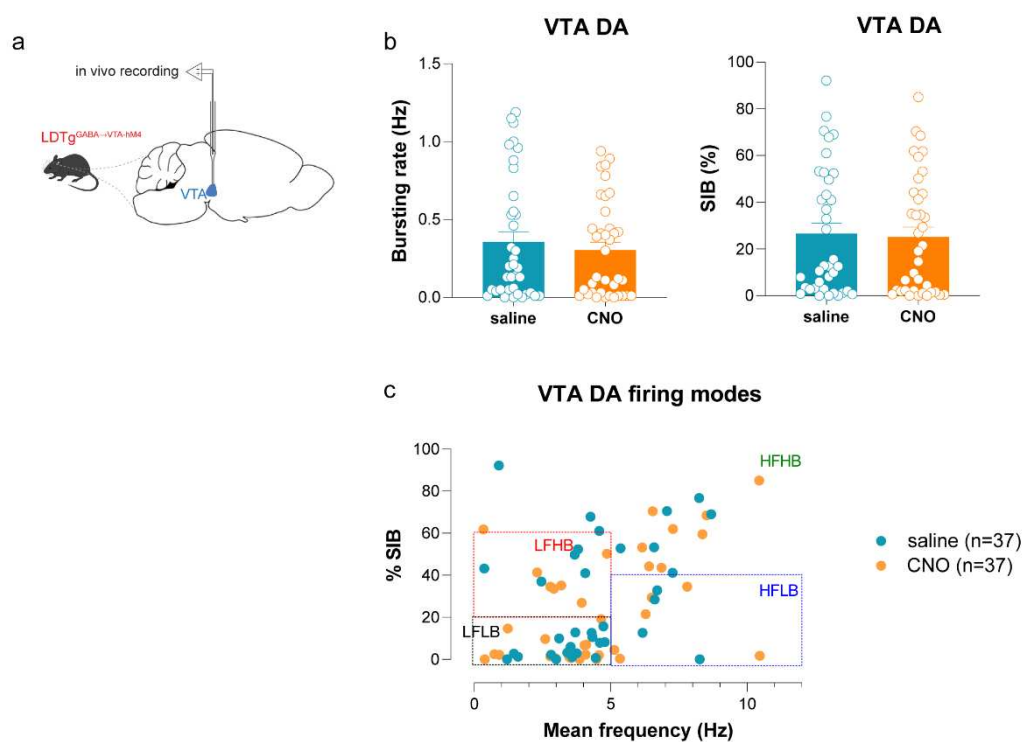


Supplementary Figure 7. Stimulation of GABAergic LDTg terminals within the VTA does not induce activation of the NAc. (a) Control and vGAT-Cre Chr2 mice were sacrificed 90 min after light stimulation as depicted in the experimental timeline. cFos-positive neurons were counted in the NAc core and shell subdivisions. No difference was found between the 2 conditions. (b) Example of freezing traces obtained when silencing or not $VTA \rightarrow^{BLA}$ projections (see Fig. 5d). (c) Example of freezing traces obtained when silencing or not $VTA \rightarrow^{LS}$ projections (see Fig. 5e).



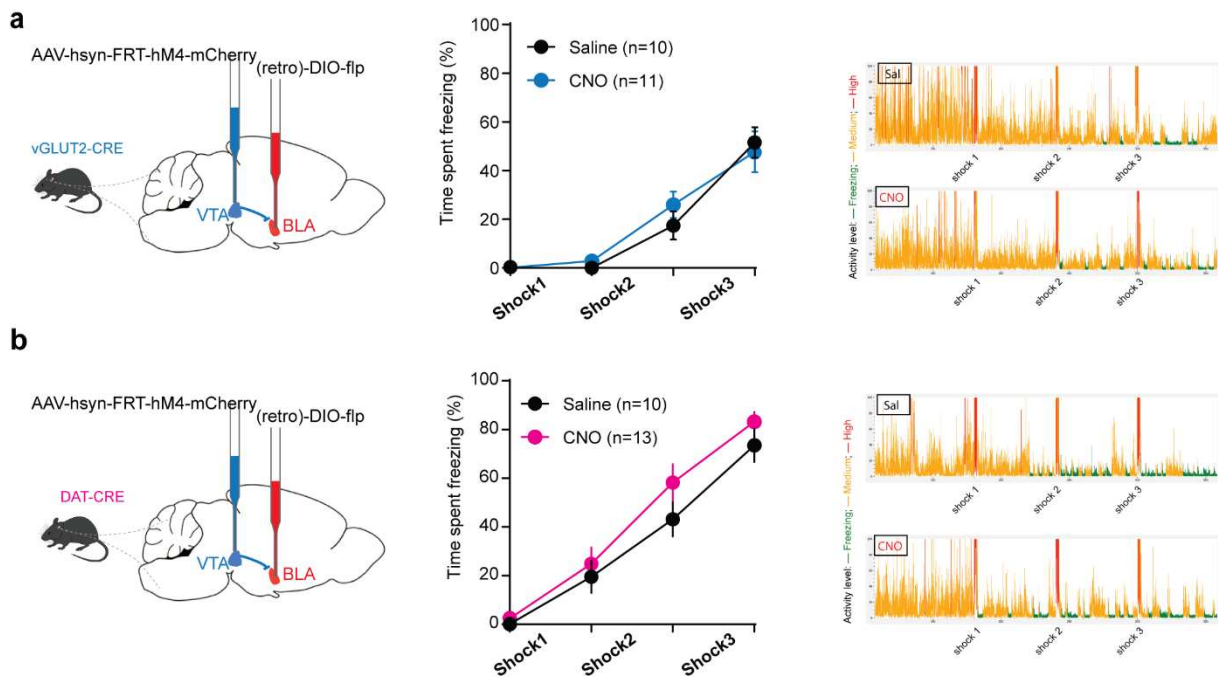
Supplementary Figure 8. Functional connectivity between LDTg GABAergic inputs and VTA cell substrates. VTA slices were obtained from vGAT-Cre Chr2 mice injected either with a retro-AAV-tdTomato in the BLA (a) or AAV-hSyn-DIO-mCherry in the VTA (b) or no viral injection in the VTA (c). We also prepared slices from vGluT2-Cre mice injected with AAV-hSyn-DIO-mCherry in the VTA and

AAV-hSyn-ChR2-YFP in the LDTg. *Ex vivo* recordings were obtained from tdTomato- or mCherry-expressing VTA neurons following light stimulation. Putative VTA DA neurons were identified as described in methods. The percentage of cells exhibiting optically-induced inhibitory postsynaptic currents (oIPSC) are represented in pie charts. (e) The mean current responses of $VTA^{\rightarrow BLA}$, VTA^{GABA} , VTA^{DA} or VTA^{Glu} responding neurons is reported in pA. (f) Optically-induced inhibitory postsynaptic currents (oIPSC) were virtually abolished in the presence of picrotoxin (PTX, 50 μ M). Right panel: Amplitude of oIPSCs in VTA^{GABA} or $VTA^{\rightarrow BLA}$ neurons.

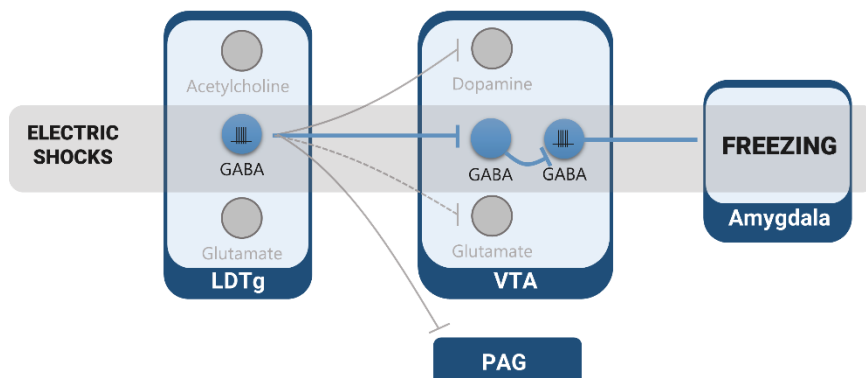


Supplementary Figure 9. Impact of silencing LDTg inhibitory inputs onto VTA DA neurons activity. (a) vGAT-Cre mice were injected with an AAV-hSyn-DIO-hM4-mCherry in the LDTg and *in vivo* recordings were performed in the VTA in anesthetized mice. The activity of putative VTA DA neurons was analysed upon systemic administration of saline or CNO. **(b)** The bursting rate (left panel) and % of spikes in bursts (SIB, right panel) did not differ between treatments. **(c)** Analysis of VTA DA neurons activity based on both the firing and bursting patterns. LFLB: low firing, low bursting; HFLB: high firing,

low bursting; LFHB: low firing, high bursting; HFHB: high firing, high bursting. The inhibition of LDTg GABAergic inputs to VTA does not alter the activity of VTA DA neurons.



Supplementary Figure 10. Lack of effect of silencing Glu or DA $VTA \rightarrow BLA$ neurons on freezing responses. vGluT2-Cre (a) or DAT-Cre (b) mice were injected with a retrograde AAV-DIO-flp in the BLA and a flippase(flippase)-dependent inhibitory DREADD in the VTA. Following exposure to electric shocks, freezing responses did not differ between saline- or CNO-treated mice. Interaction treatment x shocks $F(3, 57) = 0.751, P=0.5261$ for vGluT2 and $F(3, 63) = 0.796, P=0.500$ for DAT-Cre; repeated measures two-way ANOVA followed by Sidak's comparison test.



Supplementary Figure 11. Schematic model of the findings.

THÈSE DE DOCTORAT

DISCUSSION AND PERSPECTIVES

The global objective of my thesis was to improve our knowledge of the VTA and its involvement in anxiety and fear-related defensive behaviors. In order to do so, we assessed the role of the VTA in both anxiety and fear mainly through the study of its outputs to the amygdala but of its inputs from the LDTg. Therefore, my thesis was divided in two projects: 1) Understanding the modulatory role of the VTA glutamatergic neurons on the amygdala regulation of anxiety. 2) Understand how the VTA integrate LDTg inputs to promote defensive fear-induced freezing.

Here, we used models to either study anxiety disorders with the chronic social defeat protocol or fear response with a footshock-induced freezing paradigm. We also relied on optogenetic and pharmacogenetic tools used in transgenic mice to assess the effect on defensive behaviors of selective modulation of neuronal population in the VTA (as well as its inputs and outputs). In the first axis of my thesis, chronic stimulation of glutamate outputs of the VTA to the BLA elicit an anxiogenic response while acute stimulation or inhibition of this pathway did not alter anxiety levels. Chronic social defeat stress was also found to elicit an anxiogenic response and was matched with similar electrophysiological alterations as chronically stimulated mice. These electrophysiological alterations suggest that chronic stress induces an hyperexcitability of VTA → BLA glutamatergic efferences. In the second project of my thesis, pharmacogenetic inhibition of LDTg-inputs to the VTA was found to dampen fear-induced freezing response in mice. Selective activation of GABAergic LDTg inputs to the VTA in the absence of a threat elicited spontaneous freezing. Pharmacogenetic modulation of diverse VTA outputs revealed that VTA GABAergic projections to the BLA were likely mediating the freezing response observed in our study.

Overall, the results reveal a novel functional aspect of the VTA in the induction of defensive behaviors through the identification of a new anxiety-modulating efference of the VTA glutamatergic neurons but also through a putative LDTg-VTA-BLA pathway modulation of fear responses. Our studies reinforce the pivotal place of the VTA in the stress response by promoting defensive behaviors.

The heterogeneous role of the VTA in negative valence and defensive behaviors

a) VTA in valence assignment

Many studies that have been carried on the VTA have underlined its importance in regulating reward-seeking behaviors and motivational states. However, the view of the VTA as a structure directed mainly toward reward processing has been challenged in the last decades. Indeed, the DA neurons of the VTA were first thought to only mediate reward and to be non-responsive to aversion. Furthermore, the VTA DA projections to the striatum and the PFC were thought to direct reward-

signalling. However, this view was challenged with the emergence of the reward-prediction error principle, where a subset of VTA DA change from tonic to phasic activity when a reward better than expected is obtained (Schultz, 1998). This principle brought forth the idea that if an appetitive event promotes VTA DA activity, then aversive cues should decrease this activity or at least not change it. This idea was refuted as a non-negligible proportion of VTA DA neurons were found to be activated by aversive stimuli, underlining the presence of two neuronal VTA population mediating either aversion or reward (Bromberg-Martin et al., 2010). This evolution of the concept of the VTA as a heterogeneous structure that can mediate behaviors of opposite valence was further substantiated by studies demonstrating that excitatory inputs to the VTA DA neurons could also promote aversion. Activation of glutamatergic inputs from the LHb to the VTA DA were shown to promote aversion, hence going against the theory of a single neuronal population mediating reward when active and aversion when silenced (Lammel et al., 2012). Interestingly, in this study, different downstream effectors of VTA DA neurons are suggested to mediate reward and aversion. Another study, further strengthened this theory of two DA neuronal population in the VTA as activation of LH glutamatergic inputs to the VTA DA was associated with aversive outcome through projection to a different portion of the NAc, namely, the medial shell (De Jong et al., 2019). Overall, these studies shifted the view on the VTA DA role in mediating not only reward but also aversion. Furthermore, several studies have highlighted other non-DA dependant pathways in the VTA that can promote aversion-related behaviors (see Fig. 15 of the introduction). Together, these studies favors the view of an heterogeneous VTA that can mediate aversive signalling through different inputs and outputs structures.

b) The VTA dopamine neurons in defensive behaviors

The original studies showing that VTA neurons responded to aversive stimuli prompted investigations on whether VTA could participate in defensive behaviors in response to aversive stimuli. The place for the VTA in defensive behaviors was first investigated with electrolytic lesions and electric stimulations (Borowski & Kokkinidis, 1996). In their study, Borowski et al., showed that VTA stimulation promoted fear-startle while lesions prevented this response. Furthermore, local injection of quinpirole to block VTA DA population also blocked fear response. Further studies revealed that DA projection to the amygdala were likely responsible for the effect observed on fear. Indeed, dopamine 1 receptor (D1R) blockade through local infusion of the D1R antagonist SCH23390 in the amygdala prevented fear expression in a potentiated startle paradigm (Lamont & Kokkinidis, 1998). Furthermore, another study with the infusion in the amygdala of the same antagonist led to decreased anxiety levels in a dark-light paradigm (De La Mora et al., 2005). Overall, these studies provided the first evidence of a role of the VTA in the promotion of defensive behaviors but also indicated the BLA as the effector of the VTA in

these behaviors. Since this discovery and the development of chemogenetic and optogenetic tools have leap forward in the understanding of the role of the VTA in defensive behaviors.

While disruption of the activity of VTA DA neurons in response to aversive event such as fear conditioning has been associated with the induction of generalized anxiety (Zweifel et al., 2011), the involvement in defensive behaviors of VTA DA inputs to the amygdala remained putative until last year. While inconsistent with the previous pharmacological reports on DA action in promoting anxiety, optogenetic stimulation of VTA DA neurons projecting to the BLA was found to elicit an decreased anxious phenotype while conversely activating these inputs increases anxiety (Nguyen et al., 2021). Interestingly, another recent study found similar results. Using the CSD paradigm to induce anxiety-like disorders in mice and fiber photometry recordings revealed that anxiety was associated to DA hypoactivity for BLA projecting VTA neurons (Morel et al., 2022). Furthermore, a protocol of subthreshold social defeat was sufficient to induce an anxious state when paired with a cell-type non-selective optogenetic photoinhibition of VTA projection to the BLA. Conversely, activation of these non-selective projections after CSD protocol was found to revert the anxious phenotype. Overall, these new studies highlight a modulatory role for the VTA DA in decreasing anxiety through efferences to the BLA. However, another recent study suggested that DA may also promote anxiety in the amygdala through the disinhibition of the BLA by silencing the ITCs of the amygdala with a (Aksoy-Aksel et al., 2021). These studies highlight a complex integration of DA in the amygdala and suggest a bidirectional control of anxiety by the DA. In spite of these inconsistent reports, these studies particularly resonate with the results obtained in my thesis that demonstrate that neuromodulatory VTA inputs to the BLA can promote anxiety.

Other VTA-dependant pathways have also been shown to regulate anxiety. While I mentioned above an opposite functional role inside the VTA DA neuronal population in mediating aversion, this heterogeneity also exists between the different cell-type inside the VTA. In my introduction, I presented the seminal work of Marisela Morales and David Root in describing the heterogeneous properties of the VTA subpopulations. Their work has helped the characterization of the two other VTA cell-types involved in defensive behaviors, namely, the GABAergic and glutamatergic populations.

c) The VTA GABA neurons in defensive behaviors

VTA GABA neurons were first suggested to promote aversion through local modulation of VTA DA (Nieh et al., 2016; Tan et al., 2012), further studies demonstrated that long-range GABA could also promote aversion with efferences to the DRN (Y. Li et al., 2019). These results illustrated that VTA GABA can also regulate emotionally negative state such as aversion. These studies were closely followed by a direct association of VTA GABA projections to the amygdala in the promotion of

defensive behaviors. Indeed, a recent study has highlighted the existence of superior colliculus glutamatergic inputs to VTA GABA neurons that promote a feedforward inhibition of the CeM responsible for the induction of flight-to-escape and hiding responses (Zhou et al., 2019). These effects on hiding behaviors are interesting as a part of my thesis strongly suggest that activation of VTA GABA long-range projection to the amygdala and more precisely to the BLA elicit freezing responses. Both these pathways could therefore contribute to the VTA modulation of defensive behaviors. However, before discussing the integration of these inputs by the amygdala and their effects on anxiety and fear-related behaviors, it is important to mention the involvement of the glutamatergic population of the VTA in these behaviors.

d) The VTA glutamate neurons in defensive behaviors

Glutamatergic neurons presence in the VTA have been discovered relatively recently (Kawano et al., 2006; Yamaguchi et al., 2007). Yet, several studies have shown a role of these neurons in promoting reward (H. L. Wang et al., 2015; Yoo et al., 2016). But also in promoting aversion through efference to the LHb and NAc (J. Qi et al., 2016; Root, Mejias-Aponte, Qi, et al., 2014). Coherently, *in vivo* recordings identified VTA glutamate neurons subpopulation to be activated by aversive events (Root, Estrin, et al., 2018). Hence, similarly to the VTA-DA and VTA-GABA population, the VTA-glutamate neurons seem also involved in regulating negative valence related behaviors. However, in their study of 2018, Root et al., *in vivo* electrophysiological recordings of VTA glutamate neurons during both sucrose reward and aversive airpuff revealed the presence of two major VTA subpopulations: one active during both stimuli, therefore signalling salience; the other active in response to airpuff and silenced in response to reward. While reward-only responsive VTA glutamate neurons were also found, they were identified as a small subpopulation compared to neurons signalling only aversion and neurons signalling salience (activated by both rewarding and aversive events). Hence, these first studies have suggested that VTA glutamate neurons may be shifted toward the regulation of more negative-valence behaviors. It is these discoveries that led us to wonder if VTA glutamate could also play a role in defensive behaviors like they GABA and DA counterparts. A recent study first demonstrated a role of the VTA glutamate neurons in promoting fear-induced escape and hiding through glutamate efference from the LH (Barbano et al., 2020). More precisely, they demonstrated that genetic ablation of VTA VGLUT2 neurons was associated with a decrease in active escape behaviors while optogenetic activation and inhibition of the LH glutamate inputs to the VTA VGLUT2 was respectively associated with increase and decrease of active escape in response to a looming stimulus. Together with studies on aversion, these results of Barbano et al., suggest a strong relationship between VTA glutamate neurons and response to negative events. However, while several VTA glutamate efferences to the NAc and LHb were identified to play a role in aversion, the

downstream effector in defensive behaviors of VTA glutamate neurons has only been recently assessed. My thesis project and another recent study have illustrated those projections from the VTA glutamate to the amygdala to be involved in defensive behaviors. However, in these two studies the results obtained were for different effector subregions of the amygdala, namely the CeA for Chen et al., and the BLA for my project. Indeed, in their study Shang-Yi Chen et al., studied the interaction between the VTA glutamate neurons and the CeA in the context of arousal and defence (Chen et al., 2022). They found that an important role for these projections in promoting arousal as optogenetic activation of this efference was associated with fast transition from sleep to sustained wakefulness. Furthermore, this stimulation also triggered a wide behavioral range of defensive responses such as avoidance, burrowing, escape and flight-to-shelter. Overall, this study shows an important role for VTA glutamatergic neurons projections to the CeA in mediating both anxiety- and fear-related defensive responses. However, it is to be noted that inhibition of this projection by pharmacogenetic or optogenetic means with or without the use of threatening-cues were not assessed here. Therefore, the contribution of VTA glutamate efference to the CeA in innate defensive response remains to be tested. In my thesis, the anatomical and functional studies of VTA glutamatergic projections to the amygdala led us to study the BLA rather than the CeA. Indeed, the first figure of my thesis manuscript highlights the pattern of innervation of the amygdala by the VTA glutamatergic neurons as well as their functional connectivity. Interestingly, while both BLA and CeA are innervated by VTA glutamate inputs, these efferences seems to target more profusely the BLA. Furthermore, while most of the recorded BLA neurons received functionally connected inputs from VTA glutamate neurons, this was not the case for the CeA. More precisely, only half of the recorded neurons were found to be connected. These results guided us to preferentially study the BLA and its role in anxiety. It is important however to mention that we also used chemogenetic and optogenetic tools to acutely modulate the VTA glutamate efference to the CeA and found no effect on anxiety levels in mice (see Fig. 16). However, these differences with the study of Chen et al., could arise from the restricted span of anxiety tests we used but also from differences in the technical parameters and viral approach used to target these projecting neurons. Our study of the VTA glutamate efference to the BLA however revealed that a chronic activation of these terminals could increase basal anxiety levels as assessed 24h after the last optogenetic stimulation session while acute modulation did not yield any effect on anxiety levels. Overall, these studies of the different VTA populations have highlighted an important role for the VTA in modulating adaptive response to environmental stimuli by controlling valence signalling (i.e. reward and aversion) but also by controlling the induction of defensive behaviors related to both anxiety and fear. While the signalling of reward seems to be mediated by the VTA through different downstream effectors structures, this seems not to be the case so far for defensive behaviors. Up to my knowledge so far, the only identified effector of the VTA in promoting anxiety- and fear-related defensive response

has been the amygdala. Therefore, I will discuss next the integration of these inputs by the amygdala and their modulatory role in promoting either anxiety or fear.

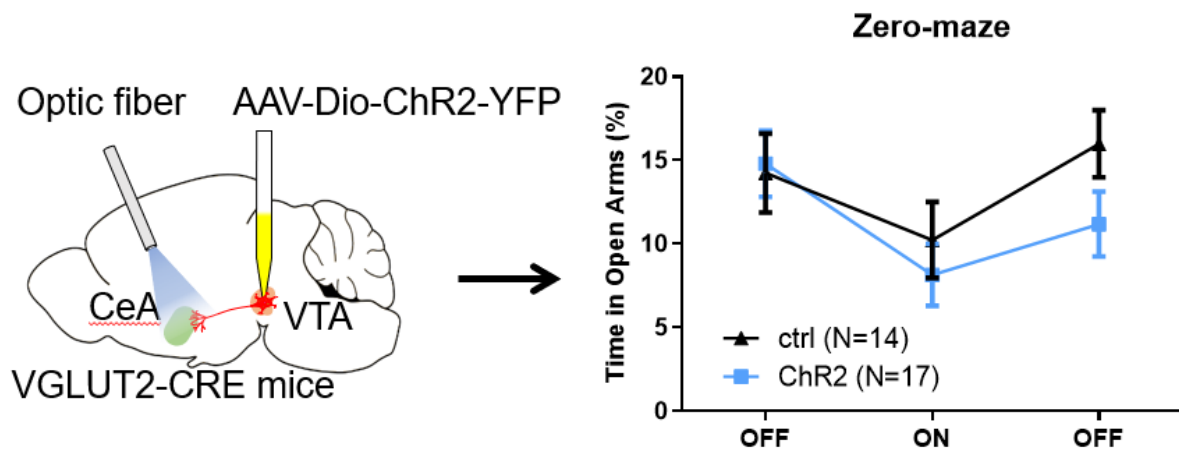


Fig. 16 – Acute optogenetic stimulation of VTA glutamate terminals in the CeA did not change anxiety levels in our study. We wanted to test if an acute stimulation of VTA glutamate neurons terminals in the CeA was sufficient to elicit changes in anxiety levels recorded in the zero maze test. Therefore, mice were injected with a AAV-Dio-ChR2-YFP in the VTA. Five weeks later, an optical fiber was implanted on top of CeA. Two weeks later, mice anxiety levels were tested in a zero-maze test divided in three phase of 1min30sec each. During the ON phase, mice received an acute optogenetic stimulation (pulses of 10mW, 20Hz, 20ms).

Focus on the amygdala: involvement in defensive behavior through VTA inputs integration

The amygdala circuitry is complex and processing sensory information into fear or anxiety requires several steps. These steps are fundamentally: 1) Integration of sensory inputs by the LA and BLA) 2) transmission of the information from the LA to the BLA 3) excitation of the CeM by direct and indirect inputs from the BLA (see chapter II.B of the introduction for more information). Although the amygdala processing described here is simplified, the VTA inputs to the amygdala can virtually have profound different and even opposite effects on defensive behaviors depending on the subregion targeted. The evidence gathered from our study and the literature have highlighted a connectivity of the VTA toward two main regions of the amygdala: the BLA and CeA. However, even inside each of these regions exist an important local network gating the transfer of information to the main output subregion, the CeM. Hence, in the following paragraph I will discuss the integration of VTA inputs in each of these subregions.

a) Integration of VTA DA inputs by the amygdala in defensive behaviors

As previously mentioned the BLA is comprised of two neuronal population, the glutamatergic principal neurons and the local inhibitory GABAergic interneurons (Vereczki et al., 2021). Two studies using in vivo optogenetic tools has illustrated that VTA DA projections interact with the BLA to regulate anxiety levels (Morel et al., 2022; Nguyen et al., 2021). In both of these studies, activation of BLA projecting DA neurons were found to decrease anxiety levels in mice while conversely silencing these inputs did the opposite. Mechanistically, this effect suggests that DA inputs to the BLA would inhibit this subregion, hence preventing the activation of the CeM and the induction of anxiety. While the BLA contains GABA interneurons, their response to DA inputs are quite complex. Indeed, while DA promotes an hyperpolarization of the GABAergic neurons in the ITC surrounding the BLA, DA can also promote activation of BLA interneurons but also of the principal neurons (Kröner et al., 2005; Muller et al., 2009). Hence, while my goal here is not to delve into the mechanisms of DA modulation of the amygdala, it seems plausible that in response to stress-induced anxiety, different VTA DA pathway may be activated and promote an inhibition of the BLA through putative enhanced interneuron local inhibitory tone. Interestingly, while not directly associated with modulation of VTA DA inputs to the BLA, the study of Zhou et al., showed that optogenetic inhibition of VTA DA neurons during a threat-mimicking looming stimulus was associated with an increase of hiding behavior. Furthermore, activation of SC glutamatergic inputs to the VTA was found to globally inhibit VTA DA neurons activity. Hence, this study suggests inhibition of VTA DA promotes defensive behavior such as hiding. Mechanistically, evidence have emerged showing that activation of the CeM leads to passive defensive (hiding, freezing, avoidance) response while its inhibition leads to more active defensive behaviors (active escape) through CeL CRF and somatostatin interneurons interaction with the CeM (Fadok et al., 2017). Therefore, one study suggests that VTA DA promote anxiety by inhibiting the BLA while the other suggest the same projection to promote more active defensive behavior. These, somehow, contradictory results further highlight the complexity of DA neuromodulation of the amygdala of anxiety and fear.

b) Integration of VTA GABA inputs by the amygdala in defensive behaviors

As previously mentioned, a role has been observed in defensive behaviors for the GABAergic inputs from the VTA to the BLA. Indeed, activation of SC glutamatergic inputs to the VTA GABA as well as optogenetic stimulation of VTA GABA terminals in the CeM results in hiding and increased flight-to-
nest behaviors (Zhou et al., 2019). Interestingly, in the second part of my thesis I studied how LDTg

inputs to the VTA can promote another type of passive defensive response which is freezing. We showed that LDTg GABA projection to the VTA mediates freezing and that GABA neurons of the VTA are responsible for this effect through modulation of the BLA. More precisely, chemogenetic inhibition of VTA GABA projection to BLA was associated with a decreased freezing response in a contextual fear conditioning paradigm. Therefore, our study, in accordance to the one of Zhou et al., suggest that VTA GABA efference to the amygdala promotes defensive behaviors through a direct (Zhou et al., 2019) and a putative indirect inhibition or lack of activation (Brousot et al., provisionally accepted) of the CeM.

Overall, these results would also suggest the presence of different functional subpopulation in the CeM as the model of Fadok et al, suggest that direct GABA inputs to the CeM should favor their inhibition and therefore promote more active defensive behaviors such as escape. Importantly, in their study, Zhou et al., found no inhibitory post synaptic current in the CeL neurons in response to VTA GABA terminals stimulation, therefore limiting the chance of a putative disinhibition of the CeM through silencing the CeL.

c) Integration of VTA glutamate inputs by the amygdala in defensive behaviors

Finally, the results from my thesis as well as the study of Chen et al., suggest that both VTA glutamatergic inputs to the BLA and CeA promote anxiety. Acute optogenetic activation of VTA glutamate terminals in the CeA elicited avoidance, burrowing, escape and flight-to-shelter (Chen et al., 2022). Our study however, showed that an acute optogenetic stimulation of the VTA glutamate inputs to the BLA do not change anxiety levels in mice. Only a chronic activation is sufficient to trigger an increase of basal anxiety. Interestingly these results and the ineffective chronic silencing of VTA glutamate terminals to the BLA PN to revert CSD-driven anxiety seems to indicate a complex role for these neuronal projections to the BLA in promoting anxiety. Several putative models could account for such unexpected results, however, I will not delve deeper into this subjected here, but I refer the reader to read the discussion of my article manuscript where those putative models are described.

Mechanistically, the induction of anxious defensive behaviors in both BLA and CeA stimulated VTA glutamate neurons are coherent with the model of Fadok et al, as both would be linked with an activation of the CeM. However, several potential caveats are to be taken into consideration. First, the study of Chen et al., did not only elicit anxiety-related passive defensive behavior but also escape behavior. This effect on an active defensive behavior could arise from the innervation of the CeA by the VTA glutamate neurons. Indeed, projections to both CeL and CeM neurons could account for these results as they would respectively promote active and passive defensive behaviors through direct or indirect modulation of the CeM. However, our results suggest otherwise. Indeed, we parsed the VTA

glutamate the functional connectivity and innervation of the different amygdala subregion and found very little innervation and functional connectivity with the CeL. Hence, these results support the existence of distinct population in the CeM with opposite role on active vs passive defensive behaviors. A second point of debate between our study and the one of Chen et al., is the model and test used. We used the chronic social defeat model, a well-known model to induce depression and anxiety-related behaviors in mice, but restricted our behavioral testing mainly to measuring risk-assessment/avoidance behaviors. Therefore, we showed that chronic optogenetic stimulation of VTA glutamate efference to the BLA triggers an increase of risk-assessment/avoidance behavior in a similar fashion as the one observed during CSD. Furthermore, CSD and chronic stimulation had matched increase of anxiety levels with similar synaptic plasticity alterations. Hence, while our behavioral testing range was more limited, our study suggests a relevant role for these projections in a context more linked to pathological anxiety. However, this was not the case for the study of Chen et al. Furthermore, the ethological relevance of their anxiety test can be challenged as none were used that rely on stressful environmental stimulus. Therefore, they study do not provide information on the relevance of VTA glutamate projection to the CeA in modulating innate defensive behaviors.

Together, these aforementioned studies on the different VTA populations highlights the importance of their connectivity with the amygdala in the regulation of defensive behaviors. Furthermore, the need for more studies on the CeM circuitry is also warranted by these findings in order to better understand how active vs passive defensive behaviors are implemented. However, it is to be noted the existence of other VTA efferences to structures involved in the regulation of defensive behaviors that have, as of yet, not been studied. These efferences are from all VTA cell-types (DA, GABA, glutamate) and encompass the PAG, the LH, the LHb and others (Aransay et al., 2015; Taylor et al., 2014). Afferences from the BNST, NAc and basal forebrain to the VTA have also been identified to play a role in modulating anxiety. However, because of the lack of clarity in the CeA regulation of defensive behavior and the lack of study on other VTA effectors, discussing here how these inputs contribute to anxiety would be highly hypothetical. Therefore, I will not discuss further the role of these afference and refer the viewer to each of the respective article (BNST: (Jennings et al., 2013) ; NAc: (G. Qi et al., 2022) ; BF: (P. Cai et al., 2022)).

Translational relevance of the study of VTA outputs to the amygdala in anxiety and fear

My thesis axes have suggested a role in defensive behaviors for glutamatergic and GABAergic afference from the VTA to the BLA. However, a more general goal for my projects in the studies in the same field is to provide new insights on the anxiety and fear circuitry that might help guide to the development of improved therapies for anxiety disorders. However, several limits need to be acknowledged when trying to assess the translational aspect of my projects. Hence, in this chapter, I will highlight the limits of the mouse models and but also of the tools we use in laboratories to study defensive behaviors.

The important difference in brain anatomy between human and mice as well as the higher cognitive function found in humans enables it to feel psychologically complex emotions. It is these complex emotions that are found in a numerous types of human anxiety disorders but cannot be replicated in mice (Cryan & Holmes, 2005). For instance, low self-esteem, suicidal thought or even the anticipatory fear of panic attacks found in humans have been attributed to the evolution of the cortex and cannot be studied in mice. However, subcortical structures are well conserved between mammals and humans, including their subdivisions as well as their connectivity, therefore suggesting similarities of the function of the circuitry of complex emotional states such as anxiety. Early lesions and fMRI studies have shown that the amygdala involvement in fear is well conserved between human and rodents (Etkin et al., 2009; Janak & Tye, 2015). However, a profound anatomical change is observed between the two species regarding the BLA and CeA. More precisely, the further a mammal species is evolved that more the size of the BLA is greater while the CeA is smaller. This shift in proportion is thought to be linked to greater cortical inputs in more evolved species enabling more complex emotional processing (Chareyron et al., 2011). While studies have established an important conservation of the functionality of the amygdala between humans and rodents, the conservation of the VTA has received less interest (La Manno et al., 2016). Indeed, several studies have well characterized the conservation of DA neurons between human and rodents (German et al., 1983; Haber & Knutson, 2010). However, while no studies are available on the conservation of VTA GABA, a study has found the presence of glutamate neurons in the VTA of both primates and humans (Root et al., 2016). Interestingly, this study on VTA glutamate neurons in humans revealed similar pattern for several features found in the mice. While lower prevalence of glutamate-only neurons were found in the RLl in humans (40%) compared to mice (80%) to the profit of dopamine-only neurons, a similar lateral-to-medial decreasing gradient of VMAT2 and DAT expression was found (González-Hernández et al., 2004). Overall, these results resonate soundly with my project as they confirm the presence of a major VTA glutamate neuronal population with strong similarities in their organization in the medial VTA with our mouse model. Furthermore, several fMRI human studies found the medial VTA (RLl and

PN) to be hyper-reactive to aversive cue presentation (Hennigan et al., 2015), to threatening stimuli in GAD afflicted patient (Cha et al., 2014) and to pain anticipation (Bauch et al., 2014). While these studies were aimed at understanding the contribution of VTA DA in threat response, VTA glutamate neurons prominence in the medial VTA could play an important part in this hyper-reactivity in humans. Furthermore, our results are coherent with this hypothesis as an increased excitability following chronic social defeat was recorded for VTA glutamate neurons projecting to the BLA in mice. Hence, this excitability could underline a similar hyper-reactivity as the one found in human VTA glutamate neurons. However, while my results on VTA neurons modulation by stress is consistent with human fMRI studies, the translational aspect of the data I obtained on the effect of chronic stress on the amygdala are more debatable. human studies have not yet provided a clear pattern of activity of the amygdala in patient afflicted with GAD. Several studies have been reporting ambivalent results, with most suggesting an hyperactivity of the BLA in GAD while others did not (see review of (Duval et al., 2015)). Therefore, while a strong conservation of both functionality and structure is found between human and mouse amygdala, the impact of the BLA hyper-reactivity our results suggested remains to be taken with caution.

Taken together, these studies about VTA and the amygdala suggest a strong conservation of functionality and organization between mice and human. Therefore, the study of this VTA glutamate projection to the BLA in human could be relevant for potential therapeutic targets as our results suggest a role for the VTA glutamate efference to the BLA in promoting anxiety disorders.

Technical considerations

While more invasive because of the need of implantation of optical fibers directly in the brain of animals, optogenetic remains an unmatched technique for neuronal modulation. Indeed, optogenetic allows for an incredible temporal resolution where the stimulation can be stopped following the will of the experimenter unlike DREADDs. Furthermore, this technique enables a incredible precision in the pattern of activation or inhibition administrated. Unlike DREADDs, the frequency, periods and intensity of the stimulation can be decided by the experimenter. Therefore, this tool has a greater physiological relevance as it enables to mimic pattern of stimulation found in the neurons. For my project, I used this property to my advantage as electrophysiological recordings enabled us to determine the firing rates for the VTA glutamate neurons after social defeat stress. Therefore, I used this frequency to chronically stimulate the VTA glutamate neurons which resulted in increased anxiety in a similar pattern as would chronic social defeat. Overall, while both chemogenetic and optogenetic tools have their respective advantages and limits, their use has been key in the field

of neurobiology to parse the functionality of neuronal circuitry in behaviors. Importantly, these tools do not only provide a way to prove causality between basal neuronal activity and behaviors but also enables to assess the therapeutic potential of targeted approach directed at selective neuronal populations. Therefore, the use of chemogenetics and optogenetic in humans could provide new treatments in an incredibly number of pathologies ranging from developmental to psychiatric disorders. As of now, four clinical trials are underway in humans using optogenetics. Because of the invasiveness of current procedure, trials are currently restricted to targeting an eye pathology where light stimulation do not require implants (White & Whittaker, 2022). While time will be needed before clinical trials on mood disorders are allowed, the development rates of both chemogenetic and optogenetic tools seems to continue gaining speed (for reviews, see (Lee et al., 2020; Sternson & Bleakman, 2020)). Interestingly, some of the latest development in the optogenetic field is the development of less-invasive techniques such as SOUL (Gong et al., 2020). This technique enables transcranial optogenetic control of cortical neurons in macaques and of deep-brain structures in the mice such as the lateral hypothalamus. This technical advance and perhaps the development of new non-invasive optogenetic tools allowing modulation of even deeper brain structures could provide a way to circumvent the main limit of optogenetic in both animals and potential human therapies. However, these techniques would still require the use of viral tools to bring the expression of the opsins directly inside the brain and potentially in selective neuronal populations. This necessity highlights two main issues: the use of untested viral tools directly on human and the required stereotaxic surgery to deliver the virus inside the brain. While only cautious clinical approach will allow to ensure the lack of harm in the use of viral tools in humans, new development in the field of neurobiology may one day allow to bypass the need for surgical procedure to deliver the said viral tools. Indeed, the current work of the team of Viviana Gradinaru could provide a new non-invasive way to deliver genetic construct directly inside the brain without the use of surgery. Their work is focused on the development of viral tools that can be administered intravenously and yet still target distantly located precise cell-type (Challis et al., 2019). While still in its premise, this work could pave the way for further development of non-invasive viral tools to deliver gene in specific cells and specific locations. One could therefore hypothesize that these new viral delivery mean may one day be used to administer optogenetic tools which themselves could be controlled through transcranial optogenetic stimulation.

While only a dream, such scenario combining non-invasive techniques to treat mood disorders would not have been potentially thought a few decades ago. Imaging this scenario is only possible because of the frightening rate of development of new tools to study and potentially treat animal version of common occurring pathologies. Overall, this underline the importance of identifying specific

neuronal pathway involved in anxiety such as the VTA glutamate projections to the BLA as they may one day be targeted in therapies with optogenetic tools.

Perspectives

I have presented here the results gathered from two projects involving the VTA and the BLA in anxiety- and fear-related defensive behaviors. These findings raise questions about the complex circuitry of the amygdala and more precisely the role of the central amygdala as my results and others are not consistent with its canonical view in the literature. Indeed, while the complex network of a part of the central amygdala, namely the centrolateral portion, is starting to be unravelled, the centromedial portion remains elusive and require more study. Our data suggests that VTA glutamate neurons make efference onto BLA principal neurons. Those results will be key to further the understanding of BLA integration of glutamatergic inputs that may contribute to its hyper-(re)activity in fear and anxiety.

My thesis axes both focus on the role of VTA neuromodulatory projections to the amygdala in defensive behaviors, hence, performing other behavioral tests might be key to fully understand the reach of this projections on anxious and fear responses. As previously stated, several inputs to the VTA that contribute to the onset of defensive behaviors have been identified, including the LDTg in our study. However, many of these inputs (BF, the NAc, and BNST and LH) downstream effectors in the regulation of defensive responses remains only putative and require further investigation.

My results suggest that chronic stress and chronic activation of VTA glutamate inputs to the BLA both mediate similar behavioral and cellular adaptations in the BLA. It would therefore be of great interest to study if silencing this projection is sufficient to revert anxious phenotype after chronic stress. While our preliminary data with acute and chronic silencing after chronic do not seems to be favorable to this hypothesis (data not shown), these results need to be confirmed. Further approach to silence neuronal activation during the periods of social defeat could also be considered as *in vivo* fiber photometry recordings revealed an activation of this projections in response to aggressions (Fig. 17).

While our first approach would have more interesting putative therapeutic value, this second approach would be key to understand how this projection contribute to the dysregulation of the amygdala. From our preliminary results, we can hypothesize a potential role of VTA glutamate neurons in the induction of hyper-(re)activity of the BLA but not in sustaining this state where other inputs might take the relay.

Social defeat recordings

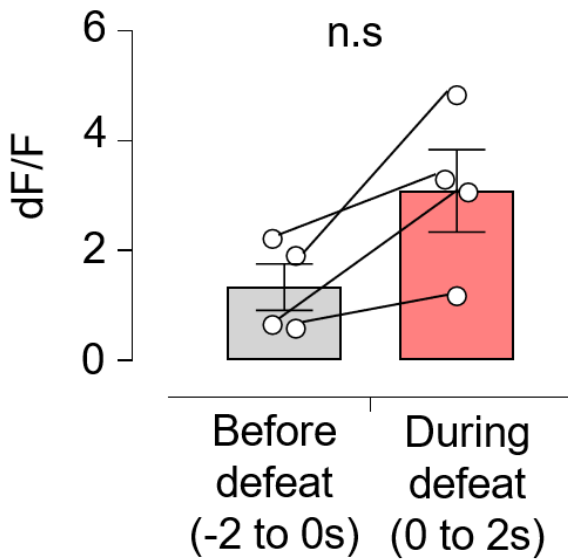


Fig. 17 – VTA glutamate neurons exhibit enhance activity during aggression by conspecific. These results were obtained by in vivo fiber photometry recordings during a social defeat session. Of note, all recorded neurons have a trend toward an increase of activity compared to baseline before aggression.

THÈSE DE DOCTORAT

Annexes

Contributions non-related to the thesis project

First contribution

Dopamine and glutamate receptors control social stress-induced striatal ERK1/2 activation

Contesse T, Broussot L, Fofu H, Vanhoutte P, Fernandez S, Barik J

Neuropharmacology volume 190, Article number: 108534 (2021)

Summary

In the following study, we determined how social stress shapes the neuronal activity of the striatum. We subjected mice to acute and chronic social stress paradigm and measured the induction of the phosphorylation of ERK1 and ERK2 as a proxy for neuronal activation in different striatal subregions. We used different type of selective antagonist of dopamine and glutamate NMDA receptors to assess the molecular pathways used for the induction of neuronal activity. Finally, we used a chemogenetic approach to identify the paraventricular nucleus of the thalamus as a source of glutamatergic inputs promoting the chronic stress-related long-lasting cellular adaptations found in the ventral striatum.

Contribution

This project was realised in the continuity of my Master internship project. The design of the project was shared between me and my two supervisors: Sebastian P FERNANDEZ and Jacques BARIK. I have participated in all the histochemical analysis. All in vivo behavioral stress protocol were performed by Loic BROUSSOT and me. I obtained most of the microscopy images with Hugo FOFO. Loïc BROUSSOT contributed to the realization of histochemical protocols. Viral injections were carried out by Jacques BARIK. Data analysis was performed by Sebastian P FERNANDEZ and me. Writing of the manuscript was performed by Sebastian P FERNANDEZ and Jacques BARIK. Peter VANHOUTTE and Loic BROUSSOT provided intellectual and technical inputs.



Dopamine and glutamate receptors control social stress-induced striatal ERK1/2 activation

Thomas Contesse^{a,b}, Loïc Broussot^{a,b}, Hugo Fofó^{a,b}, Peter Vanhoutte^{c,d,e},
Sebastian P. Fernandez^{a,b,**,1}, Jacques Barik^{a,b,*},¹

^a Université Côte d'Azur, Nice, France

^b Institut de Pharmacologie Moléculaire & Cellulaire, CNRS UMR7275, Valbonne, France

^c CNRS, UMR 8246, Neuroscience Paris Seine, F, 75005, Paris, France

^d INSERM, UMR-S 1130, Neuroscience Paris Seine, Institute of Biology Paris Seine, F, 75005, Paris, France

^e Sorbonne Université, UPMC Université Paris 06, UM CR18, Neuroscience Paris Seine, F, 75005, Paris, France

ARTICLE INFO

Keywords:

Social stress
Striatum
ERK1/2
D1 dopamine receptor
NMDA glutamate Receptor
Paraventricular thalamus

ABSTRACT

Stress has been acknowledged as one of the main risk factors for the onset of psychiatric disorders. Social stress is the most common type of stressor encountered in our daily lives. Uncovering the molecular determinants of the effect of stress on the brain would help understanding the complex maladaptations that contribute to pathological stress-related mental states. We examined molecular changes in the reward system following social defeat stress in mice, as increasing evidence implicates this system in sensing stressful stimuli. Following acute or chronic social defeat stress, the activation (i.e. phosphorylation) of extracellular signal-regulated kinases ERK1 and ERK2 (pERK1/2), markers of synaptic plasticity, was monitored in sub-regions of the reward system. We employed pharmacological antagonists and inhibitory DREADD to dissect the sequence of events controlling pERK1/2 dynamics. The nucleus accumbens (NAc) showed marked increases in pERK1/2 following both acute and chronic social stress compared to the dorsal striatum. Increases in pERK1/2 required dopamine D1 receptors and GluN2B-containing NMDA receptors. Paraventricular thalamic glutamatergic inputs to the NAc are required for social stress-induced pERK1/2. The molecular adaptations identified here could contribute to the long-lasting impact of stress on the brain and may be targeted to counteract stress-related psychopathologies.

1. Introduction

The reward system has been remarkably conserved amongst species. It promotes adaptive behaviours and therefore increases the likelihood of survival in complex environments. These responses rely on neural processes, which shape associative learning and motivated behaviours, to seek natural rewards such as food, sex and social rewards (Bromberg-Martin et al., 2010; Schultz, 2015). Within the reward system, midbrain dopamine (DA) neurons and the release of DA in targeted brain areas has by far received the most attention in the modulation of rewarding and motivational processes (Bromberg-Martin et al., 2010). Yet, accumulating evidence indicate that the activity of the reward system is sensitive to a large variety of stressors including aversive physical and psychological stimuli (Ungless et al., 2004; Marinelli and

McCutcheon, 2014). Hence, DA neurons can react to both rewarding and aversive stimuli. Social cues are abundant in our daily lives and key to establish social and territorial relationships, as well as social hierarchies in order to limit fighting for resources (Sapolsky, 2005). Thus, social stress is the most frequent type of stressor experienced in our modern society. Social stress can initiate cellular maladaptations that can culminate in stress-related mental disorders such as depression (Russo and Nestler, 2013). Indeed, we and others demonstrated that chronic social stress triggers profound dysregulations of the activity of DA neurons from the ventral tegmental area (VTA) that project to the ventral striatum (nucleus accumbens, NAc) leading to the appearance of social withdrawal and anhedonia (Barik et al., 2013; Chaudhury et al., 2013). A single social defeat episode or exposure to a social threat, in previously defeated animals, trigger a transient but significant increase

* Corresponding author. Université Côte d'Azur, Nice, France.

** Corresponding author. Université Côte d'Azur, Nice, France.

E-mail addresses: fernandez@ipmc.cnrs.fr (S.P. Fernandez), barik@ipmc.cnrs.fr (J. Barik).

¹ These authors contributed equally to this work.

<https://doi.org/10.1016/j.neuropharm.2021.108534>

Received 7 December 2020; Received in revised form 3 March 2021; Accepted 12 March 2021

Available online 27 March 2021

0028-3908/© 2021 The Author(s).

Published by Elsevier Ltd.

This is an open access article under the CC BY-NC-ND license

(<http://creativecommons.org/licenses/by-nc-nd/4.0/>).

of DA in the NAc (Tidey and Miczek, 1996; Barik et al., 2013).

Released DA from midbrain DA neurons filters excitatory glutamatergic inputs converging onto the striatum (Bamford et al., 2004b). Recent findings indicate that social stress also affect glutamate (Glu) transmission at striatal excitatory synapses, which is associated with social withdrawal (Christoffel et al., 2015). Hence, the NAc constitutes a key downstream interface that computes sensory, environmental contingencies and internal drives for both rewarding and aversive stimuli. Yet the molecular determinants of social stress outcomes are not fully understood. Key for the integration of rewarding signals are the extracellular signal-regulated kinases (ERK) 1 and 2 (ERK1/2) in medium-sized spiny neurons (MSNs), the most abundant (~95%) striatal cell type (Pascoli et al., 2014). Phosphorylation on amino acids Threonine 202 and Tyrosine 204 promotes ERK1/2 activation and trigger dynamic changes of their subcellular localization (Berti and Seger, 2017). Phosphorylated ERK1/2 (pERK1/2) rapidly translocate to the nucleus and launch chromatin remodelling, gene transcription as well as long-lasting structural and synaptic plasticity and behavioural alterations (Girault et al., 2007; Salery et al., 2020). Hence, ERK1/2 is key to translate changes from molecular adaptations into deeply engrained altered behaviours. ERK1/2 dynamics have been intensively examined for many addictive rewards, but its modulation by social stress is poorly understood. Here, we combined pharmacological and pharmacogenetic approaches to dissect the impact of social stress on striatal pERK1/2. We show that acute and chronic stress differently shape pERK1/2 induction. Also, we demonstrate that stimulation of dopamine D1 receptors as well as different NMDA receptor subtypes are required for social stress-induced pERK1/2. Last, we found that silencing paraventricular thalamus glutamatergic inputs to NAc MSNs is sufficient to dampen stress outcomes. Overall, the molecular adaptations identified here could contribute to the long-lasting impact of stress on the brain and may have relevance for stress-related disorders.

2. Material and methods

2.1. Animals

All procedures were in accordance with the recommendations of the European Commission (2010/63/EU) for care and use of laboratory animals and approved by the French National and Local Ethical Committees (*Comité Institutionnel d'Éthique Pour l'Animal de Laboratoire - AZUR*). 8-week-old Male C57Bl6J (25–30 g, Janvier Labs France), and CD1 retired breeders (30–35 g, Janvier Labs, France) were used. All the experiments were performed in accordance to the ARRIVE guidelines. Mice were kept on ventilated racks (cage size in cm: 30Lx 20l x 12H) on a 12/12 dark-light cycle (lights on at 8am). Mice had access to water and food ad libitum. Wood sticks, cotton and igloo were provided for environmental enrichment.

2.2. Drugs

Clozapine *N*-Oxyde (CNO) was purchased from Enzo Life (France), the GluN2A NMDA antagonist (PEAQX), the GluN2B NMDA antagonist (Ro 25 6981) and the DA D1 antagonist (SCH 23390) from Tocris Cookson (UK), and Xylazine/Ketamine from Centravet (France). All drugs for *in vivo* administration were diluted in saline (0.9% NaCl) and administered intraperitoneally. Drugs (salt) were injected at the following doses: CNO (1 mg/kg), PEAQX (10 mg/kg), Ro 25 6981 (10 mg/kg), SCH 23390 (0.1 mg/kg) and Xylazine/Ketamine (10 mg/kg and 150 mg/kg, respectively). Saline was administered at 10 ml/kg.

2.3. Stereotaxic injections

Stereotaxic injections were performed using a stereotaxic frame (Kopf Instruments) under general anesthesia with xylazine/ketamine (10 and 150 mg/kg respectively), as previously performed (Fernandez

et al., 2018). Surgeries were performed on 5-week old mice, therefore anatomical coordinates and maps were adjusted from Paxinos (Paxinos and Franklin, 2012). The injection rate was set at 100 nL/min. For specific manipulation of paraventricular thalamic (PVT) neurons to NAc glutamatergic projections, wild-type mice were injected bilaterally with CAV-2-CRE (Plateforme de Vectorologie de Montpellier; 400 nL/site; $2.5 \times 10e12$ pp/mL) in the NAc core (AP: + 1.2 mm, ML: ± 0.65 mm, DV: 4.4 mm from Bregma), and with AAV8-hSyn-DIO-hM4D-mCherry (400 nL; AddGene, USA; $7 \times 10e12$ pp/mL) in the PVT (AP: 1.2 mm, ML: 0 mm, DV: 3.25 mm from Bregma). Animals received carprofen in their drinking for 1 week following surgery. They were then given a 2 weeks' recovery period to allow sufficient viral expression and fully recover from surgery.

2.4. Social defeat stress

The social defeat paradigm in mice was used to induce depressive-like symptoms (Krishnan et al., 2007). It was performed as previously published (Barik et al., 2013). Briefly, wild-type mice were subjected to either a single session of defeat (acute stress group) or a session of defeat repeated every day for 10 consecutive days (chronic stress group). The session(s) of social defeat consisted in 5 min exposition to a former CD1 breeder male mouse. Under chronic stress conditions, a new CD1 was used for the social defeat every day. Directly following the social defeat, mice were housed two per cage separated with a semi-permeable barrier allowing sensory, but not physical, contacts. Control mice (naive group) were not confronted with a dominant male but lived in similar housing conditions, i. e. two per cage separated by a semi-permeable barrier. Mapping of pERK1/2-positive cells (see below) was performed on mice susceptible to stress, i.e. exhibiting social aversion (Krishnan et al., 2007). For pharmacological and pharmacogenetic manipulations all drugs (i.e. CNO, PEAQX, Ro 25 6981 and SCH 23390) were administered 30 min before the social defeat episode. Vehicle (saline) was administered accordingly.

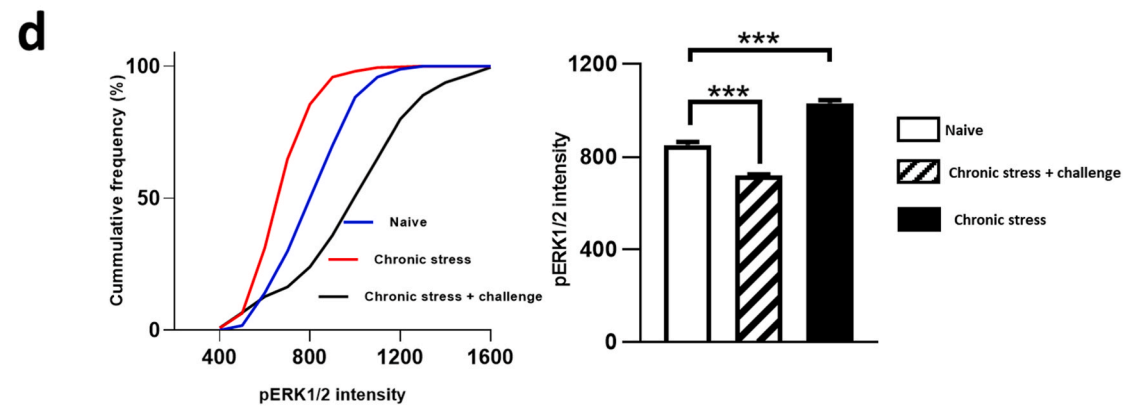
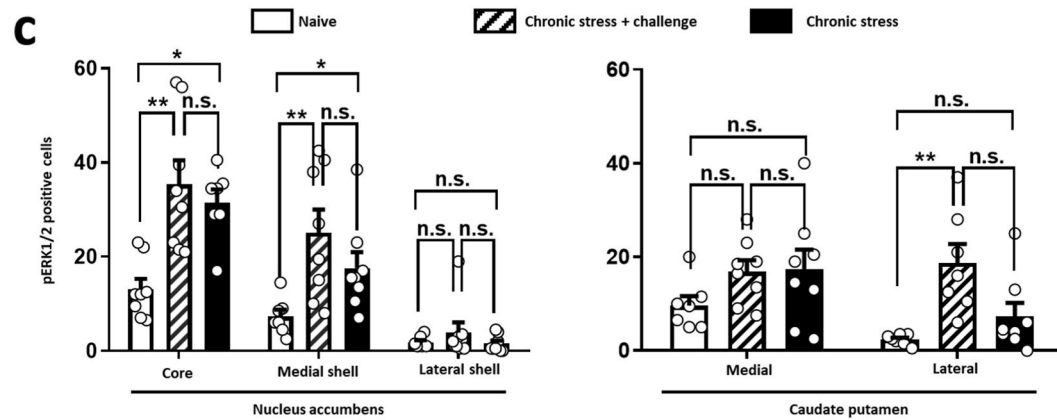
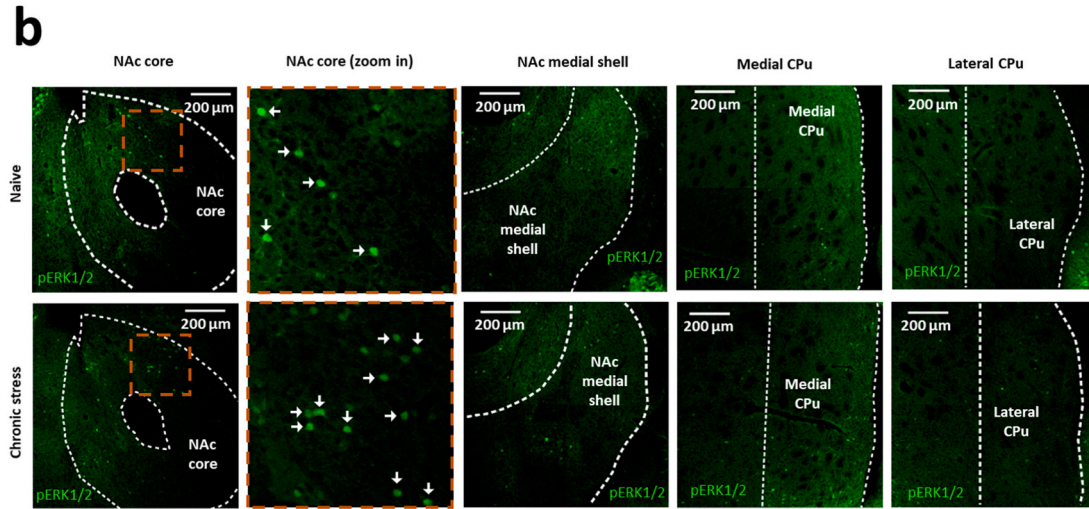
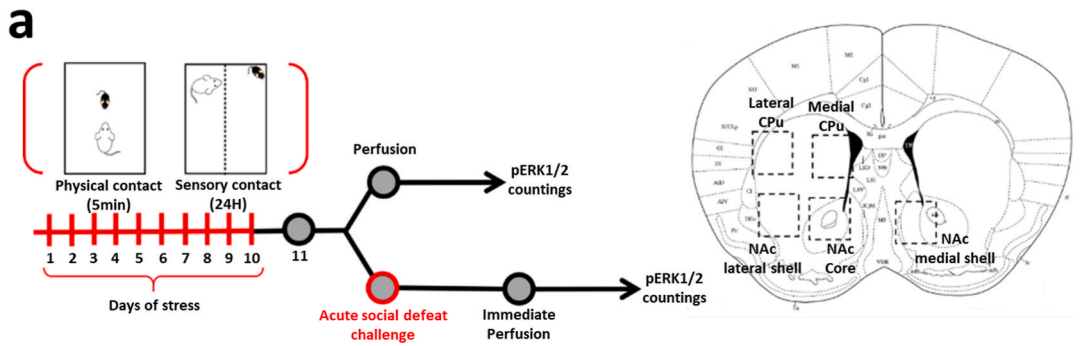
For the acute stress condition, mice were euthanized (see below) either 10 min (acute stress) or 24 h (24 h post-acute stress) following the single defeat exposure. For the chronic stress condition, mice were stressed for 10 consecutive days. Then, on day 11 mice were either sacrificed (chronic stress group) or received an additional defeat session and sacrificed 10 min after (chronic stress + challenge). All experiments were conducted between 1pm and 4pm of the light cycle.

2.5. Immuno-histofluorescence and pERK1/2 mapping

Mice were deeply anaesthetized with xylazine/ketamine as described above and transcardially perfused with cold phosphate buffer (PB: 0.1 M, $\text{Na}_2\text{HPO}_4/\text{NaH}_2\text{PO}_4$, pH 7.4), followed by 4% paraformaldehyde (PFA) in cold PB 0.1 M. Brains were post-fixed overnight in 4% PFA-PB. Free-floating vibratome striatal coronal sections (30 μm) were obtained, and correct viral injections were confirmed for each animal when appropriate.

To identify pERK1/2-positive neurons, sections were incubated (30 min) in PBS-BT (phosphate-buffered saline (PBS), 0.5% bovine serum albumin (BSA), 0.1% Triton X-100 (T)) with 10% normal goat serum (NGS). Sections were then incubated (4 °C) in PBS-BT, 1% NGS, with rabbit anti-pERK1/2 (1/500; Cell signalling #4370 S) overnight. Sections were then rinsed (30 min) in PBS at room temperature and incubated (2 h) with goat anti-rabbit Alexa 488 secondary antibody (1:1000, A32733 Invitrogen) in PBS-BT, 1% NGS. Sections were finally rinsed (30 min) with PBS and incubated 5 min with DAPI in PB before mounting with Mowiol at 10%.

Counting of pERK1/2-positive neurons were performed on the following regions of interest: nucleus accumbens core (NAc Core), NAc medial shell, NAc lateral shell, medial caudate putamen (CPu) and lateral CPu at a defined antero-posterior position (AP: + 1.2 mm). Images were acquired with an Olympus FV10 confocal microscope and a



(caption on next page)

Fig. 1. Chronic social stress produces distinct pattern of pERK1/2 induction in striatal and accumbal subregions. (a) Mice were submitted to a 10-day social defeat protocol, and on day 11th were sacrificed with or without an additional stress challenge. Number of pERK1/2+ neurons were quantified in five subregions. (b) Representative images showing ERK1/2 activation in striatal and accumbal regions after chronic stress. Arrowheads point pERK1/2+ neurons. (c) The number of pERK1/2+ neurons was significantly increased after chronic stress in the core and medial shell of the nucleus accumbens. In the caudate putamen only the lateral region responded with significantly to chronic stress with a challenge. (d) The cumulative frequency distribution of pERK1/2 fluorescence intensity in counted cells from naive, chronic stress and chronic stress + challenge groups (left panel). On the right panel, the same data is plotted as bar graph depicting pERK1/2 intensity. * $P < .05$, ** $P < .01$, *** $P < .01$ Kruskal-Wallis test followed by Dunn's comparisons. Data are expressed as mean \pm SEM. (NAc core: $H(2) = 11.95$, **; NAc medial shell: $H(2) = 10.36$, **; NAc lateral shell: $H(2) = 1.246$, $P = .5364$; Medial caudate putamen: $H(2) = 3.307$, $P = .1914$; Lateral caudate putamen: $H(2) = 12.32$, ***). Number of mice per group 7–8.

stitching of the images was done with the microscope-associated software. Viral injection site images were acquired with an epifluorescent microscope (Axioplan2 Carl Zeiss) and stitched with Adobe photoshop CC 2018 Photomerge option. A visual threshold was set by the experimenter and maintained fixed for all images. The counting was manually done using ImageJ by a blind experimenter. The number of cells labelled for pERK1/2 was averaged over two brain slices per mouse.

2.6. Data analyses

Data are presented as means \pm SEM and were analyzed using GraphPad Prism 6. Following a D'Agostino-Pearson's test, determining the normality of the distributions, statistical analyses were carried out using one-way (Figs. 1 and 2) or two-way analysis of variance (Figs. 3–5) followed by a post hoc Sidak's or Dunn's multi-comparison test. Statistical significance was set at $P < 0.05$.

3. Results

3.1. Chronic social stress produces distinct pattern of pERK1/2 induction in striatal and accumbal subregions

Long exposure to social stress produces pronounced deficits in motivation and reward-learning, two functions associated with the striatum. We first evaluated the impact of social stress in mice on pERK1/2 pattern in this region. Considering that the caudate putamen (CPu) and NAc are large areas in which different subregions are largely associated with different anatomo-functional organizations, we focused our analyses on the NAc core, medial and lateral shell, as well as the lateral and medial CPu. Because protracted stress exposure can trigger enduring adaptations, and condition reactivity to future aversive stimuli, stressed mice were stressed for.

10 consecutive days and then divided into two groups. On day 11 mice were either sacrificed (chronic stress group) to evaluate lasting effects, or received an additional defeat session and sacrificed 10 min after (chronic stress + challenge) to test for potential exacerbation of pERK1/2 induction (Fig. 1a, left panel). These groups were compared to naive mice that were not exposed to dominant males and therefore not socially defeated, and pERK1/2-positive cells were quantified in different subregions of the striatum (Fig. 1a, right panel). Representative pictograms show that chronic social stress differently increased the number of pERK1/2-positive neurons in the CPu and NAc (Fig. 1b). Specifically, marked and significant increases in pERK1/2-positive neurons were observed after chronic stress in the NAc core and medial shell, but neither in the NAc lateral shell nor in any subdivisions of the CPu (Fig. 1c). In the NAc core and medial shell, re-exposure to an acute stress challenge failed to further increase pERK1/2 positive neurons, suggesting a putative ceiling effect by chronic stress. Conversely, the lateral CPu was the only subregion analyzed that responded to chronic stress plus an acute stress challenge, but not to chronic stress per se (Fig. 1c). To address the possibility of a ceiling effect, we quantified the fluorescence intensity in each of the pERK1/2-positive cells included in Fig. 1c using. We plotted the data as a frequency distribution, and as mean intensity for cells counted in the three experimental groups (Fig. 1d). We found higher intensity in the chronic stress + challenge, suggesting that an extra defeat episode further increases pERK1/2

independently of changes in numbers of pERK1/2-positive cells. This first set of data already demonstrates the complex outcomes of chronic stress exposure on pERK1/2 patterns.

3.2. Acute social stress is sufficient to elicit ERK1/2 phosphorylation

We next tested whether an acute exposure to social stress was sufficient to elicit pERK1/2 induction. Mice were subjected to an acute social stress and killed immediately after the stress episode, or 24 h later to test for potential sustained pERK1/2 induction (Fig. 2a). These groups were compared to naive non-stressed mice. As before, representative pictograms show that acute stress has differential impact on pERK1/2 induction (Fig. 2b). Robust and significant increases were only observed in the NAc core and medial shell (Fig. 2c). No significant increase in pERK1/2-positive neurons was observed in the other subregions examined (Fig. 2c). The ability of an acute episode of social defeat to induce pERK1/2 is transient as when analyses were carried out 24 h post-stress exposure, numbers of pERK1/2-positive neurons did not differ from that of naive mice.

3.3. Dopamine D1 receptors are required for acute stress-induced ERK1/2 phosphorylation

So far, our data indicate that the NAc core and medial shell are the most sensitive subregions to social stress exposure. These parts of the NAc receive dense innervation from DA neurons located in the ventral tegmental area. In the case of addictive substances, activation of DA type 1 receptor (D1R) is key to affect intracellular signalling cascades. Hence, we tested whether a similar mechanism of action could be shared by social stress exposure. Animals were treated with either saline or the DA D1R antagonist SCH23390, and 30min after being subjected to an acute social stress. The dose of SCH23390 was selected based on previous published protocols for *in vivo* antagonism (Valjent et al., 2000). Animals were killed rapidly after the stress (Fig. 3a). As previously reported (Valjent et al., 2000), treatment with SCH23390 significantly decreased the number of pERK1/2-positive neurons in naive mice, indicative of a tonic tone of DA release that maintains basal phosphorylation of ERK1/2 (Fig. 3b and c). Nevertheless, stress failed to increase numbers of pERK1/2 positive neurons (Fig. 3b and c).

3.4. NMDA receptor subtypes mediate ERK1/2 activation after social stress

Released DA filters and selects sets of excitatory glutamatergic inputs to MSNs. Glutamate signalling involves binding to AMPA and NMDA receptors. Because activation of the latter by addictive rewards has been shown to induce strong ERK1/2 activation, we tested whether stress impact on pERK1/2 was mediated by NMDA receptors. Specifically, we used two selective antagonists: PEAQX, a selective antagonist for NMDA receptors containing the GluN2A subunit, and RO256981, a selective antagonist for NMDA receptors containing the GluN2B subunit. The doses of each drug for *in vivo* antagonism were selected based on previous reports (Bortolato et al., 2012; Kiselycznyk et al., 2015). Mice received an injection of saline, PEAQX or RO256981, and 30min after were submitted to an acute social stress and rapidly killed (Fig. 4a). In naive conditions, NMDA antagonists did not significantly alter the

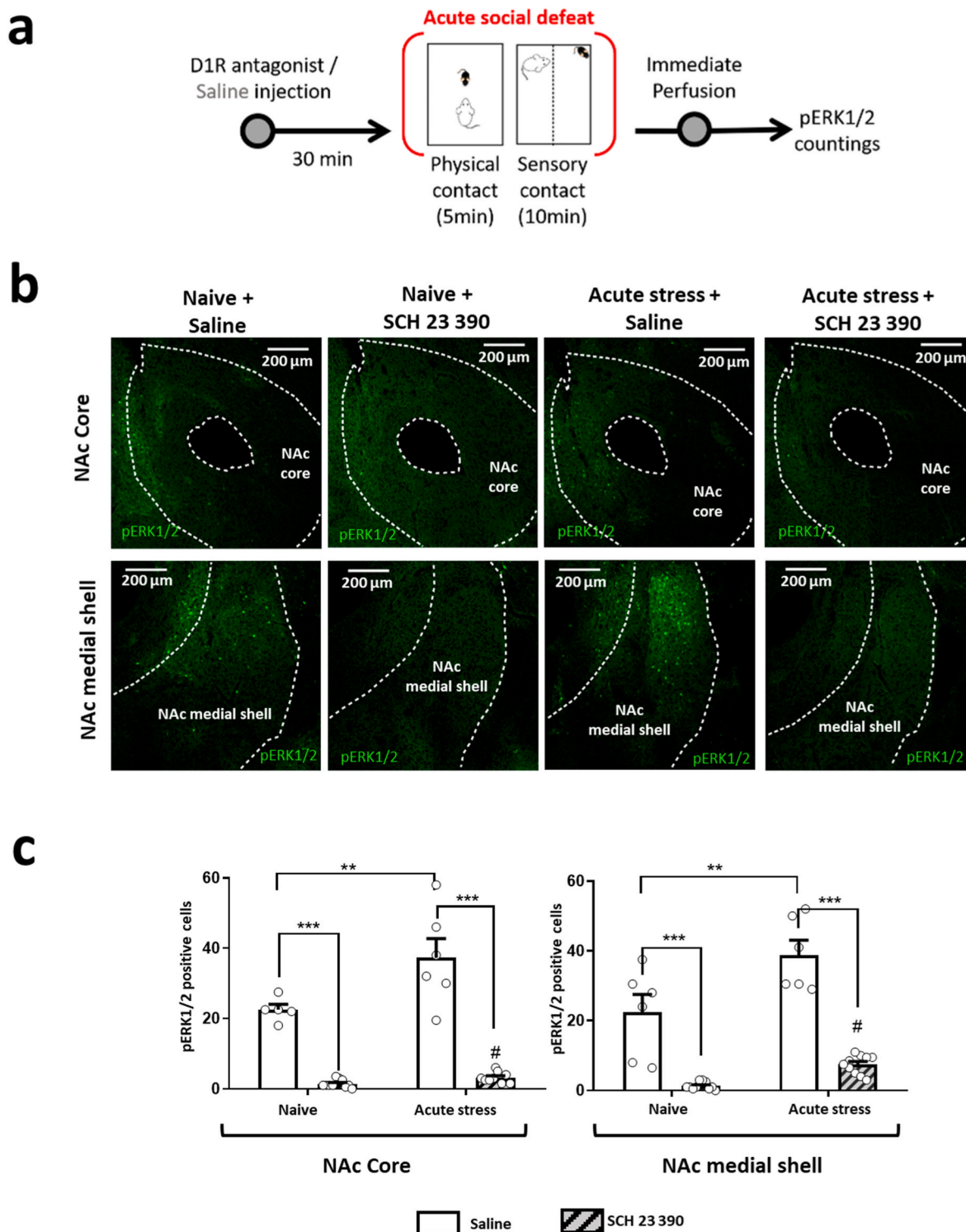
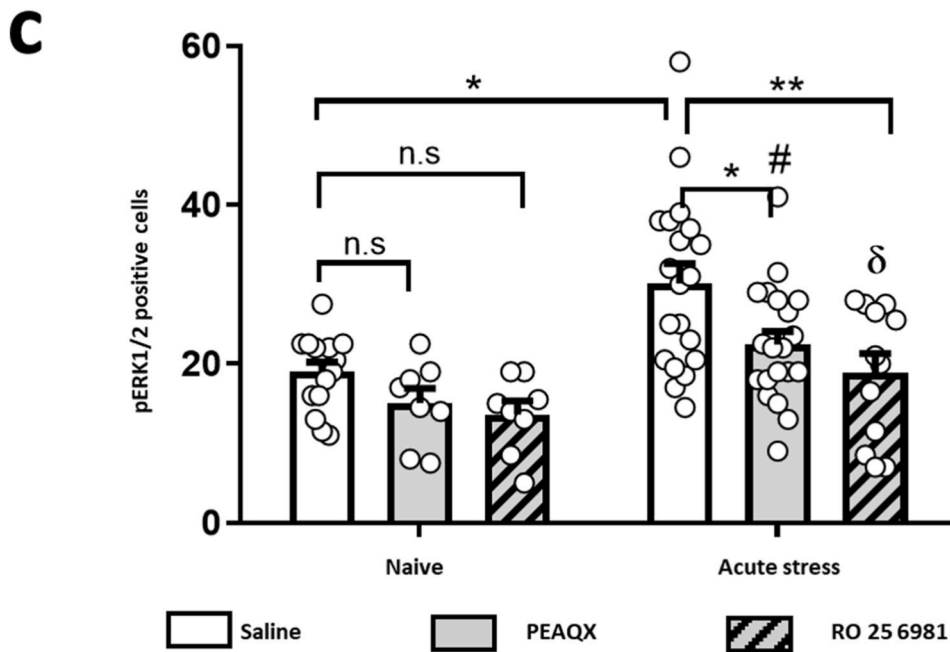
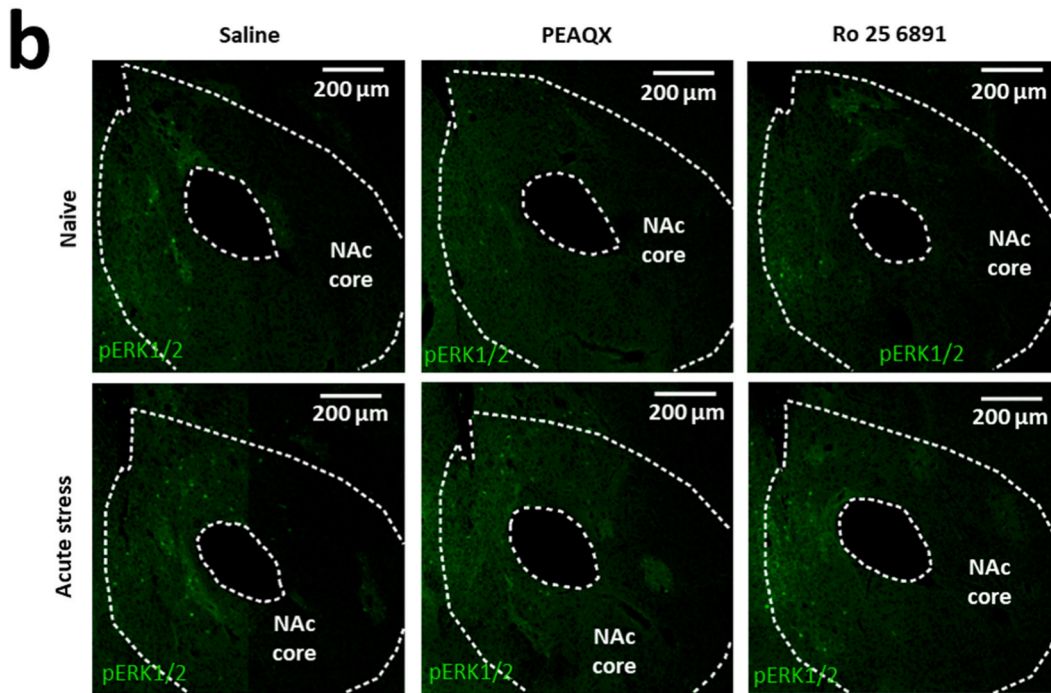
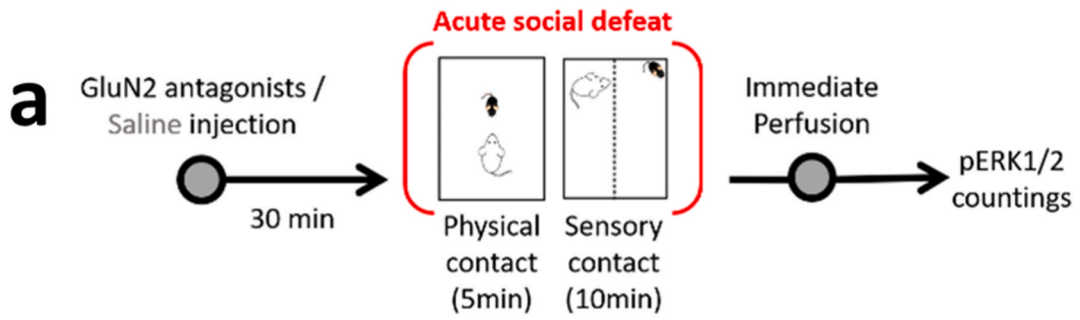


Fig. 3. Dopamine type 1 receptors contribute to stress-induced ERK1/2 activation. (a) Mice were injected ip with either saline or the D1R antagonist SCH23390 (0.1 mg/kg), and 30 min after received a single defeat stress session. Naive mice only received ip injections without stress exposure. (b) Representative images showing the blockade of stress-induced pERK1/2+ increase by D1R antagonism. (c) Acute defeat was sufficient to increase the number of pERK1/2+ neurons in the both the core (left) and medial shell (right) of the nucleus accumbens. Pre-stress treatment with the D1R antagonist SCH23390 completely abolished this effect in both regions. $^{***}P < .01$, $^{***}P < .001$ two-way ANOVA followed by Sidak's comparisons. Data are expressed as mean \pm SEM. (NAc core: interaction $F(1, 26) = 7.744$, ** ; NAc medial shell: interaction $F(1, 28) = 3.980$, $P = 0558$; stress factor $F(1, 28) = 18.96$, *** ; treatment factor $F(1, 28) = 102.9$, ***). #n. s. from naive SCH23390 in NAc core ($P = .99$) or in NAc medial shell ($P = .33$). Number of mice per group 6–10.



(caption on next page)

Fig. 4. Glutamate NMDA receptor subtypes mediate ERK1/2 activation after social stress. (a) Mice were injected ip with either saline, the NMDA-GluN2A antagonist PEAQX (10 mg/kg) or the NMDA-GluN2B antagonist Ro256981 (10 mg/kg), and 30 min after received a single defeat stress session. Naive mice only received ip injections. (b) Representative images showing the blockade of stress-induced pERK1/2+ increase by NMDA antagonism. (c) Acute defeat was sufficient to increase the number of pERK1/2+ neurons in the nucleus accumbens core. Pre-stress treatment with Ro256981 and PEAQX blocked this effect. * $P < .05$, ** $P < .01$, *** $P < .001$ two-way ANOVA followed by Sidak's comparisons. Data are expressed as mean \pm SEM. Interaction F (2, 77) = 0.9505, $P = .3911$; stress factor F (1, 77) = 18.24, ***; treatment factor F (2, 77) = 7.908, ***; #n. s. from naive PEAQX ($P = .3453$); δ n. s. from naive Ro256981 ($P = .9100$). Number of mice per group 8–19.

PVT, we next used a pharmacogenetic approach (DREADD system) to specifically silence PVT neurons projecting to the NAc. To achieve projection-specific expression of inhibitory DREADD, mice were injected in the NAc with a canine adenovirus type 2 (CAV-2) with retrograde capacity, to express the Cre recombinase in regions projecting to this structure. We also injected a cre-dependent adeno-associated virus (AAV) in the PVT to express the inhibitory DREADD (hm4D) (Fig. 5a). We achieved a transduction efficiency of 353.6 ± 16.2 cells/mm² within the PVT. This intersectional strategy allows us to selectively and timely silence PVT to NAc projections. Representative pictograms show the expression of hm4D fused with mCherry in cell bodies of the PVT, and dense presence of innervating axons into the NAc (Fig. 5a). Mice were given saline or CNO (1 mg/kg) injections 30 min prior social stress exposure (Fig. 5b). We observed that CNO treatment did not modify the number of pERK1/2-positive neurons in naive conditions (Fig. 5c and d). However, the increase in pERK1/2-positive neurons by stress was significantly reduced by silencing PVT to NAc projections (Fig. 5c and d). This result suggests that paraventricular glutamatergic inputs have a specific role in activating NAc MSNs in response to social stress.

4. Discussion

In this manuscript we described how stress, specifically social stress by conspecifics, differently activates various subregions of the CPU and NAc using pERK1/2 expression as a marker of neuronal plasticity. We show that exposure to chronic social stress produces lasting activation of the NAc core and medial shell, while the lateral shell was not affected. In the CPU, only the lateral part show susceptibility to social stress. Molecular mechanisms of acute stress reactivity in striatal subregions was dissected using pharmacological tools revealing a prominent role for DA D1R and NMDA-GluN2B and NMDA-GluN2A glutamate receptors. Our results suggest that both receptor populations are important mediators of stress, but DA D1R also participate in maintaining basal levels of pERK1/2 expression. Finally, we uncover a glutamatergic thalamic input to the nucleus accumbens, which impinges on striatal cell substrates promoting pERK1/2 expression in response to stress. Overall, our study suggest that the striatum show region-specific reactivity to social stress, mediated by glutamatergic and dopaminergic signalling.

Stress has been acknowledged as one of the main risk factor for the development of psychiatric disorders (Kloet et al., 2005). Because social interactions govern our everyday lives, the study of social stress and its effects on brain function is of great importance to understand the pathophysiology of these disorders (McEwen, 2012). Here, we used a murine model of social stress, based on inter-male aggressivity that manifests most strongly on first encounters. Long term exposure to social stress has been shown to develop lasting behavioural and biochemical abnormalities in mice, including deficits in natural rewards and increased responses to drug reward (Krishnan et al., 2007; Der-Avakian et al., 2014; Morel et al., 2018; Newman et al., 2018). The striatum is important for reward processing and value-based decision-making, and therefore a primary target to understand associations between stress exposure and reward misprocessing. Functionally, the striatum is often divided into subregions thought to participate in different aspects of reward processing. The CPU is involved in goal-directed behaviours that rely on stimulus-outcome associations, and the formation of habitual actions (Sousa and Almeida, 2012). The NAc is a limbic-motor interface, important for reinforcement and reward-motor learning (Morrison et al., 2017). Our first observation was that these striatal subregions exhibit

different stress reactivity. In the NAc, a single social encounter triggered strong but transient activation of the core and medial shell regions, which is likely to initiate plastic changes that will favour maladaptive behaviours. In turn, the CPU showed high cellular resilience to single stress exposure. This agrees with a recent study that showed that pERK1/2 is not induced in the caudal part of the striatum (i.e. tail of the striatum) by a large variety of aversive stimuli that trigger innate avoidance (Gangarossa et al., 2019).

In contrast to an acute social stress episode, chronic exposure to social stress produced a lasting activation of ERK1/2, which has also been reported following Western blot analyses on NAc punches in mice (Krishnan et al., 2007). Although not in the striatum, a recent study in depressed humans revealed alterations in pERK1/2 levels in the ventromedial prefrontal cortex (Labonté et al., 2017), highlighting the potential translational value of carefully examining pERK1/2 dynamics. Chronic stress prevented further enhancement of pERK1/2 induction in most striatal subregions examined when a new stress was encountered suggesting that repeated stress exposure could overcome homeostatic mechanisms, leading to sustained activation of cell substrates. The lateral CPU was the only subregion where a significant pERK1/2 induction was observed in chronic stressed mice challenged with a new intruder. This region has been heavily linked with habit formation, therefore this cell activation might be due to the repeated manipulation and the automation of motor responses in defensive behaviours (Sousa and Almeida, 2012).

The ERK1/2 signalling pathway plays a crucial role in regulating diverse neuronal processes in response to external stimuli. In particular, its expression in the striatum has been associated with the effects of most drugs of abuse including psychostimulants, opiates and nicotine (Valjent et al., 2004; Pascoli et al., 2014). Blocking ERK1/2 phosphorylation or inhibiting its binding to its downstream molecular targets can prevent many behavioural consequences of drugs of abuse including their rewarding and locomotor sensitizing properties as well as incubation of craving (Valjent et al., 2000; Lu et al., 2005; Besnard et al., 2011). In turn, less is known about the involvement of the ERK1/2 cascade on stress adaptations. This is of high relevance for psychiatric disorders since stress exposure is a major risk factor for drug addiction (Sinha, 2008). Indeed, we and others have proposed that stress mal-adaptations may share some molecular and circuits mechanisms with those seen in drug addiction and depression, specifically on brain reward circuits (Russo and Nestler, 2013; Morel et al., 2018). We show here that social stress exposure strongly activates striatal ERK1/2 in a manner that resembles drugs of abuse. This could explain why stress exposure is a precipitating factor in drug compulsion and relapse (Sinha, 2008), but also in brain disorders where reward processing is affected such as depression (Russo and Nestler, 2013). Understanding the molecular mechanisms mediating ERK1/2 activation is thus of importance for the development of potential novel therapies.

The ventral striatum is under strict neuronal control from midbrain dopamine inputs from the ventral tegmental area, but also from cortical, thalamic and amygdalar excitatory inputs (Hunnicutt et al., 2016). We therefore studied the contribution of these neurotransmitter systems to stress activation of ERK1/2 by using specific antagonists. Our results showed that both DA and Glu receptor types participate in stress-induced striatal pERK1/2. This is in accordance with previous data showing that ERK1/2 activation by drugs of abuse depends on the coincident detection of both dopaminergic and glutamatergic signals, with a prominent role of D1R (Bertran-Gonzalez et al., 2008; Cahill

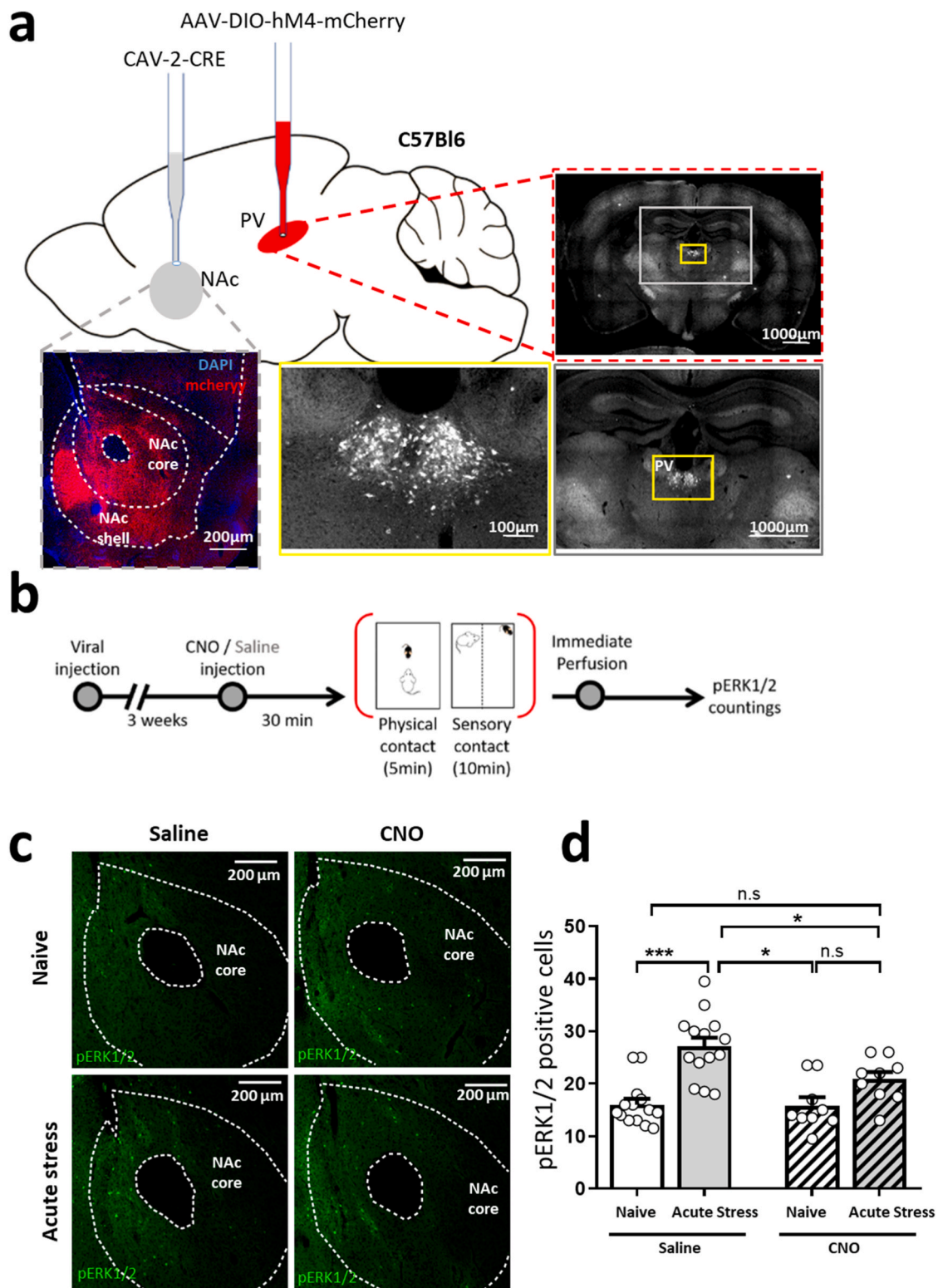


Fig. 5. Thalamic inputs mediate stress-induced activation of ERK1/2 in the NAc. (a) Intersectional viral strategy to express the inhibitory DREADD hM4 in PVT neurons projecting to the NAc. A retrograde CAV-2-CRE is injected in the NAc and an AAV is injected in the PVT to express hM4-mCherry in a CRE-dependent manner. Images show the expression of hM4-mCherry neurons correctly targeted in the PVT, and the presence of hM4-mCherry fibers in the NAc. (b) Mice were injected ip with either saline or the hM4 agonist CNO (1 mg/kg), 30 min before submitted to a single defeat stress, and sacrificed immediately after. (c) Representative images showing the blockade of stress-induced pERK1/2+ increase by silencing of the PVT to NAc neuronal pathway. (d) In saline treated mice, acute defeat was sufficient to increase the number of pERK1/2+ neurons in the NAc core an effect significantly blocked by CNO treatment. * $P < .05$, *** $P < .001$ two-way ANOVA followed by Sidak's comparisons. Data are expressed as mean \pm SEM. Interaction $F(1, 42) = 3.998$, $P = .0521$; stress factor $F(1, 42) = 28.01$, ***; treatment factor $F(1, 42) = 4.548$, *). Number of mice per group 9–14.

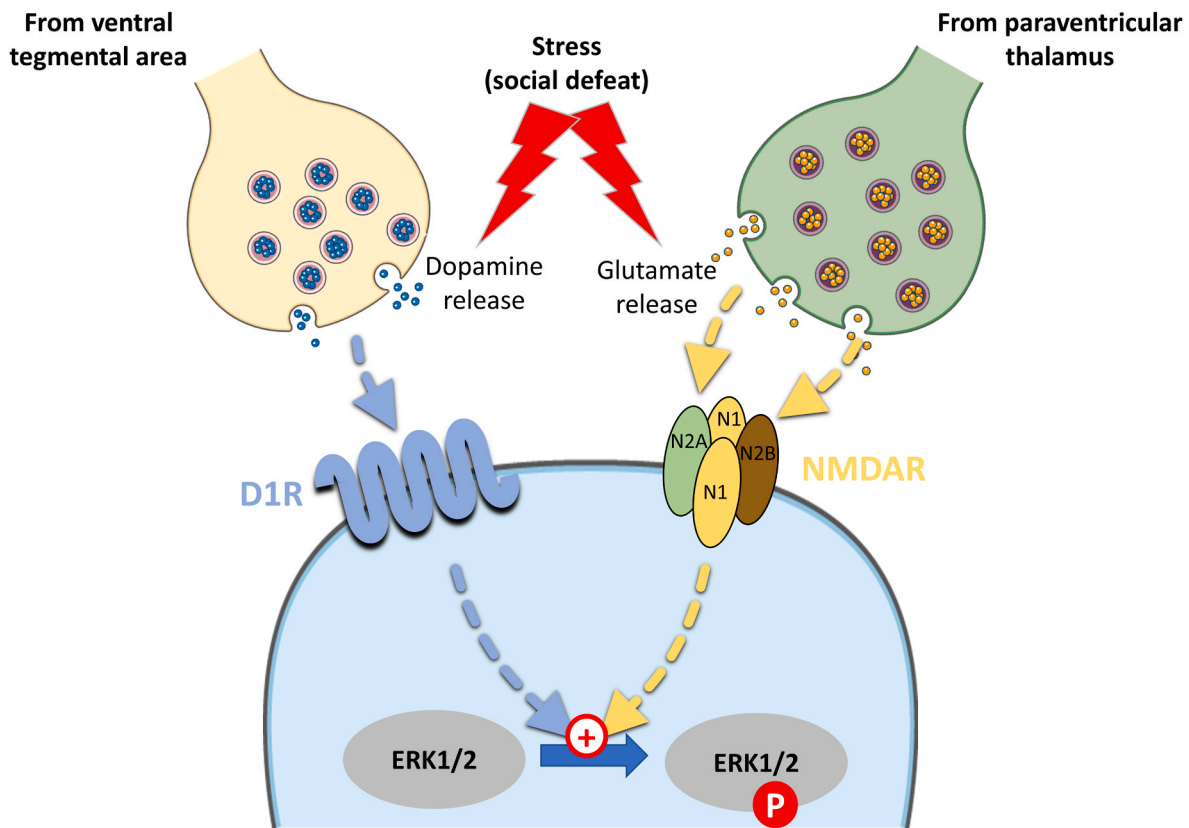


Fig. 6. Schematic model of the impact of social stress on striatal ERK1/2 induction. Social stress by con-specifics produce glutamatergic and dopaminergic release, from the thalamic paraventricular nucleus and the ventral tegmental area respectively. These neurotransmitters activate NMDA and D1 postsynaptic receptors, respectively, and their intracellular signalling pathways lead to phosphorylation of ERK1/2.

et al., 2014b), as described here for stress. Hence, once again pointing a common ground between stress and drugs of abuse. Nevertheless, our results showed that D1R antagonism abolished basal pERK1/2 levels. Hence, the failure of stress to activate ERK1/2 may not be specific to this aversive stimulus but rather reflect a generalized diminished response to any salient event. Conversely, antagonism of specific NMDA subtypes may be more promising targets as they block stress effects without affecting basal levels. Native NMDARs are assemblies composed of two GluN1 subunits and two GluN2 subunits, typically GluN2A and GluN2B (Paoletti et al., 2013). GluN2 subunits define the biophysical and pharmacological properties of the receptor. GluN2B-containing NMDARs display longer decay time constant and carry greater calcium current per unit charge (Cull-Candy and Leszkiewicz, 2004; Sobczyk et al., 2005), thus integrating excitatory post-synaptic synaptic currents across broader time intervals. Importantly, in adulthood the relative abundance of specific subunits is tightly regulated, and deviation from these native states has been associated with a number of physiological and pathological conditions (Paoletti et al., 2013). In the NAc, transient increases of GluN2B-containing NMDA receptors following repeated cocaine administration are important for subsequent long-term potentiation and behavioural abnormalities (Huang et al., 2009; Wolf, 2016). Using selective antagonist, we demonstrated that GluN2B-containing NMDA receptors significantly contribute to the induction of pERK1/2 by stress. Overall, our data shows that both dopamine and glutamate systems are involved in activating MSNs after a stressful experience, and underline the potential use of selective antagonists to prevent stress mal-adaptations that may contribute to psychiatric symptoms.

Which brain inputs contribute to stress-induced pERK activation in the striatum? Dopaminergic inputs to the CPu and NAc arise exclusively from midbrain neurons, and we have shown using microdialysis that an acute social defeat episode triggers a large dopamine transient release in

the NAc (Barik et al., 2013). This is in accordance with our data showing that D1R antagonist prevents stress-induced ERK1/2 phosphorylation. Instead, glutamatergic afferents to the striatum arise from diverse sources, including many regions of the cerebral cortex, thalamus and VTA (Hunnicutt et al.). In rats, neuronal activation has been observed in the medio-dorsal (MD) and the paraventricular thalamic nucleus (PVT) upon social interaction (Ahern et al., 2016). Recent work indicates that the thalamus can as well react to various stressors. Acute social defeat induces c-Fos expression in the MD and the PVT (Lkhagvasuren et al., 2014). The social avoidance acquired after repeated social defeat correlates with changes in thalamic volume (Anacker et al., 2016), and changes in synaptic strength at intralaminar thalamic-accumbens projections have been reported following chronic social stress (Christoffel et al., 2015). In light of these data, we tested whether excitatory PVT projections to the NAc could provide the source of glutamate that contributes to pERK1/2 induction. We used restricted DREADD expression in order to selectively silence this projection before exposure to social stress. This pharmacogenetic intervention was sufficient to block stress-induced ERK1/2 activation, while not affecting its basal levels in naive states. This suggest that the PVT provides an excitatory drive to the NAc carrying aversive information. Therefore, our data strengthen the PVT as a relay nucleus sensitive to stress.

4.1. Conclusions

Our results suggest that social stress exposure promote a prompt influx of both dopamine and glutamate release concluding in independent but eventually converging signalling cascades that promote phosphorylation of ERK1/2 (Fig. 6). We have built our conclusive Fig. 6 on different findings from our lab and others: (i) an acute social defeat episode triggers a significant increase of DA release measured by

microdialysis within the NAc (Barik et al., 2013). This is likely to impact the activity of MSNs directly via DA receptors located on these neurons or indirectly by modulating the release of glutamate release within this region. Of note, D1 DA receptors are not expressed on accumbal glutamatergic terminals (Bamford et al., 2004a); (ii) direct application of glutamate on striatal brain slices induces ERK1/2 phosphorylation in MSNs (Vanhoutte et al., 1999); (iii) in striatal cultures, stimulation of D1 DA receptors potentiates glutamate-induced pERK1/2 through activation of glutamate NMDA receptors in MSNs (Pascoli et al., 2011; Cahill et al., 2014a). Nevertheless, we cannot exclude that the systemic injections of DA and glutamate antagonists impact pERK1/2 induction by stress in the NAc via a polysynaptic pathway.

It remains to be determined whether chronic stress impact relies on transcriptional upregulation of ERK1/2, or post-translational modification, the two hypotheses not being mutually exclusive. The increased number of pERK1/2-positive cells following acute stress is likely to reflect a post-translational process due to short interval between the stimulus and its outcome. Importantly, the key point in ERK1/2 activity relies on its phosphorylation status. Hence, the fact that stress, either acute or chronic, increases its phosphorylation indicates that it should impact downstream targets of ERK1/2 and the launch of plastic changes likely impinging on the homeostasis of the NAc.

These results should be reproduced using female cohorts to evaluate for sex differences. Because social defeat stress is based on intermale aggression, this paradigm could not contemplate for sexual differences. Recent adapted protocols have been established however the basic cellular plasticity mechanisms linking stress to depressive-like behaviors are still missing (Krishnan et al., 2007; Barik et al., 2013). Could the circuit mechanism described here be exploited for the treatment of stress-related disorders? Antagonists to both NMDA and dopamine receptors have been studied, with the main disadvantage being the lack of specificity due to widespread expression of these receptors in the brain. Future refinements on circuit-based therapies such as deep brain stimulation and transcranial magnetic stimulation to achieve projection-specific modulation will surely represent an avenue to target the circuit mechanisms described here.

CRedit authorship contribution statement

Thomas Contesse: Formal analysis, Data curation, performed viral injections, behavioural experiments and histology. performed microscopy. analyzed data. **Loïc Broussot:** performed viral injections, behavioural experiments and histology. **Hugo Fofó:** performed viral injections, behavioural experiments and histology. **Peter Vanhoutte:** provided intellectual and technical inputs. **Sebastian P. Fernandez:** designed the project. wrote the manuscript. **Jacques Barik:** Writing – original draft, designed the project. wrote the manuscript. All authors provided feedback on writing the manuscript.

Declaration of competing interest

The authors declare no conflicts of interest.

Acknowledgments

This work was supported by the CNRS, Université Côte d'Azur, Fondation pour la Recherche Médicale (FRM) DEQ20180339159 to J.B., ANR-18-CE37-0003-02 to J.B and P.V, and the Institut National Du Cancer (INCa) to J.B. L.B. is the recipient of a fourth-year PhD fellowship from the FRM (FDT201904007874).

References

Ahern, M., Goodell, D.J., Adams, J., Bland, S.T., 2016. Brain regional differences in social encounter-induced Fos expression in male and female rats after post-weaning social isolation. *Brain Res.* 1630, 120–133.

- Anacker, C., Scholz, J., O'Donnell, K.J., Allemand-Grand, R., Diorio, J., Bagot, R.C., et al., 2016. Neuroanatomic differences associated with stress susceptibility and resilience. *Biol. Psychiatr.* 79, 840–849.
- Bamford, N.S., Robinson, S., Palmiter, R.D., Joyce, J.A., Moore, C., Meshul, C.K., 2004a. Dopamine modulates release from corticostriatal terminals. *J. Neurosci.* 24, 9541–9552.
- Bamford, N.S., Zhang, H., Schmitz, Y., Wu, N.-P., Cepeda, C., Levine, M.S., et al., 2004b. Heterosynaptic dopamine neurotransmission selects sets of corticostriatal terminals. *Neuron* 42, 653–663.
- Barik, J., Marti, F., Morel, C., Fernandez, S.P., Lanteri, C., Godeheu, G., et al., 2013. Chronic stress triggers social aversion via glucocorticoid receptor in dopaminergic neurons. *Science* 339, 332–335.
- Berti, D.A., Seger, R., 2017. The nuclear translocation of ERK. In: Jimenez, G. (Ed.), *ERK Signaling: Methods and Protocols*. Springer, New York, NY, pp. 175–194.
- Bertran-Gonzalez, J., Bosch, C., Maroteaux, M., Matamales, M., Hervé, D., Valjent, E., et al., 2008. Opposing patterns of signaling activation in dopamine D1 and D2 receptor-expressing striatal neurons in response to cocaine and haloperidol. *J. Neurosci.* 28, 5671–5685.
- Besnard, A., Bouveyron, N., Kappes, V., Pascoli, V., Pagès, C., Heck, N., et al., 2011. Alterations of molecular and behavioral responses to cocaine by selective inhibition of Elk-1 phosphorylation. *J. Neurosci.* 31, 14296–14307.
- Bortolato, M., Godar, S.C., Melis, M., Soggiu, A., Roncada, P., Casu, A., et al., 2012. NMDARs mediate the role of monoamine oxidase A in pathological aggression. *J. Neurosci.* 32, 8574–8582.
- Bromberg-Martin, E.S., Matsumoto, M., Hikosaka, O., 2010. Dopamine in motivational control: rewarding, aversive, and alerting. *Neuron* 68, 815–834.
- Cahill, E., Pascoli, V., Trifilieff, P., Savoldi, D., Kappes, V., Lüscher, C., et al., 2014a. D1R/GluN1 complexes in the striatum integrate dopamine and glutamate signalling to control synaptic plasticity and cocaine-induced responses. *Mol. Psychiatr.* 19, 1295–1304.
- Cahill, E., Salery, M., Vanhoutte, P., Caboche, J., 2014b. Convergence of dopamine and glutamate signaling onto striatal ERK activation in response to drugs of abuse. *Front. Pharmacol.* 4.
- Chaudhury, D., Walsh, J.J., Friedman, A.K., Juarez, B., Ku, S.M., Koo, J.W., et al., 2013. Rapid regulation of depression-related behaviours by control of midbrain dopamine neurons. *Nature* 493, 532–536.
- Christoffel, D.J., Golden, S.A., Walsh, J.J., Guise, K.G., Heshmati, M., Friedman, A.K., et al., 2015. Excitatory transmission at thalamo-striatal synapses mediates susceptibility to social stress. *Nat. Neurosci.* 18, 962–964.
- Cull-Candy, S.G., Leszkiewicz, D.N., 2004. Role of distinct NMDA receptor subtypes at central synapses. *Sci. STKE* (255), re16. <https://doi.org/10.1126/stke.2552004re16>.
- Der-Avakian, A., Mazei-Robison, M.S., Kesby, J.P., Nestler, E.J., Markou, A., 2014. Enduring deficits in brain reward function after chronic social defeat in rats: susceptibility, resilience, and antidepressant response. *Biol. Psychiatr.* 76, 542–549.
- Fernandez, S.P., Broussot, L., Marti, F., Contesse, T., Mouska, X., Soiza-Reilly, M., et al., 2018. Mesopontine cholinergic inputs to midbrain dopamine neurons drive stress-induced depressive-like behaviors. *Nat. Commun.* 9, 4449.
- Gangarossa, G., Castell, L., Castro, L., Tarot, P., Veyrunes, F., Vincent, P., et al., 2019. Contrasting patterns of ERK activation in the tail of the striatum in response to aversive and rewarding signals. *J. Neurochem.* 151, 204–226.
- Girault, J.-A., Valjent, E., Caboche, J., Hervé, D., 2007. ERK2: a logical AND gate critical for drug-induced plasticity? *Curr. Opin. Pharmacol.* 7, 77–85.
- Hsu, D.T., Kirouac, G.J., Zubieta, J.-K., Bhatnagar, S., 2014. Contributions of the paraventricular thalamic nucleus in the regulation of stress, motivation, and mood. *Front. Behav. Neurosci.* 8, 73.
- Huang, Y.H., Lin, Y., Mu, P., Lee, B.R., Brown, T.E., Wayman, G., et al., 2009. In vivo cocaine experience generates silent synapses. *Neuron* 63, 40–47.
- Hunnicutt, B.J., Jongbloets, B.C., Birdsong, W.T., Gertz, K.J., Zhong, H., and Mao, T. A comprehensive excitatory input map of the striatum reveals novel functional organization. *ELife* 5.
- Kiselycznyk, C., Jury, N.J., Halladay, L.R., Nakazawa, K., Mishina, M., Sprengel, R., et al., 2015. NMDA receptor subunits and associated signaling molecules mediating antidepressant-related effects of NMDA-GluN2B antagonism. *Behav. Brain Res.* 287, 89–95.
- Kloet, E.R. de, Joëls, M., Holsboer, F., 2005. Stress and the brain: from adaptation to disease. *Nat. Rev. Neurosci.* 6, 463–475.
- Krishnan, V., Han, M.-H., Graham, D.L., Berton, O., Renthal, W., Russo, S.J., et al., 2007. Molecular adaptations underlying susceptibility and resistance to social defeat in brain reward regions. *Cell* 131, 391–404.
- Labonté, B., Engmann, O., Purushothaman, I., Menard, C., Wang, J., Tan, C., et al., 2017. Sex-specific transcriptional signatures in human depression. *Nat. Med.* 23, 1102–1111.
- Lkhagvasuren, B., Oka, T., Nakamura, Y., Hayashi, H., Sudo, N., Nakamura, K., 2014. Distribution of Fos-immunoreactive cells in rat forebrain and midbrain following social defeat stress and diazepam treatment. *Neuroscience* 272, 34–57.
- Lu, L., Hope, B.T., Dempsey, J., Liu, S.Y., Bossert, J.M., Shaham, Y., 2005. Central amygdala ERK signaling pathway is critical to incubation of cocaine craving. *Nat. Neurosci.* 8, 212–219.
- Marinelli, M., McCutcheon, J.E., 2014. Heterogeneity of dopamine neuron activity across traits and states. *Neuroscience* 282, 176–197.
- McEwen, B.S., 2012. Brain on stress: how the social environment gets under the skin. *Proc. Natl. Acad. Sci. Unit. States Am.* 109, 17180–17185.
- Morel, C., Fernandez, S.P., Pantouli, F., Meyer, F.J., Marti, F., Tolu, S., et al., 2018. Nicotinic receptors mediate stress-nicotine detrimental interplay via dopamine cells' activity. *Mol. Psychiatr.* 23 (7), 1597–1605. <https://doi.org/10.1038/mp.2017.145>.

- Morrison, S.E., McGinty, V.B., Hoffmann, J. du, Nicola, S.M., 2017. Limbic-motor integration by neural excitations and inhibitions in the nucleus accumbens. *J. Neurophysiol.* 118, 2549–2567.
- Newman, E.L., Leonard, M.Z., Arena, D.T., Almeida, R.M.M. de, Miczek, K.A., 2018. Social defeat stress and escalation of cocaine and alcohol consumption: focus on CRF. *Neurobiology of Stress* 9, 151–165.
- Paoletti, P., Bellone, C., Zhou, Q., 2013. NMDA receptor subunit diversity: impact on receptor properties, synaptic plasticity and disease. *Nat. Rev. Neurosci.* 14, 383–400.
- Pascoli, V., Besnard, A., Hervé, D., Pagès, C., Heck, N., Girault, J.-A., et al., 2011. Cyclic adenosine monophosphate-independent tyrosine phosphorylation of NR2B mediates cocaine-induced extracellular signal-regulated kinase activation. *Biol. Psychiatr.* 69, 218–227.
- Pascoli, V., Cahill, E., Bellivier, F., Caboche, J., Vanhoutte, P., 2014. Extracellular signal-regulated protein kinases 1 and 2 activation by addictive drugs: a signal toward pathological adaptation. *Biol. Psychiatr.* 76, 917–926.
- Paxinos, George, Franklin, Keith, 2012. *Paxinos and Franklin's the Mouse Brain in Stereotaxic Coordinates* 4th Edition. Academic press.
- Russo, S.J., Nestler, E.J., 2013. The brain reward circuitry in mood disorders. *Nat. Rev. Neurosci.* 14.
- Salery, M., Trifilieff, P., Caboche, J., Vanhoutte, P., 2020. From signaling molecules to circuits and behaviors: cell-type-specific adaptations to psychostimulant exposure in the striatum. *Biol. Psychiatr.* 87, 944–953.
- Sapolsky, R.M., 2005. The influence of social hierarchy on primate health. *Science* 308, 648–652.
- Schultz, W., 2015. Neuronal reward and decision signals: from theories to data. *Physiol. Rev.* 95, 853–951.
- Sinha, R., 2008. Chronic stress, drug use, and vulnerability to addiction. *Ann. N. Y. Acad. Sci.* 1141, 105–130.
- Sobczyk, A., Scheuss, V., Svoboda, K., 2005. NMDA receptor subunit-dependent [Ca²⁺] signaling in individual hippocampal dendritic spines. *J. Neurosci.* 25, 6037–6046.
- Sousa, N., Almeida, O.F.X., 2012. Disconnection and reconnection: the morphological basis of (mal)adaptation to stress. *Trends Neurosci.* 35, 742–751.
- Tidey, J.W., Miczek, K.A., 1996. Social defeat stress selectively alters mesocorticolimbic dopamine release: an in vivo microdialysis study. *Brain Res.* 721, 140–149.
- Ungless, M.A., Magill, P.J., Bolam, J.P., 2004. Uniform inhibition of dopamine neurons in the ventral tegmental area by aversive stimuli. *Science* 303, 2040–2042.
- Valjent, E., Corvol, J.-C., Pagès, C., Besson, M.-J., Maldonado, R., Caboche, J., 2000. Involvement of the extracellular signal-regulated kinase cascade for cocaine-rewarding properties. *J. Neurosci.* 20, 8701–8709.
- Valjent, E., Pagès, C., Hervé, D., Girault, J.-A., Caboche, J., 2004. Addictive and non-addictive drugs induce distinct and specific patterns of ERK activation in mouse brain. *Eur. J. Neurosci.* 19, 1826–1836.
- Vanhoutte, P., Barnier, J.-V., Guibert, B., Pagès, C., Besson, M.-J., Hipskind, R.A., et al., 1999. Glutamate induces phosphorylation of elk-1 and CREB, along with c-fos activation, via an extracellular signal-regulated kinase-dependent pathway in brain slices. *Mol. Cell Biol.* 19, 136–146.
- Wolf, M.E., 2016. Synaptic mechanisms underlying persistent cocaine craving. *Nat. Rev. Neurosci.* 17, 351–365.

Second contribution

Mesopontine cholinergic inputs to midbrain dopamine neurons drive stress-induced depressive-like behaviors

Fernandez S.P, Broussot L, Marti F, Contesse T, Mouska X, Soiza-Reilly M, Marie H, Faure P, Barik J

Nature Communications volume 9, Article number : 4449 (2018)

Summary

In the following study, we determined the role of the LDTg in a depression-like mouse model. We subjected mice chronic social stress paradigm to induce a depression-like phenotype and used chemogenetic tools to selectively modulate the LDTg subpopulation during stress. We found silencing of the LDTg cholinergic neurons prevented long-lasting neuronal adaptations in VTA DA neurons and blocked the apparition of stress-induced social aversion. Furthermore, we show that activation of LDTg type 1 receptor to CRF promote the LDTg cholinergic neurons-mediated activation of VTA DA found in response to chronic stress.

Contribution

I contributed in this project in the realization of in vivo behavioral stress protocol and in the acquisition of microscopy data.

ARTICLE

DOI: 10.1038/s41467-018-06809-7

OPEN

Mesopontine cholinergic inputs to midbrain dopamine neurons drive stress-induced depressive-like behaviors

Sebastian P. Fernandez^{1,2}, Loïc Brousot^{1,2}, Fabio Marti ^{3,4}, Thomas Contesse^{1,2}, Xavier Mouska^{1,2}, Mariano Soiza-Reilly ^{3,5}, H  l  ne Marie^{1,2}, Philippe Faure ^{3,4} & Jacques Barik^{1,2}

Stressful life events are primary environmental factors that markedly contribute to depression by triggering brain cellular maladaptations. Dysregulation of ventral tegmental area (VTA) dopamine neurons has been causally linked to the appearance of social withdrawal and anhedonia, two classical manifestations of depression. However, the relevant inputs that shape these dopamine signals remain largely unknown. We demonstrate that chronic social defeat (CSD) stress, a preclinical paradigm of depression, causes marked hyperactivity of laterodorsal tegmentum (LDTg) excitatory neurons that project to the VTA. Selective chemogenetic-mediated inhibition of cholinergic LDTg neurons prevent CSD-induced VTA DA neurons dysregulation and depressive-like behaviors. Pro-depressant outcomes are replicated by pairing activation of LDTg cholinergic terminals in the VTA with a moderate stress. Prevention of CSD outcomes are recapitulated by blocking corticotropin-releasing factor receptor 1 within the LDTg. These data uncover a neuro-circuitry of depressive-like disorders and demonstrate that stress, via a neuroendocrine signal, profoundly dysregulates the LDTg.

¹Universit   C  te d'Azur, Nice 06560, France. ²Institut de Pharmacologie Mol  culaire & Cellulaire, CNRS, UMR7275 Valbonne, France. ³Universit   Pierre et Marie Curie, Paris 75005, France. ⁴Neurosciences Paris Seine, INSERM U1130, CNRS, UMR 8246 Paris, France. ⁵Institut du Fer    Moulin, INSERM, UMRS-839 Paris, France. Correspondence and requests for materials should be addressed to S.P.F. (email: fernandez@ipmc.cnrs.fr) or to J.B. (email: barik@ipmc.cnrs.fr)

Depression is a frequently diagnosed mental condition that has detrimental impact on psychological well-being and on health systems. It is the leading cause of disability worldwide and the World Health Organization estimates that 350 millions of people of all ages suffer from this disorder¹. Social withdrawal and anhedonia, i.e., inability to experience pleasure from normally rewarding actions, are conspicuous manifestations of major depression². These symptomatic facets of the disease have been associated with a dysregulation of the brain reward system, including dopamine (DA) neurons in the ventral tegmental area (VTA)^{3,4}.

This system has a predominant role in processing salient stimuli, both rewarding and aversive, to guide a broad range of adaptive behaviors⁵. DA neurons undergo experience-dependent plasticity, which is thought to be a cardinal cellular mechanism shaping behavioral strategies⁶. The use of preclinical models spanning from rodents to non-human primates is essential to apprehend the neurobiological complexity of depression⁷. For example, mice subjected to repeated bouts of social subordination exhibit a marked and sustained increase in the firing activity of VTA DA neurons^{8–11}. Defeated mice display a wide range of depressive-like symptoms, including social aversion and anhedonia, which can be reversed by restoring normal VTA function^{8,9}. These observations set the basis for a neuroanatomical specificity causally linking DA cellular adaptations and maladaptive behaviors to chronic stress. However, a clear understanding of how cellular adaptations within delineated neural circuits give rise to depressive-like behaviors is still largely lacking. In particular, identifying relevant inputs that shape DA neurons' responsiveness to stress is essential and has important implications for future therapeutic advances.

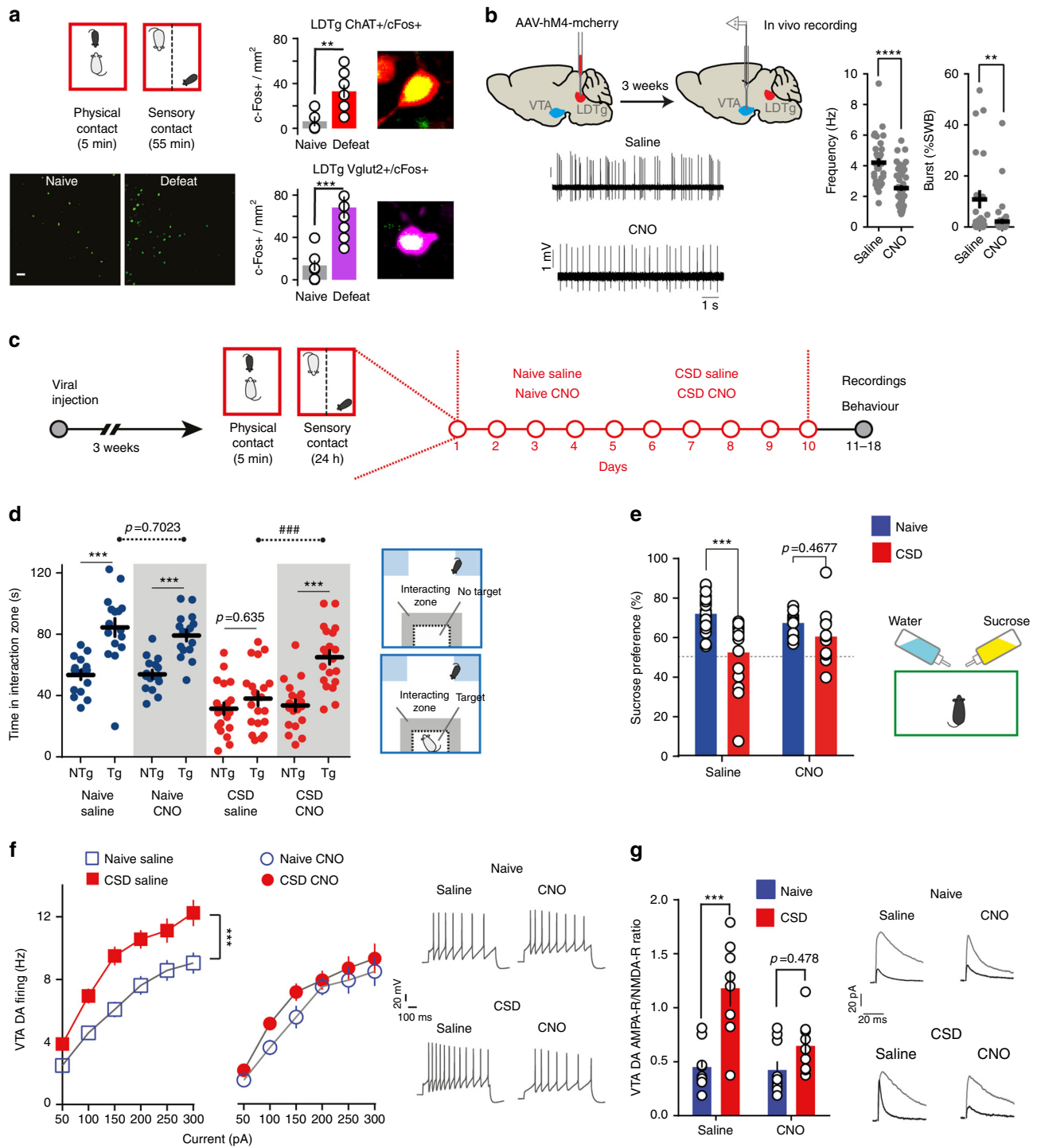
Among the many inputs received by VTA neurons¹², excitatory cholinergic and glutamatergic projections from the laterodorsal tegmentum (LDTg) are key to shape DA neurons' activity in response to salient stimuli^{13,14}. Pharmacological inhibition or excitotoxic lesions of the LDTg are detrimental to VTA DA neurons' activity^{13,15}. LDTg inputs to the VTA are key to shape reward responses^{14,16}, but their implication in stress-related experiences has yet to be addressed. We hypothesized that LDTg excitatory drive to VTA DA neurons could actively orchestrate cellular and behavioral manifestations of depressive-like behaviors. To test this, we combined retrograde labeling, and electrophysiological and behavioral approaches to assess the impact of a chemogenetic-based remote control of LDTg neurons' activity in mice subjected to a chronic social defeat (CSD) stress^{17,18}. Our data indicate that CSD, via increase of corticotropin-releasing factor (CRF), triggers a hyperactivity of LDTg cholinergic neurons projecting to the VTA. This increased cholinergic tone is a prerequisite for the subsequent stress-induced cellular adaptations of VTA DA neurons and the appearance of social aversion and anhedonia.

Results

Silencing LDTg prevents maladaptations to chronic stress. A single social defeat session exerted strong activation of excitatory LDTg neurons as evidenced by an increase in *c-Fos* expression, a classical marker of neuronal activity. Indeed, more than 5-fold *c-Fos* increase was detected in both cholinergic and glutamatergic LDTg neuronal populations (Fig. 1a). To interrogate whether the LDTg is embedded in the brain circuits that underlie the appearance of depressive-like disorders, we used a chemogenetic approach to remotely inhibit the LDTg before each daily defeat session of the chronic defeat paradigm. Wild-type (WT) mice were injected with AAV-hsyn-hM4-mcherry into the LDTg (hereafter called LDTg^{hM4} mice) and allowed a 3-week recovery

period to achieve sufficient expression reaching 71% of LDTg neurons (Supplementary Fig. 1). This approach allowed silencing of transduced LDTg neurons in the presence of the agonist clozapine N-oxide (CNO) (Supplementary Fig. 2a). Acute chemogenetic-mediated inhibition of the LDTg via CNO injection, significantly decreased spontaneous discharge frequency (~40%) and bursting activity (~80%) in all VTA DA neurons juxtacellularly recorded *in vivo* in anesthetized mice (Fig. 1b). Of note, acute injection of CNO did not alter *in vivo* firing and bursting activity of VTA DA neurons (Supplementary Fig. 3a, b) in mice injected with AAV-hSyn-GFP into the LDTg (hereafter called LDTg^{GFP} mice). This first set of data shows that the LDTg is activated by stress, and that its remote chemogenetic inhibition has a functional impact on VTA DA neurons activity. Next, LDTg^{hM4} mice were submitted to 10 days of social defeat and received an intraperitoneal (i.p.) injection of saline or CNO (1 mg/kg) 30 min before each defeat session. Naive mice were treated accordingly but without defeat (Fig. 1c). All animals were tested in a drug-free condition. As expected, defeated mice treated with saline showed strong social avoidance (Fig. 1d) and anhedonia, as evidenced by a lack of sucrose preference compared with non-stressed saline-treated mice (Fig. 1e). In contrast, LDTg inhibition during CSD prevented stress impact, as defeated CNO-treated mice showed social interaction and sucrose preference that were comparable to that of undefeated animals (Fig. 1d, e). These effects cannot be attributed to a direct action of CNO, as LDTg^{GFP} mice treated accordingly showed the expected stress-induced social aversion and anhedonia (Supplementary Fig. 3c). As these stress-related symptoms have been causally linked to pathophysiological cellular maladaptations in the DA system^{8,9}, we assessed VTA DA neuron firing and plasticity in both conditions using whole-cell current-clamp recordings. In acute brain slices from defeated saline-treated mice, VTA DA neurons exhibited increased excitability to current injection and higher AMPA-R/NMDA-R ratio when compared with undefeated mice (Fig. 1f, g). Mirroring the behavioral outcomes of LDTg inhibition, CSD failed to elicit VTA cellular adaptations. Indeed, no significant differences were observed in excitability or synaptic plasticity in VTA DA neurons from defeated LDTg^{hM4} mice treated with CNO during CSD compared with undefeated mice (Fig. 1f, g, respectively). Of note, chronic CNO injections in naive and defeated LDTg^{GFP} mice did not alter excitability of VTA DA neurons (Supplementary Fig. 3d). Altogether, these results indicate that LDTg is activated during chronic stress, and that LDTg inhibition prevents the development of depressive-like behaviors and the underlying cellular dysregulations of the VTA DA system.

Chronic stress drives hyperexcitability of LDTg neurons. The LDTg is heterogeneous containing non-overlapping VTA-projecting neurons¹⁴ and converging evidence suggest that both cholinergic and glutamatergic LDTg neurons provide excitatory inputs to VTA DA neurons^{12,16,19}. Thus, we hypothesized that these excitatory projections could be affected by chronic stress consequently leading to hyperactivity of VTA DA neurons. To unambiguously perform whole-cell patch-clamp recordings from cholinergic LDTg neurons that project to the VTA (LDTg^{→VTA}), we injected green retrobeads in the VTA of ChAT-Cre × tdTomato mice (ChAT^{tdTom} mice Fig. 2a), in which cholinergic neurons are tagged with tdTomato. To record from glutamatergic LDTg^{→VTA} neurons, we injected green retrobeads in the VTA and AAV-hsyn-DIO-mcherry in the LDTg of Vglut2-Cre mice²⁰ (Fig. 2b). Cholinergic and glutamatergic LDTg^{→VTA} neurons showed different excitability profile to depolarizing current steps, as well as different soma sizes, passive membrane properties, and action potential shape (Fig. 2c and Supplementary Fig. 4). This is



consistent with two non-overlapping neuronal populations that provide separate excitatory drive to midbrain DA neurons. CSD triggered a robust increase in excitability in both cholinergic and glutamatergic LDTg \rightarrow VTA neurons. Indeed, cholinergic LDTg \rightarrow VTA neurons responded with higher discharge frequency to depolarizing current injections in slices from defeated mice compared with undefeated animals (Fig. 2d, e). Similarly, glutamatergic LDTg \rightarrow VTA neurons showed higher intrinsic excitability after CSD than undefeated mice (Fig. 2d-f). These results suggest that CSD increases excitatory drive from LDTg cholinergic and glutamatergic neurons that innervate the VTA, possibly driving the cellular hyperexcitability of midbrain DA cells.

LDTg cholinergic neurons silencing dampens stress impact. To ascertain the individual contribution of LDTg cholinergic and/or glutamatergic neurons to depressive-like behaviors and VTA DA dysregulations, we used a Cre-dependent chemogenetic approach to specifically silence these neuronal populations. First, AAV-hSyn-DIO-hM4-mcherry was stereotaxically injected in the LDTg of ChAT-Cre mice (hereafter called LDTg ChAT-hM4 mice, Fig. 3a and Supplementary Fig. 5a). Selective inhibition of LDTg cholinergic neurons during CSD prevented the behavioral manifestations of stress. Indeed, although defeated LDTg ChAT-hM4 mice treated with saline showed strong social avoidance and anhedonic responses to sucrose solution, CNO-treated LDTg ChAT-hM4 mice

Fig. 1 Chemogenetic inhibition of the LDTg during chronic defeat prevents depressive-like behaviors and VTA DA cellular adaptations. **a** Activation of LDTg cholinergic and glutamatergic neurons after a single defeat. Images shows LDTg c-Fos positive (c-Fos +) cells (scale bar = 50 μ m). Quantification of LDTg c-Fos + cells after acute defeat stress ($n = 3$ slices/mouse, 4 mice/condition, $**P < 0.001$ unpaired t -test). **b** In vivo recordings were performed in the VTA 3 weeks after viral injection. While under anesthesia, mice were given intravenously saline or CNO and changes in activity from baseline assessed. In all instances, dopamine neurons in the VTA showed a decrease in firing frequency ($****P < 0.0001$, t -test) and bursting activity ($**P < 0.01$, Mann-Whitney) in response to CNO when compared with saline (number of cell/mice: saline $n = 33/4$ and CNO $n = 45/5$). Voltage traces are shown. **c** Schematic experimental time line. **d** Social interaction times in the absence no target (NTg) or presence target (Tg) of an unfamiliar mouse. Defeated LDTg^{hM4} mice treated with saline show marked social avoidance, which is not present in animals that received CNO before each defeat session (number of mice: Naive/Sal = 16; Naive/CNO = 16; CSD/Sal = 20; CSD/CNO = 19). Interaction treatment \times target $F(3,67) = 5.14$, $P = 0.003$, Interaction treatment \times stress $F(1,67) = 13.55$, $P < 0.001$; repeated-measures two-way ANOVA followed by Sidak's comparisons test, asterisks depict NTg vs. Tg comparisons, hash depicts comparisons between saline vs. CNO in the Tg condition; $***P < 0.001$, $####P < 0.001$. **e** Sucrose consumption is decreased in defeated saline-treated LDTg^{hM4} mice but not in CNO-treated mice (number of mice: Naive/Sal = 23; Naive/CNO = 18; CSD/Sal = 16; CSD/CNO = 15). Interaction treatment \times stress $F(1,66) = 5.39$, $P = 0.02$; two-way ANOVA followed by Sidak's comparisons test $***P < 0.001$. **f** Chemogenetic inhibition of the LDTg in defeated LDTg^{hM4} mice prevents the apparition of VTA DA hyperexcitability (number of cell/mice: Naive/Sal = 21/5; Naive/CNO = 12/4; CSD/Sal = 20/5; CSD/CNO = 18/5). Interaction treatment \times current $F(18,384) = 2.39$, $P = 0.001$; repeated-measures two-way ANOVA followed by Sidak's comparisons test $***P < 0.001$. Representative voltage traces are shown. **g** Increase in VTA DA AMPA-R/NMDA-R ratio after CSD is prevented by chemogenetic inhibition of LDTg (number of cell/mice: Naive/Sal = 10/5; Naive/CNO = 10/5; CSD/Sal = 8/6; CSD/CNO = 9/6). Interaction treatment \times stress $F(1,33) = 4.12$, $P < 0.05$; two-way ANOVA followed by Sidak's comparisons test $***P < 0.001$. Representative current traces in the absence/presence of the NMDA antagonist AP-5. All plots depict mean \pm SEM

displayed normal social interaction and sucrose intake (Fig. 3b and Supplementary Fig. 5b, respectively). Behavioral responses were comparable in undefeated LDTg^{ChAT-hM4} mice treated with either saline or CNO (Fig. 3b and Supplementary Fig. 5b). Consistent with these results, selective silencing of cholinergic LDTg neurons during CSD prevented stress-induced VTA DA neuron hyperexcitability and increases in AMPA-R/NMDA-R ratio (Fig. 3c and Supplementary Fig. 5c, respectively). We also recorded cholinergic LDTg neurons from LDTg^{ChAT-hM4} mice. Chronic CNO administration did not affect the excitability profile of these neurons in naive conditions when compared with saline but prevented CSD-induced hyperexcitability (Supplementary Fig. 5d).

In striking contrast, selective silencing of LDTg glutamatergic neurons during CSD failed to prevent behavioral and cellular adaptations to stress. To reach this observation, we injected AAV-hSyn-DIO-hM4-mcherry in the LDTg of Vglut2-Cre mice (here after LDTg^{Vglut2-hM4} mice, Fig. 3d). Defeated LDTg^{Vglut2-hM4} mice treated with either saline or CNO exhibited significant social aversion (Fig. 3e) and similar hyperexcitability in VTA DA neuron firing (Fig. 3f). Collectively, the above data indicate that cholinergic neurons of the LDTg are key orchestrators of maladaptations to chronic stress impinging on VTA DA neurons that ultimately drive social aversion and anhedonic processes. Conversely, silencing of LDTg glutamatergic neurons did not yield stress relief, which may reflect compensation from other glutamatergic inputs to the VTA.

LDTg^{→VTA} cholinergic pathway activation gates stress impact.

Due to the widespread projections of LDTg neurons, we wanted to narrow down the observed effect to LDTg projections to the VTA. Also, if activation of these projections is required for stress outcomes, this would imply that increasing activity of LDTg neurons that project to the VTA could favor stress-induced maladaptations. This would result in an enhanced sensitivity of the DA system to a moderate social stress, and the appearance of social aversion. In order to selectively activate LDTg neurons that project to the VTA, we injected a retrograde CAV-2-Cre in the VTA and AAV-hSyn-DIO-hM3-mcherry in the LDTg of WT mice (hereafter LDTg^{hM3→VTA} mice, Fig. 4a). This approach allows activation of transduced LDTg neurons in the presence of CNO (Supplementary Fig. 2b). To mimic a moderate social stress, we submitted LDTg^{hM3→VTA} mice to a subthreshold defeat

(SubSD) paradigm (Fig. 4a). We and others have previously used this protocol to evaluate the stress-potentiating effects of either optogenetic or pharmacological manipulation of VTA DA neurons^{9,21}. We observed that SubSD triggered social aversion in mice receiving CNO, whereas it was ineffective in saline-injected mice. In view of our above results, we hypothesized that this effect could be mediated by Designer Receptor Exclusively Activated by Designer Drug (DREADD)-induced activation of cholinergic inputs from the LDTg to the VTA, via activation of neuronal nicotinic acetylcholine receptors (nAChRs) that are key regulators of VTA DA neurons^{21,22}. To test this, we locally infused the non-selective nAChRs antagonist mecamylamine in the VTA, before LDTg^{hM3→VTA} mice entered the SubSD protocol (Fig. 4b). This treatment fully prevented the appearance of social aversion resulting from a mild stress combined with DREADD activation of the LDTg^{→VTA} pathway (Fig. 4b). In line with the behavioral data, LDTg^{hM3→VTA} mice submitted to SubSD showed enhanced excitability of VTA DA neurons when injected with CNO but not saline, an effect that could be reversed by systemic injection of mecamylamine (Fig. 4c). This set of data indicates that direct LDTg stimulation of VTA neurons paired with a short-lived stress is sufficient to promote behavioral and cellular adaptations, and that this effect requires activation of VTA nAChRs. To unambiguously demonstrate the involvement of LDTg cholinergic neurons projecting to the VTA in this process, we locally infused CNO in the VTA of LDTg^{ChAT-hM3} mice to selectively activate cholinergic terminals. Although vehicle-treated mice submitted to SubSD showed normal social interaction, VTA infusion of CNO combined with SubSD triggered significant social aversion (Fig. 4d). Therefore, our data demonstrate that LDTg cholinergic inputs to the VTA drive maladaptations to social stress. It also demonstrates that we can exert a bidirectional control over LDTg neurons to either favor or block adaptations to stress within VTA DA neurons.

CRF signaling affect LDTg cholinergic neurons. What is the molecular determinant of stress' action that drives hyperexcitability of cholinergic LDTg neurons? Stressors trigger the activation of the hypothalamo-pituitary adrenal axis, which is initiated by the release of CRF, a neuropeptide that act at hypothalamic and extra-hypothalamic sites²³. CRF is a potent and fast-acting mediator of endocrine and autonomic responses to stress, and regulates neurotransmission directly through two

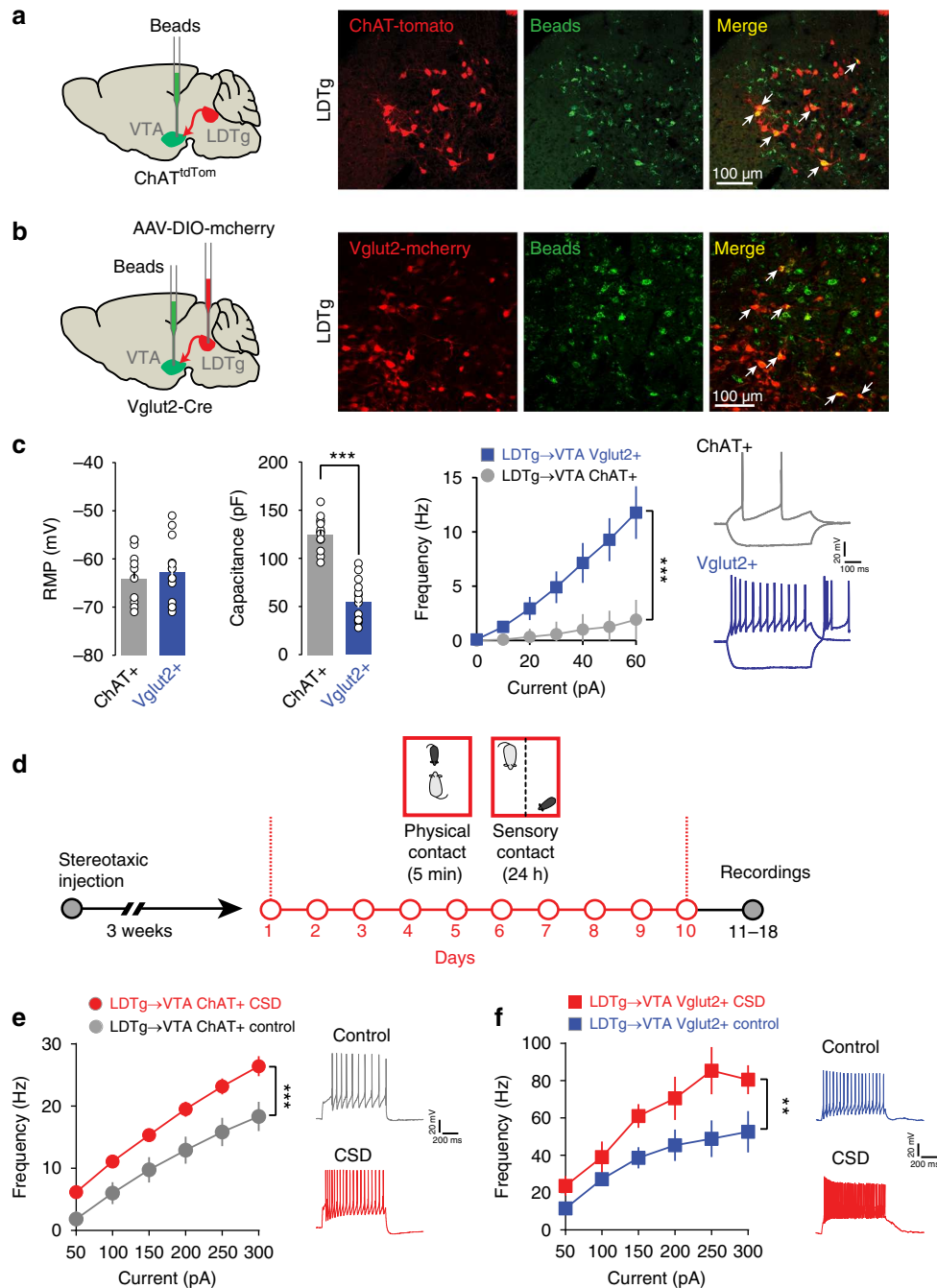
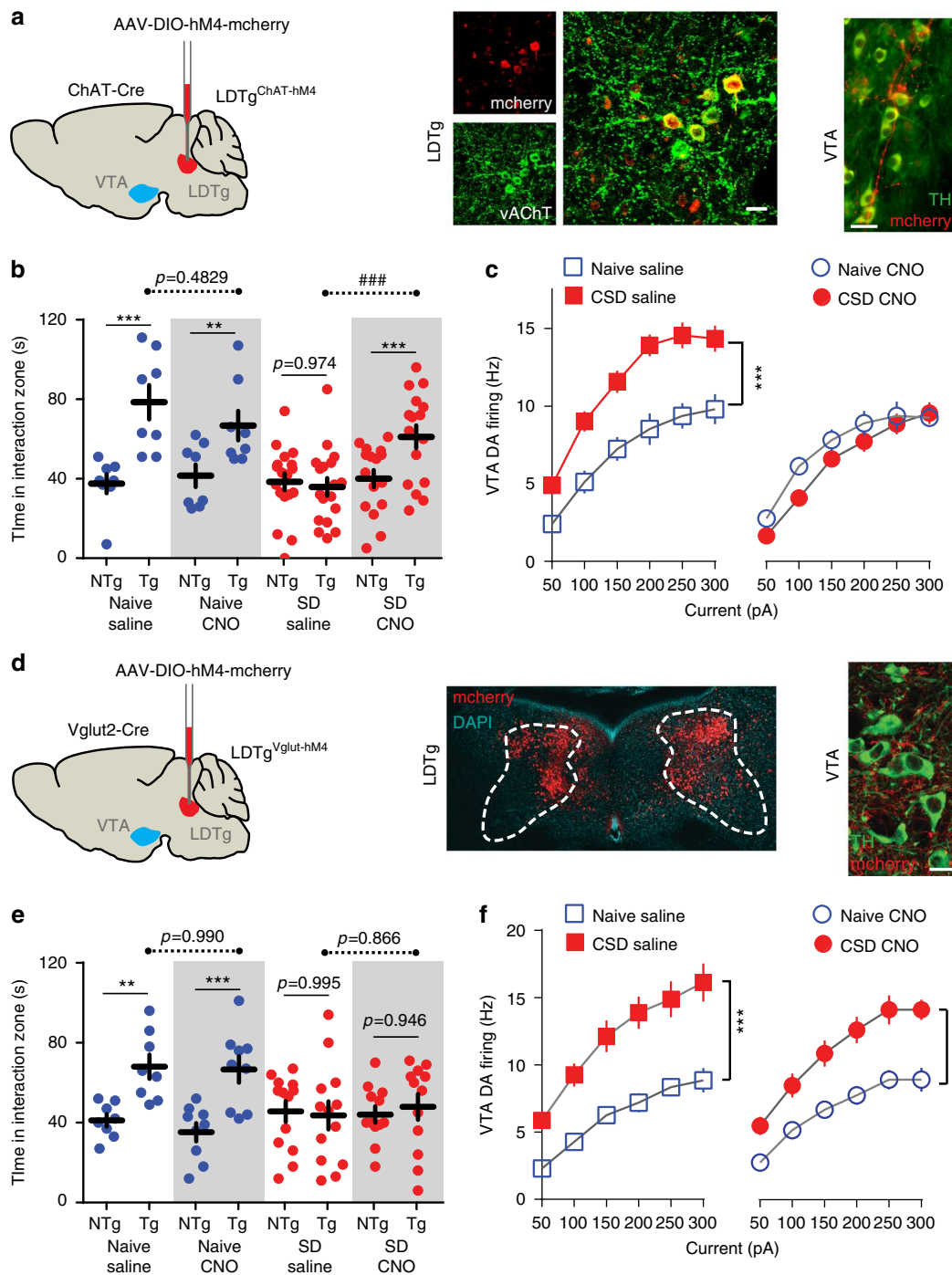


Fig. 2 Cholinergic and glutamatergic LDTg \rightarrow VTA neurons are sensitive to chronic stress. **a** ChAT-Cre::tdTomato mice were injected with green retrobeads in the VTA. Confocal images show the co-expression of green beads and tdTomato in cholinergic neurons of the LDTg. **b** Vglut2-Cre mice were injected with an AAV8-hSyn-DIO-mcherry in the LDTg and green retrobeads in the VTA. Confocal images show the co-expression of green beads and mcherry in glutamatergic neurons of the LDTg. **c** Bioelectrical properties of cholinergic and glutamatergic LDTg \rightarrow VTA neurons. Cholinergic neurons show bigger capacitance and lower firing frequencies at each current step injection (number of cell/mice: ChAT + = 15/4; Vglut + = 14/3). Interaction cell type \times current $F(6, 162) = 15.77, P < 0.0001$; repeated-measures two-way ANOVA followed by Sidak's comparisons test $***P < 0.001$. Representative voltage traces showing response to current injection (-40 and $+60$ pA) in both neuronal populations. **d** Schematic experimental time line to assess excitability in cholinergic and glutamatergic neurons after CSD. **e** Patch-clamp recordings in cholinergic LDTg \rightarrow VTA neurons revealed increased excitability after CSD (number of cell/mice: ChAT + /Naive = 15/3; ChAT + /CSD = 15/4). Interaction treatment \times current $F(6, 168) = 19.23, P = 0.0001$; repeated-measures two-way ANOVA followed by Sidak's comparisons test $***P < 0.001$. Representative voltage traces to a 300 pA current injection. **f** Patch-clamp recordings in glutamatergic LDTg \rightarrow VTA neurons also shows increased excitability after CSD (number of cell/mice: Vglut + /Naive = 13/4; Vglut/CSD = 9/4). Interaction treatment \times current $F(18, 384) = 2.39, P = 0.001$; repeated-measures two-way ANOVA followed by Sidak's comparisons test, $**P < 0.01$. Representative voltage traces to a 50 pA current injection. All plots depict mean \pm SEM



receptor subtypes, CRF receptor 1 (CRF-R1) and CRF-R2²³. It is therefore possible that the CRF system has a role in social stress processing in the LDTg consequently affecting its output connectivity. A single defeat session in naive mice led to a significant increase (1.8-fold) in plasma CRF levels (basal, 399.9 ± 116.7 pg/ml; acute aggression, 723.5 ± 178.6 pg/ml; $n = 8-12$ per group, $P < 0.05$, Mann-Whitney). To ascertain the functional role of stress-induced CRF release onto LDTg cholinergic neurons, and the respective contribution of CRF-1 or CRF-2 receptor subtypes, we performed whole-cell patch-clamp recordings in slices from ChAT^{tdTom} mice (Fig. 5a). In current-clamp mode and after reaching a stable baseline, the CRF-R1 agonist stressin I (1 μM) or the CRF-R2 agonist urocortin III (1 μM) were applied to the perfusion system. Stressin I application, but not urocortin III,

consistently initiated action potential discharge in all cholinergic neurons tested, and this effect disappeared after washout of the drug (Fig. 5a). In contrast, stressin I and urocortin III failed to elicit any notable responses in LDTg glutamatergic neurons (Fig. 5b). To further refute the involvement of CRF-R1, a subset of LDTg glutamatergic neurons were depolarized to -55 mV by current injection before applying the agonist. Even in this condition, stressin I failed to initiate action potential firing (five cells from two mice). These data suggest that after CSD, cholinergic neurons of the LDTg could be overly activated by the release of CRF via activation of excitatory CRF-R1. To answer this question, WT mice were subjected to CSD where each defeat session was preceded by a local bilateral injection of a CRF-R1-specific antagonist, CP376395 (500 ng/site), or saline. Control mice

Fig. 3 Selective chemogenetic inhibition of LDTg cholinergic but not glutamatergic neurons during CSD is sufficient to prevent depressive behaviors and VTA DA dysregulation. **a** Bilateral stereotaxic injection of AAV8-hSyn-DIO-hM4-mcherry in the LDTg of ChAT-Cre mice (LDTg^{ChAT-hM4} mice). Confocal images showing colocalization of mcherry and vesicular acetylcholinesterase transporter (vAChT) Scale bar = 20 μ m. Epifluorescence micrograph showing cholinergic fibers expressing mcherry in close interaction with tyrosine hydroxylase (TH)-positive VTA dopamine neurons. Scale bar = 25 μ m. **b** Social interaction times in undefeated or defeated LDTg^{ChAT-hM4} mice treated with saline or CNO. Saline-injected defeated mice showed marked social aversion, whereas CNO injection in the defeated group restored social interaction (number of mice: Naive/Sal = 8; Naive/CNO = 8; CSD/Sal = 18; CSD/CNO = 16). Interaction treatment \times target $F(3,46) = 9.62$, $P = 0.0001$; Interaction treatment \times stress $F(1,46) = 7.99$, $P < 0.01$; repeated-measures two-way ANOVA followed by Sidak's comparisons test, asterisks depict NTg vs. Tg comparisons, hash depicts comparisons between saline vs. CNO in the Tg condition; $**P < 0.01$, $***P < 0.001$, $###P < 0.001$. **c** Inhibition of cholinergic LDTg neurons during CSD prevented increased excitability in VTA DA neurons (number of cell/mice: Naive/Sal = 11/4; Naive/CNO = 13/4; CSD/Sal = 22/5; CSD/CNO = 18/5). Interaction treatment \times current $F(18,360) = 4.66$, $P = 0.0001$; repeated-measures two-way ANOVA followed by Sidak's comparisons test $***P < 0.001$. **d** Bilateral stereotaxic LDTg injection of AAV8-hSyn-DIO-hM4-mcherry of Vglut2-Cre mice (LDTg^{Vglut2-hM4} mice). Confocal image shows representative injection site. Confocal image showing glutamatergic fibers expressing mcherry in close interaction with TH-positive VTA dopamine neurons. Scale bar = 20 μ m. **e** Social interaction times in undefeated or defeated LDTg^{Vglut2-hM4} mice treated with saline or CNO. Silencing of LDTg glutamatergic neurons by administration of CNO during stress did not prevent the appearance of social aversion (number of mice: Naive/Sal = 8; Naive/CNO = 9; CSD/Sal = 13; CSD/CNO = 12). Interaction treatment \times target $F(3,38) = 6.80$, $P = 0.0009$; Interaction treatment \times stress $F(1,38) = 0.1619$, $P = 0.6897$; repeated-measures two-way ANOVA followed by Sidak's comparisons test, asterisks depict NTg vs. Tg comparisons, hash depicts comparisons between saline vs. CNO in the Tg condition; $**P < 0.01$, $***P < 0.001$, $###P < 0.001$. **f** Patch-clamp recordings in brain slices showed that inhibition of glutamatergic LDTg neurons during CSD did not prevent increased excitability in VTA DA neurons (number of cell/mice per condition: Naive/Sal = 12/4; Naive/CNO = 14/4; CSD/Sal = 10/5; CSD/CNO = 10/5). Interaction treatment \times current $F(6,108) = 0.95$, $P = 0.466$; repeated-measures two-way ANOVA followed by Sidak's comparisons test $***P < 0.001$. All plots depict mean \pm SEM

received the same treatment but without defeat (Fig. 5b) and animals were tested in drug-free conditions. Chronic infusion of CP376395 did not affect social approach or sucrose preference in undefeated mice; however, CP376395 fully prevented the appearance of stress-induced social aversion and anhedonia (Fig. 5c, d). We then assessed the state of VTA DA neuron excitability and, in accordance with the behavioral results, local CP376395 infusion in the LDTg prevented hyperexcitability induced by CSD (Fig. 5e). This demonstrates the ability of CRF signaling in the LDTg to promote depressive-like behaviors via dysregulation of VTA DA function.

Discussion

Here we demonstrated that chronic social stress exposure produces profound dysregulation of excitatory inputs from the LDTg to the VTA via CRF signaling. Selective inhibition of cholinergic, but not glutamatergic, LDTg neurons prevents stress-induced cellular adaptations within VTA DA neurons and the appearance of anhedonia and social withdrawal.

Central cholinergic neurotransmission is a powerful neuromodulator that, in physiological conditions, affects neuronal excitability and synaptic strength to synchronize neuronal networks, in order to guide adaptive behaviors^{24,25}. Dysregulation of acetylcholine tone in discrete brain areas can lead to pathophysiological states^{26,27}, and in particular a heightened cholinergic transmission has long been postulated to contribute to depression²⁸. This hypothesis is supported by the observations that depressive symptomatology can be induced by cholinomimetics or inhibition of acetylcholinesterase^{29–31}. Despite this evidence, the neuronal circuit underlying depression, as well as the cellular and synaptic changes driven by acetylcholine, are still poorly understood. Our data uncover a cardinal role of cholinergic neurons of the LDTg in the appearance of chronic stress-induced depressive-like behavioral manifestations. We show that CSD increased the excitability of LDTg cholinergic neurons that project to the VTA. Increased cholinergic tone would favor DA neurons firing by two mechanisms. Activation of excitatory postsynaptic nAChRs produces depolarization and firing activity of DA neurons³². In addition to direct activation, acetylcholine release can enhance the release of glutamate from other inputs via activation of presynaptic nAChRs^{33,34} (Fig. 6). We put in evidence the importance

of this cholinergic/nicotinic mechanism by pharmacological blockade of VTA nAChRs. This is in line with our previous data showing that constitutive ablation of nAChRs is sufficient to prevent CSD-induced hyperactivity of DA neurons²¹.

Although the mechanisms underlying CSD-induced increases in DA firing are at present unclear, our study suggests that adaptations in both intrinsic and synaptic plasticity could contribute to this process³⁵. For example, we showed that CSD induces changes in AMPA-R/NMDA-R ratio, a proxy for glutamatergic synaptic strength. Our data suggest that cholinergic LDTg inputs may serve as a permissive signal. Indeed, silencing of the LDTg cholinergic pathway was effective in preventing stress-induced changes in activity and glutamatergic plasticity of DA neurons. Unlike cholinergic neurons, silencing of LDTg glutamatergic neurons did not produce stress relief. This may be explained by the fact that the VTA receives numerous sources of glutamatergic inputs^{12,36}, which have been shown to be strengthened by aversive stimuli³⁷. It is evident that the glutamatergic synapse undergoes significant remodeling that are likely to contribute to deregulation of VTA DA neurons activity but the molecular mechanisms and input sources affected by stress are yet to be elucidated.

VTA DA neurons not only respond to rewarding stimuli but they can also adapt to aversive and stressful events⁵. Inputs to the VTA likely have a role in shaping stress-induced depressive-like behaviors. For example, a recent study shows that pallidal parvalbumin neurons adapt their activity in response to chronic stress, affecting VTA DA excitatory/inhibitory balance³⁸. In another study, noradrenergic inputs from the locus coeruleus were shown to promote stress resilience putatively through an inhibitory mechanism³⁹. The LDTg to VTA pathway has been studied for its role in reward. For example, direct optogenetic-mediated activation of LDTg terminals in the VTA is sufficient to produce conditioned place preference¹⁶ and a similar effect is achieved when the stimulation is restricted to cholinergic terminals⁴⁰. Our study addresses the role of this pathway in stress processing and demonstrates that aversive encounters with a dominant male can produce activation of LDTg neurons. Importantly, chemogenetic activation of the LDTg to VTA pathway paired with a mild social stress promotes the development of depressive-like symptoms and the aberrant increase in VTA DA neurons activity. These results indicate that LDTg

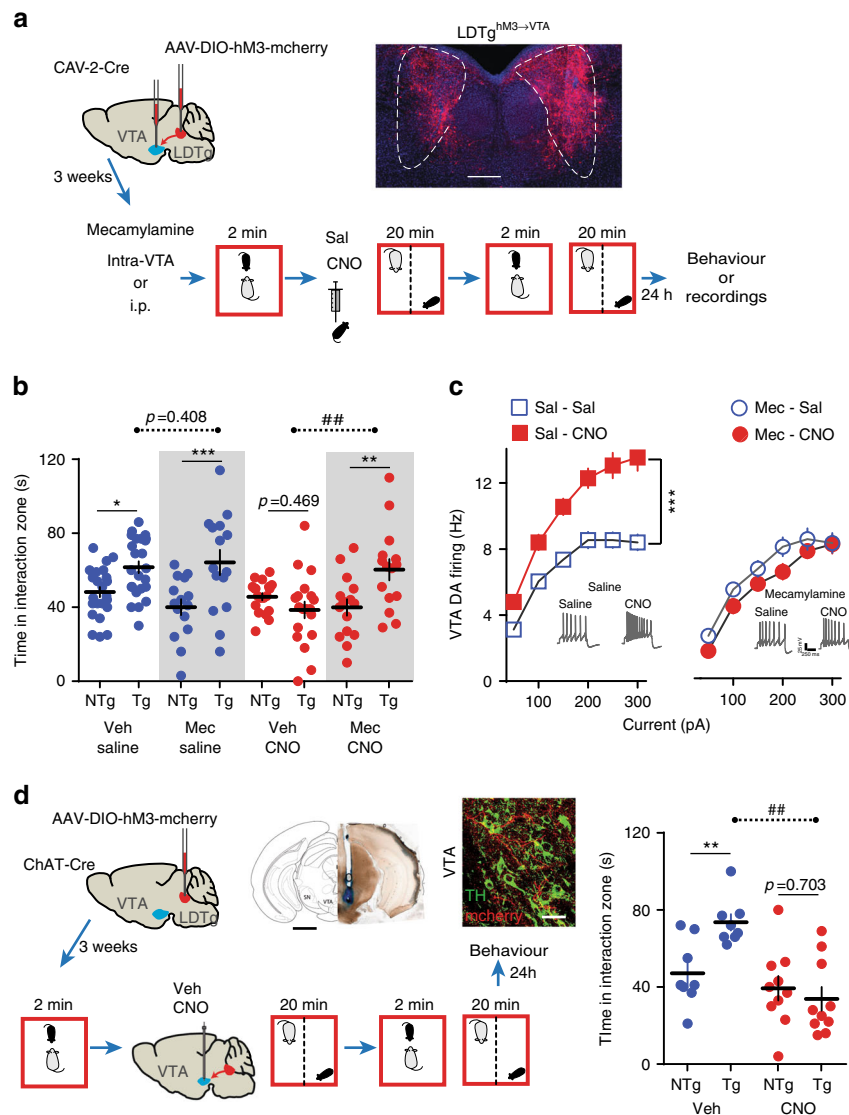


Fig. 4 LDTg cholinergic inputs to the VTA promote depressive-like maladaptations. **a** Bilateral stereotaxic injection of a retrograde CAV-2-Cre in the VTA combined with a bilateral injection of an AAV8-hSyn-DIO-hM3-mcherry in the LDTg of wild-type mice ($LDTg^{hM3 \rightarrow VTA}$). Representative image depicting hM3-mCherry expression in LDTg neurons projecting to the VTA and schematic experimental time line. Mice were implanted with cannula guides over the VTA, allowing for local infusion. **b** A subthreshold defeat (SubSD) exposure combined with CNO-induced activation of LDTg neurons projecting to the VTA elicits social aversion. Mecamylamine (Mec; $1 \mu\text{g}/\text{site}$) infusion in the VTA before SubSD is sufficient to prevent this effect (number of mice: Vehicle/Sal = 24; Mec/Sal = 15; Vehicle/CNO = 19; Mec/CNO = 15). Interaction treatment \times target $F(3,69) = 7.69$, $P = 0.0002$; Interaction treatment \times stress $F(1,69) = 0.1564$, $P = 0.2156$; repeated-measures two-way ANOVA followed by Sidak's comparisons test, asterisks depict NTg vs. Tg comparisons, hash depicts comparisons between saline vs. CNO in the Tg condition; * $P < 0.05$, ** $P < 0.01$, *** $P < 0.001$, ### $P < 0.01$. **c** A different cohort of $LDTg^{hM3 \rightarrow VTA}$ mice received either systemic saline or mecamlamine ($1 \text{ mg}/\text{kg}$) before being submitted to SubSD. CNO-induced activation of LDTg neurons projecting to the VTA combined with SubSD produced hyperactivity of VTA DA neurons. This effect was fully prevented by mecamlamine. Number of cell/mice: Sal/Sal = 18/4; Sal/CNO = 18/5; Mec/Sal = 12/4; Mec/CNO = 16/5. Interaction treatment \times current $F(18,360) = 6.58$, $P = 0.0001$; repeated-measures two-way ANOVA followed by Sidak's comparisons test *** $P < 0.001$. Representative voltage traces from each experimental condition are shown. **d** ChAT-Cre mice were injected with an AAV8-hSyn-DIO-hM3-mcherry in the LDTg and guides were implanted bilaterally over the VTA. Representative image shows cannula placement, scale bar = 1.2 mm. Confocal image showing cholinergic fibers expressing mcherry in close interaction with TH-positive VTA dopamine neurons. Scale bar = $30 \mu\text{m}$. Local VTA infusion of CNO combined with a SubSD resulted in strong social aversion, an effect not seen in vehicle-treated mice (number of mice per condition: Vehicle = 8; CNO = 10). Interaction $F(1,16) = 8.83$, $P = 0.009$; repeated-measures two-way ANOVA followed by Sidak's comparisons test, asterisks depict NTg vs. Tg comparisons, hash depicts comparisons between saline vs. CNO in the Tg condition; ** $P < 0.01$, ### $P < 0.01$. All plots depict mean \pm SEM

projections to the mesolimbic pathway not only convey rewarding information but also promote alertness in cases of threatening situations. The LDTg is therefore a more versatile brain structure than originally thought and should therefore be considered as a key upstream regulator of the VTA that shapes responses to salient stimuli, either rewarding or aversive.

There is at present substantial evidence for the involvement of the DA system in the pathophysiology of depressive-like disorders⁴. Most preclinical models of depression rely on exposure to stressful experiences⁴¹. Despite inducing shared behavioral maladaptations, these models are underpinned by different, and sometimes opposite, cellular changes within the DA system.

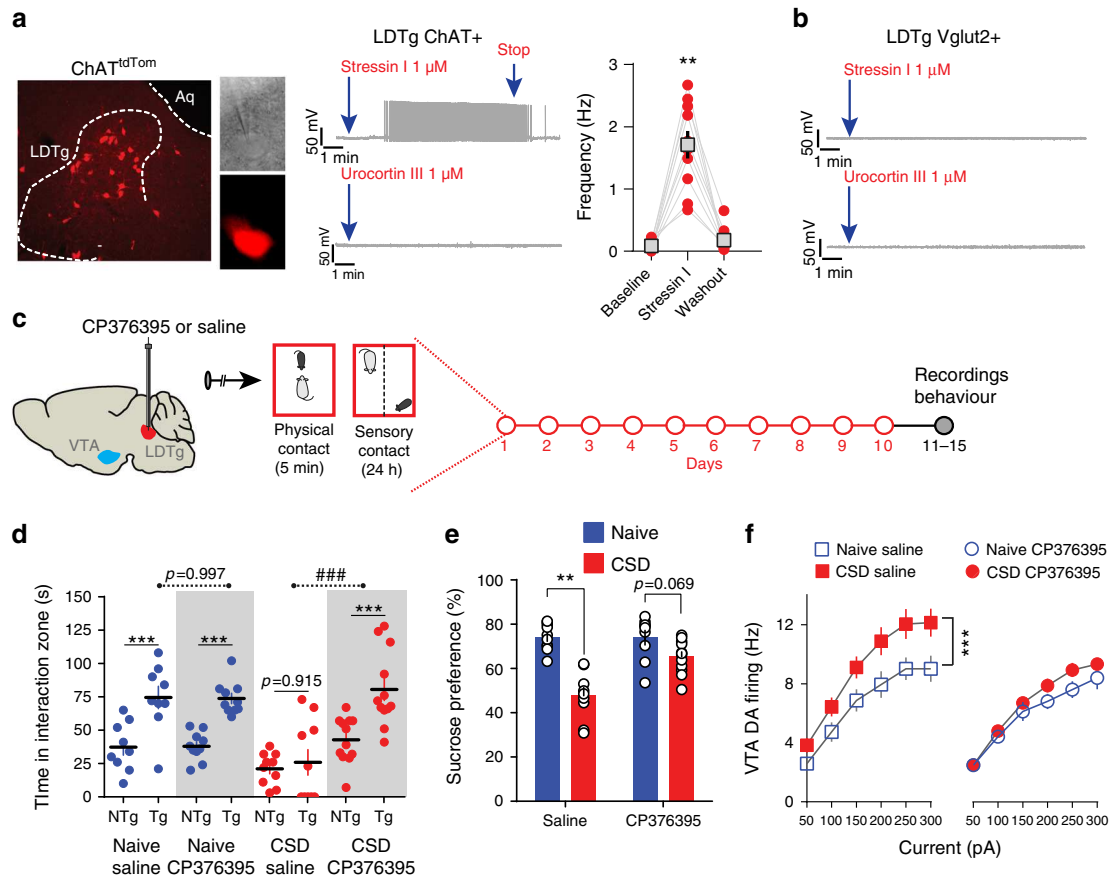


Fig. 5 CRF-1 receptors expressed in cholinergic LDTg neurons mediate stress-induced depressive-like behaviors and dysregulation of VTA DA neurons. **a** Confocal image depicting the LDTg in a ChAT-Cre::tdTomato (ChAT^{tdTom}) mouse coronal section. Visualization of tdTomato-tagged cholinergic neurons in the electrophysiological set-up during patch-clamp recordings. In current-clamp mode, most cholinergic neurons were silent, but bath application of the CRF receptor 1 agonist stressin I initiated action potential discharge. This effect was not seen with bath application of the CRF receptor 2 agonist urocortin III (number of cell/mice = 7/3). Quantification of the firing frequency in the absence and presence of stressin I (number of cell/mice = 10/4, ** $P < 0.01$, repeated-measures one-way ANOVA). **b** To visualize LDTg glutamatergic neurons, Vglut2-Cre mice were injected with an AAV8-hSyn-DIO-mcherry. Representative current-clamp recordings showing that stressin I (number of cell/mice = 9/3) or urocortin III (number of cell/mice = 9/3) failed to elicit discharge activity in this neuronal population. **c** Schematic experimental time line. Wild-type mice were implanted with cannula guides over the LDTg, allowing for local infusion before each social defeat session. **d** Local LDTg infusion of the CRF-1 antagonist CP376395 before defeat prevented the appearance of social aversion (number of mice: Naive/Vehicle = 9; Naive/CP376395 = 10; CSD/Vehicle = 10; CSD/CP376395 = 12). Interaction treatment \times target $F(3,37) = 6.33$, $P = 0.0014$; Interaction treatment \times target $F(1,69) = 7.69$, $P = 0.0002$; Interaction treatment \times stress $F(1,37) = 12.23$, $P = 0.0012$; repeated-measures two-way ANOVA followed by Sidak's comparisons test, asterisks depict NTg vs. Tg comparisons, hash depicts comparisons between saline vs. CNO in the Tg condition; *** $P < 0.001$, #### $P < 0.001$. Anatomical coordinates and maps were adjusted from Paxinos⁴⁸. **e** Sucrose preference was absent in saline-treated defeated mice, but infusion of CP376395 in the LDTg during CSD restored sucrose consumption (number of mice: Naive/Vehicle = 9; Naive/CP376395 = 10; CSD/Vehicle = 10; CSD/CP376395 = 11). Interaction treatment \times stress $F(1,36) = 10.63$, $P = 0.0024$; two-way ANOVA followed by Sidak's comparisons test *** $P < 0.001$. **f** Patch-clamp recordings in brain slices showed that increased excitability to current injection in VTA DA neurons was observed in saline-treated but not in CP376395-treated mice (number of cell/mice: Naive/Sal = 14/5; Naive/CP376395 = 11/4; CSD/Sal = 14/5; CSD/CP376395 = 19/5). Interaction current \times treatment $F(18,324) = 3.19$, $P < 0.0001$; repeated-measures two-way ANOVA followed by Sidak's comparisons test, *** $P < 0.001$. All plots depict mean \pm SEM

Indeed, the two most widely used mouse models of depression, the unpredictable chronic mild stress (UCMS), and the CSD produce decreases^{42,43} or increases^{8,9,11} in VTA DA neurons' activity, respectively. Presently, the nature of these discrepancies is not clear and may be related to differences in the duration of stress (4–6 weeks for UCMS vs. 10 days for CSD) or protocol (unpredictable stress vs. contextual association with an aggressor). Importantly, in both models, antidepressant-like effects can be achieved by phasic optogenetic stimulation of VTA DA neurons^{42,44}, likely restoring cellular homeostasis and synaptic flexibility within the system.

In the last decade, technological advances have allowed scientists to modulate specific cellular pathways in freely moving animals, in

order to dissect brain functions. Among these, chemogenetic (DREADD) approaches, which combine the use of modified G-coupled protein receptors that are activated by CNO, have become increasingly popular¹⁸. A recent publication by Gomez et al.⁴⁵ raised potential caveats due to the back-metabolism of CNO into clozapine in vivo. Nevertheless, these findings do not discount our conclusions since we have shown in non-DREADD-expressing mice that CNO per se did not impinge on two classical patterns of activity of VTA DA neurons in vivo (slow, single-spike firing, and fast-bursting activity) and did not alter behavioral and cellular adaptations to CSD. Moreover, given that we did not observe stress relief when inhibiting LDTg glutamatergic neurons further reinforces the absence of unwanted CNO side effects in this paradigm.

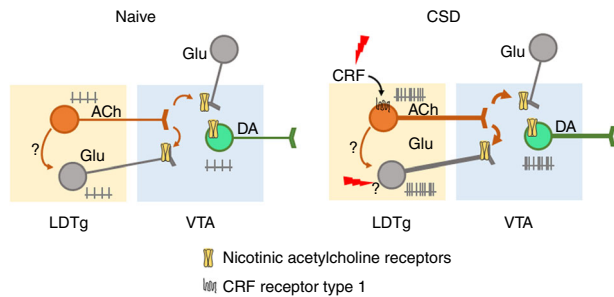


Fig. 6 Schematic model of the findings. In naive conditions, LDTg excitatory projections regulate the firing and bursting activity of VTA DA neurons. Chronic social defeat (CSD) increases the excitability of LDTg cholinergic and glutamatergic neurons that project to the VTA. Enhanced acetylcholine release increases VTA DA firing via direct activation of neuronal acetylcholine nicotinic receptors, but also by enhancing glutamatergic release via presynaptic modulation. CRF binds to CRF-1 receptors in cholinergic but not glutamatergic neurons, to promote firing in response to stress. The mechanisms by which LDTg glutamatergic neurons increase excitability after CSD are not clear, but may involve local cholinergic innervation, direct stress-related signaling, or others inputs to LDTg glutamatergic neurons

In response to stressful situations, CRF initiates neuroendocrine changes to orchestrate rapid bodily responses to ensure adequate behavioral endpoints²³. However, due to the broad central distribution of CRF receptors, the precise site(s) of action and the CRF-sensitive cell populations need to be identified. More than 90% of cholinergic neurons in the LDTg express CRF-R1⁴⁶. In accordance, we show here that acute activation of CRF-R1, but not CRF-R2, markedly increased firing of cholinergic LDTg neurons. This is likely to be the molecular event by which chronic stress triggers hyperactivity of cholinergic LDTg neurons. Indeed, we report that locally antagonizing CRF-R1 in the LDTg is sufficient to reverse cellular and behavioral marks of stress. Novel therapies involving modulation of brain pathways are showing encouraging results so far⁴⁷. However, future advances in these therapies will rely on accurate identification of cell-to-cell miscommunication within delineated neural circuits, and its involvement in pathological mental states. Our data point to a dysregulation of a tegmental cholinergic pathway arising to the VTA as a cardinal contributor to stress-induced depressive-like behaviors (Fig. 6). This imbalance could be targeted by either pharmacological antagonism to CRF receptors or, in the future, with novel selective techniques of brain stimulation.

Methods

Animals. All procedures were in accordance with the recommendations of the European Commission (2010/63/EU) for care and use of laboratory animals, and approved by the French National Ethical Committee. We used only male C57BL/6J (Janvier Labs, France), choline acetyltransferase ChAT-IRES-Cre Knock-In mice (ChAT-Cre mice, The Jackson Laboratory, stock number: 006410) and *vglut2-Cre* mice²⁰. To specifically label cholinergic neurons, ChAT-Cre mice were crossed with *tdTomato* reporter line (The Jackson Laboratory, stock number 007909). Experimental transgenic animals were heterozygous and backcrossed on a C57BL/6J background.

Reagents. Clozapine N-oxide was purchased from Enzo Life (France), Stressin I, mecamylamine and CP376395 from Tocris Cookson (UK), Urocortin III from Sigma-Aldrich (France), and Xylazine/Ketamine from Centravet (France). All drugs for *in vivo* administration were diluted in saline (0.9% NaCl). For bath application of drugs on brain slices, dilution was done in aCSF (artificial cerebrospinal fluid).

Stereotaxic injections and cannula implantation. Stereotaxic injections were performed using a stereotaxic frame (Kopf Instruments) under general anesthesia with xylazine and ketamine (10 mg/kg and 150 mg/kg, respectively). Anatomical coordinates and maps were adjusted from Paxinos⁴⁸. The injection rate was set at

100 nl/min. To identify LDTg neurons projecting to the VTA, mice (5 weeks old) were injected with green fluorescent retrobeads (200 nl/site; LumaFluor, Inc.) bilaterally in the VTA (AP: -3.2 mm, ML: ± 0.6 mm, DV: -3.7 mm from the bregma). AAV8-hSyn-hM4D-mCherry and hSyn-DIO-hM3D-mCherry (titration 10^{12} particles/ml) were purchased from the U.N.C. (University of North Carolina, USA) vector core facility and bilaterally injected (300 nl/site) in the LDTg (anteroposterior AP: -4.7 mm, mediolateral ML: ± 0.5 mm, dorsoventral DV: -3.6 mm from the bregma) of either WT, ChAT-Cre, or *Vglut2-Cre* mice (5 weeks old). Animals were given a 3 weeks' recovery period to allow sufficient viral expression.

For projection-specific manipulation, WT mice (5 weeks old) were injected with CAV-2-Cre (200 nl/site) in the VTA and with hSyn-DIO-hM3D-mCherry (300 nl/site) in the LDTg (hereafter named LDTg^{hM3→VTA} mice). We thank E.J. Kremer and the Plateforme de Vectorologie de Montpellier for providing CAV-2-Cre. Two weeks later, LDTg^{hM3→VTA} mice were implanted with double-guide cannulas above the VTA for local injections of vehicle or mecamylamine. Double-guide cannulas (ref. C235G, Plastic One), containing dummies (ref. C235DC, Plastic One) and protected by a dust cap (ref 303DC, Plastic One) were placed 1 mm above the VTA (AP: -3.2 mm, ML: ± 0.6 mm, DV: -3.7 mm from the bregma) and fixed to the skull with four screws and dental cement. LDTg^{hM3→VTA} mice were allowed to recover for a minimum of 1 week. To target the VTA, cannulas were inserted through the guides to allow drug delivery at DV: -4.7 mm.

For bilateral drug injections in freely moving mice of CP376395, double-guide cannulas containing dummies and protected by a dust cap were placed 1 mm above the LDTg (AP: -4.7 mm, ML: ± 0.5 mm, DV: -2.6 mm from the bregma) of 7 weeks old WT mice and fixed to the skull with four screws and dental cement. Mice were allowed to recover for a minimum of 1 week. To target the LDTg, cannulas were inserted through the guides to allow drug delivery at DV: -3.6 mm.

Drugs or vehicle were injected at flow rate of 100 nl/min. Cannulas were left in place for another 5 min to avoid backflow.

CSD stress and behavioral tests. The CSD stress paradigm was performed as previously⁸. WT, transgenic mice, and their respective control littermates were subjected to 10 consecutive days of social defeat by former CD1 breeder male mice. Each experimental mouse faced a new CD1 every day and sessions of defeat were limited to a maximum of 5 min. Mice were then maintained in sensory, but not physical, contacts with the dominant male through a semi-permeable barrier. Undeclared mice (Naive) were not confronted with a dominant male but lived in similar housing conditions, separated by a semi-permeable barrier. For CNO experiments, CNO (1 mg/kg, *i.p.*) or saline (10 ml/kg, *i.p.*) were administered 30 min before each defeat session. Undeclared mice were treated accordingly without being defeated. For CP376395 experiments, local infusion within the LDTg of either CP376395 (500 ng/site in a final volume of 300 nl) or saline (300 nl/site) was done at a rate of 100 nl/min. Cannulas were then left in place for 5 min to prevent backflow. For CSD mice, confrontation with the CD1 occurred after an additional 2 min period (*i.e.*, 10 min after starting local drug infusion). Naive animals were returned to their home cage. Cannula placements were confirmed postmortem. All behavioral tests were performed in drug-free conditions.

Social interaction was performed 24 h after the last defeat (day 11) in a low luminosity environment (7 ± 2 lux). Experimental mice were exposed to two consecutive sessions (150 s each) in an open-field containing initially an empty perforated box ("target -" condition), which was then replaced by a box containing an unfamiliar CD1 mouse ("target +" condition). The time spent in the interaction zone surrounding the box was recorded and used as an index of social interaction.

Anhedonia was measured in a two-bottles choice procedure for assessing sucrose preference. Mice were acclimatized to two bottles containing water during the last 3 days of the CSD paradigm. Following the social interaction test, mice were allowed to freely drink from a bottle of water or sucrose (0.5%). Bottles were weighed and rotated daily. Sucrose preference was calculated as a percentage $100 \times [\text{volume of sucrose consumed}/(\text{volume of sucrose} + \text{volume of water consumed})]$ and was averaged over a period of 3 days.

Subthreshold social defeat. The subthreshold social defeat paradigm was based on Morel *et al.*²¹.

LDTg^{hM3→VTA} mice received locally vehicle (saline 300 nl/site) or mecamylamine (1 μg in 300 nl/site)⁴⁹ in the VTA with the same technical details as described above for CP376395 experiments. LDTg^{hM3→VTA} mice were then individually introduced into a CD1 cage for 2 min of social defeat. Following this, LDTg^{hM3→VTA} mice received a single saline (10 ml/kg) or CNO (1 mg/ml) injection and were maintained with the CD1 mice separated through a partition for 20 min. The social defeat was repeated once and mice assessed in the social interaction test approximately 24 h later as described for the CSD paradigm. For electrophysiological recordings, LDTg^{hM3→VTA} mice were treated accordingly but received acute saline (10 ml/kg) or mecamylamine (1 mg/kg) *i.p.* 10 min before the first SubSD episode.

To selectively activate LDTg cholinergic terminals in the VTA, guides were placed bilaterally above the VTA of LDTg^{ChAT-hM3} mice to locally infuse CNO. Local CNO infusion has been recently used for remote control of terminals activity^{50,51}. LDTg^{ChAT-hM3} mice were submitted to SubSD as described above. Immediately after the first session of brief social defeat, CNO (10 μM ; 300 nl) or vehicle were infused at a rate of 100 nl/min, while mice were still facing the CD1

mouse through the partition preventing physical contacts. Cannulas were left in place for 5 min and mice remained facing the CD1 for another 11 min (i.e., total time of visual and olfactory contacts of 20 min) before entering the second brief social defeat session. Mice were then returned to their home cage and tested for social interaction 24 h later.

In vitro patch-clamp recordings. Mice were anesthetized (Ketamine 150 mg/kg/ Xylazine 10 mg/kg) and transcardially perfused with aCSF for slice preparation on days 11–14. For VTA recordings, horizontal 250 μm slices were obtained in bubbled ice-cold 95% O_2 /5% CO_2 aCSF containing (in mM): KCl 2.5, NaH_2PO_4 1.25, MgSO_4 10, CaCl_2 0.5, glucose 11, sucrose 234, NaHCO_3 26. Slices were then incubated in aCSF containing (in mM): NaCl 119, KCl 2.5, NaH_2PO_4 1.25, MgSO_4 1.3, CaCl_2 2.5, NaHCO_3 26, glucose 11, at 37 °C for 1 h, and then kept at room temperature. For LDTg recordings, coronal 250 μm slices were obtained using the same solutions but recovery at 37 °C lasted 15 min.

Slices were transferred and kept at 32–34 °C in a recording chamber superfused with 2.5 ml/min aCSF. Visualized whole-cell voltage-clamp or current-clamp recording techniques were used to measure synaptic responses or excitability, respectively, using an upright microscope (Olympus France). Putative DA neurons were recorded in the lateral VTA and identified using common criteria such as localization, cell body size, broad action potential, and large Ih current⁵². We compared the profile of putative VTA DA neurons with those recorded using the DA reporter mouse line PITX3-GFP⁵³ yielding identical profiles (Supplementary Fig. 6). As reported, this method might introduce bias and neglect VTA DA neurons with short action potentials⁵⁴; however, previous results have shown that chronic social stress-induced depressive behaviors is mostly associated with maladaptations in DA neurons with broad spikes^{44,55}, which are more abundant in the lateral part of the VTA⁵⁶.

Current-clamp experiments were obtained using a Multiclamp 700B (Molecular Devices, Sunnyvale, CA). Signals were collected and stored using a Digidata 1440 A converter and pCLAMP 10.2 software (Molecular Devices, CA). In all cases, access resistance was monitored by a step of -10 mV (0.1 Hz) and experiments were discarded if the access resistance increased more than 20%. Internal solution contained (in mM): K-D-gluconate 135, NaCl 5, MgCl_2 2, HEPES 10, EGTA 0.5, MgATP 2, NaGTP 0.4. Depolarizing (0–300 pA) or hyperpolarizing (0–450 pA) 800 ms current steps were used to assess excitability and membrane properties of LDTg and VTA neurons.

AMPA-R/NMDA-R ratio was assessed in voltage-clamp mode using an internal solution containing (in mM) 130 CsCl, 4 NaCl, 2 MgCl_2 , 1.1 EGTA, 5 HEPES, 2 Na_2ATP , 5 sodium creatine phosphate, 0.6 Na_3GTP , and 0.1 spermine. Synaptic currents were evoked by stimuli (60 μs) at 0.1 Hz through a glass pipette placed 200 μm from the patched neurons. Evoked-EPSCs were obtained at $V = +40$ mV in the absence and presence of the NMDA-R antagonist APV as previously described²¹. In all cases, offline analyses were performed using Clampfit 10.2 (Axon Instruments, USA) and Prism (Graphpad, USA).

In vivo electrophysiological recordings. Single-unit extracellular recordings of VTA DA cells were performed in anesthetized (chloral hydrate 8%, 400 mg/kg i.p.) mice as described previously⁵⁷. Glass electrodes (0.5% sodium acetate) were lowered in the VTA according to stereotaxic coordinates (AP: -3 to -4 mm; ML: 0.1 to 0.7 mm; DV: -4 to -4.8 mm from the bregma). To distinguish DA from non-DA neurons the following parameters were used: (1) firing rate (between 1 and 10 Hz); (2) action potential duration between the beginning and the negative trough superior to 1.1 ms. The spontaneous frequency and bursting activity of DA neurons were compared in naive LDTg^{GFP} and LDTg^{hM4} mice receiving an acute injection of either saline or CNO. The neuron response to these i.p. injections was determined by the differences between the maximum of fluctuation on a 3 min period before and after injection.

Immunohistochemistry. Mice were deeply anaesthetized with pentobarbital (Centravet, France) and transcardially perfused with cold phosphate buffer (PB: 0.1 M $\text{Na}_2\text{HPO}_4/\text{NaH}_2\text{PO}_4$, pH 7.4), followed by 4% paraformaldehyde (PFA) in PB 0.1 M. Brains were post-fixed overnight in 4% PFA-PB. Free-floating vibratome sections (50 μm) were obtained, and correct retrobeads and AAVs injections were confirmed for each animal.

To specifically label VTA DA neurons, midbrain sections were incubated (30 min) in PBS-BT (phosphate-buffered saline (PBS), 0.5% bovine serum albumin, 0.1% Triton X-100) with 10% normal goat serum (NGS). Sections were then incubated (4 °C) in PBS-BT, 1% NGS, with mouse anti-tyrosine hydroxylase (1/1000; Millipore Cat MAB318 lot 2211927) for 36 h. Sections were rinsed in PBS and incubated (2 h) in goat anti-mouse Alexa488 secondary antibody (1:1000, Vector Laboratories, Burlingame, CA) in PBS-BT, 1% NGS. Sections were rinsed with PBS and incubated 5 min with DAPI before mounting with Moviol. Similar procedures were followed to label c-Fos-, NeuN-, and cholinergic-positive neurons, using primary anti-c-Fos (1:1000, anti-rabbit, Abcam Cat Ab190289 lot GR266619-1), anti-NeuN (1:1000; anti-mouse, Millipore Cat MAB377 lot 2279235), anti-DsRed (1:1000, anti-rabbit, Clontech Cat 632496 lot 632496), anti-mCherry (1:1000, anti-chicken, Abcam Cat ab205402 lot AV4500E), and anti-vesicular acetylcholine transporter (1:1000, anti-guinea pig, Chemicon Cat AB1588 lot 52817⁵⁸), respectively. For c-Fos counting, LDTg^{CHAT-mCherry} or LDTg^{Vglut-mCherry}

mice were killed one hour after an acute social defeat episode (5 min) and brain sections obtained as described above. Double c-Fos/mCherry immunohistochemistry was conducted and images acquired with an Olympus FV10 confocal microscope. Cell counting was done manually by an experimenter blind to the conditions using Image J.

Data analysis. Data are presented as means \pm SEM and were analyzed using GraphPad Prism 7. Following a D'Agostino-Pearson's test, determining the normality of the distributions, statistical analyses were carried out using two-way analysis of variance with repeated measures when required. Post hoc Sidak's test was used when appropriate. Statistical significance was set at $P < 0.05$.

Data availability

The data that support these findings of this study are available from the corresponding author upon reasonable request.

Received: 26 October 2017 Accepted: 19 September 2018

Published online: 25 October 2018

References

- Smith, K. Mental health: a world of depression. *Nat. News* **515**, 180 (2014).
- Slattery, D. A. & Cryan, J. F. Modelling depression in animals: at the interface of reward and stress pathways. *Psychopharmacology (Berl.)* **234**, 1451–1465 (2017).
- Admon, R. & Pizzagalli, D. A. Dysfunctional reward processing in depression. *Curr. Opin. Psychol.* **4**, 114 (2015).
- Russo, S. J. & Nestler, E. J. The brain reward circuitry in mood disorders. *Nat. Rev. Neurosci.* **14**, 609–625 (2013).
- Bromberg-Martin, E. S., Matsumoto, M. & Hikosaka, O. Dopamine in motivational control: rewarding, aversive, and alerting. *Neuron* **68**, 815–834 (2010).
- Pignatelli, M. & Bonci, A. Role of dopamine neurons in reward and aversion: A Synaptic Plasticity Perspective. *Neuron* **86**, 1145–1157 (2015).
- Gray, J. M., Chaouloff, F. & Hill, M. N. To in *Current Protocols in Neuroscience* (John Wiley & Sons, Inc., 2001). <https://doi.org/10.1002/0471142301.ns0833s70>
- Barik, J. et al. Chronic stress triggers social aversion via glucocorticoid receptor in dopaminergic neurons. *Science* **339**, 332–335 (2013).
- Chaudhury, D. et al. Rapid regulation of depression-related behaviours by control of midbrain dopamine neurons. *Nature* **493**, 532–536 (2013).
- Krishnan, V. & Nestler, E. J. The molecular neurobiology of depression. *Nature* **455**, 894–902 (2008).
- Krishnan, V. et al. Molecular adaptations underlying susceptibility and resistance to social defeat in brain reward regions. *Cell* **131**, 391–404 (2007).
- Watabe-Uchida, M., Zhu, L., Ogawa, S. K., Vamanrao, A. & Uchida, N. Whole-brain mapping of direct inputs to midbrain dopamine neurons. *Neuron* **74**, 858–873 (2012).
- Lodge, D. J. & Grace, A. A. The laterodorsal tegmentum is essential for burst firing of ventral tegmental area dopamine neurons. *Proc. Natl Acad. Sci. USA* **103**, 5167 (2006).
- Wang, H.-L. & Morales, M. Pedunculopontine and laterodorsal tegmental nuclei contain distinct populations of cholinergic, glutamatergic and GABAergic neurons in the rat. *Eur. J. Neurosci.* **29**, 340–358 (2009).
- Blahe, C. D. et al. Modulation of dopamine efflux in the nucleus accumbens after cholinergic stimulation of the ventral tegmental area in intact, pedunculopontine tegmental nucleus-lesioned, and laterodorsal tegmental nucleus-lesioned rats. *J. Neurosci.* **16**, 714–722 (1996).
- Lammel, S. et al. Input-specific control of reward and aversion in the ventral tegmental area. *Nature* **491**, 212–217 (2012).
- Golden, S. A., Iii, H. E. C., Berton, O. & Russo, S. J. A standardized protocol for repeated social defeat stress in mice. *Nat. Protoc.* **6**, 1183–1191 (2011).
- Roth, B. L. DREADDs for neuroscientists. *Neuron* **89**, 683–694 (2016).
- Juarez, B. & Han, M.-H. Diversity of dopaminergic neural circuits in response to drug exposure. *Neuropsychopharmacology* **41**, 2424–2446 (2016).
- Borgius, L., Restrepo, C. E., Leao, R. N., Saleh, N. & Kiehn, O. A transgenic mouse line for molecular genetic analysis of excitatory glutamatergic neurons. *Mol. Cell. Neurosci.* **45**, 245–257 (2010).
- Morel, C. et al. Nicotinic receptors mediate stress-nicotine detrimental interplay via dopamine cells' activity. *Mol. Psychiatry* **23**, 1597–1605 (2017).
- Dani, J. A. & Bertrand, D. Nicotinic acetylcholine receptors and nicotinic cholinergic mechanisms of the central nervous system. *Annu. Rev. Pharmacol. Toxicol.* **47**, 699–729 (2007).

23. Henckens, M. J. A. G., Deussing, J. M. & Chen, A. Region-specific roles of the corticotropin-releasing factor-urocortin system in stress. *Nat. Rev. Neurosci.* **17**, 636–651 (2016).
24. Gonzales, K. K. & Smith, Y. Cholinergic interneurons in the dorsal and ventral striatum: anatomical and functional considerations in normal and diseased conditions. *Ann. N. Y. Acad. Sci.* **1349**, 1–45 (2015).
25. Picciotto, M. R., Higley, M. J. & Mineur, Y. S. Acetylcholine as a neuromodulator: cholinergic signaling shapes nervous system function and behavior. *Neuron* **76**, 116–129 (2012).
26. Hikida, T. et al. Increased sensitivity to cocaine by cholinergic cell ablation in nucleus accumbens. *Proc. Natl Acad. Sci. USA* **98**, 13351–13354 (2001).
27. Jiang, L. et al. Cholinergic signaling controls conditioned fear behaviors and enhances plasticity of cortical-amygdala circuits. *Neuron* **90**, 1057–1070 (2016).
28. Janowsky, D. S., el-Yousef, M. K., Davis, J. M. & Sekerke, H. J. A cholinergic-adrenergic hypothesis of mania and depression. *Lancet Lond. Engl.* **2**, 632–635 (1972).
29. Fritze, J. The adrenergic-cholinergic imbalance hypothesis of depression: a review and a perspective. *Rev. Neurosci.* **4**, 63–93 (1993).
30. Mineur, Y. S. et al. Cholinergic signaling in the hippocampus regulates social stress resilience and anxiety- and depression-like behavior. *Proc. Natl Acad. Sci. USA* **110**, 3573–3578 (2013).
31. Risch, S. C. et al. Physostigmine induction of depressive symptomatology in normal human subjects. *Psychiatry Res.* **4**, 89–94 (1981).
32. Faure, P., Tolu, S., Valverde, S. & Naudé, J. Role of nicotinic acetylcholine receptors in regulating dopamine neuron activity. *Neuroscience* **282**, 86–100 (2014).
33. Mansvelder, H. D. & McGehee, D. S. Long-term potentiation of excitatory inputs to brain reward areas by nicotine. *Neuron* **27**, 349–357 (2000).
34. Jones, I. W. & Wonnacott, S. Precise localization of $\alpha 7$ nicotinic acetylcholine receptors on glutamatergic axon terminals in the rat ventral tegmental area. *J. Neurosci.* **24**, 11244–11252 (2004).
35. Kourrich, S., Calu, D. J. & Bonci, A. Intrinsic plasticity: an emerging player in addiction. *Nat. Rev. Neurosci.* **16**, 173–184 (2015).
36. Beier, K. T. et al. Circuit architecture of VTA dopamine neurons revealed by systematic input-output mapping. *Cell* **162**, 622–634 (2015).
37. Daftary, S. S., Panksepp, J., Dong, Y. & Saal, D. B. Stress-induced, glucocorticoid-dependent strengthening of glutamatergic synaptic transmission in midbrain dopamine neurons. *Neurosci. Lett.* **452**, 273–276 (2009).
38. Knowland, D. et al. Distinct ventral pallidal neural populations mediate separate symptoms of depression. *Cell* **170**, 284–297.e18 (2017).
39. Isingrini, E. et al. Resilience to chronic stress is mediated by noradrenergic regulation of dopamine neurons. *Nat. Neurosci.* **19**, 560–563 (2016).
40. Xiao, C. et al. Cholinergic mesopontine signals govern locomotion and reward through dissociable midbrain pathways. *Neuron* **90**, 333–347 (2016).
41. Cryan, J. F. & Holmes, A. The ascent of mouse: advances in modelling human depression and anxiety. *Nat. Rev. Drug. Discov.* **4**, 775–790 (2005).
42. Tye, K. M. et al. Dopamine neurons modulate neural encoding and expression of depression-related behaviour. *Nature* **493**, 537–541 (2013).
43. Chang, C. & Grace, A. A. Amygdala-ventral pallidum pathway decreases dopamine activity after chronic mild stress in rats. *Biol. Psychiatry* **76**, 223–230 (2014).
44. Friedman, A. K. et al. Enhancing depression mechanisms in midbrain dopamine neurons achieves homeostatic resilience. *Science* **344**, 313–319 (2014).
45. Gomez, J. L. et al. Chemogenetics revealed: DREADD occupancy and activation via converted clozapine. *Science* **357**, 503–507 (2017).
46. Sauvage, M. & Steckler, T. Detection of corticotropin-releasing hormone receptor 1 immunoreactivity in cholinergic, dopaminergic and noradrenergic neurons of the murine basal forebrain and brainstem nuclei – potential implication for arousal and attention. *Neuroscience* **104**, 643–652 (2001).
47. Gordon, J. A. On being a circuit psychiatrist. *Nat. Neurosci.* **19**, 1385–1386 (2016).
48. Paxinos and Franklin's the Mouse Brain in Stereotaxic Coordinates - 4th edn. Available at: <https://www.elsevier.com/books/paxinos-and-franklins-the-mouse-brain-in-stereotaxic-coordinates/paxinos/978-0-12-391057-8> (accessed 19 September 2018)
49. Zhao-Shea, R. et al. Increased CRF signaling in a ventral tegmental area-interpeduncular nucleus-medial habenula circuit induces anxiety during nicotine withdrawal. *Nat. Commun.* **6**, 6770 (2015).
50. Burnett, C. J. & Krashes, M. J. Resolving behavioral output via chemogenetic designer receptors exclusively activated by designer drugs. *J. Neurosci.* **36**, 9268–9282 (2016).
51. Mahler, S. V. et al. Designer receptors show role for ventral pallidum input to ventral tegmental area in cocaine seeking. *Nat. Neurosci.* **17**, 577–585 (2014).
52. Ungless, M. A. & Grace, A. A. Are you or aren't you? Challenges associated with physiologically identifying dopamine neurons. *Trends Neurosci.* **35**, 422–430 (2012).
53. Zhao, S. et al. Generation of embryonic stem cells and transgenic mice expressing green fluorescence protein in midbrain dopaminergic neurons. *Eur. J. Neurosci.* **19**, 1133–1140 (2004).
54. Margolis, E. B., Mitchell, J. M., Ishikawa, J., Hjelmstad, G. O. & Fields, H. L. Midbrain dopamine neurons: projection target determines action potential duration and dopamine D2 receptor inhibition. *J. Neurosci.* **28**, 8908–8913 (2008).
55. Cao, J.-L. et al. Mesolimbic dopamine neurons in the brain reward circuit mediate susceptibility to social defeat and antidepressant action. *J. Neurosci.* **30**, 16453–16458 (2010).
56. Lammel, S., Ion, D. I., Roeper, J. & Malenka, R. C. Projection-specific modulation of dopamine neuron synapses by aversive and rewarding stimuli. *Neuron* **70**, 855–862 (2011).
57. Mameli-Engvall, M. et al. Hierarchical control of dopamine neuron-firing patterns by nicotinic receptors. *Neuron* **50**, 911–921 (2006).
58. Herzog, E. et al. Expression of vesicular glutamate transporters, VGLUT1 and VGLUT2, in cholinergic spinal motoneurons. *Eur. J. Neurosci.* **20**, 1752–1760 (2004).

Acknowledgements

This work was supported by the CNRS, Institut Universitaire de France, Fondation pour la Recherche Médicale, Fédération pour la Recherche sur le Cerveau and ANR (ANR-13-JSV4-0004 MECANOS) to J.B., ANR-16 NICOStress and INCa to P.F. and J.B. We thank Drs Borgius and Kiehn (Karolinska Institutet, Sweden) for providing the vglut2-Cre transgenic mice and Dr Mark Ungless for PITX3-GFP mice. We thank Drs Meye (University Medical Center of Utrecht) and Mameli (University of Lausanne) for critical comments on the manuscript.

Author contributions

S.P.F. performed viral injections and in vitro electrophysiology. S.P.F., J.B., and L.B. conducted behavioral experiments. L.B., T.C., and M.S.R. performed microscopy. F.M. performed viral injection, in vivo electrophysiology, and analyzed data. X.M. performed ELISA experiments. P.F. and H.M. provided intellectual and technical inputs. J.B. designed the project. J.B. and S.P.F. analyzed data and wrote the manuscript. All authors provided feedback on writing the manuscript.

Additional information

Supplementary Information accompanies this paper at <https://doi.org/10.1038/s41467-018-06809-7>.

Competing interests: The authors declare no competing interests.

Reprints and permission information is available online at <http://npg.nature.com/reprintsandpermissions/>

Publisher's note: Springer Nature remains neutral with regard to jurisdictional claims in published maps and institutional affiliations.



Open Access This article is licensed under a Creative Commons Attribution 4.0 International License, which permits use, sharing, adaptation, distribution and reproduction in any medium or format, as long as you give appropriate credit to the original author(s) and the source, provide a link to the Creative Commons license, and indicate if changes were made. The images or other third party material in this article are included in the article's Creative Commons license, unless indicated otherwise in a credit line to the material. If material is not included in the article's Creative Commons license and your intended use is not permitted by statutory regulation or exceeds the permitted use, you will need to obtain permission directly from the copyright holder. To view a copy of this license, visit <http://creativecommons.org/licenses/by/4.0/>.

© The Author(s) 2018

Third contribution

Dopamine and stress signalling interplay patterns of social organization in mice

Battivelli D, Vernochet C, Nguyen C, Zayed A, Meirsmann A.C, Messaoudene S, Fieggen A, Dreux G, Marti F, Contesse T, Barik J, Tassin J, Faure P, Parnaudeau S, Tronche F

In preparation, early access on BioRxiv, Article number: 856781

Summary

In the following study, we parsed the mechanisms of social hierarchy in mouse colony. We combined the use of behavioral and chemogenetic tools to assess the function of VTA in social hierarchy. We found social rankings to be correlated to susceptibility to aspects of cocaine addiction and depression-like phenotype in mice. We illustrated that DA neurons activity in the VTA and that the glucocorticoid receptor in dopamine-sensing neurons modulate social rank. Finally, we show that VTA DA neuronal activity inversely correlates with social rankings in mice.

Contribution

I contributed in this project in the formation of behavioral groups and the realization of viral injections to chemogenetically modulate the activity of VTA DA neurons.

Dopamine and stress signalling interplay patterns social organization in mice.

Dorian Battivelli¹, Cécile Vernochet¹, Claire Nguyen², Abdallah Zayed¹, Aura Carole Meirsman¹, Sarah Messaoudene¹, Alexandre Fieggen¹, Gautier Dreux¹, Fabio Marti², Thomas Contesse^{3,4}, Jacques Barik^{3,4}, Jean-Pol Tassin¹, Philippe Faure², Sébastien Parnaudeau^{1*}, François Tronche^{1*}

¹ Gene Regulation and Adaptive Behaviours group, Neuroscience Paris Seine, UMR8246, Centre National de la Recherche Scientifique (CNRS), INSERM U1130, Sorbonne Université (SU) UMCR18, Institut de Biologie Paris Seine, 75005, Paris, France.

² Neurophysiology and Behaviour group, Neuroscience Paris Seine, UMR8246, Centre National de la Recherche Scientifique (CNRS), INSERM U1130, Sorbonne Université (SU) UMCR18, Institut de Biologie Paris Seine, 75005, Paris, France.

³ Université Côte d'Azur, Nice, France

⁴ Institut de Pharmacologie Moléculaire & Cellulaire, CNRS UMR7275, Valbonne, France.

* co-last authors.

Correspondence to François Tronche (francois.tronche@sorbonne-universite.fr) and Sébastien Parnaudeau (sebastien.parnaudeau@upmc.fr)

Keywords: social ranking, interindividual behavioural differences, dopamine, psychopathologies, glucocorticoid receptor.

Abstract

The rules leading to the emergence of a social organization and the role of social hierarchy on normal and pathological behaviours remain elusive. Here we show that groups of four isogenic male mice rapidly form enduring social ranks in a dominance hierarchy. Highest ranked individuals display enhanced anxiety and working memory, are more social and more susceptible to stress-related maladaptive behaviours. Are these differences causes or consequences to social life? We show that anxiety emerges from life in colony whereas sociability is a pre-existing trait. Strikingly, highest ranked individuals exhibit lower bursting activity of VTA dopamine neurons. Both pharmacogenetic inhibition of this neuronal population and the genetic inactivation of glucocorticoid receptor signalling in dopamine-sensing brain areas promote the accession to higher social ranks. Altogether, these results indicate that the shaping of social fate relies upon the interplay of dopamine system and stress response, impacting individual behaviour and potentially mental health.

Introduction

Social organization is readily observable across vertebrate species and can result in the establishment of a social hierarchy that may minimize energy costs due to direct competitions for resources among congeners (Tinbergen, 1939; Francis, 1984). At the group level this may improve adaptation to the environmental demands. At the individual level, it exposes different congeners to distinct experiences and participates to the emergence of individuality that distinguishes it from others (Bergmüller and Taborsky, 2010; Lathe, 2004). This corresponds to repeatability and consistency of an animal individual behaviour in the face of environmental and social challenges, which translates into different strategies to find food, deal with predators, or compete with conspecifics.

Mice are social vertebrates, living in hierarchical structures of 4 to 12 adult members (Berry and Bronson, 1992; Beery and Kaufer, 2015) that share territorial defence and exhibit a large repertoire of behaviours (e.g. physical exploration, vocal communication, aggression, social

recognition, imitation, empathy) that characterize sociability. The social rank of individuals can be determined based on observations of antagonistic interactions, territorial marking, access to limited resources and by precedence behaviours (Zhou *et al.*, 2018). The driving forces underlying the emergence of social organization remain largely unknown. Although these include genetic factors, however, the fact that social hierarchy is observed within groups of genetically identical congeners suggests that environmental factors are in play. Among these, the stress response and more specifically glucocorticoids release has been suspected to influence social dominance in a variety of species, although a clear link has yet to be drawn (Sapolsky, 2004; Creel *et al.*, 2013).

Hierarchy establishment involves iterative pairwise interactions that have consequences on the behavioural fate of each individual (Cordero and Sandi, 2007; Timmer and Sandi, 2010). Indeed, specific behavioural patterns emerge in genetically identical mice raised in semi-naturalistic environments (Freund *et al.*, 2013; Hager *et al.*, 2014; Torquet *et al.*, 2018), and differences in behavioural traits have been attributed to social ranking in smaller colonies (Wang *et al.*, 2011; Larrieu *et al.*, 2017). Whether such individual differences pre-exist the formation of the social group is unclear, and the physiological mechanisms implicated in hierarchical segregation remain elusive. Beyond understanding the principles of interindividual behavioural diversity in animals, these questions are also relevant in humans, in a psychopathological context, since social status is recognized as a vulnerability risk factor for psychiatric diseases including mood disorders and addiction (Kessler, 1994; Wilkinson, 1999; Lorant, 2003; Singh-Manoux *et al.*, 2005).

The mesocorticolimbic system that encompasses the prefrontal cortex (PFC), the nucleus accumbens (NAcc) and their dopaminergic input from the ventral tegmental area (VTA) could participate to the emergence of social hierarchy and behavioural diversity. This brain system modulates a broad spectrum of behaviours, including motivation and decision-making involved in social context (Gunaydin *et al.*, 2014). VTA dopamine neurons activity conditions social avoidance following social defeats (Chaudhury *et al.*, 2013; Barik *et al.*, 2013). The interaction between stress-evoked release of glucocorticoids and dopamine system is critical for this effect

and relies on the activation of glucocorticoid receptors (GR) present in dopamine-sensing areas neurons (Barik *et al.*, 2013). Several structures receiving dopaminergic inputs have been recently associated with the emergence of social ranking. Modulating the synaptic efficacy in medial PFC neurons causes individual bidirectional shifts within social ranking (Wang *et al.*, 2011), and lower mitochondrial activity within the NAcc is associated to lower social ranking in both rats and mice (Hollis *et al.*, 2015; Larrieu *et al.*, 2017).

In this study, we examine the segregation of individual behaviours with social status in colonies of four genetically identical male mice (tetrads). We investigated whether pre-existing behavioural and physiological differences shape the social fate of individuals or whether such differences emerge from social life. Finally, we provide evidence for an implication of mesocorticolimbic dopamine system and stress response signalling in the establishment of social hierarchy and individuation of behaviours.

Results

Social ranks within tetrads are stable over long periods

We formed colonies of four age and weight matched adult C57BL/6J male mice of six weeks, previously unknown to each other. Two to four weeks later, we analysed the social ranks of animals. We first used a precedence test based on encounters within a plastic tube between each possible congener pairs among a tetrad. It allows to identify lower ranked individuals as they come out of the tube walking backward (Wang *et al.*, 2011) (Fig. 1a). The six possible pairwise combinations of individuals from a tetrad were tested three consecutive times a day, and the one with the highest number of forward exits was classified as higher ranked. We tested each tetrad daily, for at least six days, until the highest (rank 1 rated R1) and the lowest ranks (rank 4 rated R4) were stable over 3 consecutive days.

Among 60 tetrad colonies, the stability criterion was reached faster for the extreme ranks (Fig. 1b). Half of R1 and R4 mice were already having a stable status on days 3 and 5, respectively. All of them were stable after 12 days whereas a quarter of ranks 2 (R2) and rank 3 (R3) animals

were not. As observed by Wang *et al.*, 2011, the rank of individuals conditioned the duration of contests. Confrontations between R1 and R2 individuals lasted for an average of 18 seconds whereas confrontations involving R4 lasted twice less (Fig. 1c).

Once established, social ranking was stable over long periods. Fig. 1d pictures social fate of individuals from 12 tetrads repeatedly assessed through 5 sessions during a period of 3 months. This is particularly true for R4 individuals (Fig. 1d, lighter blue lines) as 17 weeks later, eleven out of twelve mice remained at the lowest rank. Among initially highest ranked individuals, ten and seven, out of twelve, kept the same ranking, 14 and 17 weeks later, respectively (Fig. 1d, darker blue lines). One progressively decreased ranking, to end in R4, one ended in R3 and three in R2. Animals with initial intermediate ranks displayed the highest switching in rankings but 19 out of 24 still ended by reaching an intermediate rank (Fig. 1d, medium blue and grey lines). During this period of time, mice were regularly weighted, and no correlation between social rank and weight evolution was found (data not shown).

To validate precedence behaviour as a reliable proxy for social ranking we quantified other expressions of social dominance, such as access to shared resources or territoriality. Higher ranked individuals in the tube-test showed significantly longer total occupancy of a small warm spot within a cold cage during the 20 minutes of the test (Fig. 1e) compared to their three other cage-mates, with 3 to 4 times longer episodes. Urine marking patterns were collected on absorbent paper from a box occupied by R1 and R4 individuals separated by a transparent and perforated wall for 2 hours and visualized under U.V. light (extended data Fig. 1a). 17 out of 23 top-ranked individuals in the tube-test also showed dominant urine marking patterns, in either the number of marks or their cumulated area, when compared with lower ranked congeners.

Social rank correlates with behavioural differences.

We compared behaviour between higher (R1) and lower (R4) socially ranked individuals. We did not see differences neither in locomotor activity, measured in an open-field (data not

shown), nor in stress-coping, measured by quantifying immobility and escape behaviours in the forced-swim test for two consecutive days (Fig. 2a).

In contrast, anxiety-like behaviour and sociability markedly differed between social ranks, highest ranked individuals being more anxious and more sociable than lower ranked ones. We quantified anxiety-like behaviour approach-avoidance conflict tests based on the mouse innate avoidance of open and lit spaces (Fig. 2b). When measuring anxiety of isogenic mice, high interindividual differences are classically observed, as in Fig. 2b (grey dots). Considering individual social ranks allow to stratify the population into two distinct groups with regards to anxiety-like behaviours. R1 individuals, more anxious, spent significantly less time in the open section of an elevated O-maze (Fig. 2b, left dark blue), as well as in the lit compartment of a dark-light box (Fig. 2b, right dark blue). We also compared sociability and social memory between R1 and R4 mice in a three-chamber test. As expected, C57BL/6 mice display a marked preference for a social stimulus (Fig. 2c, social preference, grey bars). Stratification of the results taking into account the social rank of individuals shows that only the R1 individuals, and not the R4, displayed social preference (Fig. 2c, social preference, right panel, dark and light blue bars, respectively). However, social rank does not affect social memory or social novelty. Mice of both ranks have a similar natural preference for interacting with an unfamiliar conspecific vs a familiar one (Fig. 2c, lower panel).

During manipulations of the tetrads, R4 mice frequently showed aggressive behaviours towards their cage-mates. We performed a resident-intruder test, repeated for two consecutive days with individuals from 10 tetrads. From half of them, at least one R1 or R4 mice attacked the intruder. For these pairs, we quantified the interactions with the intruder (extended data Fig 2). On the first day, R4 individuals displayed significantly more aggressive behaviours, including clinch attacks, lateral threats, chases, upright postures and bite attempts whereas R1 individuals had more prosocial behaviour (grooming of the intruder). On the second day this difference was more pronounced. Whereas none of the R1 individuals attacked the intruder, all R4 mice did within the first 130 seconds and did significantly more rattling.

We then addressed whether social ranking could also affect cognitive abilities. We studied spatial working memory in a non-match-to-sample T-maze task (Fig. 2d, upper panel). In this task, mice are placed within a T-Maze and can access a reward placed into the unique open arm (forced phase). They are required to retain a memory trace of a recently sampled maze location during a delay period (delay phase) and then prompted to select the opposite location in order to receive a reward (choice phase). Each mouse was tested 10 times a day, and the learning criterion was defined as a minimum of 7 correct choices for 3 consecutive days. Although both groups of mice learned the task, R1 individuals did it significantly faster compared to R4 (Fig. 2d, lower panel).

Differences in sociability but not anxiety-like behaviours pre-exist to social rank establishment

The behavioural differences between ranks could emerge from initially similar mice as a consequence of social adaptation within members of a tetrad. Alternatively, these differences could pre-exist before their gathering, and shape individual social ranking trajectories. To address this question, we compared behaviours of individuals before grouping them in tetrads, and after the formation of the social colony. As mentioned before, anxiety-like behaviours were markedly enhanced for highest ranked individuals compared to lowest ones. This behavioural difference seems to emerge from social organization since no difference was observed between future R1 and R4 mice, before they were pooled together, in elevated O-maze and in dark-light tests. The time spent in open arms and in the lit compartment were similar for these two groups, as well as for the future ranks 2 and 3 (Fig. 3b). In contrast differences in sociability seem to pre-exist to life in colony. Future R1 mice have already a marked interest for social interactions before social life in tetrads, similar to that observed once the tetrad is formed (Fig. 3c, dark blue bars, left panel), whereas future R4 have not. Interestingly, intermediate ranks have an intermediate phenotype with a significant but lower preference. R1 and R4 mice did not present differences in despair-like behaviour, thus as expected we did not observe any differences between future R1 and R4 (Fig. 3a) individuals.

Social rank conditions sensitivity to some preclinical models of psychopathologies

In human, low social status, is associated with reduced life span (Stringhini *et al.*, 2017) and negative health consequences including chronic cardiovascular, immune, metabolic and psychiatric disorders). In a variety of social vertebrate species, associations between social rank and health outcomes have been documented (Sapolsky, 2005). We investigated whether highest and lowest ranked individuals within tetrads would respond distinctly to two established preclinical models of mental disorders in mice.

The locomotor sensitization to cocaine is a gradual and enduring facilitation of locomotor activity promoted by repeated cocaine exposure, believed to reflect the reinforcing effects of abused drugs (Robinson and Berridge, 2000). Five days of daily cocaine injections (10 mg.kg^{-1}) led to a gradual increase of locomotion during the hour following the drug administration in both R1 and R4 mice (Fig. 4a). This increased locomotor response was maintained after a withdrawal period of 6 days as assessed after a challenge injection (Fig. 4a, day 12). While this result clearly shows that both R1 and R4 individuals exhibit significant locomotor sensitization to cocaine, R4 individuals appeared more sensitive. Indeed, R4 mice showed enhanced responses during the five consecutive cocaine injection days, and an even more pronounced hypersensitivity during the challenge day (Fig 4a, right panel).

Repeated social defeats is a well-validated mouse model of depression, marked by a lasting social aversion, which allows to distinguish animals that exhibit depressive-like symptoms (susceptible) from those which are resilient to stress (Krishnan *et al.*, 2007). Highest and lowest ranked mice from eight tetrads were daily subjected to 5 minutes social defeats for 10 consecutive days by an unfamiliar aggressor and remain in sensory (but physical) contacts for the rest of the day (Fig. 4b, left panel). We quantified in an open field the time of interaction with an empty plastic box vs a box containing an unfamiliar male mouse, before and after social defeat (Fig 4b middle panel). After social defeats, 7 out of the 16 mice challenged developed a social aversion (Fig. 4b right panel, orange lines). Among them only one was a

R1 individual. In other words, majority of R1 individuals (87.5%) were resilient whereas only 25% of R4 ones were.

Dopamine neurons activity in the ventral tegmental area and glucocorticoid receptor in dopamine-sensing neurons modulate social rank attainment.

Stress response and glucocorticoids release is a major risk factor for psychopathologies. We and other have shown that the interplay between stress response and the dopamine reward pathway plays a major role in stress-induced depressive behaviour and responses to addictive drugs (Ambroggi *et al.*, 2009; Barik *et al.*, 2010; Barik *et al.*, 2013). Several lines of evidence suggest that both systems could play a significant role in rank establishment. We first compared dopamine utilization in R1 and R4 individuals in key brain regions innervated by midbrain dopamine neurons.

We measured in the caudate putamen (CPu), the NAcc, and the PFC the tissue contents of dopamine (DA) and 3,4- dihydroxyphenylacetic acid (DOPAC), a metabolite produced following dopamine reuptake. The DOPAC/DA ratio thus gives an index of dopamine utilization (Fig. 5a left graph). We did not observe any difference in the CPu, a structure mostly innervated by dopamine cells located in the substantia nigra pars compacta (SNc). In the NAcc, we noted a trend towards a decreased dopamine utilization in R1 individuals when compared to R4 ones, although the difference did not reach significance (Fig. 5a). In striking contrasts, in the PFC, R1 individuals displayed a marked increase of dopamine release. Overall, we showed a dopamine utilization characterized by a stronger PFC/NAcc ratio in R1 mice compared to R4 ones (Fig. 5a right graph). Since both the NAcc and the PFC are mainly innervated by dopamine cells located in the VTA, we investigated whether differences could exist in their activity between R1 and R4 individuals. We performed juxtacellular single-unit recordings in anesthetized mice. The analysis of 186 neurons from 10 R1 mice and 157 neurons from 10 R4 mice revealed that whereas the frequency of spontaneous firing was similar in both ranks (Fig. 5b, left graph), the percentage of spikes within bursts was significantly lower in R1 individuals (Fig. 5b, right graph).

Reduced activity of VTA dopamine neurons facilitates higher ranking.

Glucocorticoid receptor (GR) gene inactivation in dopamine innervated areas results in lower VTA dopamine neurons activity, similar to that observed in R1 mice (Ambroggi *et al.*, 2009; Barik *et al.*, 2013). Further, we showed that it facilitates resilience to social defeat by preventing the appearance of social withdrawal and reduces behavioural responses to cocaine (Ambroggi *et al.*, 2009; Barik *et al.*, 2010; Barik *et al.*, 2013). We thus examined whether GR signalling within the dopamine reward pathway could influence social ranking in tetrads. We grouped one adult GR^{D1aCre} mice with three unfamiliar control (GR^{loxP/loxP}) individuals (Fig 5c, left graph) and assessed their social rank in tube-test two weeks later. Within 5 tetrads out of 7, GR^{D1aCre} mice ended on the highest rank, in one it was ranked second and in one fourth (Fig 5c, middle panel). Analysing tube-test individual contests during the last three days of ranking determination, we observed that mutant mice have a significantly higher probability to win. Out of 189 contests involving a mutant and a control mouse, mutant ones won 139.

These results raise the possibility that stress-response might influence social fate by impacting on the mesolimbic dopamine neurons. To test the causality between low VTA dopamine neurons activity and higher social rank, we assessed the impact of inhibiting this cell population on social hierarchy. To do so, we expressed a modified human muscarinic receptor Gi coupled hM4D specifically in VTA dopamine neurons, using an adeno-associated virus expression system (AAV8-hSyn-DIO-hM4D(Gi)-mCherry), stereotactically injected into the VTA of mice expressing the Cre recombinase in dopamine neurons (BAC-DATiCre -Turiault *et al.*, 2007-, VTA^{inhib} mice, Fig. 5d). The hM4D receptor is activated solely by a pharmacologically inert compound, clozapine-N-oxide (CNO). Upon CNO activation, hM4D hyperpolarizes neurons through a Gi protein mediated activation of inward-rectifying potassium channels (Armbruster *et al.*, 2007). Control animals were C57B/L6 mice similarly injected with AAV8-hSyn-GFP particles. Tetrads composed of one VTA^{inhib} mouse and three control mice were formed and permanently treated with CNO in drinking water (10 mg L⁻¹, Fig. 5d left). After analysis of the social hierarchy in these tetrads, we observed that permanently reducing the activity of VTA

dopamine neurons increased the probability of the individual to reach the highest rank, (Fig. 5d middle) and significantly increased the number of tube test wins. Out of 171 contests involving a VTA^{inhib} and a control mouse, VTA^{inhib} ones won 118 (Fig. 5d right). In another experimental design, we tested the effect of acute dopamine neurons inhibition on tube test performance. We found that a single injection of CNO (1 mg kg⁻¹) 30 minutes before tube test contests changed neither the rank of VTA^{inhib} mice, nor their probability to win a contest in already established tetrads (extended data Fig. 5, Day 1). However, after several days of CNO injections, their probability to win a contest seemed to increase (from 49,2 ± 15,9 % on day 1 to 67,5 ± 14,7 % on day 5, n=7 individuals), strengthening the idea that VTA dopamine neurons activity is rather important for the process of hierarchy establishment than for punctual tube test performance (extended data Fig. 5).

Discussion

Within a few days, genetically identical mice living in small groups of four individuals establish a social organization. The social hierarchy can be determined observing differential precedence in displacements as in tube-test (Wang *et al.*, 2011; Larrieu *et al.*, 2017) and differential access to resources, as a warm spot in a cold environment. The attained social rank is stable over month periods, with limited switch between ranks within a tetrad. These switches are almost absent for the lowest ranked individuals and rarely observed for the highest ones. They are frequent for the two intermediate ranks that also take a longer time to stabilize during the first tube-test session. Behavioural analyses usually present an important interindividual variability and social ranking might at least partly account for this phenomenon. We showed, in agreement with Larrieu *et al.* (2017) that used the same ranking methods, that highest ranked mice exhibit indeed higher anxiety-like behaviours and increased social interactions. Varholick *et al.* (2018) did not however observe this correlation. This discrepancy may rely on the limited number of animals tested, or on the approach they chose to identify ranking, with sparser tube tests, performed once a week for three weeks. Few other studies

that used other criteria to identify dominant individuals, such as aggressiveness, have been carried out leading to conflicting results. As such, Hilakivi *et al.* (1989) reported no difference whereas Ferrari *et al.* (1998) saw an increased anxiety for dominant individuals. Similarly, the high dispersion of individual interaction time with a congener during sociability tests in isogenic mice can also be in part explained by their social rank. Highest ranked ones are indeed more sociable, in agreement with Kunkel and Wang (2018). This association of high anxiety and high sociability is surprising as in both humans and rodents, low anxiety is usually paired with increased sociability (Allsop *et al.*, 2014; Beery and Kaufer, 2015). For instance, oxytocin facilitates social behaviors and has well-known anxiolytic properties (Insel, 2010). In the same line, optogenetic stimulation of basolateral amygdala to ventral hippocampus circuit facilitates anxiety and impairs social interaction (Felix-Ortiz *et al.*, 2013; Felix-Ortiz and Tye, 2014). This associative rule is nevertheless not systematic. Similar to our observation in top ranked individuals, vasopressin promotes social behaviour and is also anxiogenic (Bielsky *et al.*, 2004).

A central but poorly explored question is whether the emergence of social ranks precedes the appearance of specific individual behavioural traits, or whether pre-existing individual differences channel the social status trajectory of an individual. Our study indicates that both situations occur. The anxiety of highest ranked animals clearly emerged following social life since no differences existed prior to rank establishment. A similar observation was made in outbred Swiss mice, housed in dyads and ranked upon their aggressiveness (Hilakivi-Clarke and Lister, 1992). On the contrary, in rats, a study showed that a high level of anxiety is a predisposing factor for social submission (Hollis *et al.*, 2015). In our study, while the increased anxiety seems to be the consequence of social ranking, the difference in sociability clearly pre-exists to the formation of the ranks within the colonies. The origin of this individual difference in behaviour most likely arises due to previous breeding and social housing conditions. It could have emerged in the first colony in which these animals were grouped. It could also occur from differences that appeared early, before weaning, since a study suggested that maternal care could shape adult social behaviour (Starr-Phillips and Beery, 2014).

Several studies point at the mesocorticolimbic system as a potential substrate for social ranking. In the NAcc, low mitochondrial activity has been causally linked with lower rank in dyadic contests (Hollis *et al.*, 2015). Also, increased activity and higher strength of excitatory inputs to the PFC layer V has been linked with higher social ranking (Wang *et al.*, 2011). Our study shows that VTA dopamine neurons exhibit differential activity depending on the rank, with a marked reduction of the bursting activity in R1 individuals. Several studies suggest a role for dopamine in social ranking from insects to mammals (Yamaguchi *et al.*, 2015). In ants, brain dopamine concentration is higher in socially dominant individuals (Penick *et al.*, 2014; Okada *et al.*, 2015). In birds and lizards, increased levels of dopamine in striatal structure have been observed in higher ranked individuals (McIntyre and Chew, 1983; Korzan *et al.*, 2006). In line with our results, reduced levels of dopamine have been shown in the NAcc of dominant rats (Jupp *et al.*, 2016).

Genetic evidence also sustains a link between dopaminergic neurotransmission and social status. Dopamine transporter gene is essential for sensing dopamine release and dopaminergic neurotransmission. Its inactivation in mice disorganizes social colonies (Rodríguez *et al.*, 2004), and genetic variants of the DAT gene are associated with social dominance in macaques (Miller-Butterworth *et al.*, 2007). Imaging studies in humans and non-human primates showed an enhanced availability of the striatal D2 receptor for individuals with dominant status. This could result from either higher level of D2 receptors or lower dopamine release (Nader *et al.*, 2012; Cervenka *et al.*, 2010; Martinez *et al.*, 2010). Neuropharmacological approaches also suggest a role for dopamine signalling in social ranking but the differences in strategies deployed (e.g. systemic vs local striatal injections in the NAcc) do not allow clear interpretation. Systemic administration of D2 receptor antagonist reduced social dominance in both mice and monkeys (Yamaguchi *et al.*, 2017a) whereas local injection into the NAcc of an agonist did not have an effect in rats (van der Kooij *et al.*, 2018). Similar experiments with a D1 receptor antagonist facilitated or did not modify social dominance in mice and monkeys (Yamaguchi *et al.*, 2017b) whereas local injection into the NAcc of an agonist increased dominance in rats (van der Kooij *et al.*, 2018). Interestingly,

changes in VTA dopamine cells activity are observed during the emergence of behavioural categories occurring within groups of dozens of mice living in complex semi-naturalistic environments (Torquet *et al.*, 2018). It would be interesting to study social ranking between these categories using precedence tests such as the tube test. The decreased firing in R1 mice was associated with a trend of decreased dopamine release in the NAcc as measured by the ratio DOPAC/DOPA, but also more surprisingly with an increased release in the PFC which could explain their enhanced working memory ability. This apparent discrepancy between our electrophysiology data and the increased cortical release of dopamine is likely due to the fact that only a minority of the dopamine cells in the VTA project to the PFC (Bjorklund and Lindvall, 1984).

Dysregulation of the mesocorticolimbic system is a key feature of several stress-related behavioural psychopathologies, including addiction and depression that develop with a high interindividual variation that is not fully understood (Robinson and Berridge, 2000; Russo *et al.*, 2012). The differences of cortical/subcortical dopaminergic balance between the higher and lower ranked individual we reported, may provide a physiological ground underlying differential vulnerability to psychopathology-like phenotypes. Indeed, the reduction in locomotor sensitization to cocaine in highest ranked individuals is coherent with the reduction of VTA bursting activity in these individuals (Runegaard *et al.*, 2018). Repeated social defeat in mice has been intensively used as a preclinical model of depression. In a subset of animals, so-called susceptible, this chronic stress induces enduring anxiety and social avoidance that depends on enduring increase of VTA dopamine activity (Cao *et al.*, 2010). Optogenetic stimulation of VTA neurons projecting to the NAcc induces a susceptible phenotype whereas optogenetic inhibition induces resilience (Chaudhury *et al.*, 2013). We demonstrated that lowest ranked mice, with higher VTA dopamine tone are more likely to develop social aversion following ten days of repeated defeats. Two other studies made observations that differ from ours on the consequences of repeated social defeat depending on social rank. Lehmann *et al.* (2013) did not observe a correlation whereas Larrieu *et al.* (2017) observed the opposite (*i.e.* resilience for lower ranked individuals). Differences may reside in the intensity of the defeats

to which individual were exposed, the lower number of R1 and R4 tested (8 here vs 4) and the fact that pooled data from ranks 1 and 2 were compared to that of ranks 3 and 4 in the Larrieu's study. Furthermore, our experiment was performed on tetrads established for 5 months that have been tested regularly to ensure their stability over time. This repeated solicitation of animals in the context of chronic social competitions may have reinforced the phenotypes of each rank.

Studies in human and animals suggested the existence of a correlation between social rank and differences in stress hormones. Elevated circulating glucocorticoids are usually associated with subordinate status in non-mammals, and mammals including rodents and primates, although conflicting results have been reported (Sapolsky, 2004; Sapolsky, 2005; Creel *et al.*, 2013; Cavigelli and Caruso, 2015). In human, the common perception that dominant individuals may have higher glucocorticoid levels has been challenged. Higher socio-economic status (SES) has been linked to lower evening glucocorticoid levels (Cohen *et al.*, 2006). Studies in military leaders, as well as in influential individuals from a Bolivian forager-farmer population, different for individuals with higher SES, showed lower glucocorticoid levels (Sherman *et al.*, 2012; von Rueden *et al.*, 2014). We studied the social fate of mice deprived of the glucocorticoid receptor gene in dopamine innervated neurons. This targeted mutation clearly promotes higher social ranking in our tetrads. This result is consistent with our recent observation made on mice raised by two (Papilloud *et al.*, 2020). Interestingly, we also showed that these mice exhibit a lower VTA dopamine cells bursting activity (Ambroggi *et al.*, 2009), a decreased sensitization to cocaine (Barik *et al.*, 2010) and a shift toward resiliency following repeated social defeat (Barik *et al.*, 2013). These phenotypes are strikingly similar to that of R1 individuals suggesting that stress response and its impact on dopamine pathway might play a principle organizational role in shaping the behavioural trajectories leading to the establishment of social ranking. This hypothesis is reinforced by our data showing increased social ranking upon VTA dopamine neurons inhibition. In contrast, optogenetic stimulation of VTA dopamine neurons seems to favour dominant behaviour for competitive access to reward, which could rather reflect the role of this brain region in reward processing (Lozano-Montes *et*

al., 2019). Importantly, in our experiment, whereas a transient reduction of dopamine activity during dominance measurement in tube-test has no detectable effect, a permanent reduction during the formation of the social organization upwards rank attainment, suggesting that this activity does not affect the expression of dominance but rather shapes its establishment. This process may occur under the continuous influence of the glucocorticoid stress-response.

Material and methods

Animals

C57BL/6JRj, 129/SvEv, and CD1 male mice of 6 weeks were purchased from Janvier (Le Genest-Saint-Isle, France) and housed under standard conditions, at 22°C, 55% to 65% humidity, with a 12-hour light/dark cycle (7 am/7 pm) and free access to water and a rodent diet. BAC-DATiCrefto mice (Turiault *et al.*, 2007) were heterozygous and backcrossed on a C57BL/6J background. *Nr3c1* (*GR*) gene inactivation was selectively targeted in dopaminoceptive neurons (*Nr3c1*^{loxP/loxP};Tg:D1aCre (Lemberger *et al.*, 2007), here after designed GR^{D1aCre}), as described in Ambroggi *et al.* (2009). Experimental animals were obtained by mating *Nr3c1*^{loxP/loxP} females with *Nr3c1*^{loxP/loxP};Tg:D1aCre males. Half of the progeny were mutant animals the other half were control littermates. When required, thymus and adrenal glands of animals were dissected and weighted after fat tissue removal under a binocular loupe. Experiments were performed in accordance with the European Directive 2010/63/UE and the recommendation 2007/526/EC for care of laboratory animals and approved by the Sorbonne Université committee for animal care and use.

Stereotaxic injections

Stereotaxic injections were performed using a stereotaxic frame (Kopf Instruments) under general anaesthesia with xylazine and ketamine (10 mg kg⁻¹ and 150 mg kg⁻¹, respectively). Anatomical coordinates and maps were adjusted from Watson and Paxinos, 2010. The injection rate was set at 100 nl min⁻¹. To express hM4D in VTA dopamine neurons, we injected BAC-DATiCrefto mice (6 weeks old) with AAV8-hSyn-DIO-hM4D-mCherry (300 nl L⁻¹, titration 10¹² particles ml⁻¹, University of North Carolina, USA vector core facility) bilaterally in the VTA (AP -3.2 mm, ML ±0.6 mm, DV -4.7mm from the bregma). For control, C57BL/6J mice issued from the same breedings than BAC-DATiCrefto mice, but not carrying the transgene, were injected similarly but with an AAV8-hSyn-GFP (titration 10¹² particles ml⁻¹, University of North Carolina, USA vector core facility). Animals were given a 4 weeks' recovery period to allow

sufficient viral expression.

Constitution of tetrads

Mice were weighted upon arrival and were then grouped by four (tetrads) gathering mice of similar weights. When behavioural testing was performed before the constitution of the tetrads, mice were singly housed for one week. Mice were regularly weighted. For tetrads including GR^{D1aCre} mutant mice, animals were genotyped at 4 weeks of age. Tetrads were formed with animals unfamiliar to each other issued from different litters, grouping one mutant with three age-matched control mice (GR^{loxP/loxP}).

Social rank identification

Tube-test. Mice gathered by groups of four individuals for two to four weeks were first trained to move forward a transparent Plexiglas tube (diameter, 2.5 cm; length, 30 cm) for 2 consecutive days, performing 8 trials the first day and 4 the second one. Each individual alternatively entered the tube from right and left extremities and was let for a maximum of 30 seconds to exit the tube at the opposite end. After 30 seconds if still present within the tube, the mouse was gently pushed out. The diameter of the tube allowed passing one individual but and did not permit it to reverse direction. During the following days, social ranks were assessed daily through the six possible pairwise confrontations in the tube, performing for each a trial composed of 3 confrontations. Two mice were simultaneously introduced within the tube from the 2 opposite ends taking care that they met in the middle of the tube. The first mouse to exit the tube was designed as the loser of the contest. The individual that won at least 2 confrontations was ranked higher. Mice were classified from rank 1 (3 wins) to rank 4 (no win). Contests exceeding 2.5 minutes were stopped and immediately repeated. After each trial, the tube was cleaned with 20% ethanol and dried. Among 84 tetrads analysed, we always observed a non-ambiguous ranking. The order of confrontations was randomized day after day using a round-robin design. Social ranks were initially assessed during a minimum period of 6 days and considered stable if both ranks 1 and 4 were stable for the last three days. Tetrads

that did not reach this criterion were analysed further, until reaching three days stability for ranks 1 and 4. All 84 tetrads reached stability within 12 days. Social rank was repeatedly analysed every three to four weeks for a minimum of three consecutive days.

For tetrads composed of one mouse stereotaxically injected with AAV8-hSyn-DIO-hM4D-mCherry and three mice with AAV8-hSyn-GFP, once both ranks 1 and 4 were stable for three consecutive days, tube test was pursued for five more days but each individual received an injection of CNO (*i.p.* 1mg kg⁻¹), 30 minutes before tube-test. Three weeks later, tetrads were treated for 24h with CNO in drinking water (10 mg L⁻¹), then dismantled and new tetrads were formed with similar composition but with individuals unknown to each other and were permanently treated with CNO in drinking water (10 mg L⁻¹). After two weeks, social ranking was determined by tube test.

Territory urine marking assay. R1 and R4 mice from a tetrad were placed in an empty PVC box (42x42x15 cm), separated by a central transparent perforated Plexiglas divider and were let free to explore and mark their own territory for 2 hrs. Absorbent paper (Whatmann), partially covered by fresh sawdust was set in the bottom of each compartment to collect urine deposited by mice during the session. Absorbent paper was then pictured under UV light (312 nm). Both the number of urine marks and the total area of urine marks were quantified.

Warm spot assay. Tetrads were placed in a transparent plastic cage (35x20x18 cm) without litter, placed on ice (bottom cage temperature 4 °C). 20 minutes later, a warm plate (11x9 cm, 28-30 °C) was introduced on the floor of the cage, at a corner. Mice activity was recorded for 20 min, and warm plate occupancy, by each individual, scored by an experimenter blind to conditions.

Spontaneous locomotor activity in open field

Mice were placed in a corner of a squared PVC white box (42x42 cm, 15 cm depth), and let free to explore for 10 min, under 50 lux. A video camera system placed above enabled the automatic quantification of locomotor activity (Noldus Ethovision 11.0 XT).

Anxiety-like behaviour

Dark-Light box. The dark-light box apparatus consisted of a plastic rectangular box (45x20 cm, 25 cm high) divided into a white compartment (30 cm, open) and a black compartment (15 cm, covered with a removable lid), that communicate through a central door (5x5 cm). Animals were initially placed into the black compartment, and exploration recorded for 10 min, under 30 lux. The time spent in each compartment was blindly scored by two experimenters.

Elevated O-maze. The maze consisted of a circular path (width 5.5 cm, outer diameter 56 cm) elevated 30 cm above the floor and made of black PVC. It was divided in four sections of equal lengths, two opposite bordered with bilateral black plastic walls (15.5 cm high) and two open ones. Mice were positioned at one extremity of a closed section, the head directed inward, under 50 lux in the open sections and 10 lux in the closed one. Their exploration was recorded for 10 minutes and the time spent into closed and open sections was blindly scored by two experimenters. A mouse was considered to be in a section when the 4 paws were introduced.

Despair, forced swim test

Glass cylinders (40 cm tall, 12 cm diameter) were filled with tepid water (23°C) until reaching a depth of 10 cm. Mice, placed on a large spoon, were gently introduced into cylinders and videotaped for 6 min. Cumulative length of time of immobility, balance and escape movements were blindly scored. Escape behaviour was defined as movements involving the 4 paws of the animal beating against the wall of the cylinder mimicking a climbing-like behaviour. Balance movements refer to brief movements involving mainly only the 2 posterior paws of the animal and aiming to displace in water without trying to climb up the cylinder's wall. Mice were considered immobile when floating passively, doing neither escape nor balance movements. The experiment was repeated 24 h later when planned in the experimental design.

Sociability, three-chambers test

Sociability was measured under 50 lux in a rectangular box containing three chambers (30x20, 15 cm high for each compartment) with removable doors (5x5 cm) at the centre of each

partition. In the opposite sides of the 2 lateral compartments, 2 clear perforated plastic boxes (10x7 cm, 7 cm high) were placed. One contained an unfamiliar adult male mouse (C57BL/6J), the other was left empty. During habituation phase (5 min), the challenged individual was placed in closed central compartment. Doors were then opened and the mouse free to explore the display for 5 min. The sessions were recorded, and the close interaction time with the empty box and with the box containing an unknown congener were blindly scored. The interaction time was defined as the periods during which the animal was oriented with the head towards the box, and in direct contact with it. To measure the preference for social novelty, and social memory, the mouse was let, closed, in the chamber containing the social cue for 5 min. It was then placed again in the central chamber, free to investigate the three compartments. The time length spent in close interaction with boxes containing, either a familiar mouse, previously encountered, or an unfamiliar one was scored, for 5 minutes session.

Aggressiveness, resident intruder challenge

Ranks 1 and 4 males were individually housed for 48 hours before starting the resident intruder test. 10 weeks old 129/SvEv males (Janvier laboratory, Saint-Berthevin, France) were used as intruders. The experimental sessions were carried out between 9.30 am and 3 pm. The intruder was placed in the cage of the challenged mouse and social interactions were videotaped for 20 minutes for ulterior manual scoring by an experimenter blind to the conditions. A second session was repeated 24 h later with a new intruder. Sessions in which either R1 or R4 individuals from on tetrad displayed aggressive behaviour were scored.

Non-matching to sample T-maze task

The test was performed as previously described (Sigurdsson *et al.*, 2010). Briefly, mice underwent for 3 days a moderate food reduction (2 g/mouse/day), taking care not to go below 85% of their initial weight. Animals were then trained on a spatial working memory task (non-match-to-sample task) in a T-maze (61 cm large x 51 cm width x 15 cm high, with a path 11

cm large). Mice were habituated to the maze for two days during which they had 15 minutes to collect food pellets (20 mg dustless sugar pellets, Bioserv). The next three days, mice had to complete 4 forced runs each day, during which one of the two arms were alternatively closed in order to habituate to the guillotine doors (Fig. 2D). Mice were then daily tested on 10 trials per day. Each trial consisting of two runs, a forced run and a choice run. At the beginning of the trial both arms are baited. In the forced run the right or left arm is randomly chosen to be opened, while the other arm is closed. At the beginning of the forced run, the mouse was placed at end of the longest T-maze arm. After running down this arm, it could enter into the open goal arm and have access to a food reward. Once the mouse reached back the starting arm, it was blocked by a door at its end for a delay of 6 s. Then started the choice run. During it, the mouse ran down the centre arm, where it had to choose between the two open goal arms. To obtain a reward, animals were required to enter the non-visited arm during the sample phase. This was scored as a correct choice. Animals were exposed to daily sessions of 10 trials, until they reached a criterion performance, defined as having a minimum of seven correct choices a day, for three consecutive days. The inter-trial time was 45 s.

Social defeat and interaction paradigms

Social defeat was performed as previously described (Barik *et al.*, 2013). Six months old CD1 breeder male mice were screened for their aggressiveness. 6 months old individuals were subjected to 10 consecutive days of social defeat with new encounters. Each defeat consisted of 5 minutes physical interactions with a resident CD1 mouse, followed by a 24 h exposure to the CD1 in its home cage but separated by a perforated transparent plastic wall which allowed visual, auditory, and olfactory communication whilst preventing physical contact. Social interaction was first performed the day before the first social defeat (pre-defeat) and performed again 24 h after the last social defeat (post-defeat). Challenged mice were placed for 150 seconds in a plastic white open-field (42x42 cm, 30 cm high, 20 lux) containing an empty transparent and perforated plastic box. Mice were rapidly removed and an unfamiliar CD1 mouse was placed in the box, and the challenged mouse re-exposed to the open field for 150

seconds. Sessions were recorded and the time spent in direct interaction with the boxes were manually quantified by an experimenter blind to conditions.

Locomotor sensitization to cocaine

Locomotor sensitization to cocaine was conducted on 3 months old R1 and R4 individuals. Mice were placed in a circular corridor (4.5-cm width, 17 cm-external diameter, 30-50 lux) crossed by four infrared captors (1.5 cm above the base), equally spaced (Imetronic, Pessac, France). The locomotor activity was automatically quantified by counting the quarters of turn travelled by the mouse that corresponded to the interruption of two successive beams. Animals were habituated to the apparatus for 3 hours during 3 consecutive days and received a saline injection on days 2 and 3 (NaCl 0.9% saline solution, 10 ml kg⁻¹, *i.p.*). On the five following days, mice were placed in the apparatus for 90 min, then injected with cocaine hydrochloride (Sigma-Aldrich, 10mg kg⁻¹ *i.p.*) and left inside 180 minutes after injection. Following 7 days of withdrawal, mice received a challenge injection of cocaine (10mg kg⁻¹ *i.p.*). At the end of each session, mice were placed back in their tetrads. Social ranks were tested at the end of the experiment, and only mice of R1 and R4 that did not change were considered for the analysis. The behavioural sensitization experiment has been carried out from 9 am to 13 pm.

In vivo electrophysiological recordings

3 to 5 months old R1 and R4 mice were anesthetized with chloral hydrate (8%), 400 mg kg⁻¹ *i.p.* supplemented as required to maintain optimal anaesthesia throughout the experiment and positioned in a stereotaxic frame. A hole was drilled in the skull above midbrain dopaminergic nuclei (coordinates: 3.0 ± 1.5 mm posterior to bregma, 1 ± 1 mm [VTA] lateral to the midline, Watson and Paxinos, 2010). Recording electrodes were pulled from borosilicate glass capillaries (with outer and inner diameters of 1.50 and 1.17 mm, respectively) with a Narishige electrode puller. The tips were broken under microscope control and filled with 0.5% sodium acetate. Electrodes had tip diameters of 1-2 µm and impedances of 20–50 MΩ. A reference electrode was placed in the subcutaneous tissue. The recording electrodes were lowered

vertically through the hole with a micro drive. Electrical signals were amplified by a high-impedance amplifier and monitored with an oscilloscope and an audio monitor. The unit activity was digitized at 25 kHz and stored in Spike2 program. The electrophysiological characteristics of dopamine neurons were analysed in the active cells encountered when systematically passing the microelectrode in a stereotaxically defined block of brain tissue including the VTA (1). Its margins ranged from -2.9 to -3.5 mm posterior to bregma (AP), 0.3 to 0.6 mm (ML) and -3.9 to -5 mm ventral (DV) (Grace and Bunney, 1984). Sampling was initiated on the right side and then on the left side. Extracellular identification of dopamine neurons was based on their location as well as on the set of unique electrophysiological properties that distinguish dopamine from non-dopamine neurons *in vivo*: (i) a typical triphasic action potential with a marked negative deflection; (ii) a long duration (>2.0 ms); (iii) an action potential width from start to negative trough >1.1 ms; (iv) a slow firing rate (<10 Hz and >1 Hz). Electrophysiological recordings were analysed using the R software (⁴⁹). Dopamine cell firing was analysed with respect to the average firing rate and the percentage of spikes within bursts (%SWB, number of spikes within burst divided by total number of spikes). Bursts were identified as discrete events consisting of a sequence of spikes such that: their onset is defined by two consecutive spikes within an interval <80 ms whenever and they terminate with an inter-spike interval >160 ms. Firing rate and % of spikes within bursts were measured on successive windows of 60 s, with a 45 seconds overlapping period. Responses to nicotine are presented as the mean of percentage of firing frequency variation from the baseline \pm SEM. For statistical analysis, maximum of firing variation induced by nicotine occurring 180 seconds after the injection are compared to spontaneous variation from the baseline occurring 180 seconds just before the injection by non-parametric Mann-Whitney test.

Quantification of dopamine and DOPAC

Animals were decapitated and brains were rapidly dissected and frozen at -12°C on the stage of a Leitz-Wetzlar microtome. Coronal sections (300 μ m thick) were cut and placed onto the refrigerated stage. Three dopaminergic terminal fields were assayed: the mPFC, the CPU and

the NAcc. For each structure, two or four tissue punches (1 mm diameter) from two consecutive sections were taken bilaterally and each side analysed separately for the CPU, the NAcc and mPFC, respectively. Tissue punches were immersed into 50 μ l of 0.1 N HClO₄ containing Na₂S₂O₅ (0.5%), disrupted by sonication and centrifuged at 15000 g for 20 min. Aliquots (10 μ l) of supernatant were diluted with high pressure liquid chromatography mobile phase and injected into a reverse-phase system consisting of a C18 column (HR-80 Catecholamine 80 x 4.6 mm, Thermo Scientific, USA) and a 0.1 M NaH₂PO₄ mobile phase containing 1-octanesulfonic acid (2.75 mM), triethylamine (0.25 mM), EDTA (0.1 mM), methanol (6 %) and adjusted to pH 2.9 with phosphoric acid. Flow rate was set at 0.6 mL/min by an ESA-580 pump. Electrochemical detection was performed with an ESA coulometric detector (Coulochem II 5100A, with a 5014B analytical cell; Eurosep, Cergy, France). The conditioning electrode was set at - 0.175 mV and the detecting electrode at + 0.175 mV, allowing a good signal-to-noise ratio. External standards were regularly injected to determine the elution times (9.8 and 21.5 min) and the sensitivity (0.3 and 0.4 pg), for DOPAC and dopamine respectively.

Immunostaining

Following CNO treatment, anesthetized mice were perfused (intra cardiac) with 4% paraformaldehyde. Brains were removed, post-fixed over-night in the same solution and sliced with a vibratome (30 μ m). Sections containing SN and VTA were incubated with antibodies directed against tyrosine hydroxylase (mouse monoclonal, 1:1000, Merck-Millipore MAB318) and mCherry (rabbit polyclonal, 1:500, Abcam ab167453) overnight at 4°C with constant shaking. Sections were then incubated for 2 h at room temperature with anti-mouse Alexa 488 (Invitrogen A-1101, 1:500) and anti-rabbit Cy3 (Invitrogen A-10520, 1:500) antibodies. Sections were mounted using Vectashield with DAPI (Vectorlabs) and analysed by fluorescence microscopy.

Statistical Analysis

Data are expressed as mean \pm SEM. Statistical analyses were performed by using Mann-Whitney non-parametric test and two-way ANOVA. When primary effect was found to be significant, post hoc comparisons were made using a Bonferroni/Dunn test. Differences of $P \leq 0.05$ were considered statistically significant. Statistical analyses were carried out using PRISM software.

Data and materials availability. The that support the findings in this study are available from the corresponding authors upon request. Source data are provided with this paper.

Acknowledgements

This project has been supported by grants from the LabEx BioPsy, the French Agence Nationale de la Recherche (ANR3053NEUR31438301 to FT and ANR-14-CE35-0029-01 to SP), by the Foundation for Medical Research (FRM Equipe grant DEQ20140329552 to FT and DEQ20180339159 to JB), by the INCA (TABAC grant to PF, JB and FT), Université Côte d'Azur and Sorbonne Université. The authors warmly thank S. Bhattacharya, C Sandi, L. Amar and S. Vyas for helpful discussions and S.B., L. A and S.V. for critical reading of the manuscript. We also thank F. Machulka and the IBPS mouse facility for their technical assistance.

Contributions

F.T. and S.P conceived and co-supervised the study. F.T., S.P, D.B. and P.F. designed the experiments, acquired and analysed the data. D.B., C.V., C.N., S.P., A.Z., A.C.M., S.M., A.F., J.P.T., T.C., J.B. and F.M. acquired and analysed the data. F.T., D.B. and S.P, wrote the manuscript.

Competing interests Statement

The authors declare no competing interests.

References

- Allsop, S.A., Vander Weele, C.M., Wichmann, R., and Tye, K.M. (2014). Optogenetic insights on the relationship between anxiety-related behaviors and social deficits. *Front. Behav. Neurosci.* *8*.
- Ambroggi, F., Turiault, M., Milet, A., Deroche-Gamonet, V., Parnaudeau, S., Balado, E., Barik, J., van der Veen, R., Maroteaux, G., Lemberger, T., et al. (2009). Stress and addiction: glucocorticoid receptor in dopaminergic neurons facilitate cocaine seeking. *Nat. Neurosci.* *12*, 247–249.
- Armbruster, B.N., Li, X., Pausch, M.H., Herlitze, S., and Roth, B.L. (2007). Evolving the lock to fit the key to create a family of G protein-coupled receptors potentially activated by an inert ligand. *Proc. Natl. Acad. Sci.* *104*, 5163–5168.
- Barik, J., Parnaudeau, S., Saint Amax, A.L., Guiard, B.P., Golib Dzib, J.F., Bocquet, O., Bailly, A., Benecke, A., and Tronche, F. (2010). Glucocorticoid receptors in dopaminergic neurons, key for cocaine, are dispensable for molecular and behavioral morphine responses. *Biol. Psychiatry* *68*, 231–239.
- Barik, J., Marti, F., Morel, C., Fernandez, S.P., Lanteri, C., Godeheu, G., Tassin, J.-P., Mombereau, C., Faure, P., and Tronche, F. (2013). Chronic stress triggers social aversion via glucocorticoid receptor in dopaminergic neurons. *Science* *339*, 332–335.
- Beery, A.K., and Kaufer, D. (2015). Stress, social behavior, and resilience: Insights from rodents. *Neurobiol. Stress* *1*, 116–127.
- Bergmüller, R., and Taborsky, M. (2010). Animal personality due to social niche specialisation. *Trends Ecol. Evol.* *25*, 504–511.
- Berry, R.J., and Bronson, F.H. (1992). Life history and bioeconomy of the house mouse. *Biol. Rev.* *67*, 519–550.
- Bielsky, I.F., Hu, S.-B., Szegda, K.L., Westphal, H., and Young, L.J. (2004). Profound impairment in social recognition and reduction in anxiety-like behavior in vasopressin V1a receptor knockout mice. *Neuropsychopharmacology* *29*, 483–493.
- Bjorklund, A., and Lindvall, O. (1984). Dopamine containing systems in the CNS. In *Handbook of Chemical Neuroanatomy*, (Amsterdam: Elsevier), pp. 55–122.
- Cao, J.-L., Covington, H.E., Friedman, A.K., Wilkinson, M.B., Walsh, J.J., Cooper, D.C., Nestler, E.J., and Han, M.-H. (2010). Mesolimbic dopamine neurons in the brain reward circuit mediate susceptibility to social defeat and antidepressant action. *J. Neurosci.* *30*, 16453–16458.
- Cavigelli, S.A., and Caruso, M.J. (2015). Sex, social status and physiological stress in primates: the importance of social and glucocorticoid dynamics. *Philos. Trans. R. Soc. B Biol. Sci.* *370*, 20140103.
- Cervenka, S., Gustavsson, J.P., Halldin, C., and Farde, L. (2010). Association between striatal and extrastriatal dopamine D2-receptor binding and social desirability. *NeuroImage* *50*, 323–328.

- Chaudhury, D., Walsh, J.J., Friedman, A.K., Juarez, B., Ku, S.M., Koo, J.W., Ferguson, D., Tsai, H.-C., Pomeranz, L., Christoffel, D.J., et al. (2013). Rapid regulation of depression-related behaviours by control of midbrain dopamine neurons. *Nature* 493, 532–536.
- Cohen, S., Schwartz, J.E., Epel, E., Kirschbaum, C., Sidney, S., and Seeman, T. (2006). Socioeconomic Status, Race, and Diurnal Cortisol Decline in the Coronary Artery Risk Development in Young Adults (CARDIA) Study: *Psychosom. Med.* 68, 41–50.
- Cordero, M.I., and Sandi, S. (2007). Stress amplifies memory for social hierarchy. *Front. Neurosci.* 1, 175–184.
- Creel, S., Dantzer, B., Goymann, W., and Rubenstein, D.R. (2013). The ecology of stress: effects of the social environment. *Funct. Ecol.* 27, 66–80.
- Felix-Ortiz, A.C., and Tye, K.M. (2014). Amygdala inputs to the ventral hippocampus bidirectionally modulate social behavior. *J. Neurosci.* 34, 586–595.
- Felix-Ortiz, A.C., Beyeler, A., Seo, C., Leppla, C.A., Wildes, C.P., and Tye, K.M. (2013). BLA to vHPC inputs modulate anxiety-related behaviors. *Neuron* 79, 658–664.
- Ferrari, P.F., Palanza, P., Parmigiani, S., and Rodgers, R.J. (1998). Interindividual variability in Swiss male mice: relationship between social factors, aggression, and anxiety. *Physiol. Behav.* 63, 821–827.
- Francis, R.C. (1984). The effects of bidirectional selection for social dominance on agonistic behavior and sex ratios in the paradise fish (*Macropodus Opercularis*). *Behaviour* 90, 25–44.
- Freund, J., Brandmaier, A.M., Lewejohann, L., Kirste, I., Kritzler, M., Kruger, A., Sachser, N., Lindenberger, U., and Kempermann, G. (2013). Emergence of Individuality in Genetically Identical Mice. *Science* 340, 756–759.
- Grace, A., and Bunney, B. (1984). The control of firing pattern in nigral dopamine neurons: burst firing. *J. Neurosci.* 4, 2877–2890.
- Gunaydin, L.A., Grosenick, L., Finkelstein, J.C., Kauvar, I.V., Fenno, L.E., Adhikari, A., Lammel, S., Mirzabekov, J.J., Airan, R.D., Zalocusky, K.A., et al. (2014). Natural neural projection dynamics underlying social behavior. *Cell* 157, 1535–1551.
- Hager, T., Jansen, R.F., Pieneman, A.W., Manivannan, S.N., Golani, I., van der Sluis, S., Smit, A.B., Verhage, M., and Stiedl, O. (2014). Display of individuality in avoidance behavior and risk assessment of inbred mice. *Front. Behav. Neurosci.* 8.
- Hilakivi, L.A., Lister, R.G., Duncan, M.J., Ota, M., Eskay, R.L., Mefford, I., and Linnoila, M. (1989). Behavioral, hormonal and neurochemical characteristics of aggressive α -mice. *Brain Res.* 502, 158–166.
- Hilakivi-Clarke, L.A., and Lister, R.G. (1992). Are there preexisting behavioral characteristics that predict the dominant status of male NIH Swiss mice (*Mus musculus*)? *J. Comp. Psychol.* 106, 184–189.
- Hollis, F., van der Kooij, M.A., Zanoletti, O., Lozano, L., Cantó, C., and Sandi, C. (2015). Mitochondrial function in the brain links anxiety with social subordination. *Proc. Natl. Acad. Sci.* 112, 15486–15491.

- Insel, T.R. (2010). The challenge of translation in social neuroscience: a review of oxytocin, vasopressin, and affiliative behavior. *Neuron* 65, 768–779.
- Jupp, B., Murray, J.E., Jordan, E.R., Xia, J., Fluharty, M., Shrestha, S., Robbins, T.W., and Dalley, J.W. (2016). Social dominance in rats: effects on cocaine self-administration, novelty reactivity and dopamine receptor binding and content in the striatum. *Psychopharmacology (Berl.)* 233, 579–589.
- Kessler, R.C. (1994). Lifetime and 12-month prevalence of DSM-III-R psychiatric disorders in the United States: results from the national comorbidity survey. *Arch. Gen. Psychiatry* 51, 8.
- van der Kooij, M.A., Hollis, F., Lozano, L., Zalachoras, I., Abad, S., Zanoletti, O., Grosse, J., Guillot de Suduiraut, I., Canto, C., and Sandi, C. (2018). Diazepam actions in the VTA enhance social dominance and mitochondrial function in the nucleus accumbens by activation of dopamine D1 receptors. *Mol. Psychiatry* 23, 569–578.
- Korzan, W.J., Forster, G.L., Watt, M.J., and Summers, C.H. (2006). Dopaminergic activity modulation via aggression, status, and a visual social signal. *Behav. Neurosci.* 120, 93–102.
- Krishnan, V., Han, M.-H., Graham, D.L., Berton, O., Renthal, W., Russo, S.J., LaPlant, Q., Graham, A., Lutter, M., Lagace, D.C., et al. (2007). Molecular adaptations underlying susceptibility and resistance to social defeat in brain reward regions. *Cell* 131, 391–404.
- Kunkel, T., and Wang, H. (2018). Socially dominant mice in C57BL6 background show increased social motivation. *Behav. Brain Res.* 336, 173–176.
- Larrieu, T., Cherix, A., Duque, A., Rodrigues, J., Lei, H., Gruetter, R., and Sandi, C. (2017). Hierarchical status predicts behavioral vulnerability and nucleus accumbens metabolic profile following chronic social defeat stress. *Curr. Biol.* 27, 2202-2210.e4.
- Lathe, R. (2004). The individuality of mice. *Genes Brain Behav.* 3, 317–327.
- Lehmann, M.L., Geddes, C.E., Lee, J.L., and Herkenham, M. (2013). Urine scent marking (USM): a novel test for depressive-like behavior and a predictor of stress resiliency in mice. *PLoS ONE* 8, e69822.
- Lemberger, T., Parlato, R., Dasselze, D., Westphal, M., Casanova, E., Turiault, M., Tronche, F., Schiffmann, S.N., and Schütz, G. (2007). Expression of Cre recombinase in dopaminergic neurons. *BMC Neurosci.* 8, 4.
- Lorant, V. (2003). Socioeconomic inequalities in depression: A meta-analysis. *Am. J. Epidemiol.* 157, 98–112.
- Lozano-Montes, L., Astori, S., Abad, S., Guillot de Suduiraut, I., Sandi, C., and Zalachoras, I. (2019). Latency to reward predicts social dominance in rats: a causal role for the dopaminergic mesolimbic system. *Front. Behav. Neurosci.* 13, 69.
- Martinez, D., Orłowska, D., Narendran, R., Slifstein, M., Liu, F., Kumar, D., Broft, A., Van Heertum, R., and Kleber, H.D. (2010). Dopamine type 2/3 receptor availability in the striatum and social status in human volunteers. *Biol. Psychiatry* 67, 275–278.
- McIntyre, D.C., and Chew, G.L. (1983). Relation between social rank, submissive behavior, and brain catecholamine levels in ring-necked pheasants (*Phasianus cholchicus*). *Behav. Neurosci.* 97, 595–601.

- Miller-Butterworth, C.M., Kaplan, J.R., Shaffer, J., Devlin, B., Manuck, S.B., and Ferrell, R.E. (2007). Sequence variation in the primate dopamine transporter gene and its relationship to social dominance. *Mol. Biol. Evol.* 25, 18–28.
- Nader, M.A., Nader, S.H., Czoty, P.W., Riddick, N.V., Gage, H.D., Gould, R.W., Blaylock, B.L., Kaplan, J.R., Garg, P.K., Davies, H.M.L., et al. (2012). Social dominance in female monkeys: dopamine receptor function and cocaine reinforcement. *Biol. Psychiatry* 72, 414–421.
- Okada, Y., Sasaki, K., Miyazaki, S., Shimoji, H., Tsuji, K., and Miura, T. (2015). Social dominance and reproductive differentiation mediated by dopaminergic signaling in a queenless ant. *J. Exp. Biol.* 218, 1091–1098.
- Papilloud, A., Weger, M., Bacq, A., Zalachoras, I., Hollis, F., Larrieu, T., Battivelli, D., Grosse, J., Zanoletti, O., Parnaudeau, S., et al. (2020). The glucocorticoid receptor in the nucleus accumbens plays a crucial role in social rank attainment in rodents. *Psychoneuroendocrinology* 112, 104538.
- Penick, C.A., Brent, C.S., Dolezal, K., and Liebig, J. (2014). Neurohormonal changes associated with ritualized combat and the formation of a reproductive hierarchy in the ant *Harpegnathos saltator*. *J. Exp. Biol.* 217, 1496–1503.
- Robinson, T.E., and Berridge, K.C. (2000). The psychology and neurobiology of addiction: an incentive–sensitization view. *Addiction* 95, 91–117.
- Rodriguez, R.M., Chu, R., Caron, M.G., and Wetsel, W.C. (2004). Aberrant responses in social interaction of dopamine transporter knockout mice. *Behav. Brain Res.* 148, 185–198.
- von Rueden, C.R., Trumble, B.C., Emery Thompson, M., Stieglitz, J., Hooper, P.L., Blackwell, A.D., Kaplan, H.S., and Gurven, M. (2014). Political influence associates with cortisol and health among egalitarian forager-farmers. *Evol. Med. Public Health* 2014, 122–133.
- Runegaard, A.H., Sørensen, A.T., Fitzpatrick, C.M., Jørgensen, S.H., Petersen, A.V., Hansen, N.W., Weikop, P., Andreasen, J.T., Mikkelsen, J.D., Perrier, J.-F., et al. (2018). Locomotor and reward-enhancing effects of cocaine are differentially regulated by chemogenetic stimulation of Gi-signaling in dopaminergic neurons. *Eneuro* 5, ENEURO.0345-17.2018.
- Russo, S.J., Murrough, J.W., Han, M.-H., Charney, D.S., and Nestler, E.J. (2012). Neurobiology of resilience. *Nat. Neurosci.* 15, 1475–1484.
- Sapolsky, R.M. (2004). Social status and health in humans and other animals. *Annu. Rev. Anthropol.* 33, 393–418.
- Sapolsky, R.M. (2005). The influence of social hierarchy on primate health. *Science* 308, 648–652.
- Sherman, G.D., Lee, J.J., Cuddy, A.J.C., Renshon, J., Oveis, C., Gross, J.J., and Lerner, J.S. (2012). Leadership is associated with lower levels of stress. *Proc. Natl. Acad. Sci.* 109, 17903–17907.
- Sigurdsson, T., Stark, K.L., Karayiorgou, M., Gogos, J.A., and Gordon, J.A. (2010). Impaired hippocampal–prefrontal synchrony in a genetic mouse model of schizophrenia. *Nature* 464, 763–767.

- Singh-Manoux, A., Marmot, M.G., and Adler, N.E. (2005). Does subjective social status predict health and change in health status better than objective status?: *Psychosom. Med.* 67, 855–861.
- Starr-Phillips, E.J., and Beery, A.K. (2014). Natural variation in maternal care shapes adult social behavior in rats: maternal care influences adult social behavior. *Dev. Psychobiol.* 56, 1017–1026.
- Stringhini, S., Carmeli, C., Jokela, M., Avendaño, M., Muennig, P., Guida, F., Ricceri, F., d’Errico, A., Barros, H., Bochud, M., et al. (2017). Socioeconomic status and the 25 × 25 risk factors as determinants of premature mortality: a multicohort study and meta-analysis of 1.7 million men and women. *The Lancet* 389, 1229–1237.
- Timmer, M., and Sandi, C. (2010). A role for glucocorticoids in the long-term establishment of a social hierarchy. *Psychoneuroendocrinology* 35, 1543–1552.
- Tinbergen, N. (1939). On the analysis of social organization among vertebrates, with special reference to birds. *Am. Midl. Nat.* 21, 210.
- Torquet, N., Marti, F., Campart, C., Tolu, S., Nguyen, C., Oberto, V., Benallaoua, M., Naudé, J., Didienne, S., Debray, N., et al. (2018). Social interactions impact on the dopaminergic system and drive individuality. *Nat. Commun.* 9, 3081.
- Turialt, M., Parnaudeau, S., Milet, A., Parlato, R., Rouzeau, J.-D., Lazar, M., and Tronche, F. (2007). Analysis of dopamine transporter gene expression pattern – generation of DAT-iCre transgenic mice: Cre-mediated recombination in dopaminergic cells. *FEBS J.* 274, 3568–3577.
- Varholick, J.A., Bailoo, J.D., Palme, R., and Würbel, H. (2018). Phenotypic variability between Social Dominance Ranks in laboratory mice. *Sci. Rep.* 8, 6593.
- Wang, F., Zhu, J., Zhu, H., Zhang, Q., Lin, Z., and Hu, H. (2011). Bidirectional control of social hierarchy by synaptic efficacy in medial prefrontal cortex. *Science* 334, 693–697.
- Watson, C., and Paxinos, G. (2010). *Chemoarchitectonic atlas of the mouse brain*. (San Diego: Elsevier Academic Press).
- Wilkinson, R.G. (1999). Health, hierarchy, and social anxiety. *Ann. N. Y. Acad. Sci.* 896, 48–63.
- Yamaguchi, Y., Lee, Y.-A., and Goto, Y. (2015). Dopamine in socioecological and evolutionary perspectives: implications for psychiatric disorders. *Front. Neurosci.* 9.
- Yamaguchi, Y., Lee, Y.-A., Kato, A., Jas, E., and Goto, Y. (2017a). The roles of dopamine D2 receptor in the social hierarchy of rodents and primates. *Sci. Rep.* 7, 43348.
- Yamaguchi, Y., Lee, Y.-A., Kato, A., and Goto, Y. (2017b). The roles of dopamine D1 receptor on the social hierarchy of rodents and non-human primates. *Int. J. Neuropsychopharmacol.* 20, 324–335.
- Zhou, T., Sandi, C., and Hu, H. (2018). Advances in understanding neural mechanisms of social dominance. *Curr. Opin. Neurobiol.* 49, 99–107.

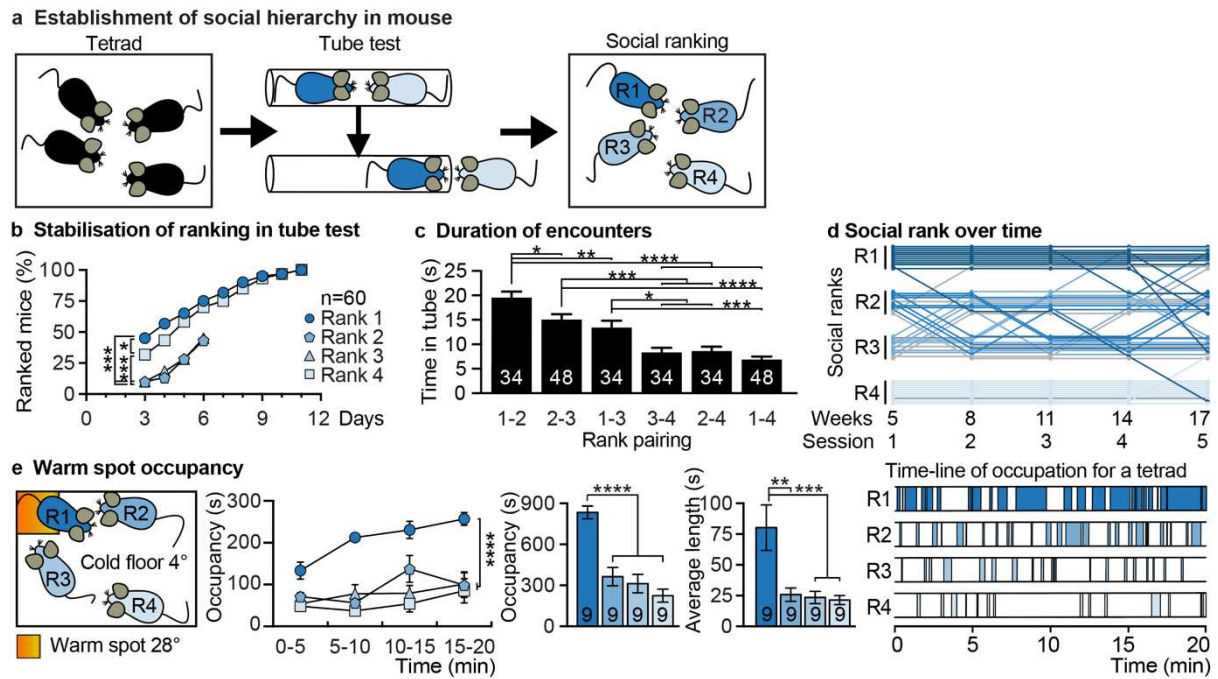


Figure 1. Social hierarchy establishment and stability in mice.

a, Design of social hierarchy establishment and analysis. Unfamiliar male mice were grouped by four. After 3 to 4 weeks, their social rank was determined by a precedence test (tube-test), and further tested four times until week 17. **b**, Rapidity of rank identification in the tube-test. The cumulated percentage of stable ranked individuals for each rank is pictured for each day of tube-test (n=60 tetrads). The data for ranks 2 and 3 are indicated for days 3 to 6 since rank identification was stopped when ranks 1 and 4 were stable. Gehan-Breslow-Wilcoxon Test. **c**, Mean duration of the confrontation in the tube-test performed during the three last days when ranks were stable. Each possible rank combination is pictured. The numbers of tetrads that have been analysed are indicated for each rank combination; n=48 or 34 in cases of unstable ranks 2 and 3. Wilcoxon rank sum test. **d**, Social ranks were stable from week 5 and for over three months for most animals. The dynamic of social ranking in the tube-test is pictured for a set of 12 tetrads. Each line depicts an individual mouse, its position within its social rank pool indicates the tetrad which it belongs to. Different blue intensities indicate the rank defined at the first tube-test session. The 6 individuals of ranks 2 and 3 that did not reach stability at the end of the first session are pictured with by grey lines. **e**, Left : representation of the warm spot

test. The position of the warm spot is pictured by an orange box. Middle : time course occupancy of the warm spot, total occupancy, and average length occupancy by differently ranked individuals (n=9 tetrads). Right : representative occupancy periods of the warm spot by individuals of a tetrad. *p < 0.05; **p < 0.01; ***p < 0.001. Error bars, \pm SEM.

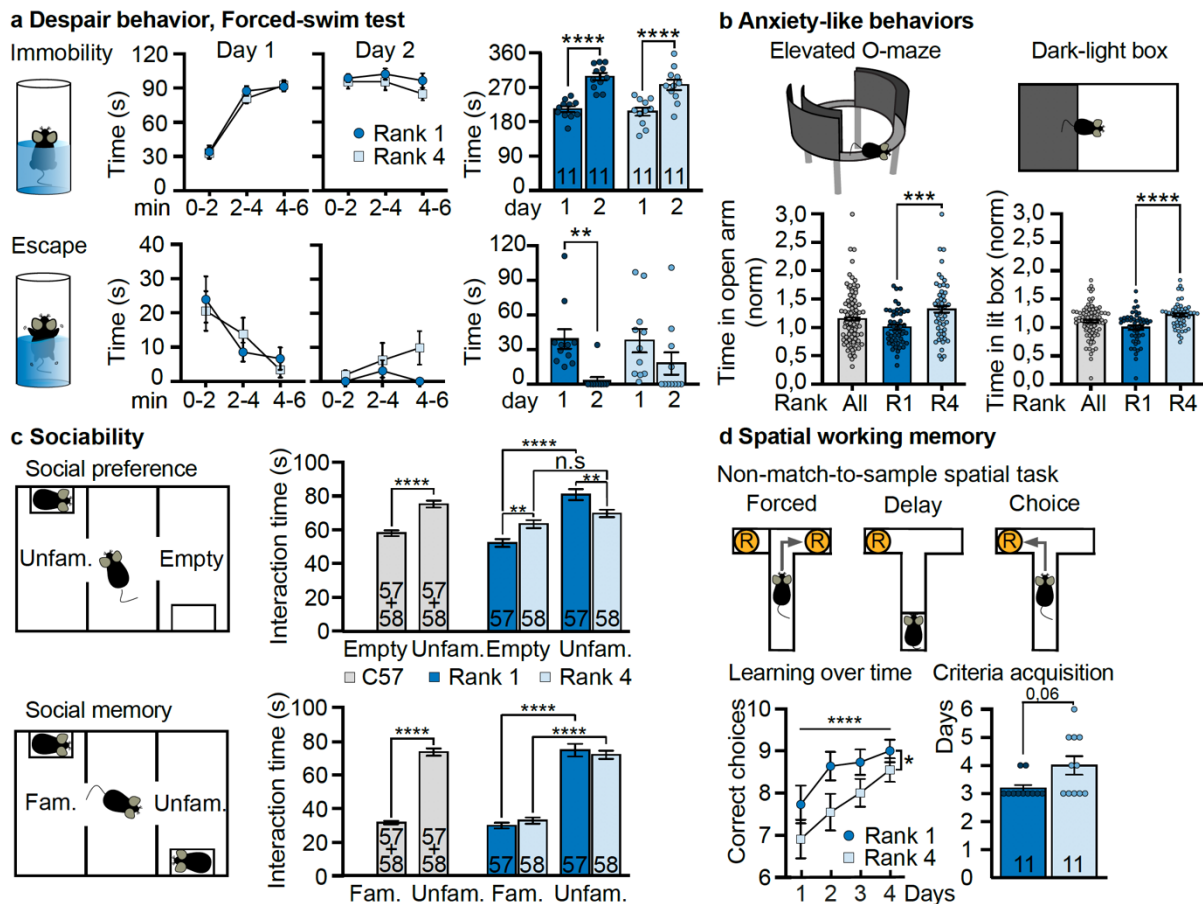


Figure 2. Differences in social rank correlates with differences in behaviour in genetically identical mice.

a, Highest and lowest ranked animals display similar depression-like behaviour in the forced-swim test. The length of immobility in tepid water is presented by 2 minutes periods (upper panel, left) and for the 6 minutes of the test (upper panel, right) for R1 and R4 mice ($n=11$ per group). Results obtained on the first day (Day 1) and 24 h later (Day 2) are pictured. The lower panels present, in the same way, the quantification of escape behaviour of the same individuals. Error bars, \pm SEM. **b**, Rank 1 individuals display increased anxiety-like behaviours. The experimental setups are pictured. The time spent for all C57B/L6 ($n=96$), Rank 1 ($n=48$, dark blue) and Rank 4 ($n=48$, light blue) individuals in the open-section of an elevated O-maze and in the lit compartment of a dark-light box are pictured. Time values were normalized from the R1 means. Respectively, $t_{94}=3.55$, $***p<0.001$ and $t_{94}=4.213$, $****p<0.001$, unpaired t-tests, two-tailed. Error bars, \pm SEM. **c**, Highest ranked mice display increased sociability but a

social memory similar to that of lowest ranked individuals. The three-chambers test is depicted (left). The duration of time spent interacting with an empty box (Empty) and with a box containing an unfamiliar mouse (Unfam.) are pictured in the upper row for C57B/L6 (grey, $n=115$), R1 (dark blue, $n=57$) and R4 (light blue, $n=58$) individuals. The duration of time spent interacting with a box containing a familiar mouse (Fam.) vs an unfamiliar one (Unfam.) are represented in the lower row. Upper row: $t_{114}=6.012$, **** $p<0.0001$, unpaired t-test, two-tailed. Right graph: effect of interaction, **** $p<0.0001$, $F_{(1,113)}=17.07$; effect of social cue, **** $p<0.0001$, $F_{(1,113)}=41.7$; no effect of social rank, $p=0.97$, $F_{(1,113)}=0.002$. Empty box: R1 vs empty box: R4, ** $p<0.01$; Social cue R1 vs social cue R4, ** $p<0.01$; Empty box vs social cue for R1 mice, **** $p<0.0001$. Empty box vs social cue for R4 mice, $p=0.20$. Two-way mixed ANOVA, Bonferroni's test. Error bars, \pm SEM. Lower row : $t_{114}=15.19$, **** $p<0.0001$, unpaired t-test, two-tailed. Right graph: no effect of interaction, $p=0.30$, $F_{(1,113)}=1.097$; effect of familiarity, **** $p<0.0001$, $F_{(1,113)}=231.1$; no effect of social rank, $p=0.003$, $F_{(1,113)}=0.97$. R1: familiar vs unfamiliar, **** $p<0.0001$; R4: familiar vs unfamiliar, **** $p<0.0001$. Two-way mixed ANOVA, Bonferroni's test. Error bars, \pm SEM. **d**, Rank 1 individuals display better performances in the Non-match-to-sample-spatial task, a spatial working memory task. Upper row illustrates the task design. The learning curve of 11 mice from both ranks, indicates the progression of correct choices over the days (lower row, left). The number of days required to reach the learning criterion is indicated (mean and individual scores, right). Effect of time, **** $p<0.0001$, $F_{(3,60)}=7.87$; effect of social rank, * $P<0.05$, $F_{(1,20)}=4.85$; no effect of interaction, $p=0.78$, $F_{(3,60)}=0.36$. Two-way mixed ANOVA. Right panel indicates for each rank the average number of days required to acquire the criterion. $U=34.5$, $p=0.056$ Mann-Whitney U test, two tailed. Error bars, \pm SEM.

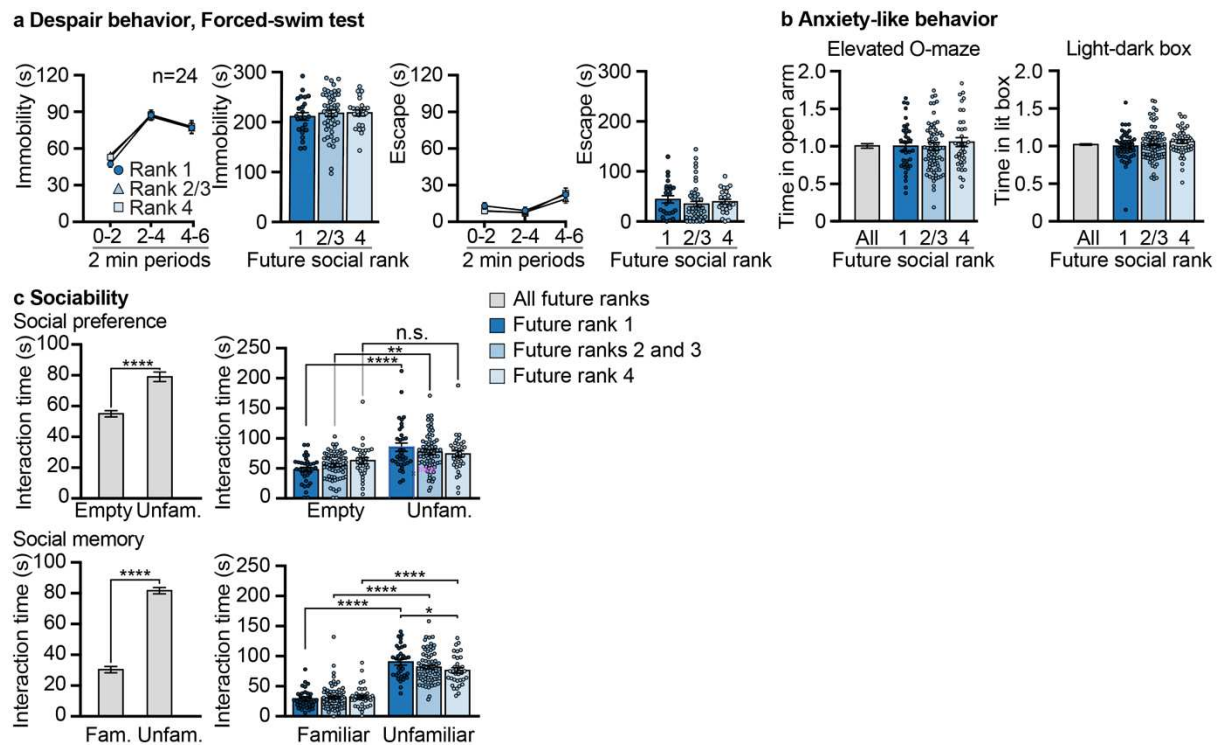


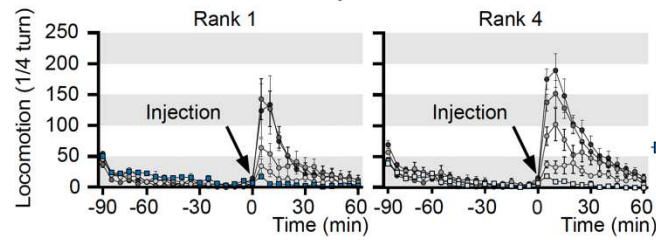
Figure 3. Difference in anxiety-like behaviour emerge for social life but difference in sociability is a trait pre-existing to social life.

a, Future rank 1 and rank 4 individuals have similar despair behaviour in a forced swim test. The time length of immobility and escape are pictured for each periods of two minutes (lines), and for the six minutes of the test (bars). For future R1 (n=24), R4 (n=24), and R2/3 (n=48) (dark, medium and light blue, respectively) Error bars, \pm SEM. **b**, Future rank 1 and rank 4 individuals display similar anxiety-like behaviours. The time spent to explore the open segments of an elevated O-maze and the lit compartment of a dark-light box are pictured for all C57BL/6 mice (grey bars, n=144 and n=192, respectively), and among them the future R1 (dark blue bars, n=36 and n=48, respectively), the future ranks 2 and 3 (medium blue bars, n=72 and n=95, respectively), and the future R4 (light blue bars, n=36 and n=48, respectively). For the O-maze, one dot out of scale (3.25) was omitted for ranks 2/3. Scores are normalized from the R1 means. Error bars, \pm SEM. **c**, Social behaviour. Social preference (left), Future rank 4 mice did not display social preference unlike future R1 individuals. Duration of interactions with an empty box vs a box containing an unfamiliar (Unfam.) congener is pictured

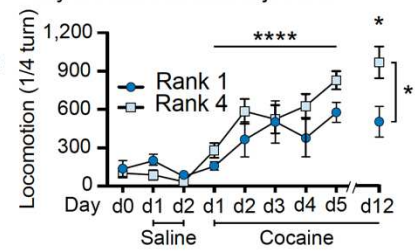
for 136 mice C57BL/6 mice from tetrads (grey bars) and, among them, the future R1 (dark blue bars, n=34), R2/3 (medium blue bars, n=68) and R4 (light blue bars, n=34). Left: $t_{135}=5.435$, **** $p<0.0001$, unpaired t-test, two tailed. Right: no effect of interaction, $p=0.09$, $F_{(2,133)}=2.41$; effect of social cue, **** $p<0.0001$, $F_{(1,133)}=27.55$; no effect of social rank, $p=0.77$, $F_{(2,133)}=0.28$. Empty box vs social cue for R1 mice, **** $p<0.0001$; empty box vs social cue for R2/3 mice, ** $p\leq 0.001$. Two-way mixed ANOVA, Bonferroni's test. Error bars, \pm SEM. Social memory. The time length interaction with the box containing a familiar (Fam.) social cue vs a box containing an unfamiliar (Unfam.) mouse is pictured. Left: $t_{135}=17.71$, **** $p<0.0001$, unpaired t-test, two tailed. Right: no effect of interaction, $p=0.01$, $F_{(2,133)}=2.31$; effect of familiarity, **** $p<0.0001$, $F_{(1,133)}=291.6$; no effect of social rank, $p=0.34$, $F_{(2,133)}=1.10$. Familiar vs unfamiliar for R1 mice, **** $p<0.0001$; Familiar vs unfamiliar for R2/3 mice, **** $p<0.0001$; Familiar vs unfamiliar for R4 mice, **** $p<0.0001$. Unfamiliar social cue: R1 vs R4, * $p<0.05$. Two-way mixed ANOVA, Bonferroni's test. Error bars, \pm SEM.

a Locomotor sensitization to cocaine

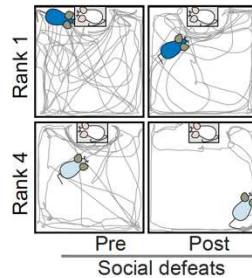
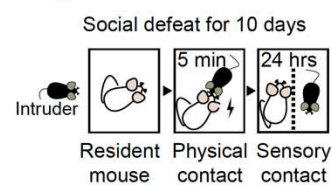
Time course of locomotor activity



Daily locomotion after injection



b Repeated social defeat



Social interaction

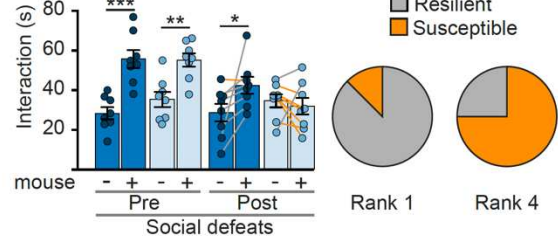
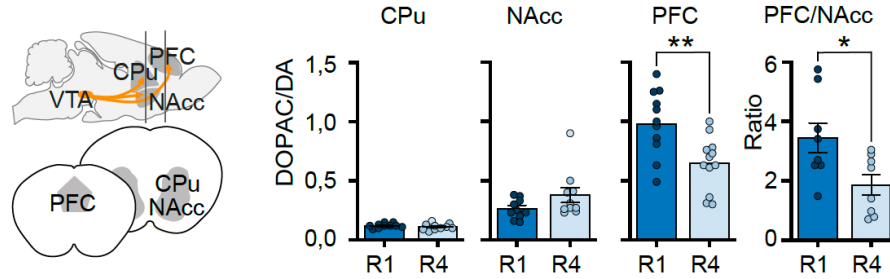


Figure 4. Social rank correlates with differences in preclinical models of behavioural disorders.

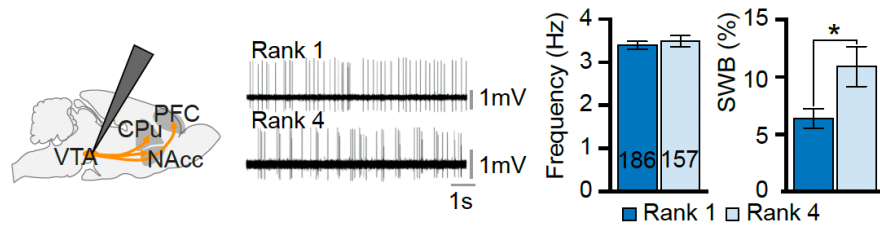
a, Locomotor sensitization to cocaine. Left, time course of Rank 1 (left panel, $n=8$) and Rank 4 (middle panel, $n=9$) individuals locomotion expressed as $\frac{1}{4}$ turn within a circular corridor for indicated sessions. Time 0 correspond to the injection of cocaine (Coc, 10 mg kg^{-1}) or saline (Sal). Right panel, cumulated locomotor activity of R1 and R4 individuals (dark and light blue, respectively) for 1 hour following habituation (day 0), saline (days 1 and 2) and cocaine (days 1 to 5 and a challenge on day 12) injections. Effect of time, **** $p < 0.0001$, $F_{(5,75)}=7.55$; effect of social rank, * $p < 0.05$, $F_{(1,15)}=5.376$; no effect of interaction, $p=0.32$, $F_{(5,75)}=1.198$. Coc d12 R1 vs Coc d12 R4, * $p < 0.05$. Two-way mixed ANOVA, Bonferroni's test. Error bars, \pm SEM. **b**, Depression-like behaviour induced by repeated social defeats. Left, protocol design. Middle left, representation of the open field in which social interactions were measured. The position of the box containing a CD1 mouse is indicated. Representative trajectories of R1 and R4 individuals before and after repeated social defeats are pictured. Middle right panel, R1 (dark blue, $n=8$) and R4 (light blue, $n=8$) interaction time with an empty box (mouse -) or a CD1 mouse (mouse +), before and after repeated social defeat. Right panel, susceptible individuals, developing social aversion are indicated with orange lines, resilient ones with grey ones. Right, representation of susceptible (orange) and resilient (grey) individuals among R1 and R4 males.

Pre-social defeats: effect of social cue, **** $p < 0.0001$, $F_{(1,14)} = 41.2$; no effect of social rank, $p = 0.39$, $F_{(1,14)} = 0.76$; no effect of interaction, $p = 0.33$, $F_{(1,14)} = 1.04$. Empty box vs social cue for R1 mice, *** $p < 0.001$; empty box vs social cue for R4 mice, ** $p < 0.01$. Post-social defeats: no effect of social cue, $p = 0.19$, $F_{(1,14)} = 1.89$; no effect of social rank, $p = 0.60$, $F_{(1,14)} = 0.29$; effect of interaction, * $p < 0.05$, $F_{(1,14)} = 4.95$. Empty box vs social cue for R1 mice, * $p < 0.05$. Two-way mixed ANOVA, Bonferroni's test. Error bars, \pm SEM.

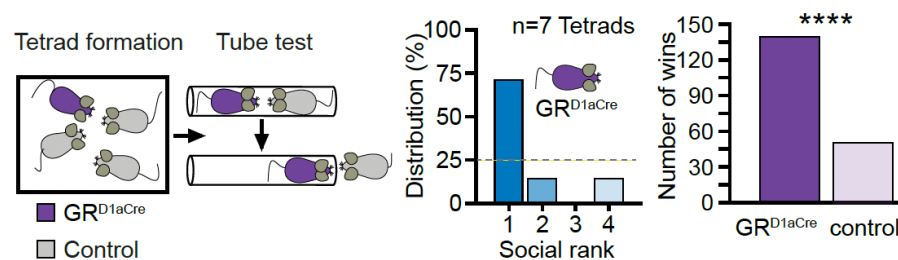
a Rank 1 and Rank 4 present differences in dopamine utilization



b Rank 1 mice have lower VTA dopamine neurons bursting activity



c GR deletion in dopaminergic neurons upwards social ranking



d Decreased CPU VTA DA neurons activity during colonization upwards social ranking

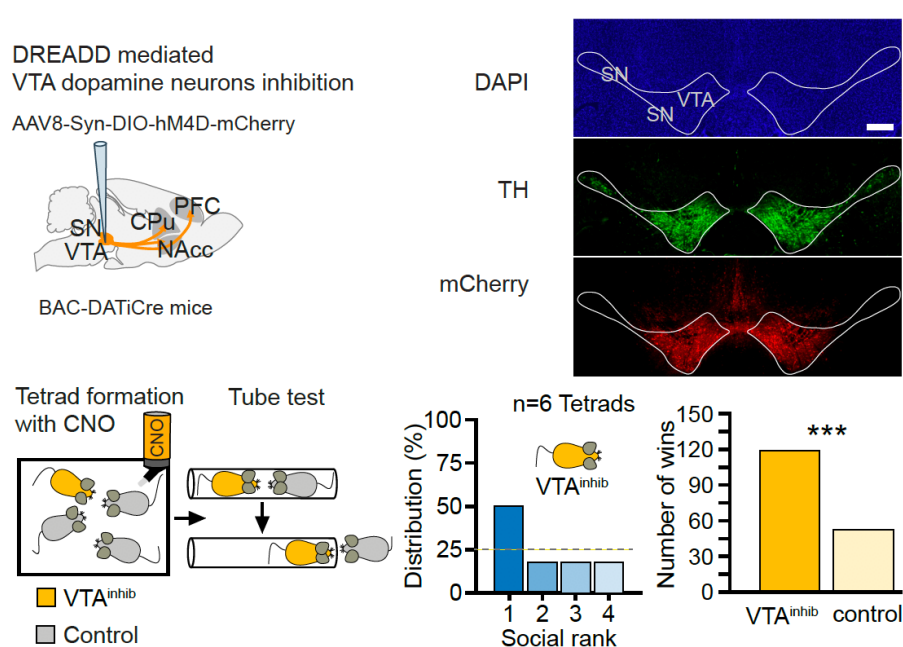


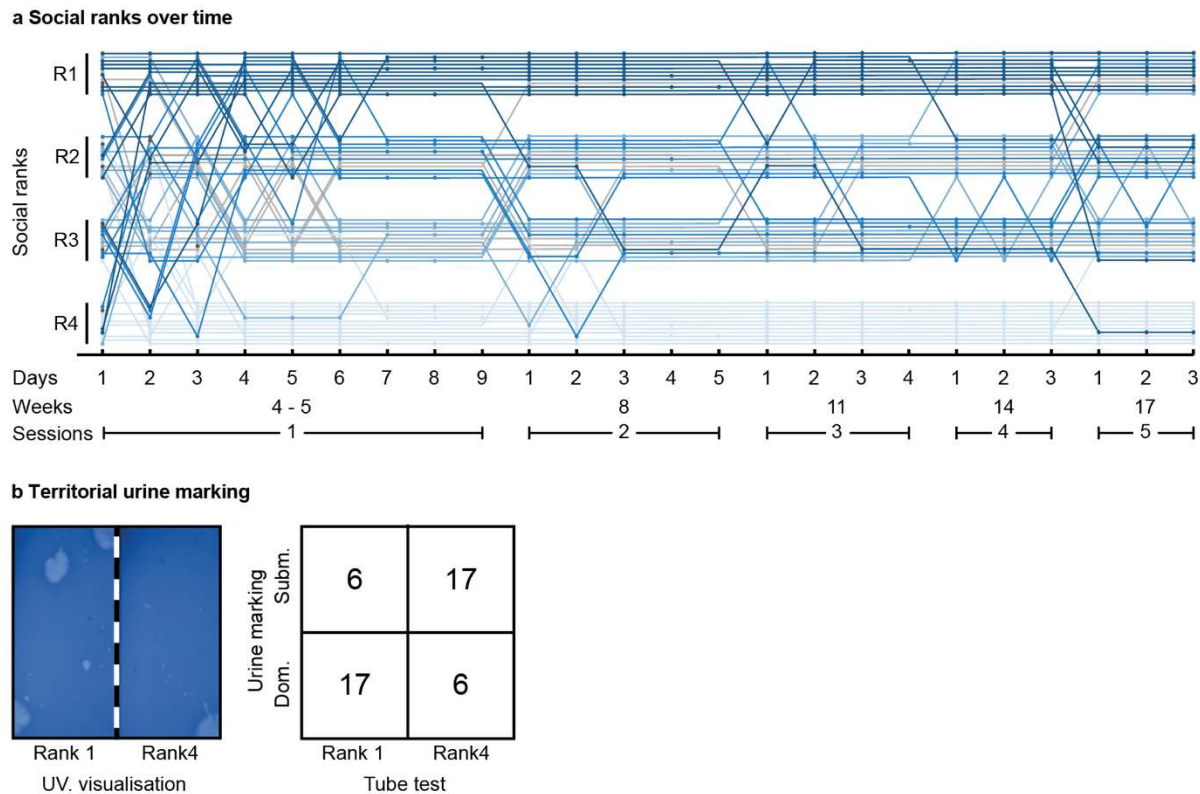
Figure 5. Dopamine neurons activity in the ventral tegmental area and Glucocorticoid Receptor in dopaminergic neurons modulate social rank attainment.

a, Differences in dopamine utilization between Rank 1 and Rank 4 males. Left, sagittal representation sketches the section lines for tissue punches along the mesocorticolimbic

pathway (bottom, coronal view). Dopamine utilization was estimated measuring the ratio DOPAC/DA in the caudate putamen (CPu, n=10, 5 mice), the nucleus accumbens (NAcc, n=10, 5 mice) and the prefrontal cortex (PFC, n=12, 6 mice) of both R1 and R4 mice. The PFC/NAcc ratio was calculated for 4 mice (n=8). For PFC, $t_{22}=3.256$, $**p<0.01$, For PFC/NAcc $t_{14}=2.51$, $*p<0.05$, unpaired t-tests, two-tailed. n represents the number of hemispheres for each group. Error bars, \pm SEM. VTA: ventral tegmental area. **b**, Rank 1 individuals have lower VTA dopamine neurons bursting activity. Schematic representation of electrode positioning (left). Representative traces of recording for individuals of each rank (middle). Mean frequency (Hz) and percentage of spikes within bursts (SWB) of dopamine cells basal firing mice belonging to R1 (n=186, 10 individuals) and R4 (n=157, 10 individuals) (right). For SWB data: $t_{341}=2.362$, $p^*=0.02$, unpaired t-test, two-tailed. Error bars, \pm SEM. **c**, GR deletion in dopaminergic neurons promotes higher social ranking in tetrads. Left, tetrads were constituted with one mutant (GR^{D1aCre}) and three control ($GR^{lox/lox}$) mice, for three weeks. The middle graph indicates the percentage of GR^{D1aCre} mice reaching each rank, among the 7 tetrads tested. The right graph pictures the number of won tube test contests between GR^{D1aCre} and control mice, out of 189 encounters during the 3 last days of tube test sessions. Fischer's exact test, two-tailed, $****p<0.0001$, Error bars, \pm SEM. **d**, Decreased VTA dopaminergic neurons activity during colonization upwards social ranking. Upper row, schematic representation of the DREADD expressing AAV8 particles injection site (left). Representative analysis of injection site (right). Upper panel, DAPI staining, VTA: ventral tegmental area, SN: substantia nigra. Bar: 250 μ m. Middle panel, immunofluorescence staining detecting Tyrosine Hydroxylase (TH) expression. Lower panel, immunofluorescence staining detecting mCherry expression. Lower row, tetrads were constituted with one mouse expressing CNO-dependent hM4D (VTA^{inhib}) and three expressing GFP in the VTA (control) mice. CNO was permanently delivered in drinking water. After two weeks, social hierarchy was determined. The middle graph indicates the percentage of VTA^{inhib} mice reaching each possible rank, among the 6 tetrads tested. The right graph pictures the total number of won tube test contests between

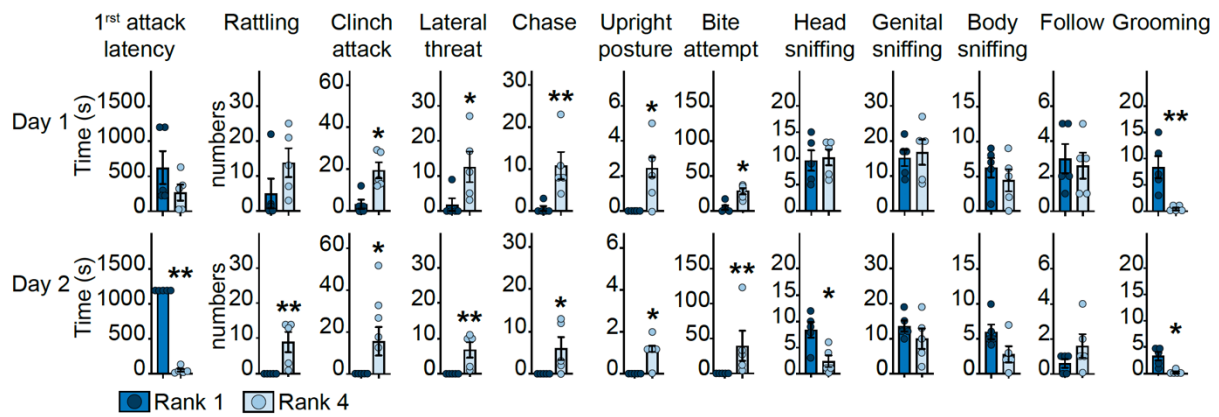
VTA^{inhib} and control mice, out of 171 encounters during the 3 last days of tube test sessions.

Fischer's exact test, two-tailed, **** p<0.0001, *** p<0.001 Error bars, ± SEM.



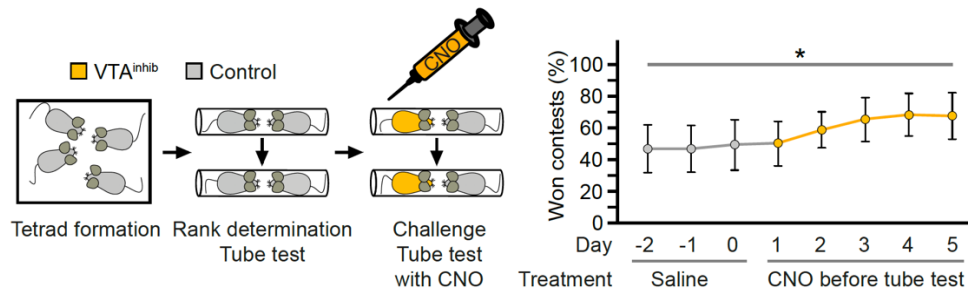
Extended data Figure 1. Stability of hierarchical classification and territoriality

a, Rank assessment in tube-test is pictured with daily resolution for 12 tetrads. As in Fig. 1, each line corresponds to an individual mouse and indicates the tetrad to which it belongs to (1 to 12). The blue intensity indicates its rank attainment after the first session. R1-4 indicates its social rank. Dots on the lines indicate that a tube-test was performed during the corresponding day. Note that there is no dot after hierarchy has reached the stability criterion during a session (*i.e.* that R1 and R4 mice were stable for three consecutive days, with an initial period of at least 6 days of testing). Grey lines correspond to mice of intermediate ranks that did not reach stability at the end of the first session. On days 1, 2 and 3, dark grey dots indicate individuals for which the rank could not be determined. **b**, Territorial urine marking reflects ranking obtained in tube-test. Left : representative picture of a urine marking during a 2 h confrontation between a R1 and a R4 mice, visualized under UV light. Right : contingency table of the ranking correspondences between the tube- and the urine marking- tests. Dom. : dominant; Subm : submissive. Fisher's exact test, two-tailed, ** $p < 0.01$, $n = 23$ per group.



Extended data Figure 2. Aggressiveness of rank 1 and rank 4 mice

The latencies to the first attack during resident-intruder challenges were scored for rank 1 (dark blue) and rank 4 individuals (light blue, left graph). The occurrences of aggressive and not aggressive behaviours were scored during 20 min. Data are expressed as mean ± SEM. Statistical analyses were performed by using Mann-Whitney non-parametric test. *p<0.05; **p<0.01 (n=5 per group).



Extended data Figure 5. Reducing VTA dopamine neurons activity during tube test only does not affect social ranking.

Left, tetrads were constituted with one mouse expressing CNO-dependent hM4D and (VTA^{inhib}) and three expressing GFP in the VTA (control) mice, in absence of CNO treatment. After two weeks, social hierarchy was determined (n=7 cages). During the five following days, tube tests were repeated with mice receiving an injection of CNO, 30 minutes before. The right graph pictures the percentage of won tube test contests by VTA^{inhib} mice on the last three days without CNO treatment (days -2 till day 0, saline) and the five following days, after a CNO injection. Data are expressed as mean \pm SEM. Repeated ANOVA. * p<0.05.

Thesis references table

- Adhikari, A., Lerner, T. N., Finkelstein, J., Pak, S., Jennings, J. H., Davidson, T. J., Ferenczi, E., Gunaydin, L. A., Mirzabekov, J. J., Ye, L., Kim, S. Y., Lei, A., & Deisseroth, K. (2015). Basomedial amygdala mediates top-down control of anxiety and fear. *Nature*, *527*(7577), 179. <https://doi.org/10.1038/NATURE15698>
- AGGLETON, J. P., & MISHKIN, M. (1986). THE AMYGDALA: SENSORY GATEWAY TO THE EMOTIONS. *Biological Foundations of Emotion*, 281–299. <https://doi.org/10.1016/B978-0-12-558703-7.50018-8>
- Aksoy-Aksel, A., Gall, A., Seewald, A., Ferraguti, F., & Ehrlich, I. (2021). Midbrain dopaminergic inputs gate amygdala intercalated cell clusters by distinct and cooperative mechanisms in male mice. *ELife*, *10*. <https://doi.org/10.7554/ELIFE.63708>
- American Psychiatric Association. (2013). *Diagnostic and Statistical Manual of Mental Disorders*. <https://doi.org/10.1176/APPI.BOOKS.9780890425596>
- Anstrom, K. K., & Woodward, D. J. (2005). Restraint increases dopaminergic burst firing in awake rats. *Neuropsychopharmacology: Official Publication of the American College of Neuropsychopharmacology*, *30*(10), 1832–1840. <https://doi.org/10.1038/SJ.NPP.1300730>
- Anthony, T. E., Dee, N., Bernard, A., Lerchner, W., Heintz, N., & Anderson, D. J. (2014). Control of stress-induced persistent anxiety by an extra-amygdala septohypothalamic circuit. *Cell*, *156*(3), 522. <https://doi.org/10.1016/J.CELL.2013.12.040>
- Aransay, A., Rodríguez-López, C., García-Amado, M., Clascá, F., & Prensa, L. (2015). Long-range projection neurons of the mouse ventral tegmental area: a single-cell axon tracing analysis. *Frontiers in Neuroanatomy*, *9*(MAY). <https://doi.org/10.3389/FNANA.2015.00059>
- Asede, D., Bosch, D., Lüthi, A., Ferraguti, F., & Ehrlich, I. (2015). Sensory inputs to intercalated cells provide fear-learning modulated inhibition to the basolateral amygdala. *Neuron*, *86*(2), 541–554. <https://doi.org/10.1016/J.NEURON.2015.03.008/ATTACHMENT/5FE4A46C-2BB3-4C3C-ABF9-9AC10F76CCB3/MMC2.XLSX>
- Asok, A., Draper, A., Hoffman, A. F., Schulkin, J., Lupica, C. R., & Rosen, J. B. (2018). Optogenetic silencing of a corticotropin-releasing factor pathway from the central amygdala to the bed nucleus of the stria terminalis disrupts sustained fear. *Molecular Psychiatry*, *23*(4), 914. <https://doi.org/10.1038/MP.2017.79>
- Babaev, O., Piletti Chatain, C., & Krueger-Burg, D. (2018). Inhibition in the amygdala anxiety circuitry. *Experimental & Molecular Medicine* *2018 50:4*, *50*(4), 1–16. <https://doi.org/10.1038/s12276-018-0063-8>
- Balakathiresan, N. S., Chandran, R., Bhomia, M., Jia, M., Li, H., & Maheshwari, R. K. (2014). Serum and amygdala microRNA signatures of posttraumatic stress: Fear correlation and biomarker potential. *Journal of Psychiatric Research*, *57*(1), 65–73. <https://doi.org/10.1016/J.JPSYCHIRES.2014.05.020>
- Bandler, R., & Shipley, M. T. (1994). Columnar organization in the midbrain periaqueductal gray: modules for emotional expression? *Trends in Neurosciences*, *17*(9), 379–389. [https://doi.org/10.1016/0166-2236\(94\)90047-7](https://doi.org/10.1016/0166-2236(94)90047-7)
- Barbano, M. F., Wang, H. L., Morales, M., & Wise, R. A. (2016). Feeding and Reward Are Differentially Induced by Activating GABAergic Lateral Hypothalamic Projections to VTA. *The Journal of Neuroscience: The Official Journal of the Society for Neuroscience*, *36*(10), 2975–2985. <https://doi.org/10.1523/JNEUROSCI.3799-15.2016>

- Barbano, M. F., Wang, H. L., Zhang, S., Miranda-Barrientos, J., Estrin, D. J., Figueroa-González, A., Liu, B., Barker, D. J., & Morales, M. (2020). VTA Glutamatergic Neurons Mediate Innate Defensive Behaviors. *Neuron*, *107*(2), 368-382.e8. <https://doi.org/10.1016/J.NEURON.2020.04.024>
- Barik, J., Marti, F., Morel, C., Fernandez, S., Lanteri, C., Godeheu, G., Tassin, J.-P., Mombereau, C., Faure, P., & Tronche, F. (2013). Chronic Stress Triggers Social Aversion via Glucocorticoid Receptor in Dopaminergic Neurons. In *Science (New York, N.Y.)* (Vol. 339). <https://doi.org/10.1126/science.1226767>
- Baritaki, S., de Bree, E., Chatzaki, E., & Pothoulakis, C. (2019). Chronic Stress, Inflammation, and Colon Cancer: A CRH System-Driven Molecular Crosstalk. *Journal of Clinical Medicine*, *8*(10). <https://doi.org/10.3390/JCM8101669>
- Bass, C. E., Grinevich, V. P., Gioia, D., Day-Brown, J. D., Bonin, K. D., Stuber, G. D., Weiner, J. L., & Budygin, E. A. (2013). Optogenetic stimulation of VTA dopamine neurons reveals that tonic but not phasic patterns of dopamine transmission reduce ethanol self-administration. *Frontiers in Behavioral Neuroscience*, *7*(NOV). <https://doi.org/10.3389/FNBEH.2013.00173>
- Bauch, E. M., Rausch, V. H., & Bunzeck, N. (2014). Pain anticipation recruits the mesolimbic system and differentially modulates subsequent recognition memory. *Human Brain Mapping*, *35*(9), 4594. <https://doi.org/10.1002/HBM.22497>
- Beier, K. T., Steinberg, E. E., Deloach, K. E., Xie, S., Miyamichi, K., Schwarz, L., Gao, X. J., Kremer, E. J., Malenka, R. C., & Luo, L. (2015). Circuit Architecture of VTA Dopamine Neurons Revealed by Systematic Input–Output Mapping. *Cell*, *162*(3), 622. <https://doi.org/10.1016/J.CELL.2015.07.015>
- Birmingham, M. K., Stumpf, W. E., & Sar, M. (1979). Nuclear localization of aldosterone in rat brain cells assessed by autoradiography. *Experientia*, *35*(9), 1240–1241. <https://doi.org/10.1007/BF01963313>
- Björklund, A., & Dunnett, S. B. (2007). Dopamine neuron systems in the brain: an update. *Trends in Neurosciences*, *30*(5), 194–202. <https://doi.org/10.1016/J.TINS.2007.03.006>
- Blanchard, D. C., Griebel, G., & Blanchard, R. J. (2003). The Mouse Defense Test Battery: pharmacological and behavioral assays for anxiety and panic. *European Journal of Pharmacology*, *463*(1–3), 97–116. [https://doi.org/10.1016/S0014-2999\(03\)01276-7](https://doi.org/10.1016/S0014-2999(03)01276-7)
- Blanchard, D. C., Griebel, G., Pobbe, R., & Blanchard, R. J. (2011). Risk assessment as an evolved threat detection and analysis process. *Neuroscience & Biobehavioral Reviews*, *35*(4), 991–998. <https://doi.org/10.1016/J.NEUBIOREV.2010.10.016>
- Blanchard, R. J., Hebert, M. A., Ferrari, P., Palanza, P., Figueira, R., Blanchard, D. C., & Parmigiani, S. (1998). Defensive behaviors in wild and laboratory (Swiss) mice: the mouse defense test battery. *Physiology & Behavior*, *65*(2), 201–209. [https://doi.org/10.1016/S0031-9384\(98\)00012-2](https://doi.org/10.1016/S0031-9384(98)00012-2)
- Borowski, T. B., & Kokkinidis, L. (1996). Contribution of ventral tegmental area dopamine neurons to expression of conditional fear: effects of electrical stimulation, excitotoxin lesions, and quinpirole infusion on potentiated startle in rats. *Behavioral Neuroscience*, *110*(6), 1349–1364. <https://doi.org/10.1037//0735-7044.110.6.1349>
- Bota, M., Sporns, O., & Swanson, L. W. (2012). Neuroinformatics analysis of molecular expression patterns and neuron populations in gray matter regions: the rat BST as a rich exemplar. *Brain Research*, *1450*, 174–193. <https://doi.org/10.1016/J.BRAINRES.2012.02.034>
- Bouarab, C., Thompson, B., & Polter, A. M. (2019). VTA GABA Neurons at the Interface of Stress and Reward. *Frontiers in Neural Circuits*, *13*. <https://doi.org/10.3389/FNCIR.2019.00078>

- Bouret, S., Duvel, A., Onat, S., & Sara, S. J. (2003). Phasic Activation of Locus Ceruleus Neurons by the Central Nucleus of the Amygdala. *Journal of Neuroscience*, 23(8), 3491–3497. <https://doi.org/10.1523/JNEUROSCI.23-08-03491.2003>
- Britt, J. P., Benaliouad, F., McDevitt, R. A., Stuber, G. D., Wise, R. A., & Bonci, A. (2012). Synaptic and Behavioral Profile of Multiple Glutamatergic Inputs to the Nucleus Accumbens. *Neuron*, 76(4), 790. <https://doi.org/10.1016/J.NEURON.2012.09.040>
- Bromberg-Martin, E. S., Matsumoto, M., & Hikosaka, O. (2010). Dopamine in motivational control: rewarding, aversive, and alerting. *Neuron*, 68(5), 815. <https://doi.org/10.1016/J.NEURON.2010.11.022>
- Brown, A. C., & Waslien, C. I. (2003). STRESS AND NUTRITION. *Encyclopedia of Food Sciences and Nutrition*, 5628–5636. <https://doi.org/10.1016/B0-12-227055-X/01156-1>
- Buffalari, D. M., & Grace, A. A. (2007). Noradrenergic Modulation of Basolateral Amygdala Neuronal Activity: Opposing Influences of α -2 and β Receptor Activation. *The Journal of Neuroscience*, 27(45), 12358. <https://doi.org/10.1523/JNEUROSCI.2007-07.2007>
- Cádiz-Moretti, B., Otero-García, M., Martínez-García, F., & Lanuza, E. (2014). Afferent projections to the different medial amygdala subdivisions: a retrograde tracing study in the mouse. *Brain Structure and Function* 2014 221:2, 221(2), 1033–1065. <https://doi.org/10.1007/S00429-014-0954-Y>
- Cai, H., Haubensak, W., Anthony, T. E., & Anderson, D. J. (2014). Central amygdala PKC- δ (+) neurons mediate the influence of multiple anorexigenic signals. *Nature Neuroscience*, 17(9), 1240–1248. <https://doi.org/10.1038/NN.3767>
- Cai, P., Chen, H. Y., Tang, W. T., Hu, Y. D., Chen, S. Y., Lu, J. S., Lin, Z. H., Huang, S. N., Hu, L. H., Su, W. K., Li, Q. X., Lin, Z. J., Kang, T. R., Yan, X. Bin, Liu, P. C., Chen, L., Yin, D., Wu, S. Y., Li, H. Y., & Yu, C. (2022). A glutamatergic basal forebrain to midbrain circuit mediates wakefulness and defensive behavior. *Neuropharmacology*, 208, 108979. <https://doi.org/10.1016/J.NEUROPHARM.2022.108979>
- Calhoun, G. G., & Tye, K. M. (2015). Resolving the neural circuits of anxiety. *Nature Neuroscience*, 18(10), 1394. <https://doi.org/10.1038/NN.4101>
- Cao, J. L., Covington, H. E., Friedman, A. K., Wilkinson, M. B., Walsh, J. J., Cooper, D. C., Nestler, E. J., & Han, M. H. (2010). Mesolimbic Dopamine Neurons in the Brain Reward Circuit Mediate Susceptibility to Social Defeat and Antidepressant Action. *The Journal of Neuroscience*, 30(49), 16453. <https://doi.org/10.1523/JNEUROSCI.3177-10.2010>
- Carli, G., & Farabollini, F. (2022). Introduction to defensive behavior in vertebrates. *Progress in Brain Research*, 271(1), 37–49. <https://doi.org/10.1016/BS.PBR.2022.02.002>
- Casseday, J. H., Fremouw, T., & Covey, E. (2002). *The Inferior Colliculus: A Hub for the Central Auditory System*. 238–318. https://doi.org/10.1007/978-1-4757-3654-0_7
- Cerminara, N. L., Koutsikou, S., Lumb, B. M., & Apps, R. (2009). The periaqueductal grey modulates sensory input to the cerebellum: a role in coping behaviour? *The European Journal of Neuroscience*, 29(11), 2197–2206. <https://doi.org/10.1111/J.1460-9568.2009.06760.X>
- Cha, J., Carlson, J. M., DeDora, D. J., Greenberg, T., Proudfit, G. H., & Mujica-Parodi, L. R. (2014). Hyper-Reactive Human Ventral Tegmental Area and Aberrant Mesocorticolimbic Connectivity in Overgeneralization of Fear in Generalized Anxiety Disorder. *The Journal of Neuroscience*, 34(17), 5855. <https://doi.org/10.1523/JNEUROSCI.4868-13.2014>

- Challis, R. C., Ravindra Kumar, S., Chan, K. Y., Challis, C., Beadle, K., Jang, M. J., Kim, H. M., Rajendran, P. S., Tompkins, J. D., Shivkumar, K., Deverman, B. E., & Gradinaru, V. (2019). Systemic AAV vectors for widespread and targeted gene delivery in rodents. *Nature Protocols*, *14*(2), 379–414. <https://doi.org/10.1038/S41596-018-0097-3>
- Chareyron, L. J., Banta Lavenex, P., Amaral, D. G., & Lavenex, P. (2011). Stereological Analysis of the Rat and Monkey Amygdala. *The Journal of Comparative Neurology*, *519*(16), 3218. <https://doi.org/10.1002/CNE.22677>
- Chen, S. Y., Yao, J., Hu, Y. D., Chen, H. Y., Liu, P. C., Wang, W. F., Zeng, Y. H., Zhuang, C. W., Zeng, S. X., Li, Y. P., Yang, L. Y., Huang, Z. X., Huang, K. Q., Lai, Z. T., Hu, Y. H., Cai, P., Chen, L., & Wu, S. (2022). Control of Behavioral Arousal and Defense by a Glutamatergic Midbrain-Amygdala Pathway in Mice. *Frontiers in Neuroscience*, *16*, 415. <https://doi.org/10.3389/FNINS.2022.850193/BIBTEX>
- Chiodo, L. A., Bannon, M. J., Grace, A. A., Roth, R. H., & Bunney, B. S. (1984). Evidence for the absence of impulse-regulating somatodendritic and synthesis-modulating nerve terminal autoreceptors on subpopulations of mesocortical dopamine neurons. *Neuroscience*, *12*(1), 1–16. [https://doi.org/10.1016/0306-4522\(84\)90133-7](https://doi.org/10.1016/0306-4522(84)90133-7)
- Christianson, J. P., Ragole, T., Amat, J., Greenwood, B. N., Strong, P. V., Paul, E. D., Fleshner, M., Watkins, L. R., & Maier, S. F. (2010). 5-hydroxytryptamine 2C receptors in the basolateral amygdala are involved in the expression of anxiety after uncontrollable traumatic stress. *Biological Psychiatry*, *67*(4), 339. <https://doi.org/10.1016/J.BIOPSYCH.2009.09.011>
- Ciccocioppo, R., de Guglielmo, G., Hansson, A. C., Ubaldi, M., Kallupi, M., Cruz, M. T., Oleata, C. S., Heilig, M., & Roberto, M. (2014). Restraint Stress Alters Nociceptin/Orphanin FQ and CRF Systems in the Rat Central Amygdala: Significance for Anxiety-Like Behaviors. *The Journal of Neuroscience*, *34*(2), 363. <https://doi.org/10.1523/JNEUROSCI.2400-13.2014>
- Coimbra, B., Domingues, A. V., Soares-Cunha, C., Correia, R., Pinto, L., Sousa, N., & Rodrigues, A. J. (2021). Laterodorsal tegmentum-ventral tegmental area projections encode positive reinforcement signals. *Journal of Neuroscience Research*, *99*(11), 3084–3100. <https://doi.org/10.1002/JNR.24931>
- Colyn, L., Venzala, E., Marco, S., Perez-Otaño, I., & Tordera, R. M. (2019). Chronic social defeat stress induces sustained synaptic structural changes in the prefrontal cortex and amygdala. *Behavioural Brain Research*, *373*, 112079. <https://doi.org/10.1016/J.BBR.2019.112079>
- Courtjol, E., Menezes, E. C., & Teixeira, C. M. (2021). Serotonergic regulation of the dopaminergic system: Implications for reward-related functions. *Neuroscience and Biobehavioral Reviews*, *128*, 282–293. <https://doi.org/10.1016/J.NEUBIOREV.2021.06.022>
- Cryan, J. F., & Holmes, A. (2005). The ascent of mouse: advances in modelling human depression and anxiety. *Nature Reviews Drug Discovery* *2005* *4*:9, *4*(9), 775–790. <https://doi.org/10.1038/nrd1825>
- Datta, D., & Arnsten, A. F. T. (2019). Loss of Prefrontal Cortical Higher Cognition with Uncontrollable Stress: Molecular Mechanisms, Changes with Age, and Relevance to Treatment. *Brain Sciences*, *9*(5). <https://doi.org/10.3390/BRAINSCI9050113>
- Davis, M., Walker, D. L., Miles, L., & Grillon, C. (2010). Phasic vs Sustained Fear in Rats and Humans: Role of the Extended Amygdala in Fear vs Anxiety. *Neuropsychopharmacology*, *35*(1), 105. <https://doi.org/10.1038/NPP.2009.109>
- De Jong, J. W., Afjei, A., Pollak, I., Tian, L., Deisseroth, K., & Correspondence, S. L. (2019). A Neural Circuit Mechanism for Encoding Aversive Stimuli in the Mesolimbic Dopamine System. *Neuron*,

101, 133-151.e7. <https://doi.org/10.1016/j.neuron.2018.11.005>

- De La Mora, M. P., Cárdenas-Cachón, L., Vázquez-García, M., Crespo-Ramírez, M., Jacobsen, K., Höistad, M., Agnati, L., & Fuxe, K. (2005). Anxiolytic effects of intra-amygdaloid injection of the D1 antagonist SCH23390 in the rat. *Neuroscience Letters*, 377(2), 101–105. <https://doi.org/10.1016/J.NEULET.2004.11.079>
- de la Mora, M. P., Gallegos-Cari, A., Arizmendi-García, Y., Marcellino, D., & Fuxe, K. (2010). Role of dopamine receptor mechanisms in the amygdaloid modulation of fear and anxiety: Structural and functional analysis. *Progress in Neurobiology*, 90(2), 198–216. <https://doi.org/10.1016/j.pneurobio.2009.10.010>
- Deng, H., Xiao, X., & Wang, Z. (2016). Periaqueductal Gray Neuronal Activities Underlie Different Aspects of Defensive Behaviors. *Journal of Neuroscience*, 36(29), 7580–7588. <https://doi.org/10.1523/JNEUROSCI.4425-15.2016>
- Di Chiara, G., & Imperato, A. (1988). Drugs abused by humans preferentially increase synaptic dopamine concentrations in the mesolimbic system of freely moving rats. *Proceedings of the National Academy of Sciences of the United States of America*, 85(14), 5274–5278. <https://doi.org/10.1073/PNAS.85.14.5274>
- Diano, M., Celeghein, A., Bagnis, A., & Tamietto, M. (2017). Amygdala response to emotional stimuli without awareness: Facts and interpretations. *Frontiers in Psychology*, 7(JAN). <https://doi.org/10.3389/FPSYG.2016.02029/FULL>
- Duval, E. R., Javanbakht, A., & Liberzon, I. (2015). Neural circuits in anxiety and stress disorders: a focused review. *Therapeutics and Clinical Risk Management*, 11, 115. <https://doi.org/10.2147/TCRM.S48528>
- Duvarci, S., & Pare, D. (2014). AMYGDALA MICROCIRCUITS CONTROLLING LEARNED FEAR. *Neuron*, 82(5), 966. <https://doi.org/10.1016/J.NEURON.2014.04.042>
- Duvarci, S., & Paré, D. (2007). Glucocorticoids enhance the excitability of principal basolateral amygdala neurons. *The Journal of Neuroscience: The Official Journal of the Society for Neuroscience*, 27(16), 4482–4491. <https://doi.org/10.1523/JNEUROSCI.0680-07.2007>
- Enoch, M. A., Xu, K., Ferro, E., Harris, C. R., & Goldman, D. (2003). Genetic origins of anxiety in women: a role for a functional catechol-O-methyltransferase polymorphism. *Psychiatric Genetics*, 13(1), 33–41. <https://doi.org/10.1097/00041444-200303000-00006>
- Etkin, A., Prater, K. E., Schatzberg, A. F., Menon, V., & Greicius, M. D. (2009). Disrupted amygdalar subregion functional connectivity and evidence of a compensatory network in generalized anxiety disorder. *Archives of General Psychiatry*, 66(12), 1361–1372. <https://doi.org/10.1001/ARCHGENPSYCHIATRY.2009.104>
- Fadok, J. P., Krabbe, S., Markovic, M., Courtin, J., Xu, C., Massi, L., Botta, P., Bylund, K., Müller, C., Kovacevic, A., Tovote, P., & Lüthi, A. (2017). A competitive inhibitory circuit for selection of active and passive fear responses. *Nature*, 542(7639), 96–99. <https://doi.org/10.1038/NATURE21047>
- Fadok, J. P., Markovic, M., Tovote, P., & Lüthi, A. (2018). New perspectives on central amygdala function. *Current Opinion in Neurobiology*, 49, 141–147. <https://doi.org/10.1016/J.CONB.2018.02.009>
- Faget, L., Osakada, F., Duan, J., Ressler, R., Johnson, A. B., Proudfoot, J. A., Yoo, J. H., Callaway, E. M., & Hnasko, T. S. (2016). Afferent inputs to neurotransmitter-defined cell types in the ventral tegmental area. *Cell Reports*, 15(12), 2796. <https://doi.org/10.1016/J.CELREP.2016.05.057>

- Faget, L., Zell, V., Souter, E., McPherson, A., Ressler, R., Gutierrez-Reed, N., Yoo, J. H., Dulcis, D., & Hnasko, T. S. (2018). Opponent control of behavioral reinforcement by inhibitory and excitatory projections from the ventral pallidum. *Nature Communications* 2018 9:1, 9(1), 1–14. <https://doi.org/10.1038/s41467-018-03125-y>
- Farook, J. M., Wang, Q., Moochhala, S. M., Zhu, Z. Y., Lee, L., & Wong, P. T. H. (2004). Distinct regions of periaqueductal gray (PAG) are involved in freezing behavior in hooded PVG rats on the cat-freezing test apparatus. *Neuroscience Letters*, 354(2), 139–142. <https://doi.org/10.1016/J.NEULET.2003.10.011>
- Felix-Ortiz, A. C., Burgos-Robles, A., Bhagat, N. D., Leppla, C. A., & Tye, K. M. (2016). Bidirectional modulation of anxiety-related and social behaviors by amygdala projections to the medial prefrontal cortex. *Neuroscience*, 321, 197–209. <https://doi.org/10.1016/J.NEUROSCIENCE.2015.07.041>
- Felix-Ortiz, Ada C., Beyeler, A., Seo, C., Leppla, C. A., Wildes, C. P., & Tye, K. M. (2013). BLA to vHPC inputs modulate anxiety-related behaviors. *Neuron*, 79(4), 658–664. <https://doi.org/10.1016/J.NEURON.2013.06.016>
- Forster, G. L., Novick, A. M., Scholl, J. L., & Watt, M. J. (2012). The Role of the Amygdala in Anxiety Disorders. *The Amygdala - A Discrete Multitasking Manager*. <https://doi.org/10.5772/50323>
- Gasparini, S., Howland, J. M., Thatcher, A. J., & Geerling, J. C. (2020). Central afferents to the nucleus of the solitary tract in rats and mice. *The Journal of Comparative Neurology*, 528(16), 2708. <https://doi.org/10.1002/CNE.24927>
- German, D. C., Schlusselberg, D. S., & Woodward, D. J. (1983). Three-dimensional computer reconstruction of midbrain dopaminergic neuronal populations: from mouse to man. *Journal of Neural Transmission*, 57(4), 243–254. <https://doi.org/10.1007/BF01248996>
- Gerrits, M. A. F. M., & Van Ree, J. M. (1996). Effect of nucleus accumbens dopamine depletion on motivational aspects involved in initiation of cocaine and heroin self-administration in rats. *Brain Research*, 713(1–2), 114–124. [https://doi.org/10.1016/0006-8993\(95\)01491-8](https://doi.org/10.1016/0006-8993(95)01491-8)
- Gilabert-Juan, J., Castillo-Gomez, E., Pérez-Rando, M., Moltó, M. D., & Nacher, J. (2011). Chronic stress induces changes in the structure of interneurons and in the expression of molecules related to neuronal structural plasticity and inhibitory neurotransmission in the amygdala of adult mice. *Experimental Neurology*, 232(1), 33–40. <https://doi.org/10.1016/J.EXPNEUROL.2011.07.009>
- Gilpin, N. W., Herman, M. A., & Roberto, M. (2015). The Central Amygdala as an Integrative Hub for Anxiety and Alcohol Use Disorders. *Biological Psychiatry*, 77(10), 859–869. <https://doi.org/10.1016/J.BIOPSYCH.2014.09.008>
- Gjerstad, J. K., Lightman, S. L., & Spiga, F. (2018). Role of glucocorticoid negative feedback in the regulation of HPA axis pulsatility. *Stress (Amsterdam, Netherlands)*, 21(5), 403. <https://doi.org/10.1080/10253890.2018.1470238>
- Godar, S. C., Bortolato, M., Frau, R., Dousti, M., Chen, K., & Shih, J. C. (2011). Maladaptive defensive behaviours in monoamine oxidase A-deficient mice. *The International Journal of Neuropsychopharmacology / Official Scientific Journal of the Collegium Internationale Neuropsychopharmacologicum (CINP)*, 14(9), 1195. <https://doi.org/10.1017/S1461145710001483>
- Gomez-Sanchez, E. P. (2004). Brain mineralocorticoid receptors: Orchestrators of hypertension and end-organ disease. *Current Opinion in Nephrology and Hypertension*, 13(2), 191–196. <https://doi.org/10.1097/00041552-200403000-00007>

- Gong, X., Mendoza-Halliday, D., Ting, J. T., Kaiser, T., Sun, X., Bastos, A. M., Wimmer, R. D., Guo, B., Chen, Q., Zhou, Y., Pruner, M., Wu, C. W. H., Park, D., Deisseroth, K., Barak, B., Boyden, E. S., Miller, E. K., Halassa, M. M., Fu, Z., ... Feng, G. (2020). An Ultra-Sensitive Step-Function Opsin for Minimally Invasive Optogenetic Stimulation in Mice and Macaques. *Neuron*, *107*(1), 38-51.e8. <https://doi.org/10.1016/J.NEURON.2020.03.032>
- González-Hernández, T., Barroso-Chinea, P., Acevedo, A., Salido, E., & Rodríguez, M. (2001). Colocalization of tyrosine hydroxylase and GAD65 mRNA in mesostriatal neurons. *European Journal of Neuroscience*, *13*(1), 57–67. <https://doi.org/10.1111/J.1460-9568.2001.01371.X>
- González-Hernández, T., Barroso-Chinea, P., De La Cruz Muros, I., Del Mar Pérez-Delgado, M., & Rodríguez, M. (2004). Expression of dopamine and vesicular monoamine transporters and differential vulnerability of mesostriatal dopaminergic neurons. *The Journal of Comparative Neurology*, *479*(2), 198–215. <https://doi.org/10.1002/CNE.20323>
- Goode, T. D., Ressler, R. L., Acca, G. M., Miles, O. W., & Maren, S. (2019). Bed nucleus of the stria terminalis regulates fear to unpredictable threat signals. *ELife*, *8*. <https://doi.org/10.7554/ELIFE.46525>
- Gordon-Fennell, A., Gordon-Fennell, L., Desai, S., & Marinelli, M. (2020). The Lateral Preoptic Area and Its Projection to the VTA Regulate VTA Activity and Drive Complex Reward Behaviors. *Frontiers in Systems Neuroscience*, *14*, 71. <https://doi.org/10.3389/FNSYS.2020.581830/BIBTEX>
- Gottschalk, M. G., & Domschke, K. (2017). Genetics of generalized anxiety disorder and related traits. *Dialogues in Clinical Neuroscience*, *19*(2), 159. <https://doi.org/10.31887/DCNS.2017.19.2/KDOMSCHKE>
- Grace, A. A., & Bunney, B. S. (1984). THE CONTROL OF FIRING PATTERN IN NIGRAL DOPAMINE NEURONS: BURST FIRING'. *The Journal of Neuroscience*, *4*(11).
- Grace, A. A., & Bunney, B. S. (1984). The control of firing pattern in nigral dopamine neurons: single spike firing. *The Journal of Neuroscience*, *4*(11), 2866. <https://doi.org/10.1523/JNEUROSCI.04-11-02866.1984>
- Grace, Anthony A., Floresco, S. B., Goto, Y., & Lodge, D. J. (2007). Regulation of firing of dopaminergic neurons and control of goal-directed behaviors. *Trends in Neurosciences*, *30*(5), 220–227. <https://doi.org/10.1016/J.TINS.2007.03.003>
- Grace, Anthony A., & Rosenkranz, J. A. (2002). Regulation of conditioned responses of basolateral amygdala neurons. *Physiology & Behavior*, *77*(4–5), 489–493. [https://doi.org/10.1016/S0031-9384\(02\)00909-5](https://doi.org/10.1016/S0031-9384(02)00909-5)
- Groeneweg, F. L., Karst, H., de Kloet, E. R., & Joëls, M. (2012). Mineralocorticoid and glucocorticoid receptors at the neuronal membrane, regulators of nongenomic corticosteroid signalling. *Molecular and Cellular Endocrinology*, *350*(2), 299–309. <https://doi.org/10.1016/J.MCE.2011.06.020>
- Gudsnuk, K., & Champagne, F. A. (2012). Epigenetic Influence of Stress and the Social Environment. *ILAR Journal*, *53*(3–4), 279. <https://doi.org/10.1093/ILAR.53.3-4.279>
- Gungor, N. Z., & Paré, D. (2016). Functional Heterogeneity in the Bed Nucleus of the Stria Terminalis. *The Journal of Neuroscience*, *36*(31), 8038. <https://doi.org/10.1523/JNEUROSCI.0856-16.2016>
- Haber, S. N., & Knutson, B. (2010). The reward circuit: linking primate anatomy and human imaging. *Neuropsychopharmacology: Official Publication of the American College of Neuropsychopharmacology*, *35*(1), 4–26. <https://doi.org/10.1038/NPP.2009.129>

- Halliday, G. M., & Törk, I. (1986). Comparative anatomy of the ventromedial mesencephalic tegmentum in the rat, cat, monkey and human. *Journal of Comparative Neurology*, 252(4), 423–445. <https://doi.org/10.1002/CNE.902520402>
- Haramati, S., Navon, I., Issler, O., Ezra-Nevo, G., Gil, S., Zwang, R., Hornstein, E., & Chen, A. (2011). microRNA as Repressors of Stress-Induced Anxiety: The Case of Amygdalar miR-34. *The Journal of Neuroscience*, 31(40), 14191. <https://doi.org/10.1523/JNEUROSCI.1673-11.2011>
- Hennigan, K., D'Ardenne, K., & McClure, S. M. (2015). Distinct midbrain and habenula pathways are involved in processing aversive events in humans. *The Journal of Neuroscience: The Official Journal of the Society for Neuroscience*, 35(1), 198–208. <https://doi.org/10.1523/JNEUROSCI.0927-14.2015>
- Herman, J. P. (2013). Neural control of chronic stress adaptation. *Frontiers in Behavioral Neuroscience*, 0(MAY), 61. <https://doi.org/10.3389/FNBEH.2013.00061/BIBTEX>
- Herman, J. P., Cullinan, W. E., & Watson, S. J. (1994). Involvement of the Bed Nucleus of the Stria Terminalis in Tonic Regulation of Paraventricular Hypothalamic CRH and AVP mRNA Expression. *Journal of Neuroendocrinology*, 6(4), 433–442. <https://doi.org/10.1111/J.1365-2826.1994.TB00604.X>
- Herry, C., Ciocchi, S., Senn, V., Demmou, L., Müller, C., & Lüthi, A. (2008). Switching on and off fear by distinct neuronal circuits. *Nature* 2008 454:7204, 454(7204), 600–606. <https://doi.org/10.1038/nature07166>
- Hettema, J. M., Neale, M. C., & Kendler, K. S. (2001). A review and meta-analysis of the genetic epidemiology of anxiety disorders. *The American Journal of Psychiatry*, 158(10), 1568–1578. <https://doi.org/10.1176/APPI.AJP.158.10.1568>
- Hill, M. N., Kumar, S. A., Filipowski, S. B., Iverson, M., Stuhr, K. L., Keith, J. M., Cravatt, B. F., Hillard, C. J., Chattarji, S., & McEwen, B. S. (2012). Disruption of fatty acid amide hydrolase activity prevents the effects of chronic stress on anxiety and amygdalar microstructure. *Molecular Psychiatry* 2013 18:10, 18(10), 1125–1135. <https://doi.org/10.1038/mp.2012.90>
- Hnasko, T. S., Hjelmstad, G. O., Fields, H. L., & Edwards, R. H. (2012). Ventral Tegmental Area Glutamate Neurons: Electrophysiological Properties and Projections. *Journal of Neuroscience*, 32(43), 15076–15085. <https://doi.org/10.1523/jneurosci.3128-12.2012>
- Ito, M., Nagase, M., Tohyama, S., Mikami, K., Kato, F., & Watabe, A. M. (2021). The parabrachial-to-amygdala pathway provides aversive information to induce avoidance behavior in mice. *Molecular Brain*, 14(1), 1–9. <https://doi.org/10.1186/S13041-021-00807-5/FIGURES/3>
- Jaenisch, R., & Bird, A. (2003). Epigenetic regulation of gene expression: how the genome integrates intrinsic and environmental signals. *Nature Genetics*, 33 Suppl(3S), 245–254. <https://doi.org/10.1038/NG1089>
- Janak, P. H., & Tye, K. M. (2015). From circuits to behaviour in the amygdala. *Nature*, 517(7534), 284. <https://doi.org/10.1038/NATURE14188>
- Jennings, J. H., Sparta, D. R., Stamatakis, A. M., Ung, R. L., Pleil, K. E., Kash, T. L., & Stuber, G. D. (2013). Distinct extended amygdala circuits for divergent motivational states. *Nature*, 496(7444), 224–228. <https://doi.org/10.1038/NATURE12041>
- Jhou, T. C., Fields, H. L., Baxter, M. G., Saper, C. B., & Holland, P. C. (2009). The rostromedial tegmental nucleus (RMTg), a major GABAergic afferent to midbrain dopamine neurons, selectively encodes aversive stimuli and promotes behavioral inhibition. *Neuron*, 61(5), 786. <https://doi.org/10.1016/J.NEURON.2009.02.001>

- Joëls, M., Angela Sarabdjitsingh, R., & Karst, H. (2012). Unraveling the Time Domains of Corticosteroid Hormone Influences on Brain Activity: Rapid, Slow, and Chronic Modes. *Pharmacological Reviews*, 64(4), 901–938. <https://doi.org/10.1124/PR.112.005892>
- Joëls, M., & de Kloet, E. R. (2017). 30 YEARS OF THE MINERALOCORTICOID RECEPTOR: The brain mineralocorticoid receptor: a saga in three episodes. *Journal of Endocrinology*, 234(1), T49–T66. <https://doi.org/10.1530/JOE-16-0660>
- Kawano, M., Kawasaki, A., Sakata-Haga, H., Fukui, Y., Kawano, H., Nogami, H., & Hisano, S. (2006). Particular subpopulations of midbrain and hypothalamic dopamine neurons express vesicular glutamate transporter 2 in the rat brain. *The Journal of Comparative Neurology*, 498(5), 581–592. <https://doi.org/10.1002/CNE.21054>
- Kempadoo, K. A., Tourino, C., Cho, S. L., Magnani, F., Leininger, G. M., Stuber, G. D., Zhang, F., Myers, M. G., Deisseroth, K., de Lecea, L., & Bonci, A. (2013). Hypothalamic Neurotensin Projections Promote Reward by Enhancing Glutamate Transmission in the VTA. *The Journal of Neuroscience*, 33(18), 7618. <https://doi.org/10.1523/JNEUROSCI.2588-12.2013>
- Kim, J. I., Ganesan, S., Luo, S. X., Wu, Y. W., Park, E., Huang, E. J., Chen, L., & Ding, J. B. (2015). Aldehyde dehydrogenase 1a1 mediates a GABA synthesis pathway in midbrain dopaminergic neurons. *Science (New York, N.Y.)*, 350(6256), 102–106. <https://doi.org/10.1126/SCIENCE.AAC4690>
- Kim, J., Pignatelli, M., Xu, S., Itohara, S., & Tonegawa, S. (2016). Antagonistic negative and positive neurons of the basolateral amygdala. *Nature Neuroscience* 2016 19:12, 19(12), 1636–1646. <https://doi.org/10.1038/nn.4414>
- Kim, J., Zhang, X., Muralidhar, S., LeBlanc, S. A., & Tonegawa, S. (2017). Basolateral to Central Amygdala Neural Circuits for Appetitive Behaviors. *Neuron*, 93(6), 1464-1479.e5. <https://doi.org/10.1016/J.NEURON.2017.02.034>
- Kim, S. Y., Adhikari, A., Lee, S. Y., Marshel, J. H., Kim, C. K., Mallory, C. S., Lo, M., Pak, S., Mattis, J., Lim, B. K., Malenka, R. C., Warden, M. R., Neve, R., Tye, K. M., & Deisseroth, K. (2013). Diverging neural pathways assemble a behavioural state from separable features in anxiety. *Nature*, 496(7444), 219–223. <https://doi.org/10.1038/NATURE12018>
- Klaassen, F. H., Held, L., Figner, B., O'Reilly, J. X., Klumpers, F., de Voogd, L. D., & Roelofs, K. (2021). Defensive freezing and its relation to approach–avoidance decision-making under threat. *Scientific Reports*, 11(1), 12030. <https://doi.org/10.1038/S41598-021-90968-Z>
- Koller, K., Rafal, R. D., Platt, A., & Mitchell, N. D. (2019). Orienting toward threat: Contributions of a subcortical pathway transmitting retinal afferents to the amygdala via the superior colliculus and pulvinar. *Neuropsychologia*, 128, 78–86. <https://doi.org/10.1016/J.NEUROPSYCHOLOGIA.2018.01.027>
- Korotkova, T. M., Ponomarenko, A. A., Brown, R. E., & Haas, H. L. (2004). Functional diversity of ventral midbrain dopamine and GABAergic neurons. *Molecular Neurobiology*, 29(3), 243–259. <https://doi.org/10.1385/MN:29:3:243>
- Koutsikou, S., Crook, J. J., Earl, E. V., Leith, J. L., Watson, T. C., Lumb, B. M., & Apps, R. (2014). Neural substrates underlying fear-evoked freezing: the periaqueductal grey–cerebellar link. *The Journal of Physiology*, 592(Pt 10), 2197. <https://doi.org/10.1113/JPHYSIOL.2013.268714>
- Koutsikou, S., Watson, T. C., Crook, J. J., Leith, J. L., Lawrenson, C. L., Apps, R., & Lumb, B. M. (2015). The Periaqueductal Gray Orchestrates Sensory and Motor Circuits at Multiple Levels of the Neuraxis. *The Journal of Neuroscience: The Official Journal of the Society for Neuroscience*, 35(42), 14132–14147. <https://doi.org/10.1523/JNEUROSCI.0261-15.2015>

- Kouzarides, T. (2007). Chromatin modifications and their function. *Cell*, 128(4), 693–705. <https://doi.org/10.1016/J.CELL.2007.02.005>
- Krauzlis, R. J., Lovejoy, L. P., & Zénon, A. (2013). Superior Colliculus and Visual Spatial Attention. *Annual Review of Neuroscience*, 36, 165–182. <https://doi.org/10.1146/ANNUREV-NEURO-062012-170249>
- Kröner, S., Rosenkranz, J. A., Grace, A. A., & Barrionuevo, G. (2005). Dopamine modulates excitability of basolateral amygdala neurons in vitro. *Journal of Neurophysiology*, 93(3), 1598–1610. <https://doi.org/10.1152/JN.00843.2004>
- Kršiak, M., Šulcová, A., Tomašiková, Z., Dlohožková, N., Kosař, E., & Mašek, K. (1981). Drug Effects on Attack, Defense and Escape in Mice. *Pharmacology Biochemistry and Behavior*, 14, 47–52. [https://doi.org/10.1016/S0091-3057\(81\)80010-X](https://doi.org/10.1016/S0091-3057(81)80010-X)
- La Manno, G., Gyllborg, D., Codeluppi, S., Nishimura, K., Salto, C., Zeisel, A., Borm, L. E., Stott, S. R. W., Toledo, E. M., Villaescusa, J. C., Lönnerberg, P., Ryge, J., Barker, R. A., Arenas, E., & Linnarsson, S. (2016). Molecular Diversity of Midbrain Development in Mouse, Human, and Stem Cells. *Cell*, 167(2), 566. <https://doi.org/10.1016/J.CELL.2016.09.027>
- Lahti, L., Haugas, M., Tikker, L., Airavaara, M., Voutilainen, M. H., Anttila, J., Kumar, S., Inkinen, C., Salminen, M., & Partanen, J. (2016). Differentiation and molecular heterogeneity of inhibitory and excitatory neurons associated with midbrain dopaminergic nuclei. *Development (Cambridge, England)*, 143(3), 516–529. <https://doi.org/10.1242/DEV.129957>
- Lammel, S., Hetzel, A., Häckel, O., Jones, I., Liss, B., & Roeper, J. (2008). Unique properties of mesoprefrontal neurons within a dual mesocorticolimbic dopamine system. *Neuron*, 57(5), 760–773. <https://doi.org/10.1016/J.NEURON.2008.01.022>
- Lammel, S., Lim, B. K., Ran, C., Huang, K. W., Betley, M. J., Tye, K. M., Deisseroth, K., & Malenka, R. C. (2012). Input-specific control of reward and aversion in the ventral tegmental area. *Nature*, 491(7423), 212–217. <https://doi.org/10.1038/nature11527>
- Lamont, E. W., & Kokkinidis, L. (1998). Infusion of the dopamine D1 receptor antagonist SCH 23390 into the amygdala blocks fear expression in a potentiated startle paradigm. *Brain Research*, 795(1–2), 128–136. [https://doi.org/10.1016/S0006-8993\(98\)00281-9](https://doi.org/10.1016/S0006-8993(98)00281-9)
- Lebow, M. A., & Chen, A. (2016). Overshadowed by the amygdala: the bed nucleus of the stria terminalis emerges as key to psychiatric disorders. *Molecular Psychiatry* 2016 21:4, 21(4), 450–463. <https://doi.org/10.1038/mp.2016.1>
- LeDoux, J. E., Iwata, J., Cicchetti, P., & Reis, D. J. (1988). Different projections of the central amygdaloid nucleus mediate autonomic and behavioral correlates of conditioned fear. *Journal of Neuroscience*, 8(7), 2517–2529. <https://doi.org/10.1523/JNEUROSCI.08-07-02517.1988>
- LeDoux, Joseph E., Cicchetti, P., Xagoraris, A., & Romanski, L. M. (1990). The lateral amygdaloid nucleus: sensory interface of the amygdala in fear conditioning. *The Journal of Neuroscience : The Official Journal of the Society for Neuroscience*, 10(4), 1062–1069. <https://doi.org/10.1523/JNEUROSCI.10-04-01062.1990>
- Lee, C., Lavoie, A., Liu, J., Chen, S. X., & Liu, B. H. (2020). Light Up the Brain: The Application of Optogenetics in Cell-Type Specific Dissection of Mouse Brain Circuits. *Frontiers in Neural Circuits*, 14, 18. <https://doi.org/10.3389/FNCIR.2020.00018/BIBTEX>
- Lesicko, A. M. H., Hristova, T. S., Maigler, K. C., & Llano, D. A. (2016). Connectional Modularity of Top-Down and Bottom-Up Multimodal Inputs to the Lateral Cortex of the Mouse Inferior Colliculus. *The Journal of Neuroscience : The Official Journal of the Society for Neuroscience*, 36(43), 11037–

11050. <https://doi.org/10.1523/JNEUROSCI.4134-15.2016>

- Li, G., Amano, T., Pare, D., & Nair, S. S. (2011). Impact of infralimbic inputs on intercalated amygdala neurons: a biophysical modeling study. *Learning & Memory (Cold Spring Harbor, N.Y.)*, *18*(4), 226–240. <https://doi.org/10.1101/LM.1938011>
- Li, Hao, Namburi, P., Olson, J. M., Borio, M., Lemieux, M. E., Beyeler, A., Calhoun, G. G., Hitora-Imamura, N., Coley, A. A., Libster, A., Bal, A., Jin, X., Wang, H., Jia, C., Choudhury, S. R., Shi, X., Felix-Ortiz, A. C., de la Fuente, V., Barth, V. P., ... Tye, K. M. (2022). Neurotensin orchestrates valence assignment in the amygdala. *Nature*. <https://doi.org/10.1038/S41586-022-04964-Y>
- Li, Hao, Pullmann, D., Cho, J. Y., Eid, M., & Jhou, T. C. (2019). Generality and opponency of rostromedial tegmental (RMTg) roles in valence processing. *ELife*, *8*. <https://doi.org/10.7554/ELIFE.41542>
- Li, Haohong, Penzo, M. A., Taniguchi, H., Kopec, C. D., Huang, Z. J., & Li, B. (2013). Experience-dependent modification of a central amygdala fear circuit. *Nature Neuroscience*, *16*(3), 332. <https://doi.org/10.1038/NN.3322>
- Li, X., Qi, J., Yamaguchi, T., Wang, H. L., & Morales, M. (2013). Heterogeneous composition of dopamine neurons of the rat A10 region: Molecular evidence for diverse signaling properties. *Brain Structure and Function*, *218*(5), 1159–1176. <https://doi.org/10.1007/S00429-012-0452-Z/TABLES/2>
- Li, Y., Li, C. Y., Xi, W., Jin, S., Wu, Z. H., Jiang, P., Dong, P., He, X. Bin, Xu, F. Q., Duan, S., Zhou, Y. D., & Li, X. M. (2019). Rostral and Caudal Ventral Tegmental Area GABAergic Inputs to Different Dorsal Raphe Neurons Participate in Opioid Dependence. *Neuron*, *101*(4), 748-761.e5. <https://doi.org/10.1016/J.NEURON.2018.12.012>
- Li, Z., Wei, J. X., Zhang, G. W., Huang, J. J., Zingg, B., Wang, X., Tao, H. W., & Zhang, L. I. (2021). Corticostriatal control of defense behavior in mice induced by auditory looming cues. *Nature Communications 2021 12:1*, *12*(1), 1–13. <https://doi.org/10.1038/s41467-021-21248-7>
- Likhtik, E., & Paz, R. (2015). Amygdala-prefrontal interactions in (mal)adaptive learning. *Trends in Neurosciences*, *38*(3), 158. <https://doi.org/10.1016/J.TINS.2014.12.007>
- Lisman, J., Schulman, H., & Cline, H. (2002). The molecular basis of CaMKII function in synaptic and behavioural memory. *Nature Reviews. Neuroscience*, *3*(3), 175–190. <https://doi.org/10.1038/NRN753>
- Liu, Z. P., Song, C., Wang, M., He, Y., Xu, X. Bin, Pan, H. Q., Chen, W. B., Peng, W. J., & Pan, B. X. (2014). Chronic stress impairs GABAergic control of amygdala through suppressing the tonic GABAA receptor currents. *Molecular Brain*, *7*(1), 1–14. <https://doi.org/10.1186/1756-6606-7-32/TABLES/1>
- Lodge, D. J., & Grace, A. A. (2006). The laterodorsal tegmentum is essential for burst firing of ventral tegmental area dopamine neurons. *Proceedings of the National Academy of Sciences of the United States of America*, *103*(13), 5167–5172. <https://doi.org/10.1073/PNAS.0510715103>
- Mackintosh, N. J. (1987). Neurobiology, psychology and habituation. *Behaviour Research and Therapy*, *25*(2), 81–97. [https://doi.org/10.1016/0005-7967\(87\)90079-9](https://doi.org/10.1016/0005-7967(87)90079-9)
- Maggio, N., & Segal, M. (2012). Steroid modulation of hippocampal plasticity: switching between cognitive and emotional memories. *Frontiers in Cellular Neuroscience*, *6*(MARCH). <https://doi.org/10.3389/FNCEL.2012.00012>
- Makovac, E., Meeten, F., Watson, D. R., Herman, A., Garfinkel, S. N., D. Critchley, H., & Ottaviani, C. (2016). Alterations in Amygdala-Prefrontal Functional Connectivity Account for Excessive Worry

- and Autonomic Dysregulation in Generalized Anxiety Disorder. *Biological Psychiatry*, 80(10), 786–795. <https://doi.org/10.1016/J.BIOPSYCH.2015.10.013>
- Margolis, E. B., Lock, H., Hjelmstad, G. O., & Fields, H. L. (2006). The ventral tegmental area revisited: is there an electrophysiological marker for dopaminergic neurons? *The Journal of Physiology*, 577(Pt 3), 907–924. <https://doi.org/10.1113/JPHYSIOL.2006.117069>
- Margules, D. L., & Olds, J. (1962). Identical “feeding” and “rewarding” systems in the lateral hypothalamus of rats. *Science (New York, N.Y.)*, 135(3501), 374–375. <https://doi.org/10.1126/SCIENCE.135.3501.374>
- Marowsky, A., Yanagawa, Y., Obata, K., & Vogt, K. E. (2005). A specialized subclass of interneurons mediates dopaminergic facilitation of amygdala function. *Neuron*, 48(6), 1025–1037. <https://doi.org/10.1016/J.NEURON.2005.10.029>
- Martel, P., & Fantino, M. (1996). Mesolimbic dopaminergic system activity as a function of food reward: a microdialysis study. *Pharmacology, Biochemistry, and Behavior*, 53(1), 221–226. [https://doi.org/10.1016/0091-3057\(95\)00187-5](https://doi.org/10.1016/0091-3057(95)00187-5)
- Masneuf, S., Lowery-Gionta, E., Colacicco, G., Pleil, K. E., Li, C., Crowley, N., Flynn, S., Holmes, A., & Kash, T. (2014). Glutamatergic mechanisms associated with stress-induced amygdala excitability and anxiety-related behavior. *Neuropharmacology*, 85, 190–197. <https://doi.org/10.1016/J.NEUROPHARM.2014.04.015>
- Matsumoto, M., & Hikosaka, O. (2009). How do dopamine neurons represent positive and negative motivational events? *Nature*, 459(7248), 837. <https://doi.org/10.1038/NATURE08028>
- McCall, J. G., Al-Hasani, R., Siuda, E. R., Hong, D. Y., Norris, A. J., Ford, C. P., & Bruchas, M. R. (2015). CRH Engagement of the Locus Coeruleus Noradrenergic System Mediates Stress-Induced Anxiety. *Neuron*, 87(3), 605–620. <https://doi.org/10.1016/J.NEURON.2015.07.002>
- McCorry, L. K. (2007). Physiology of the Autonomic Nervous System. *American Journal of Pharmaceutical Education*, 71(4). <https://doi.org/10.5688/AJ710478>
- Mcdonald, A. J. (1998). Cortical pathways to the mammalian amygdala. *Progress in Neurobiology*, 55(3), 257–332. [https://doi.org/10.1016/S0301-0082\(98\)00003-3](https://doi.org/10.1016/S0301-0082(98)00003-3)
- McEwen, B. S., & Stellar, E. (1993). Stress and the Individual: Mechanisms Leading to Disease. *Archives of Internal Medicine*, 153(18), 2093–2101. <https://doi.org/10.1001/ARCHINTE.1993.00410180039004>
- McHenry, J. A., Otis, J. M., Rossi, M. A., Robinson, J. E., Kosyk, O., Miller, N. W., McElligott, Z. A., Budygin, E. A., Rubinow, D. R., & Stuber, G. D. (2017). Hormonal gain control of a medial preoptic area social reward circuit. *Nature Neuroscience* 2017 20:3, 20(3), 449–458. <https://doi.org/10.1038/nn.4487>
- Meerson, A., Cacheaux, L., Goosens, K. A., Sapolsky, R. M., Soreq, H., & Kaufer, D. (2010). Changes in brain MicroRNAs contribute to cholinergic stress reactions. *Journal of Molecular Neuroscience*, 40(1–2), 47–55. <https://doi.org/10.1007/S12031-009-9252-1/FIGURES/2>
- Miranda-Barrientos, J., Chambers, I., Mongia, S., Liu, B., Wang, H. L., Mateo-Semidey, G. E., Margolis, E. B., Zhang, S., & Morales, M. (2021). Ventral tegmental area GABA, glutamate, and glutamate-GABA neurons are heterogeneous in their electrophysiological and pharmacological properties. *European Journal of Neuroscience*, 54(1), 4061–4084. <https://doi.org/10.1111/EJN.15156>
- Mitra, R., Jadhav, S., McEwen, B. S., Vyas, A., & Chattarji, S. (2005). Stress duration modulates the spatiotemporal patterns of spine formation in the basolateral amygdala. *Proceedings of the*

National Academy of Sciences of the United States of America, 102(26), 9371–9376.
<https://doi.org/10.1073/PNAS.0504011102/ASSET/09F39965-0DCD-4B6F-8C20-0D6C2AF0C581/ASSETS/GRAPHIC/ZPQ0260586800002.JPEG>

- Mogenson, G. J., Jones, D. L., & Yim, C. Y. (1980). From motivation to action: Functional interface between the limbic system and the motor system. *Progress in Neurobiology*, 14(2–3), 69–97. [https://doi.org/10.1016/0301-0082\(80\)90018-0](https://doi.org/10.1016/0301-0082(80)90018-0)
- Mongeau, R., Miller, G. A., Chiang, E., & Anderson, D. J. (2003). Neural correlates of competing fear behaviors evoked by an innately aversive stimulus. *The Journal of Neuroscience: The Official Journal of the Society for Neuroscience*, 23(9), 3855–3868. <https://doi.org/10.1523/JNEUROSCI.23-09-03855.2003>
- Monsey, M. S., Ota, K. T., Akingbade, I. F., Hong, E. S., & Schafe, G. E. (2011). Epigenetic Alterations Are Critical for Fear Memory Consolidation and Synaptic Plasticity in the Lateral Amygdala. *PLOS ONE*, 6(5), e19958. <https://doi.org/10.1371/JOURNAL.PONE.0019958>
- Montag, C., Basten, U., Stelzel, C., Fiebach, C. J., & Reuter, M. (2010). The BDNF Val66Met polymorphism and anxiety: support for animal knock-in studies from a genetic association study in humans. *Psychiatry Research*, 179(1), 86–90. <https://doi.org/10.1016/J.PSYCHRES.2008.08.005>
- Montardy, Q., Zhou, Z., Lei, Z., Liu, X., Zeng, P., Chen, C., Liu, Y., Sanz-Leon, P., Huang, K., & Wang, L. (2019). Characterization of glutamatergic VTA neural population responses to aversive and rewarding conditioning in freely-moving mice. *Science Bulletin*, 64(16), 1167–1178. <https://doi.org/10.1016/J.SCIB.2019.05.005>
- Morales, M., & Margolis, E. B. (2017). Ventral tegmental area: Cellular heterogeneity, connectivity and behaviour. *Nature Reviews Neuroscience*, 18(2), 73–85. <https://doi.org/10.1038/NRN.2016.165>
- Morel, C., Montgomery, S. E., Li, L., Durand-de Cuttoli, R., Teichman, E. M., Juarez, B., Tzavaras, N., Ku, S. M., Flanigan, M. E., Cai, M., Walsh, J. J., Russo, S. J., Nestler, E. J., Calipari, E. S., Friedman, A. K., & Han, M. H. (2022). Midbrain projection to the basolateral amygdala encodes anxiety-like but not depression-like behaviors. *Nature Communications* 2022 13:1, 13(1), 1–13. <https://doi.org/10.1038/s41467-022-29155-1>
- Moreno-Martínez, S., Tendilla-Beltrán, H., Sandoval, V., Flores, G., & Terrón, J. A. (2022). Chronic restraint stress induces anxiety-like behavior and remodeling of dendritic spines in the central nucleus of the amygdala. *Behavioural Brain Research*, 416, 113523. <https://doi.org/10.1016/J.BBR.2021.113523>
- Muller, J. F., Mascagni, F., & McDonald, A. J. (2009). Dopaminergic innervation of pyramidal cells in the rat basolateral amygdala. *Brain Structure & Function*, 213(3), 275–288. <https://doi.org/10.1007/S00429-008-0196-Y>
- Murphy, C. P., & Singewald, N. (2019). Role of MicroRNAs in Anxiety and Anxiety-Related Disorders. *Current Topics in Behavioral Neurosciences*, 42, 185–219. https://doi.org/10.1007/7854_2019_109/TABLES/2
- Murrough, J. W., Huang, Y., Hu, J., Henry, S., Williams, W., Gallezot, J. D., Bailey, C. R., Krystal, J. H., Carson, R. E., & Neumeister, A. (2011). Reduced amygdala serotonin transporter binding in posttraumatic stress disorder. *Biological Psychiatry*, 70(11), 1033–1038. <https://doi.org/10.1016/J.BIOPSYCH.2011.07.003>
- Nair-Roberts, R. G., Chatelain-Badie, S. D., Benson, E., White-Cooper, H., Bolam, J. P., & Ungless, M. A. (2008). Stereological estimates of dopaminergic, GABAergic and glutamatergic neurons in the

- ventral tegmental area, substantia nigra and retrorubral field in the rat. *Neuroscience*, *152*(4–2), 1024. <https://doi.org/10.1016/J.NEUROSCIENCE.2008.01.046>
- Namburi, P., Beyeler, A., Yorozu, S., Calhoun, G. G., Halbert, S. A., Wichmann, R., Holden, S. S., Mertens, K. L., Anahtar, M., Felix-Ortiz, A. C., Wickersham, I. R., Gray, J. M., & Tye, K. M. (2015). A circuit mechanism for differentiating positive and negative associations. *Nature*, *520*(7549), 675–678. <https://doi.org/10.1038/NATURE14366>
- Narayanan, R., & Schratt, G. (2020). miRNA regulation of social and anxiety-related behaviour. *Cellular and Molecular Life Sciences* *2020* *77*:21, *77*(21), 4347–4364. <https://doi.org/10.1007/S00018-020-03542-7>
- Nguyen, C., Mondoloni, S., Le Borgne, T., Centeno, I., Come, M., Jehl, J., Solié, C., Reynolds, L. M., Durand-de Cuttoli, R., Tolu, S., Valverde, S., Didiene, S., Hanneke, B., Fiancette, J. F., Pons, S., Maskos, U., Deroche-Gamonet, V., Dalkara, D., Hardelin, J. P., ... Faure, P. (2021). Nicotine inhibits the VTA-to-amygdala dopamine pathway to promote anxiety. *Neuron*, *109*(16), 2604–2615.e9. <https://doi.org/10.1016/J.NEURON.2021.06.013>
- Nieh, E. H., Vander Weele, C. M., Matthews, G. A., Presbrey, K. N., Wichmann, R., Leppla, C. A., Izadmehr, E. M., & Tye, K. M. (2016). Inhibitory Input from the Lateral Hypothalamus to the Ventral Tegmental Area Disinhibits Dopamine Neurons and Promotes Behavioral Activation. *Neuron*, *90*(6), 1286–1298. <https://doi.org/10.1016/J.NEURON.2016.04.035>
- Nieto, S. J., Patriquin, M. A., Nielsen, D. A., & Kosten, T. A. (2016). Don't worry; be informed about the epigenetics of anxiety. *Pharmacology, Biochemistry, and Behavior*, *146–147*, 60. <https://doi.org/10.1016/J.PBB.2016.05.006>
- Nitschke, J. B., Sarinopoulos, I., Oathes, D. J., Johnstone, T., Whalen, P. J., Davidson, R. J., & Kalin, N. H. (2009). Anticipatory activation in the amygdala and anterior cingulate in generalized anxiety disorder and prediction of treatment response. *The American Journal of Psychiatry*, *166*(3), 302–310. <https://doi.org/10.1176/APPI.AJP.2008.07101682>
- Nobin, A., & Bjorklund, A. (1973). Topography of the monoamine neuron systems in the human brain as revealed in fetuses. *Acta Physiologica Scandinavica. Supplementum*, *388*, 40. <https://pubmed.ncbi.nlm.nih.gov/4521068/>
- O'Connell, L. A., & Hofmann, H. A. (2011). The vertebrate mesolimbic reward system and social behavior network: a comparative synthesis. *The Journal of Comparative Neurology*, *519*(18), 3599–3639. <https://doi.org/10.1002/CNE.22735>
- O'Neill, P. K., Gore, F., & Salzman, C. D. (2018). Basolateral amygdala circuitry in positive and negative valence. *Current Opinion in Neurobiology*, *49*, 175–183. <https://doi.org/10.1016/J.CONB.2018.02.012>
- Olson, V. G., & Nestler, E. J. (2007). Topographical organization of GABAergic neurons within the ventral tegmental area of the rat. *Synapse*, *61*(2), 87–95. <https://doi.org/10.1002/SYN.20345>
- Omelchenko, N., Bell, R., & Sesack, S. R. (2009). Lateral Habenula Projections to the Rat Ventral Tegmental Area: Sparse Synapses Observed Onto Dopamine and GABA Neurons. *The European Journal of Neuroscience*, *30*(7), 1239. <https://doi.org/10.1111/J.1460-9568.2009.06924.X>
- Padival, M. A., Blume, S. R., & Rosenkranz, J. A. (2013). Repeated restraint stress exerts different impact on structure of neurons in the lateral and basal nuclei of the amygdala. *Neuroscience*, *246*, 230–242. <https://doi.org/10.1016/J.NEUROSCIENCE.2013.04.061>
- Padival, M., Quinette, D., & Amiel Rosenkranz, J. (2013). Effects of Repeated Stress on Excitatory Drive of Basal Amygdala Neurons In Vivo. *Neuropsychopharmacology* *2013* *38*:9, *38*(9), 1748–1762.

<https://doi.org/10.1038/npp.2013.74>

- Palomares-Castillo, E., Hernández-Pérez, O. R., Pérez-Carrera, D., Crespo-Ramírez, M., Fuxe, K., & Pérez De La Mora, M. (2012). The intercalated paracapsular islands as a module for integration of signals regulating anxiety in the amygdala. *Brain Research*, *1476*, 211–234. <https://doi.org/10.1016/J.BRAINRES.2012.03.047>
- Pape, H. C., & Pare, D. (2010). Plastic Synaptic Networks of the Amygdala for the Acquisition, Expression, and Extinction of Conditioned Fear. *Physiological Reviews*, *90*(2), 419. <https://doi.org/10.1152/PHYSREV.00037.2009>
- Pardo-Bellver, C., Cádiz-Moretti, B., Novejarque, A., Martínez-García, F., & Lanuza, E. (2012). Differential efferent projections of the anterior, posteroventral, and posterodorsal subdivisions of the medial amygdala in mice. *Frontiers in Neuroanatomy*, *6*(AUG 2012), 1–26. <https://doi.org/10.3389/FNANA.2012.00033>
- Partridge, J. G., Forcelli, P. A., Luo, R., Cashdan, J. M., Schulkin, J., Valentino, R. J., & Vicini, S. (2016). Stress increases GABAergic neurotransmission in CRF neurons of the central amygdala and bed nucleus stria terminalis. *Neuropharmacology*, *107*, 239. <https://doi.org/10.1016/J.NEUROPHARM.2016.03.029>
- Patel, D., Anilkumar, S., Chattarji, S., & Buwalda, B. (2018). Repeated social stress leads to contrasting patterns of structural plasticity in the amygdala and hippocampus. *Behavioural Brain Research*, *347*, 314–324. <https://doi.org/10.1016/J.BBR.2018.03.034>
- Pearson, J., Goldstein, M., Markey, K., & Brandeis, L. (1983). Human brainstem catecholamine neuronal anatomy as indicated by immunocytochemistry with antibodies to tyrosine hydroxylase. *Neuroscience*, *8*(1), 3–32. [https://doi.org/10.1016/0306-4522\(83\)90023-4](https://doi.org/10.1016/0306-4522(83)90023-4)
- Perez-Bonilla, P., Santiago-Colon, K., & Leininger, G. M. (2020). Lateral hypothalamic area neuropeptides modulate ventral tegmental area dopamine neurons and feeding. *Physiology & Behavior*, *223*. <https://doi.org/10.1016/J.PHYSBEH.2020.112986>
- Persaud, N. S., & Cates, H. M. (2022). The Epigenetics of Anxiety Pathophysiology: A DNA Methylation and Histone Modification Focused Review. *ENeuro*, ENEURO.0109-21.2021. <https://doi.org/10.1523/ENEURO.0109-21.2021>
- Pessoa, L., & Adolphs, R. (2010). Emotion processing and the amygdala: from a “low road” to “many roads” of evaluating biological significance. *Nature Reviews Neuroscience* *2010 11:11*, *11*(11), 773–782. <https://doi.org/10.1038/nrn2920>
- Phillipson, O. T. (1979). The cytoarchitecture of the interfascicular nucleus and ventral tegmental area of Tsai in the rat. *The Journal of Comparative Neurology*, *187*(1), 85–98. <https://doi.org/10.1002/CNE.901870106>
- Pignatelli, M., & Beyeler, A. (2019). Valence coding in amygdala circuits. *Current Opinion in Behavioral Sciences*, *26*, 97. <https://doi.org/10.1016/J.COBEHA.2018.10.010>
- Pitkänen, A., Stefanacci, L., Farb, C. R., Go, G., Genevieve, Ledoux, J. E., & Amaral, D. G. (1995). Intrinsic connections of the rat amygdaloid complex: Projections originating in the lateral nucleus. *Journal of Comparative Neurology*, *356*(2), 288–310. <https://doi.org/10.1002/CNE.903560211>
- Pitman, R. K., Rasmusson, A. M., Koenen, K. C., Shin, L. M., Orr, S. P., Gilbertson, M. W., Milad, M. R., & Liberzon, I. (2012). Biological studies of post-traumatic stress disorder. *Nature Reviews Neuroscience* *2012 13:11*, *13*(11), 769–787. <https://doi.org/10.1038/nrn3339>
- Pomrenze, M. B., Tovar-Diaz, J., Blasio, A., Maiya, R., Giovanetti, S. M., Lei, K., Morikawa, H., Woodward

- Hopf, F., & Messing, R. O. (2019). A Corticotropin Releasing Factor Network in the Extended Amygdala for Anxiety. *The Journal of Neuroscience: The Official Journal of the Society for Neuroscience*, 39(6), 1030–1043. <https://doi.org/10.1523/JNEUROSCI.2143-18.2018>
- Qi, G., Zhang, P., Li, T., Li, M., Zhang, Q., He, F., Zhang, L., Cai, H., Lv, X., Qiao, H., Chen, X., Ming, J., & Tian, B. (2022). NAc-VTA circuit underlies emotional stress-induced anxiety-like behavior in the three-chamber vicarious social defeat stress mouse model. *Nature Communications* 2022 13:1, 13(1), 1–19. <https://doi.org/10.1038/s41467-022-28190-2>
- Qi, J., Zhang, S., Wang, H. L., Barker, D. J., Miranda-Barrientos, J., & Morales, M. (2016). VTA glutamatergic inputs to nucleus accumbens drive aversion by acting on GABAergic interneurons. *Nature Neuroscience*, 19(5), 725–733. <https://doi.org/10.1038/NN.4281>
- Qi, J., Zhang, S., Wang, H. L., Wang, H., De Jesus Aceves Buendia, J., Hoffman, A. F., Lupica, C. R., Seal, R. P., & Morales, M. (2014). A glutamatergic reward input from the dorsal raphe to ventral tegmental area dopamine neurons. *Nature Communications*, 5. <https://doi.org/10.1038/NCOMMS6390>
- Rainnie, D. G., Bergeron, R., Sajdyk, T. J., Patil, M., Gehlert, D. R., & Shekhar, A. (2004). Corticotrophin Releasing Factor-Induced Synaptic Plasticity in the Amygdala Translates Stress into Emotional Disorders. *The Journal of Neuroscience*, 24(14), 3471. <https://doi.org/10.1523/JNEUROSCI.5740-03.2004>
- Rajbhandari, A. K., Baldo, B. A., & Bakshi, V. P. (2015). Predator Stress-Induced CRF Release Causes Enduring Sensitization of Basolateral Amygdala Norepinephrine Systems that Promote PTSD-Like Startle Abnormalities. *The Journal of Neuroscience: The Official Journal of the Society for Neuroscience*, 35(42), 14270–14285. <https://doi.org/10.1523/JNEUROSCI.5080-14.2015>
- Root, D. H., Estrin, D. J., & Morales, M. (2018). Aversion or Salience Signaling by Ventral Tegmental Area Glutamate Neurons. *iScience*, 2, 51. <https://doi.org/10.1016/j.isci.2018.03.008>
- Root, D. H., Mejias-Aponte, C. A., Qi, J., & Morales, M. (2014). Role of Glutamatergic Projections from Ventral Tegmental Area to Lateral Habenula in Aversive Conditioning. *The Journal of Neuroscience*, 34(42), 13906. <https://doi.org/10.1523/JNEUROSCI.2029-14.2014>
- Root, D. H., Mejias-Aponte, C. A., Zhang, S., Wang, H. L., Hoffman, A. F., Lupica, C. R., & Morales, M. (2014). Single rodent mesohabenular axons release glutamate and GABA. *Nature Neuroscience* 2014 17:11, 17(11), 1543–1551. <https://doi.org/10.1038/nn.3823>
- Root, D. H., Wang, H. L., Liu, B., Barker, D. J., Mód, L., Szocsics, P., Silva, A. C., Maglóczy, Z., & Morales, M. (2016). Glutamate neurons are intermixed with midbrain dopamine neurons in nonhuman primates and humans. *Scientific Reports*, 6, 30615. <https://doi.org/10.1038/SREP30615>
- Root, D. H., Zhang, S., Barker, D. J., Miranda-Barrientos, J., Liu, B., Wang, H. L., & Morales, M. (2018). Selective Brain Distribution and Distinctive Synaptic Architecture of Dual Glutamatergic-GABAergic Neurons. *Cell Reports*, 23(12), 3465–3479. <https://doi.org/10.1016/j.celrep.2018.05.063>
- Rosenkranz, J. A., & Grace, A. A. (2001). Dopamine Attenuates Prefrontal Cortical Suppression of Sensory Inputs to the Basolateral Amygdala of Rats. *Journal of Neuroscience*, 21(11), 4090–4103. <https://doi.org/10.1523/JNEUROSCI.21-11-04090.2001>
- Rosenkranz, J. A., Venheim, E. R., & Padival, M. (2010). Chronic Stress Causes Amygdala Hyperexcitability in Rodents. *Biological Psychiatry*, 67(12), 1128–1136. <https://doi.org/10.1016/j.biopsych.2010.02.008>
- Rumpel, S., LeDoux, J., Zador, A., & Malinow, R. (2005). Postsynaptic receptor trafficking underlying a

- form of associative learning. *Science (New York, N.Y.)*, 308(5718), 83–88. <https://doi.org/10.1126/SCIENCE.1103944>
- Sah, P., Faber, E. S. L., De Armentia, M. L., & Power, J. (2003). The amygdaloid complex: Anatomy and physiology. *Physiological Reviews*, 83(3), 803–834. <https://doi.org/10.1152/PHYSREV.00002.2003/ASSET/IMAGES/LARGE/9J0330254010.JPEG>
- Sapolsky, R. M., Romero, L. M., & Munck, A. U. (2000). How Do Glucocorticoids Influence Stress Responses? Integrating Permissive, Suppressive, Stimulatory, and Preparative Actions. *Endocrine Reviews*, 21(1), 55–89. <https://doi.org/10.1210/EDRV.21.1.0389>
- Schiele, M. A., & Domschke, K. (2018). Epigenetics at the crossroads between genes, environment and resilience in anxiety disorders. *Genes, Brain, and Behavior*, 17(3). <https://doi.org/10.1111/GBB.12423>
- Schiffino, F. L., Siemian, J. N., Petrella, M., Laing¹, B. T., Sarsfield, S., Borja¹, C. B., Gajendiran, A., Zuccoli, M. L., & Aponte, Y. (2019). Activation of a lateral hypothalamic-ventral tegmental circuit gates motivation. *PloS One*, 14(7). <https://doi.org/10.1371/JOURNAL.PONE.0219522>
- Schratt, G. M., Tuebing, F., Nigh, E. A., Kane, C. G., Sabatini, M. E., Kiebler, M., & Greenberg, M. E. (2006). A brain-specific microRNA regulates dendritic spine development. *Nature*, 439(7074), 283–289. <https://doi.org/10.1038/NATURE04367>
- Schultz, W. (1998). Predictive reward signal of dopamine neurons. *Journal of Neurophysiology*, 80(1), 1–27. <https://doi.org/10.1152/JN.1998.80.1.1>
- Schultz, W. (2016). Dopamine reward prediction error coding. *Dialogues in Clinical Neuroscience*, 18(1), 23. <https://doi.org/10.31887/DCNS.2016.18.1/WSCHULTZ>
- Selye, H. (1950). Stress and the General Adaptation Syndrome. *British Medical Journal*, 1(4667), 1383. <https://doi.org/10.1136/BMJ.1.4667.1383>
- Shin, L. M., & Liberzon, I. (2009). The Neurocircuitry of Fear, Stress, and Anxiety Disorders. *Neuropsychopharmacology* 2010 35:1, 35(1), 169–191. <https://doi.org/10.1038/npp.2009.83>
- Silva, B. A., Gross, C. T., & Gräff, J. (2016). The neural circuits of innate fear: detection, integration, action, and memorization. *Learning & Memory*, 23(10), 544–555. <https://doi.org/10.1101/LM.042812.116>
- Smith, S. M., & Vale, W. W. (2006). The role of the hypothalamic-pituitary-adrenal axis in neuroendocrine responses to stress. *Dialogues in Clinical Neuroscience*, 8(4), 383. <https://doi.org/10.31887/DCNS.2006.8.4/SSMITH>
- Soden, M. E., Yee, J. X., Cuevas, B., Rastani, A., Elum, J., & Zweifel, L. S. (2022). Distinct Encoding of Reward and Aversion by Peptidergic BNST Inputs to the VTA. *Frontiers in Neural Circuits*, 0, 62. <https://doi.org/10.3389/FNCIR.2022.918839>
- Sotnikov, S. V., Markt, P. O., Malik, V., Chekmareva, N. Y., Naik, R. R., Sah, A., Singewald, N., Holsboer, F., Czibere, L., & Landgraf, R. (2014). Bidirectional rescue of extreme genetic predispositions to anxiety: impact of CRH receptor 1 as epigenetic plasticity gene in the amygdala. *Translational Psychiatry*, 4(2), e359. <https://doi.org/10.1038/TP.2013.127>
- Stamatakis, A. M., Jennings, J. H., Ung, R. L., Blair, G. A., Weinberg, R. J., Neve, R. L., Boyce, F., Mattis, J., Ramakrishnan, C., Deisseroth, K., & Stuber, G. D. (2013). A unique population of ventral tegmental area neurons inhibits the lateral habenula to promote reward. *Neuron*, 80(4). <https://doi.org/10.1016/j.neuron.2013.08.023>
- Stamatakis, A. M., & Stuber, G. D. (2012). Activation of lateral habenula inputs to the ventral midbrain

- promotes behavioral avoidance. *Nature Neuroscience*, *15*(8), 1105–1107. <https://doi.org/10.1038/NN.3145>
- Steidl, S., Wang, H., Ordonez, M., Zhang, S., & Morales, M. (2017). Optogenetic excitation in the ventral tegmental area of glutamatergic or cholinergic inputs from the laterodorsal tegmental area drives reward. *The European Journal of Neuroscience*, *45*(4), 559–571. <https://doi.org/10.1111/EJN.13436>
- Sternson, S. M., & Bleakman, D. (2020). Chemogenetics: drug-controlled gene therapies for neural circuit disorders. *Cell & Gene Therapy Insights*, *6*(7), 1079. <https://doi.org/10.18609/CGTI.2020.112>
- Strobel, C., Marek, R., Gooch, H. M., Sullivan, R. K. P., & Sah, P. (2015). Prefrontal and Auditory Input to Intercalated Neurons of the Amygdala. *Cell Reports*, *10*(9), 1435–1442. <https://doi.org/10.1016/J.CELREP.2015.02.008>
- Stuber, G. D., Sparta, D. R., Stamatakis, A. M., Van Leeuwen, W. A., Hardjoprajitno, J. E., Cho, S., Tye, K. M., Kempadoo, K. A., Zhang, F., Deisseroth, K., & Bonci, A. (2011). Excitatory transmission from the amygdala to nucleus accumbens facilitates reward seeking. *Nature*, *475*(7356), 377–382. <https://doi.org/10.1038/NATURE10194>
- Takahashi, L. K., Nakashima, B. R., Hong, H., & Watanabe, K. (2005). The smell of danger: a behavioral and neural analysis of predator odor-induced fear. *Neuroscience and Biobehavioral Reviews*, *29*(8), 1157–1167. <https://doi.org/10.1016/J.NEUBIOREV.2005.04.008>
- Tan, K. R., Yvon, C., Turiault, M., Mirzabekov, J. J., Doehner, J., Labouèbe, G., Deisseroth, K., Tye, K. M., & Lüscher, C. (2012). GABA Neurons of the VTA Drive Conditioned Place Aversion. *Neuron*, *73*(6), 1173. <https://doi.org/10.1016/J.NEURON.2012.02.015>
- Tang, W., Kochubey, O., Kintscher, M., & Schneggenburger, R. (2020). A VTA to Basal Amygdala Dopamine Projection Contributes to Signal Salient Somatosensory Events during Fear Learning. *Journal of Neuroscience*, *40*(20), 3969–3980. <https://doi.org/10.1523/JNEUROSCI.1796-19.2020>
- Tank, A. W., & Wong, D. L. (2015). Peripheral and central effects of circulating catecholamines. *Comprehensive Physiology*, *5*(1), 1–15. <https://doi.org/10.1002/CPHY.C140007>
- Taylor, S. R., Badurek, S., Dileone, R. J., Nashmi, R., Minichiello, L., & Picciotto, M. R. (2014). GABAergic and glutamatergic efferents of the mouse ventral tegmental area. *Journal of Comparative Neurology*, *522*(14), 3308–3334. <https://doi.org/10.1002/cne.23603>
- ter Heegde, F., De Rijk, R. H., & Vinkers, C. H. (2015). The brain mineralocorticoid receptor and stress resilience. *Psychoneuroendocrinology*, *52*(1), 92–110. <https://doi.org/10.1016/J.PSYNEUEN.2014.10.022>
- Timmermans, S., Souffriau, J., & Libert, C. (2019). A general introduction to glucocorticoid biology. *Frontiers in Immunology*, *10*(JULY), 1545. <https://doi.org/10.3389/FIMMU.2019.01545/BIBTEX>
- Tong, W. H., Abdulai-Saiku, S., & Vyas, A. (2021). Medial Amygdala Arginine Vasopressin Neurons Regulate Innate Aversion to Cat Odors in Male Mice. *Neuroendocrinology*, *111*(6), 505–520. <https://doi.org/10.1159/000508862>
- Tovote, P., Esposito, M. S., Botta, P., Chaudun, F., Fadok, J. P., Markovic, M., Wolff, S. B. E., Ramakrishnan, C., Fenno, L., Deisseroth, K., Herry, C., Arber, S., & Lüthi, A. (2016). Midbrain circuits for defensive behaviour. *Nature*, *534*(7606), 206–212. <https://doi.org/10.1038/NATURE17996>
- Tran, L., Chaloner, A., Sawalha, A. H., & Greenwood Van-Meerveld, B. (2013). Importance of epigenetic

- mechanisms in visceral pain induced by chronic water avoidance stress. *Psychoneuroendocrinology*, *38*(6), 898–906. <https://doi.org/10.1016/J.PSYNEUEN.2012.09.016>
- Trezza, V., Damsteegt, R., Marijke Achterberg, E. J., & Vanderschuren, L. J. M. J. (2011). Nucleus Accumbens μ -Opioid Receptors Mediate Social Reward. *The Journal of Neuroscience*, *31*(17), 6362. <https://doi.org/10.1523/JNEUROSCI.5492-10.2011>
- Tritsch, N. X., Granger, A. J., & Sabatini, B. L. (2016). Mechanisms and functions of GABA co-release. *Nature Reviews. Neuroscience*, *17*(3), 139–145. <https://doi.org/10.1038/NRN.2015.21>
- Tritsch, N. X., Oh, W. J., Gu, C., & Sabatini, B. L. (2014). Midbrain dopamine neurons sustain inhibitory transmission using plasma membrane uptake of GABA, not synthesis. *ELife*, *2014*(3). <https://doi.org/10.7554/ELIFE.01936>
- Trutti, A. C., Mulder, M. J., Hommel, B., & Forstmann, B. U. (2019). Functional neuroanatomical review of the ventral tegmental area. *NeuroImage*, *191*, 258–268. <https://doi.org/10.1016/j.neuroimage.2019.01.062>
- Tsai, C. (1925). The optic tracts and centers of the opossum. *Didelphis virginiana*. *Journal of Comparative Neurology*, *39*(2), 173–216. <https://doi.org/10.1002/CNE.900390202>
- Tsai, H. C., Zhang, F., Adamantidis, A., Stuber, G. D., Bond, A., De Lecea, L., & Deisseroth, K. (2009). Phasic firing in dopaminergic neurons is sufficient for behavioral conditioning. *Science (New York, N.Y.)*, *324*(5930), 1080–1084. <https://doi.org/10.1126/SCIENCE.1168878>
- Ulrich-Lai, Y. M., & Herman, J. P. (2009). Neural regulation of endocrine and autonomic stress responses. *Nature Reviews Neuroscience* *2009* *10*:6, *10*(6), 397–409. <https://doi.org/10.1038/nrn2647>
- Ungless, M. A., & Grace, A. A. (2012). Are you or aren't you? Challenges associated with physiologically identifying dopamine neurons. *Trends in Neurosciences*, *35*(7), 422. <https://doi.org/10.1016/J.TINS.2012.02.003>
- Valentino, R. J., & Van Bockstaele, E. (2008). Convergent regulation of locus coeruleus activity as an adaptive response to stress. *European Journal of Pharmacology*, *583*(2–3), 194–203. <https://doi.org/10.1016/J.EJPHAR.2007.11.062>
- Van Kerkhof, L. W. M., Trezza, V., Mulder, T., Gao, P., Voorn, P., & Vanderschuren, L. J. M. J. (2014). Cellular activation in limbic brain systems during social play behaviour in rats. *Brain Structure & Function*, *219*(4), 1181. <https://doi.org/10.1007/S00429-013-0558-Y>
- Vereczki, V. K., Müller, K., Krizsán, É., Máté, Z., Fekete, Z., Rovira-Esteban, L., Veres, J. M., Erdélyi, F., & Hájos, N. (2021). Total Number and Ratio of GABAergic Neuron Types in the Mouse Lateral and Basal Amygdala. *Journal of Neuroscience*, *41*(21), 4575–4595. <https://doi.org/10.1523/JNEUROSCI.2700-20.2021>
- Viviani, D., Charlet, A., Van Den Burg, E., Robinet, C., Hurni, N., Abatis, M., Magara, F., & Stoop, R. (2011). Oxytocin selectively gates fear responses through distinct outputs from the central amygdala. *Science*, *333*(6038), 104–107. <https://doi.org/10.1126/SCIENCE.1201043>
- Voltas, N., Aparicio, E., Arija, V., & Canals, J. (2015). Association study of monoamine oxidase-A gene promoter polymorphism (MAOA-uVNTR) with self-reported anxiety and other psychopathological symptoms in a community sample of early adolescents. *Journal of Anxiety Disorders*, *31*, 65–72. <https://doi.org/10.1016/J.JANXDIS.2015.02.004>
- Vyas, A., Bernal, S., & Chattarji, S. (2003). Effects of chronic stress on dendritic arborization in the central and extended amygdala. *Brain Research*, *965*(1–2), 290–294.

[https://doi.org/10.1016/S0006-8993\(02\)04162-8](https://doi.org/10.1016/S0006-8993(02)04162-8)

- Wang, H. L., Qi, J., Zhang, S., Wang, H., & Morales, M. (2015). Rewarding Effects of Optical Stimulation of Ventral Tegmental Area Glutamatergic Neurons. *The Journal of Neuroscience*, *35*(48), 15948. <https://doi.org/10.1523/JNEUROSCI.3428-15.2015>
- Wang, L., Herman, J. P., & Krauzlis, R. J. (2022). Neuronal modulation in the mouse superior colliculus during covert visual selective attention. *Scientific Reports*, *12*(1). <https://doi.org/10.1038/S41598-022-06410-5>
- Weera, M. M., Shackett, R. S., Kramer, H. M., Middleton, J. W., & Gilpin, N. W. (2021). Central Amygdala Projections to Lateral Hypothalamus Mediate Avoidance Behavior in Rats. *Journal of Neuroscience*, *41*(1), 61–72. <https://doi.org/10.1523/JNEUROSCI.0236-20.2020>
- Weidenfeld, J., & Ovadia, H. (2017). The Role of the Amygdala in Regulating the Hypothalamic-Pituitary-Adrenal Axis. *The Amygdala - Where Emotions Shape Perception, Learning and Memories*. <https://doi.org/10.5772/67828>
- White, M., & Whittaker, R. G. (2022). <p>Post-Trial Considerations for an Early Phase Optogenetic Trial in the Human Brain</p>. *Open Access Journal of Clinical Trials*, *14*, 1–9. <https://doi.org/10.2147/OAJCT.S345482>
- Xiao, C., Cho, J. R., Zhou, C., Treweek, J. B., Chan, K., McKinney, S. L., Yang, B., & Gradinaru, V. (2016). Cholinergic Mesopontine Signals Govern Locomotion and Reward through Dissociable Midbrain Pathways. *Neuron*, *90*(2), 333–347. <https://doi.org/10.1016/J.NEURON.2016.03.028>
- Yamaguchi, T., Qi, J., Wang, H. L., Zhang, S., & Morales, M. (2015). Glutamatergic and Dopaminergic Neurons in the Mouse Ventral Tegmental Area. *The European Journal of Neuroscience*, *41*(6), 760. <https://doi.org/10.1111/EJN.12818>
- Yamaguchi, T., Sheen, W., & Morales, M. (2007). Glutamatergic neurons are present in the rat ventral tegmental area. *The European Journal of Neuroscience*, *25*(1), 106–118. <https://doi.org/10.1111/J.1460-9568.2006.05263.X>
- Yamaguchi, T., Wang, H. L., Li, X., Ng, T. H., & Morales, M. (2011). Mesocorticolimbic Glutamatergic Pathway. *Journal of Neuroscience*, *31*(23), 8476–8490. <https://doi.org/10.1523/JNEUROSCI.1598-11.2011>
- Yang, Y., Lee, J., & Kim, G. (2020). Integration of locomotion and auditory signals in the mouse inferior colliculus. *ELife*, *9*. <https://doi.org/10.7554/ELIFE.52228>
- Yi, E. S., Oh, S., Lee, J. kyu, & Leem, Y. H. (2017). Chronic stress-induced dendritic reorganization and abundance of synaptosomal PKA-dependent CP-AMPA receptor in the basolateral amygdala in a mouse model of depression. *Biochemical and Biophysical Research Communications*, *486*(3), 671–678. <https://doi.org/10.1016/J.BBRC.2017.03.093>
- Yoo, J. H., Zell, V., Gutierrez-Reed, N., Wu, J., Ressler, R., Shenasa, M. A., Johnson, A. B., Fife, K. H., Faget, L., & Hnasko, T. S. (2016). Ventral tegmental area glutamate neurons co-release GABA and promote positive reinforcement. *Nature Communications* *2016 7:1*, *7*(1), 1–13. <https://doi.org/10.1038/ncomms13697>
- You, J. S., Hu, S. Y., Chen, B., & Zhang, H. G. (2005). Serotonin transporter and tryptophan hydroxylase gene polymorphisms in Chinese patients with generalized anxiety disorder. *Psychiatric Genetics*, *15*(1), 7–11. <https://doi.org/10.1097/00041444-200503000-00002>
- You, Z. B., Chen, Y. Q., & Wise, R. A. (2001). Dopamine and glutamate release in the nucleus accumbens and ventral tegmental area of rat following lateral hypothalamic self-stimulation. *Neuroscience*,

107(4), 629–639. [https://doi.org/10.1016/S0306-4522\(01\)00379-7](https://doi.org/10.1016/S0306-4522(01)00379-7)

- Young, E. A., Abelson, J., & Lightman, S. L. (2004). Cortisol pulsatility and its role in stress regulation and health. *Frontiers in Neuroendocrinology*, 25(2), 69–76. <https://doi.org/10.1016/J.YFRNE.2004.07.001>
- Yuen, E. Y., Liu, W., Karatsoreos, I. N., Ren, Y., Feng, J., McEwen, B. S., & Yan, Z. (2011). Mechanisms for acute stress-induced enhancement of glutamatergic transmission and working memory. *Molecular Psychiatry*, 16(2), 156–170. <https://doi.org/10.1038/MP.2010.50>
- Zell, V., Steinkellner, T., Hollon, N. G., Warlow, S. M., Souter, E., Faget, L., Hunker, A. C., Jin, X., Zweifel, L. S., & Hnasko, T. S. (2020). VTA Glutamate Neuron Activity Drives Positive Reinforcement Absent Dopamine Co-release. *Neuron*, 107(5), 864–873.e4. <https://doi.org/10.1016/J.NEURON.2020.06.011>
- Zhang, G. W., Shen, L., Tao, C., Jung, A. H., Peng, B., Li, Z., Zhang, L. I., & Tao, H. W. (2021). Medial preoptic area antagonistically mediates stress-induced anxiety and parental behavior. *Nature Neuroscience*, 24(4), 516–528. <https://doi.org/10.1038/S41593-020-00784-3>
- Zhang, J. Y., Liu, T. H., He, Y., Pan, H. Q., Zhang, W. H., Yin, X. P., Tian, X. L., Li, B. M., Wang, X. D., Holmes, A., Yuan, T. F., & Pan, B. X. (2019). Chronic Stress Remodels Synapses in an Amygdala Circuit–Specific Manner. *Biological Psychiatry*, 85(3), 189–201. <https://doi.org/10.1016/J.BIOPSYCH.2018.06.019>
- Zhang, S., Qi, J., Li, X., Wang, H. L., Britt, J. P., Hoffman, A. F., Bonci, A., Lupica, C. R., & Morales, M. (2015). Dopaminergic and glutamatergic microdomains in a subset of rodent mesoaccumbens axons. *Nature Neuroscience*, 18(3), 386–396. <https://doi.org/10.1038/NN.3945>
- Zhang, T. A., Placzek, A. N., & Dani, J. A. (2010). In vitro identification and electrophysiological characterization of dopamine neurons in the ventral tegmental area. *Neuropharmacology*, 59(6), 431–436. <https://doi.org/10.1016/J.NEUROPHARM.2010.06.004>
- Zhang, W. H., Zhang, J. Y., Holmes, A., & Pan, B. X. (2021). Amygdala Circuit Substrates for Stress Adaptation and Adversity. *Biological Psychiatry*, 89(9), 847–856. <https://doi.org/10.1016/J.BIOPSYCH.2020.12.026>
- Zhang, X., Ge, T. T., Yin, G., Cui, R., Zhao, G., & Yang, W. (2018). Stress-induced functional alterations in amygdala: Implications for neuropsychiatric diseases. *Frontiers in Neuroscience*, 12(MAY), 1–9. <https://doi.org/10.3389/fnins.2018.00367>
- Zhou, Z., Liu, X., Chen, S., Feng, G., Xu, F., & Correspondence, L. W. (2019). A VTA GABAergic Neural Circuit Mediates Visually Evoked Innate Defensive Responses. *Neuron*, 103, 473–488.e6. <https://doi.org/10.1016/j.neuron.2019.05.027>
- Zhuo, M. (2016). Neural Mechanisms Underlying Anxiety–Chronic Pain Interactions. *Trends in Neurosciences*, 39(3), 136–145. <https://doi.org/10.1016/J.TINS.2016.01.006>
- Zinebi, F., Xie, J., Liu, J., Russell, R. T., Gallagher, J. P., McKernan, M. G., & Shinnick-Gallagher, P. (2003). NMDA Currents and Receptor Protein Are Downregulated in the Amygdala during Maintenance of Fear Memory. *The Journal of Neuroscience*, 23(32), 10283. <https://doi.org/10.1523/JNEUROSCI.23-32-10283.2003>
- Zoccal, D. B., Furuya, W. I., Bassi, M., Colombari, D. S. A., & Colombari, E. (2014). The nucleus of the solitary tract and the coordination of respiratory and sympathetic activities. *Frontiers in Physiology*, 5 JUN, 238. <https://doi.org/10.3389/FPHYS.2014.00238/BIBTEX>
- Zweifel, L. S., Fadok, J. P., Argilli, E., Garelick, M. G., Jones, G. L., Dickerson, T. M. K., Allen, J. M.,

Mizumori, S. J. Y., Bonci, A., & Palmiter, R. D. (2011). Activation of Dopamine Neurons is Critical for Aversive Conditioning and Prevention of Generalized Anxiety. *Nature Neuroscience*, *14*(5), 620. <https://doi.org/10.1038/NN.2808>